Journal of the Asociación Argentina de Ortopedia y Traumatología

AN ORGAN OF THE ASOCIACIÓN ARGENTINA DE ORTOPEDIA Y TRAUMATOLOGÍA

VOL. 91, N.° 2 / APRIL 2026 PP. 77-187

www.aaot.org.ar • https://raaot.org.ar

Full english text available. Indexed in SciELO, LILACS, Latindex, Dialnet, Doaj, Redib, AmeliCA y JournalTOCs • Included in the Núcleo Básico de Revistas Científicas Argentinas del CONICET.

ISSN 1852-7434 (ONLINE)

Fabricated Bibliographic Citations Generated by Artificial Intelligence in Scientific Research

Dr. Ernesto Bersusky
AAOT Journal Editor

The use of artificial intelligence (AI) is undoubtedly a valuable tool in the preparation of academic work. However, we are increasingly aware that one of its new risks is the generation of academic texts containing entirely fabricated or nonexistent bibliographic references.

These AI-generated texts often cite references that appear legitimate but are nonexistent. As a result, the content cannot be verified in databases or primary sources and therefore lacks scientific validity.

This represents a real threat to the credibility of science, as the problem is not only the falsified references but also the generated text itself, which may appear authentic.

We have identified this phenomenon in several manuscripts submitted to our journal. The use of AI is clearly regulated by the AAOT journal (see the Publications Guidelines section), and authors are required to disclose its use and ensure the accuracy and reliability of the text.

Literature searches before the advent of AI were often slow and tedious, and reviewing these texts frequently required considerable effort. With AI, this process can now be performed with a personal computer in almost no time. AI tools can extract and process information from scientific journals, databases, and books. Finally, the appeal of these tools is extremely strong, and authors may be tempted to use them in ways that are not acceptable.

The use of AI in scientific and technical writing has many advantages and a critical limitation: the accuracy of data and information. For this reason, every text must be carefully reviewed and edited by authors and subject-matter experts prior to publication or submission.

The Editorial Board of this journal monitors the use of AI through plagiarism and AI detection software and verifies all references.

In some cases, we have helped authors resolve these issues; in others, we have been forced to reject the manuscript.

We strongly recommend that authors:

1. Read and adhere to the Publications Guidelines and use AI in accordance with the instructions provided therein.
2. Carefully verify both the text and the references.
3. Share any ideas or suggestions with us to improve the ethical use of AI in research submitted to the journal.
4. This is a novel topic and we remain open to proposals within the limits established by international indexing services and databases.

Authors share responsibility with editors for the work that is published.

Dr. ERNESTO BERSUSKY • ebersusky@gmail.com https://orcid.org/0000-0002-3121-9326

How to cite this article: Bersusky E. Fabricated Bibliographic Citations Generated by Artificial Intelligence in Scientific Research. *Rev Asoc Argent Ortop Traumatol* 2026;91(2):77-78. https://doi.org/10.15417/issn.1852-7434.2026.91.2.2329

WORKS CONSULTED

- Walters WH, Wilder EI. Fabrication and errors in the bibliographic citations generated by ChatGPT. Scie Rep 2023;13:14045. https://doi.org/10.1038/s41598-023-41032-5
- Paz-Enrique LE. Citas fantasmas en artículos científicos: problemática creciente ante el uso de la inteligencia artificial. Rev Med Electron 2023;45(6). Available at: http://scielo.sld.cu/scielo.php?script=sci_arttext&pid=S1684-18242023000600892&lng=es

Case Presentation

Juan Pablo Ghisi,[*] Joaquín Escotorín[**]
[*]Magnetic Resonance Imaging Department, Hospital General de Agudos "Dr. Juan A. Fernández", Autonomous City of Buenos Aires, Argentina
[**]Diagnostic Imaging Department, Sanatorio San Lucas, San Isidro, Buenos Aires, Argentina

Case Resolution on page 184.

Knee Pain

ABSTRACT
Two cases with similar clinical presentations are reported. In both cases, imaging evaluation showed comparable findings involving the capsuloligamentous structures of the medial aspect of the knee.
Keywords: Knee; calcifications; pain
Level of Evidence: IV

Gonalgia

RESUMEN
Se presentan dos casos con un cuadro clínico similar. En ambos, los estudios por imágenes mostraron hallazgos comparables, localizados en relación con las estructuras capsuloligamentarias de la cara medial de la rodilla.
Palabras clave: Rodilla; calcificaciones; dolor.
Nivel de Evidencia: IV

INTRODUCTION

Two cases with similar clinical presentations are reported. In both cases, imaging evaluation showed comparable findings involving the capsuloligamentous structures of the medial aspect of the knee.

CASE 1

A 40-year-old man presented with predominantly medial knee pain, with pain-related functional limitation and no relevant history of trauma. Imaging studies, including plain radiographs and magnetic resonance imaging (MRI), were requested due to suspected involvement of the medial capsuloligamentous compartment. Laboratory tests showed no clinically significant abnormalities; acute-phase reactants were not elevated, and there were no signs of systemic involvement.

CASE 2

A 50-year-old man presented with medial knee pain. As an initial evaluation, a soft-tissue ultrasound focused on the medial aspect of the knee was requested. Based on the findings, the evaluation was completed with MRI for better anatomical characterization of the lesion and its relationship to adjacent capsuloligamentous structures.

Received on March 13th, 2026. Accepted after evaluation on March 19th, 2026 • Dr. JUAN PABLO GHISI • jpghisi@gmail.com https://orcid.org/0000-0001-7991-9228
How to cite this article: Ghisi JP, Escotorín J. Postgraduate Orthopedic Instruction – Imaging. Case Presentation. *Rev Asoc Argent Ortop Traumatol* 2026;91(2):79-82. https://doi.org/10.15417/issn.1852-7434.2026.91.2.2324

IMAGING FINDINGS AND INTERPRETATION

CASE 1

The knee radiograph (Figure 1) showed faint calcifications projected over the medial aspect. On MRI (Figures 2 and 3), multiple foci of signal void with a multilobulated morphology and irregular margins were observed around the capsule and anterior to the femoral insertion of the medial collateral ligament, associated with edema of the adjacent soft tissues. The medial collateral ligament was thickened, with altered signal intensity in its proximal segment, consistent with reactive changes.

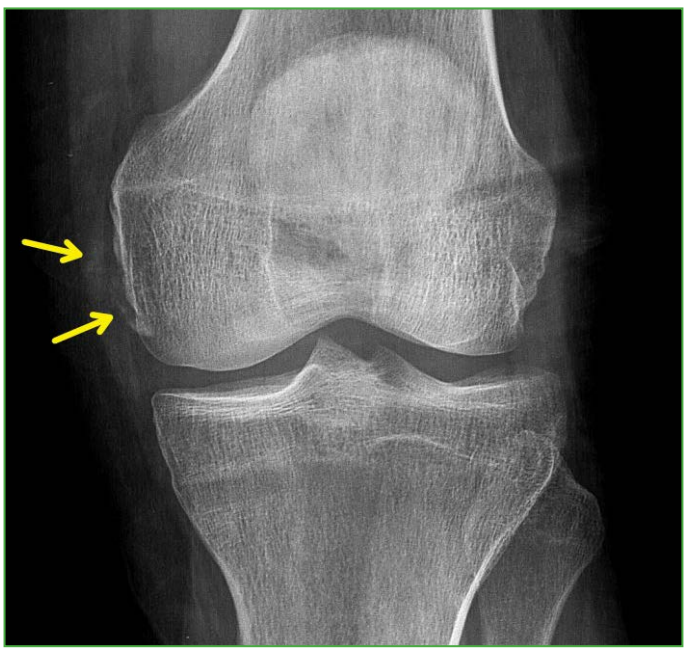

Figure 1. Case 1. Anteroposterior knee radiograph. Faint periarticular calcifications are observed in the medial compartment, projected anterior to the medial femoral condyle, at the femoral insertion of the medial collateral ligament (arrows).

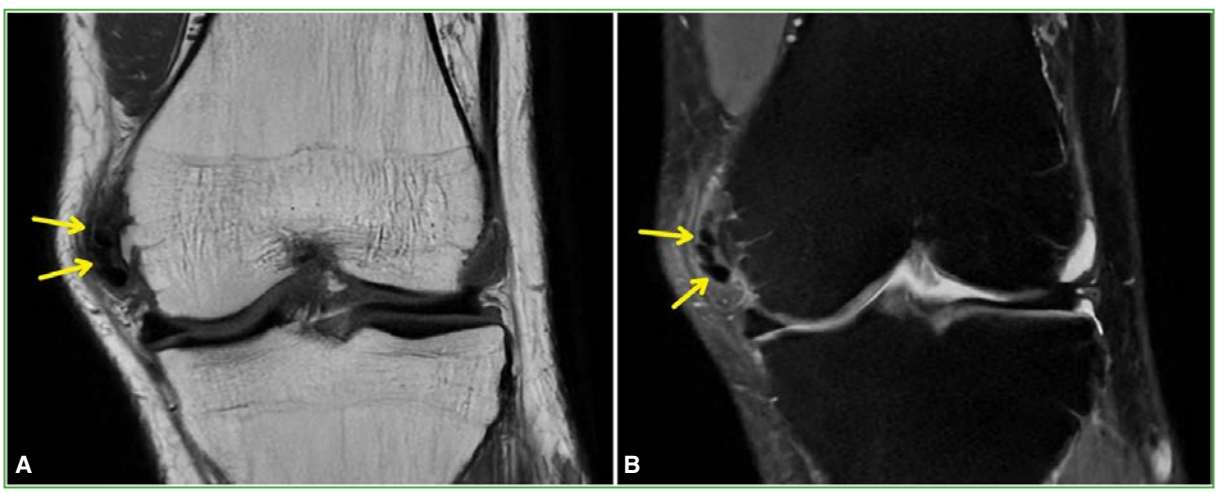

Figure 2. Case 1. MRI of the knee, coronal images: T1-weighted (**A**) and proton density fat-suppressed (**B**) sequences. Multiple foci of signal void corresponding to calcifications are identified, associated with edema of the adjacent soft tissues.

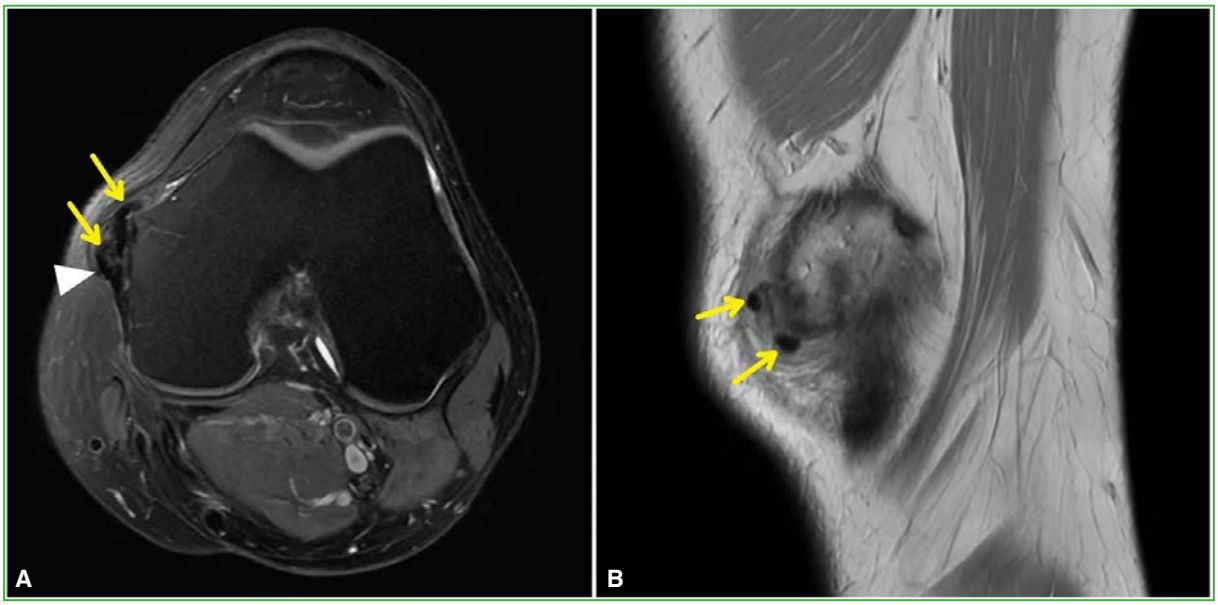

Figure 3. Case 1. MRI of the knee: axial proton density fat-suppressed (**A**) and sagittal proton density (**B**) images. At least two foci of signal void (arrows) are identified in a pericapsular location, anterior to the femoral insertion of the medial collateral ligament (arrowhead).

CASE 2

Ultrasound of the medial aspect of the knee (Figure 4) showed two focal echogenic foci with mild posterior acoustic shadowing, located immediately anterior to the femoral insertion of the medial collateral ligament. MRI (Figures 5 and 6) confirmed, in the same medial pericapsular location, two foci of signal void associated with perilesional inflammatory edema, without evidence of ligament discontinuity.

In both cases, imaging studies demonstrated calcium deposits at the insertion of the medial capsuloligamentous complex, associated with inflammatory changes in the adjacent soft tissues.

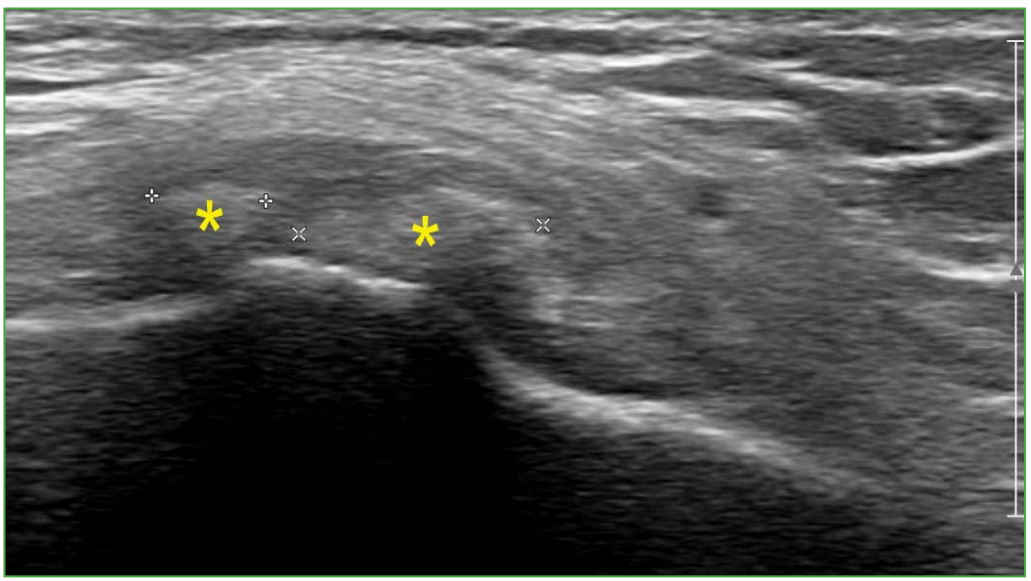

Figure 4. Case 2. Knee ultrasound, longitudinal view. Two focal echogenic foci (*) are observed immediately anterior to the femoral insertion of the medial collateral ligament, with mild posterior acoustic shadowing, consistent with soft-tissue calcifications.

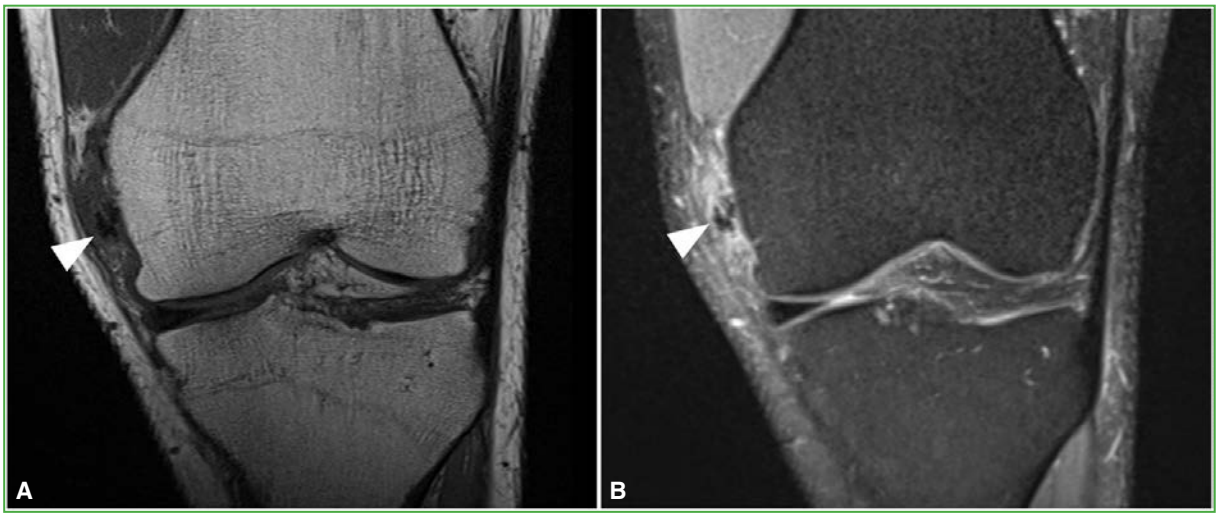

Figure 5. Case 2. MRI of the knee, coronal images: T1-weighted (**A**) and proton density fat-suppressed (**B**) sequences. Two hypointense foci are observed adjacent to the femoral insertion of the medial collateral ligament (arrowheads), with perilesional hyperintensity on fluid-sensitive sequences, consistent with edema.

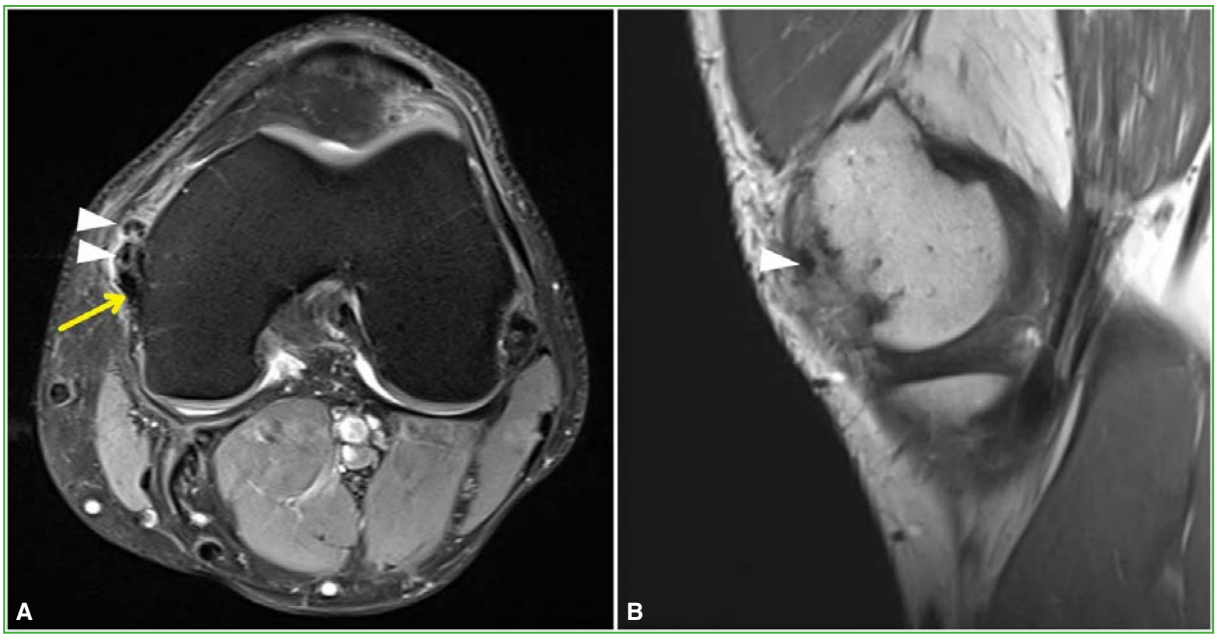

Figure 6. Case 2. MRI of the knee: axial proton density fat-suppressed (**A**) and sagittal proton density (**B**) images. Pericapsular calcifications (arrowheads) are identified at the insertion of the medial collateral ligament (arrow), with adjacent soft-tissue edema on fat-suppressed sequences.

J. Escotorín ORCID ID: https://orcid.org/0009-0006-4115-1034

Reverse Palmar Flaps for Triphalangeal Finger Defects: An Anatomical Study and Case Series

Martín J. Pastrana,[*] Laura Togneri,[*] Ezequiel Zaidenberg,[**] José A. Pastrana,[#] Carlos R. Zaidenberg[**]

[*]*Orthopedics and Traumatology Service, Hospital de Pediatría SAMIC "Prof. Dr. Juan P. Garrahan", Autonomous City of Buenos Aires, Argentina*

[**]*Musculoskeletal Study Unit, 1st Chair of Anatomy, School of Medicine, Universidad Nacional de Buenos Aires, Autonomous City of Buenos Aires, Argentina*

[#]*Hand and Upper Limb Reconstructive Surgery Unit, Sanatorio Güemes, Buenos Aires, Argentina*

ABSTRACT

Objective: To describe the anatomical consistency of palmar cutaneous branches and commissural arteries, and to evaluate patients treated with reverse palmar flaps. **Materials and Methods:** Anatomical study: five cadaveric hands were analyzed to assess the consistency of palmar cutaneous branches, as well as commissural and transverse interphalangeal arteries. Clinical study: patients with palmar digital injuries in triphalangeal fingers treated with palmar flaps were included, with no age restriction, no prior surgical history, with or without associated injuries, and a minimum follow-up of 24 months. Subjective evaluation included the Visual Analog Scale (VAS) for pain and the QuickDASH score. Objective evaluation included the two-point discrimination test and goniometric assessment of total active motion (TAM) according to the Strickland system. **Results:** The anatomical study demonstrated consistent palmar cutaneous branches (2–4 branches per flap island), as well as the presence of commissural and transverse interphalangeal arteries. The clinical study included 10 patients (8 men and 2 women). Eight short and two long palmar flaps were performed. The postoperative VAS score was 1/10 and the QuickDASH score was 2.5. Two-point discrimination was 7 mm. According to TAM (Strickland classification), 6 results were excellent, 3 good, and 1 fair. **Conclusions:** Palmar cutaneous branches and anastomotic systems were found to be consistent. The reverse pedicled palmar flap proved to be an effective option for the treatment of digital defects.

Keywords: Reverse pedicled palmar flaps.

Level of Evidence: IV

Colgajos inversos del hueco de la mano en defectos de dedos trifalángicos. Estudio anatómico y evaluación de una serie de casos

RESUMEN

Objetivos: Describir la constancia anatómica de ramas cutáneas de la palma de la mano y las arterias comisurales, y evaluar a pacientes tratados con colgajos inversos del hueco de la palma. **Materiales y Métodos:** *Estudio anatómico:* 5 manos cadavéricas para analizar la constancia de ramas cutáneas palmares de la mano, arterias comisurales y transversas interfalángicas. *Estudio clínico:* pacientes con heridas digitales palmares en dedos trifalángicos de la mano, tratados con colgajos del hueco de la palma, sin restricción de edad, sin antecedentes quirúrgicos, con o sin lesiones asociadas y un seguimiento mínimo de 24 meses. Las evaluaciones se realizaron con la escala analógica visual para dolor, el QuickDASH, y la prueba de discriminación de 2 puntos y goniometría del rango de movilidad activa total por el sistema de Strickland. **Resultados:** El estudio anatómico demostró la constancia de ramas cutáneas (2-4 ramas por isla) del hueco de la palma, de la arteria comisural y transversas interfalángicas. El estudio clínico incluyó a 10 pacientes (8 hombres y 2 mujeres). Se realizaron 8 colgajos del hueco de la palma cortos y 2 largos. El puntaje posoperatorio de la escala analógica visual fue de 1/10 y el del QuickDASH, 2,5; y la prueba de discriminación de 2 puntos fue de 7 mm. Según el rango de movilidad activa, 6 resultados fueron excelentes; 3, buenos y uno, regular. **Conclusiones:** Las ramas cutáneas y los sistemas anastomóticos resultaron constantes. El colgajo pediculado inverso del hueco de la palma resultó eficiente en el tratamiento de defectos digitales.

Palabras clave: Colgajos pediculados inversos; hueco; palma.

Nivel de Evidencia: IV

Received on February 16th, 2023. Accepted after evaluation on July 29th, 2024 • Dr. MARTÍN J. PASTRANA • martinjosepastrana@hotmail.com https://orcid.org/0000-0002-4843-2115

How to cite this article: Pastrana MJ, Togneri L, Zaidenberg E, Pastrana JA, Zaidenberg CR. Reverse Palmar Flaps for Triphalangeal Finger Defects: An Anatomical Study and Case Series. *Rev Asoc Argent Ortop Traumatol* 2026;91(2):83-91. https://doi.org/10.15417/issn.1852-7434.2026.91.2.1727

INTRODUCTION

Palmar injuries of the fingers involving soft-tissue, osseous, or combined defects are common conditions associated with occupational and recreational activities. When these injuries involve the distal half of the fingers, they can often be treated with random or axial advancement flaps. However, when they are located in the proximal half or involve extensive defects that exceed local coverage capacity, other reconstructive options must be considered.[1-3]

At the beginning of the 20th century, Harold Gillies, a pioneer of plastic surgery, established "the replacement of like with like" as a fundamental principle in soft-tissue reconstruction.[4] More recently, Upton et al. stated that the ideal reconstruction of palmar defects should be performed using glabrous (hairless and glandless), sensate, durable, relatively immobile, and thin tissues.[5]

The study of cutaneous vascular territories divides the hand into digital, digitopalmar, thenar, hypothenar, and, finally, the midpalmar area (MPA). The latter, with an average surface area of 18 cm² in adults, is densely supplied with cutaneous branches that can be used for flap design. Within this framework, reverse and pedicled flaps from the MPA may be considered.[6] Reverse flaps are defined as those in which blood flow is reversed through proximal pedicles or that can be rotated distally, even without true reversal of flow direction.[7]

The objectives of this study were to describe the anatomical consistency of the cutaneous branches of the MPA, together with the palmar-dorsal and digital anastomotic systems, and to clinically evaluate a series of patients with finger defects treated with reverse MPA flaps.

MATERIALS AND METHODS

Anatomical Study

Five cadaveric hands were analyzed (3 female and 2 male; mean age 70 years; range 54-80). After cannulation of the axillary artery, each specimen was injected with red-colored latex, followed by sealing of the cannulas and preservation using a mixture of formaldehyde and phenolic acid according to the Cozzi technique.

Under 3.5x magnification, the palmar vasculature of the hand was dissected. The frequency and consistency of the cutaneous branches of the MPA were analyzed, as well as the presence of commissural arteries (communicating between the palmar and dorsal systems) and of the proximal and distal transverse interphalangeal arteries, also known as Edwards' vascular arcade. Using a micrometric caliper, the mean diameter of the cutaneous branches and palmar vascular axes was measured, along with their angle of origin relative to the vascular axis.

Clinical study

A retrospective study was conducted including patients treated between January 2013 and January 2018. The inclusion criteria were: patients with palmar digital wounds involving the four fingers, treated with reverse MPA flaps (short or long), without age restriction, without prior surgical history, with or without associated injuries (partial amputation of the distal phalanx or distal interphalangeal disarticulation, digital nerve injury distal to the Edwards arcade used as the pivot point, or tendon injury), and a minimum mean follow-up of 24 months. Patients who did not meet these criteria or who had infectious processes were excluded.

All procedures were performed by a single hand surgeon in a single operative stage, at a mean of 4 days after trauma (range 1–9). The anatomosurgical classification proposed by Zancolli for reverse MPA flaps was used, based on the cutaneous branches of the arteries supplying the skin and their pivot point. This classification divides the flaps into short and long, according to the pivot point (commissural confluence or transverse interphalangeal artery, respectively) and their distal reach (Figures 1 and 2).[6] The surgical technique is described below.

Surgical Technique

The procedure is performed under supraclavicular plexus block, with gentle inflation of the tourniquet. After marking the anatomical landmarks (the common and proper digital neurovascular bundles, as well as the probable location of cutaneous perforators in the MPA), the extent of digital tissue loss is determined, and both the size and shape of the defect are transferred to the skin of the MPA (according to the finger to be reconstructed).

The first step consists of an approach at the interdigital commissure, under 3.5x magnification, to confirm the commissural communication between the dorsal and superficial palmar systems (common digital artery).

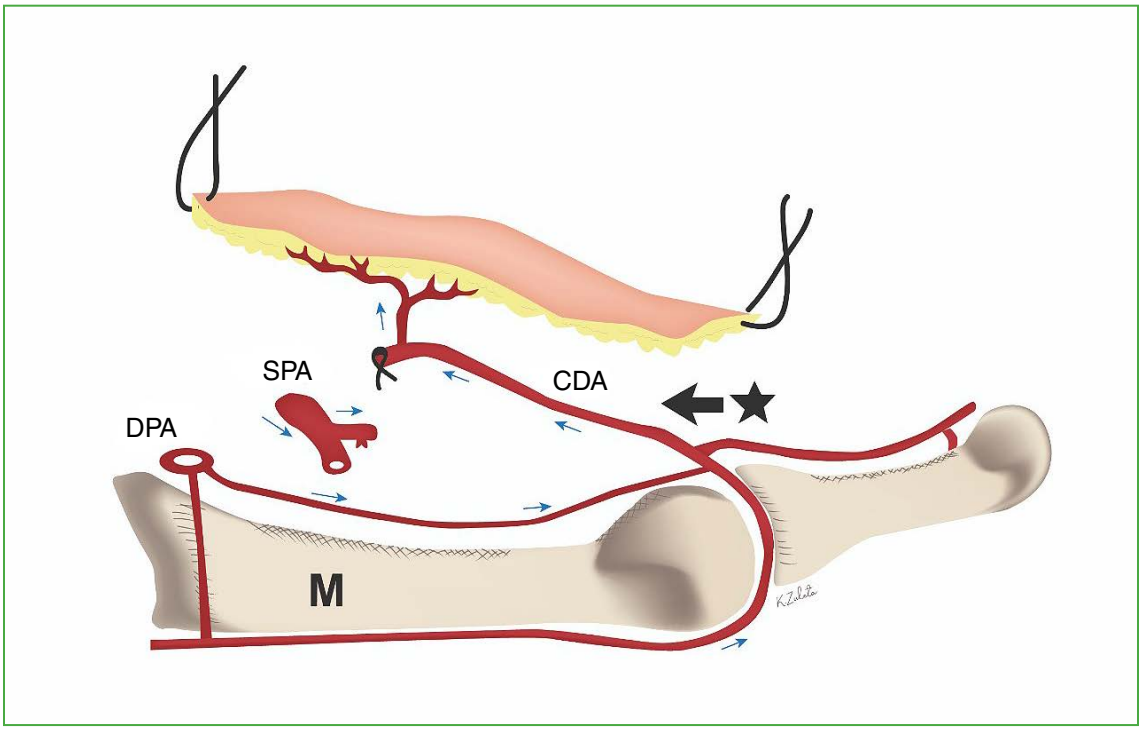

Figure 1. Illustration of the short variant of the midpalmar flap, as described by Zancolli. DPA = deep palmar arch; SPA = superficial palmar arch; CDA = common digital artery; M = metacarpal.

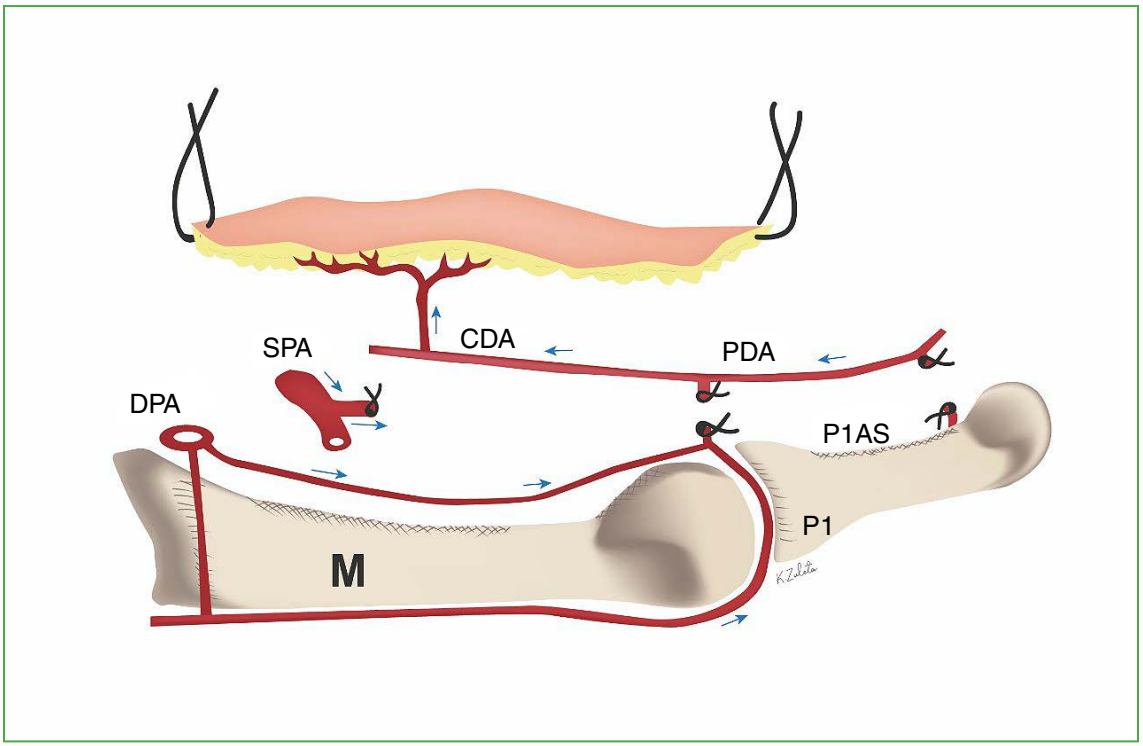

Figure 2. Illustration of the long variant of the midpalmar flap, as described by Zancolli.
DPA = deep palmar arch; SPA = superficial palmar arch; CDA = common digital artery; PDA = proper digital artery; M = metacarpal; P1 = proximal phalanx; P1AS = proximal phalanx anastomotic system.

Once confirmed, the skin island is designed, including an average of 2 to 4 cutaneous branches. The flap is dissected with the least possible amount of subcutaneous tissue. The fibers of the central palmar aponeurosis are divided; the common digital artery is dissected and ligated proximally at its junction with the superficial palmar arch. The island flap is elevated, handling the pedicle carefully and avoiding stretching or twisting along its axis. From the digitopalmar region, the approach is continued in a zigzag fashion, separating the common digital artery and the bifurcation of the proper digital arteries (with their venae comitantes) from the common digital nerve, which is preserved and protected.

Through a lateral digital approach, dissection proceeds until reaching the defect to be covered. The commissural confluence must be preserved (short midpalmar area flap [MPA]) or ligated and divided together with the collateral artery of the adjacent finger to increase advancement (long MPA). The tourniquet is released, meticulous hemostasis is performed, and flap viability is assessed by irrigation with warm saline solution. The recipient site is then covered with the skin island and approximated using 4-0 monofilament sutures, avoiding excessive tension.

Finally, a split-thickness skin graft is harvested from the elbow crease, medial aspect of the arm, or groin (with primary closure) to cover the donor site. An elastic anti-edema dressing is applied, and the hand is immobilized with a short arm plaster splint extending to the digits.

Postoperative Course

Daily wound care was performed during the first 5 days after surgery to assess flap viability (evaluating clinical parameters such as color and capillary refill, without Doppler or other adjunctive methods). Subsequent wound care was performed weekly until suture removal. The patient then began hand occupational therapy. Time to return to usual activities (work/sports) was recorded. Patients were contacted by telephone for long-term follow-up (12 and 24 months).

The sample was evaluated subjectively using the visual analog scale for pain and the QuickDASH questionnaire. Objective evaluation was performed using the two-point discrimination test, and the Strickland scoring system was used to assess total active range of motion by goniometry, defined as the sum of active flexion of the metacarpophalangeal, proximal interphalangeal, and distal interphalangeal joints minus the extension deficit of these joints.[6] Results >150° were considered excellent; 125°-149°, good; 90°-124°, fair; and <90°, poor.

Secondary complications related to the surgical procedure (partial or total necrosis, dehiscence, retractile scarring) were recorded.

RESULTS

Anatomical Study

The anatomical study demonstrated the consistent presence of cutaneous branches of the MPA. An average of 2 to 4 branches per flap island designed at the intermetacarpal level was identified in the cadaveric specimens (Figure 3). These branches emerged at an angle of approximately 70° (range 65°-75°) relative to the common digital artery, perforating the central palmar aponeurosis. In all specimens, a commissural artery (communicating between the palmar and dorsal systems) was consistently identified at the digital commissure, with a mean diameter of 0.4 mm (range 0.3-0.5) (Figure 4).

The mean diameter of the common digital arteries was 1.9 mm (range 1.7-2.1), while the mean diameter of the proper digital arteries was 1.1 mm (range 1-1.2).

In all dissections, transverse interphalangeal arteries, also known as Edwards' vascular arcade, were identified, serving an anastomotic function between the collateral vessels of the same finger. These vessels emerged at an average angle of 80° (range 78°-82°) relative to the proper digital artery and were located at the neck of the proximal and middle phalanges, respectively. They contributed to the arcade together with the articular branch of the proper digital nerve (in two specimens, two articular branches were identified per side) (Figure 5).

Clinical Study

A series of 10 patients (8 male and 2 female) with a mean age of 25 years (range 6-45) was included. The non-dominant hand was affected in 80% of cases. The most frequently involved finger was the middle finger (6 cases), followed by the index finger (3 cases) and the ring finger (1 case). In most cases, the injury was work-related. In two cases, neurorrhaphy of the injured proper digital nerve was performed. In one case, partial amputation of the distal phalanx was present, and in another, distal interphalangeal disarticulation. The mean defect size was 15.1 x 11.3 mm. In eight cases, short MPA flaps were performed, and in two cases, long MPA flaps were used due to the distal location of the defect. All flaps survived.

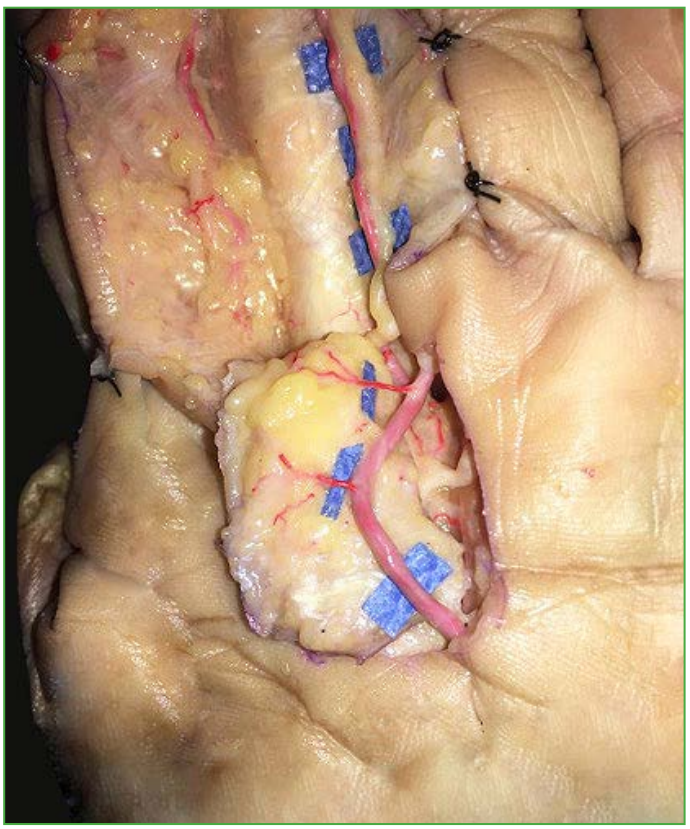

Figure 3. Anatomical dissection of the midpalmar area showing the presence of cutaneous branches within the designed flap island.

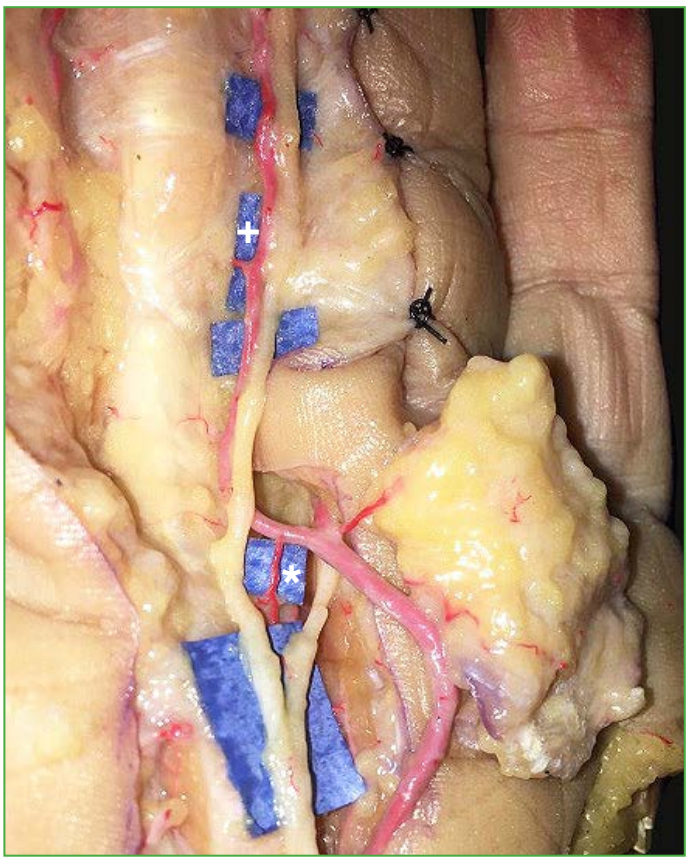

Figure 4. Anatomical dissection of the midpalmar area showing the commissural confluence (commissural artery) and the proximal transverse interphalangeal artery. (*) Commissural confluence; (+) Proximal transverse interphalangeal artery.

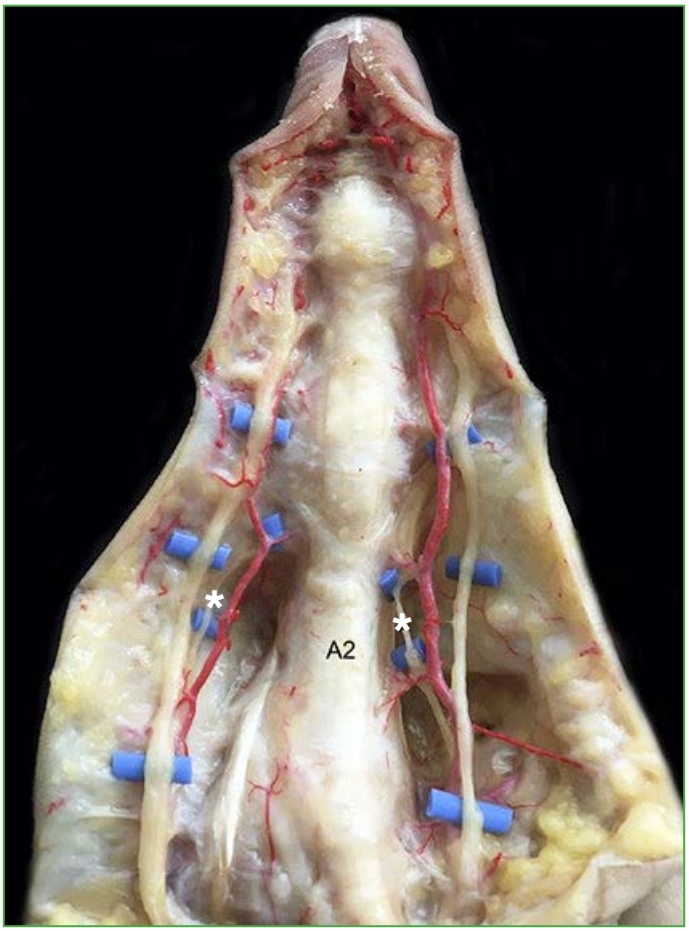

Figure 5. Digital anatomical dissection. The entry of articular nerve branches into Edwards' vascular arcade is observed on each side of the finger, together with the proximal and distal transverse interphalangeal arteries. A2 = A2 pulley; (*) articular nerve branches.

The mean time from admission to discharge, including return to work/sports activities, was 7 weeks (range 6–8). The mean postoperative pain score was 1/10 on the visual analog scale, and the mean postoperative QuickDASH score was 2.5 (Figure 6).

Mean two-point discrimination was 7 mm. Total active range of motion, according to the Strickland scoring system, showed 6 excellent, 3 good, and 1 fair result. The data for this group are summarized in the Table.

Three cases of partial wound dehiscence were recorded (2 long MPA flaps and 1 short MPA flap), all resolved by secondary intention healing. Two cases of partial necrosis of the distal flap edge (both long MPA flaps) were also managed with surgical debridement followed by secondary healing. One case of digital scar contracture (after a long MPA flap) required Z-plasty for correction.

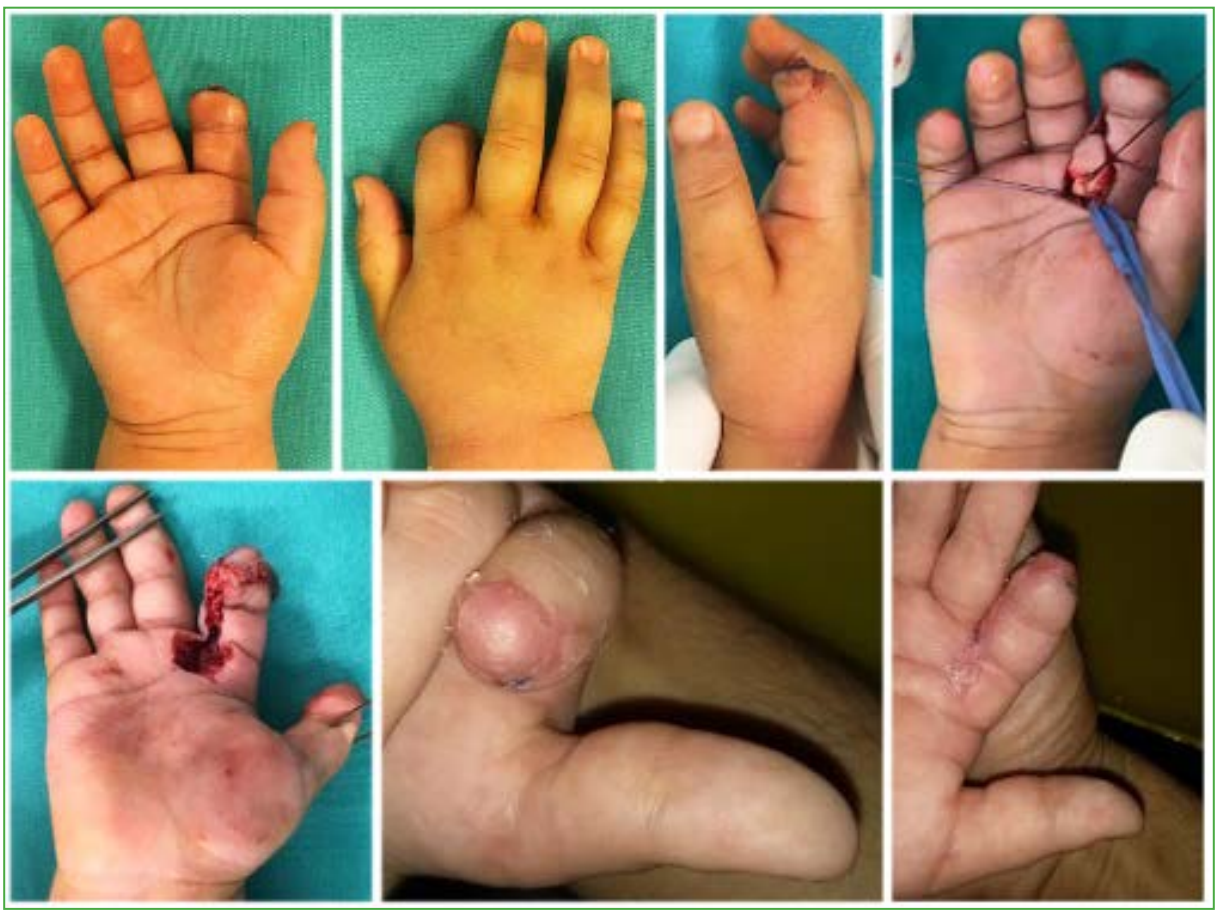

Figure 6. Chronological sequence, as an example, of distal interphalangeal disarticulation of the index finger, the surgical procedure, and long-term follow-up.

Table. Demographic data and subjective and objective assessment by patient.

Patient	Lesion size (mm)	Affected finger	Type of MPA flap	Pain according to VAS (post-op)	Quick DASH score (post-op)	2PDT (mm)	TAM Strickland System
1	19 x 12	Middle	Long	1/10	2.5	9	Average
2	15 x 10	Index	Short	0/10	2	6	Excellent
3	14 x 12	Ring	Short	2/10	3.4	7	Excellent
4	14 x 10	Middle	Short	1/10	2.3	8	Good
5	13 x 11	Middle	Short	2/10	3.5	7	Excellent
6	18 x 12	Index	Long	1/10	2.5	8	Good
7	12 x 10	Index	Short	0/10	2	7	Excellent
8	16 x 12	Middle	Short	1/10	2	7	Good
9	15 x 12	Middle	Short	1/10	2.6	6	Excellent
10	15 x 12	Middle	Short	1/10	2.8	6	Excellent
Average	15.1 x 11.3			1/10	2.5	7	

MPA = midpalmar area; VAS = visual analog scale for pain; 2PDT = 2-point discrimination test; TAM = total active motion.

DISCUSSION

Due to the characteristics of palmar skin, the range of options for intrinsic hand coverage (excluding extrinsic and free flaps) described in the literature is varied, although not extensive.

Melone et al.[8] and Dellon[9] described the random thenar flap and its variant, respectively. In both cases, these flaps are reserved for lesions predominantly involving the fingertips and the distal phalanx. They reported excellent sensory outcomes; however, flexion contracture was the main complication, related to the period of immobilization required before separation from the donor site. Their use in proximal defects is now considered obsolete.

Zancolli's description of reverse MPA flaps, in a small series of patients, represents the first report of pedicled, glabrous reverse flaps in the literature. Based on a detailed analysis of hand vascular anatomy, he indicated their use for massive palmar defects of the four fingers or the base of the thumb, with exposure of bone, tendons, vessels, or nerves. He reported acceptable outcomes, with no flap loss, although sensory outcomes at final follow-up were not addressed.[6]

Vasconez et al. reported the use of a palmar flap to correct contractures of the first web space, based on cutaneous branches of the digital artery of the index finger, with acceptable outcomes and no scar contracture.[10]

Zaidenberg and Angrigiani proposed a "rational organization" of reverse MPA flap design, incorporating digital and dorsal variants (in short and long forms). In a series of 88 patients, 24 underwent reverse MPA flaps, with a 6% rate of total loss and 3% of partial loss; however, the specific subgroup was not detailed, nor were final sensory outcomes reported.[7]

Omakawa et al. conducted an anatomical study of 30 cadaveric hands and described two regions: the distal midpalmar region, with 8 to 15 cutaneous branches (arising from the three common digital arteries) capable of perfusing an area of 5 x 3 cm, and the radial midpalmar border, with 3-6 cutaneous branches (arising from the superficial palmar arch). They proposed two flaps: a transversely designed distal midpalmar flap, with a pivot point at the proximal Edwards' arcade for finger defects, and a radial midpalmar border flap for thumb defects. They highlighted favorable aesthetic outcomes without scar contracture as an advantage.[11,12]

Meanwhile, Orbay et al., in a clinical anatomy study, proposed a reverse flap based on the superficial palmar branch of the radial artery, extending from the wrist crease to the transverse palmar crease, with a maximum width of 2.5 cm and a length of 10 cm. In a series of 36 patients, they reported a single case of necrosis, which healed by secondary intention.[13]

In the present study, the anatomical consistency of cutaneous branches, together with the palmar-dorsal and digital anastomotic systems, was analyzed, highlighting their regularity and making flap design predictable. Regarding clinical outcomes, a higher rate of complications was observed compared with the reference literature; these included wound dehiscence and marginal necrosis, which resolved by secondary intention healing, except for one case of scar contracture that required Z-plasty.

Regarding the reinnervation of a non-innervated flap, published studies support the role of axonal sprouting from the recipient bed into the flap, contributing to the final outcome in the two-point discrimination test. This is further supported by histochemical evidence of nerve regeneration at the margins of the studied flaps.[14-19]

The limitations of this study include its retrospective design, the small sample size, and the heterogeneity in age and occupations (predominantly manual workers). However, we consider as strengths the cadaveric confirmation of palmar and digital vascular anatomy, as well as the inclusion of a relatively homogeneous series of patients treated by a single surgeon.

FINAL CONSIDERATIONS

The palmar cutaneous perforating branches, together with the palmar-dorsal and digital anastomotic systems, were found to be consistent and reliable, allowing predictable flap design. The reverse pedicled midpalmar flap, in both its short and long variants, proved effective for the treatment of patients with finger defects.

Conflicts of interest: The authors declare no conflicts of interest.

L. Togneri ORCID ID: https://orcid.org/0000-0002-7165-2677
E. Zaidenberg ORCID ID: https://orcid.org/0000-0002-1535-0586
J. A. Pastrana ORCID ID: https://orcid.org/0000-0002-9341-6640
C. R. Zaidenberg ORCID ID: https://orcid.org/0000-0001-5921-0828

REFERENCES

1. Foucher G, Smith C, Pempinello C, Braun FM, Citron N. Homodigital neurovascular island flaps for digital pulp loss. *J Hand Surg Br* 1989;14(2):204-8. https://doi.org/10.1016/0266-7681(89)90127-7
2. Regmi S, Gu J, Zhang N, Liu H. A systematic review of outcomes and complications of primary fingertip reconstruction using reverse-flow homodigital island flaps. *Aesth Plast Surg* 2016;40:277-83. https://doi.org/10.1007/s00266-016-0624-y
3. Kim KS, Kim ES, Hwang JH, Lee SY. Thumb reconstruction using the radial midpalmar (perforator-based) island flap (distal thenar perforator-based island flap). *Plast Reconstr Surg* 2010;125(2):601-8. https://doi.org/10.1097/PRS.0b013e3181c82fd7
4. Zhang WY, Hallock GG. Gillies and Dunedin: the birthplace of modern plastic surgery. *J Plast Reconstr Aesthet Surg* 2020;73(6):1012-7. https://doi.org/10.1016/j.bjps.2020.02.011
5. Upton J, Havlik RJ, Khouri RK. Refinements in hand coverage with microvascular free flaps. *Clin Plast Surg* 1992;19:841-57. PMID: 1339640
6. Zancolli EA. Colgajo cutáneo en isla del hueco de la palma. *Prensa Méd Argentina* 1990;77:14-20.
7. Zaidenberg CR, Angrigiani C. Colgajos reversos para el tratamiento de las heridas graves de los dedos. *Rev Asoc Argent Ortop Traumatol* 1992;58(1):58-65. Available at: https://www.aaot.org.ar/revista/1993_2002/1993/1993_1/580107.pdf
8. Melone CP, Beasley RW, Cartsens JH. The thenar flap-an analysis of its use in 150 cases. *J Hand Surg Am* 1982;7(3):291-7. https://doi.org/10.1016/s0363-5023(82)80182-2
9. Dellon AL. The proximal inset thenar flap for fingertip reconstruction. *Plast Reconstr Surg* 1983;72:698-704. https://doi.org/10.1097/00006534-198311000-00022
10. Vasconez LO, Velazquez CA, Rumley T. Correction of the first web space contracture with an arterialized palmar flap. En: Gilbert A, Masquelet A, Hentz VR (eds). *Pedicled flaps of the upper limb*. Boston: Little Brown; 1992, p. 135-8.
11. Omokawa S, Mizumoto S, Iwai M. Innervated radial thenar flap for sensory reconstruction of fingers. *J Hand Surg Am* 1996;21:373-80. https://doi.org/10.1016/s0363-5023(96)80347-9
12. Omokawa S, Tanaka Y, Ryu J, Clovis N. Anatomical consideration of reverse-flow island flap transfers from the midpalm for finger reconstruction. *J Plast Reconstr Surg* 2001;108(7):2020-5. https://doi.org/10.1097/00006534-200112000-00029
13. Orbay JL, Rosen JG, Khouri RK, Indriago I. The glabrous palmar flap. The new free or reversed pedicled palmar fasciocutaneous flap for volar hand reconstruction. *Tech Hand Up Extrem Surg* 2009;13:145-50. https://doi.org/10.1097/BTH.0b013e3181ac9183
14. Dellon AL, Kallman CH. Evaluation of functional sensation in the hand. *J Hand Surg Am* 1983;8(6):865-70. https://doi.org/10.1016/s0363-5023(83)80083-5
15. Shindo ML, Sinha UK, Rice DH. Sensory recovery in noninnervated free flaps for head and neck reconstruction. *Laryngoscope* 1995;105(12 Pt 1):1290-3. https://doi.org/10.1288/00005537-199512000-00005
16. Meltem Ayhan Oral, Kamuran Zeynep Sevim, Metin Görgü, Hasan Yücel Öztan. Sensory recovery with innervated and noninnervated flaps after total lower lip reconstruction: a comparative study. *Plast Surg Int* 2013;2013:643061. https://doi.org/10.1155/2013/643061
17. Dykes R, Terzis J, Strauch B. Sensations from surgically transferred glabrous skin: central versus peripheral factors. *Can J Neurol Sci* 1979;6(4):437-45. https://doi.org/10.1017/s0317167100023842
18. Vriens JP, Acosta R, Soutar DS, Webster MH. Recovery of sensation in the radial forearm free flap in oral reconstruction. *Plast Reconstr Surg* 1996;98(4):649-56. https://doi.org/10.1097/00006534-199609001-00008
19. Close LG, Truelson JM, Milledfe RA, Schweitzer C. Sensory recovery in noninnervated flaps used for oral cavity and oropharyngeal reconstruction. *Arch Otolaryngol Head Neck Surg* 1995;121(9):967-72. https://doi.org/10.1001/archotol.1995.01890090011002

Large Osteochondromas During Growth: A Case Series and Literature Review

Patricio P. Manzone,[*] Claudio A. Fernández,[**] Marta Salom,[#] María Emilia Moreiro,[##] Nuria Amarilla,[§] Claudio Silveri,[§§] Pablo Stoppiello,[§§] Gottardo Bianchi,[§§] Nicolás Casales,[§§] Leticia Gaiero,[§§] Pablo Amador,[I] Silvana Fiscina,[II] Sergio Innocenti[II]

[*]Nicolás Andry" Center, Resistencia, Chaco, Argentina
[**]School of Medical Science, National University of La Plata, La Plata, Buenos Aires, Argentina
[#]Pediatric Orthopedic and Trauma Surgery Unit, Hospital Universitari i Politècnic La Fe, Valencia, Spain
[##]Pediatric Orthopedics and Traumatology Service, Hospital de Niños "Sor María Ludovica", La Plata, Buenos Aires, Argentina
[§]Orthopedics and Traumatology Service, Hospital General "Dr. Julio C. Perrando", Resistencia, Chaco, Argentina
[§§]UPOME - Musculoskeletal Oncology Unit, Universidad de la República, Montevideo, Uruguay
[I]Orthopedics and Traumatology Service, Hospital San Bernardo, Salta, Argentina
[II]Orthopedics and Traumatology Service, Hospital Nacional de Pediatría S.A.M.I.C. "Prof. Dr. Juan P. Garrahan", Autonomous City of Buenos Aires, Argentina

ABSTRACT

Introduction: Osteochondromas are the most common benign osteochondral tumors. Their size is rarely an indication for surgery, and large osteochondromas are usually reported as isolated cases. However, although rare, the potential for malignant transformation exists. We present a series of large osteochondromas in a pediatric population treated surgically, along with a review of the literature. **Materials and Methods:** A retrospective, multicenter cohort study was conducted in skeletally immature patients with large osteochondromas who underwent surgical treatment. Tumor volume was assessed using preoperative imaging. Demographic and surgical variables were analyzed. **Results:** Twenty patients (16 males and 4 females) from eight sites were included; four had multiple osteochondromatosis and the mean age at surgery was 14 years. Nineteen patients had lesions in the extremities, and one had an extraspinal osteochondroma. Four patients were asymptomatic. Magnetic resonance imaging was used to determine tumor volume; the mean volume was 65 cm³ (range: 43.75–904.78 cm³). Surgical treatment included marginal resection in 10 cases, wide resection in 8, and intralesional resection in 2. Mean follow-up was 4 years and 8 months. There were two immediate postoperative complications, two late complications, and one recurrence. **Conclusions:** Surgical removal of large osteochondromas in the extremities and in extraspinal locations should be considered even in asymptomatic patients due to the risk of malignant transformation. Intralesional resection should be avoided because of the risk of recurrence. Marginal resection is the preferred approach, although selected cases may require wide resection with reconstruction.

Keywords: Osteochondroma; pediatric; staging; surgical treatment.
Level of Evidence: IV

Osteocondromas voluminosos durante el crecimiento: serie de casos y revisión bibliográfica

RESUMEN

Introducción: Los osteocondromas son los tumores osteocartilaginosos benignos más frecuentes. Raramente su volumen es indicación de cirugía y los osteocondromas voluminosos, en general, se comunican como casos aislados. La posibilidad de malignización, aunque excepcional, existe. Se presenta una serie de osteocondromas voluminosos en una población pediátrica tratados quirúrgicamente, y se revisa la bibliografía. **Materiales y Métodos:** Investigación retrospectiva de cohorte multicéntrica de pacientes inmaduros esqueléticamente con osteocondromas voluminosos operados. Se evaluó el volumen en imágenes preoperatorias. Se analizaron diferentes variables demográficas y quirúrgicas. **Resultados:** Se incluyó a 20 pacientes (16 varones y 4 niñas) con una edad media al operarse de 14 años, provenientes de 8 centros, 4 con osteocondromatosis múltiple. Diecinueve tenían osteocondromas en las extremidades y uno, un osteocondroma extracanal en el raquis. Cuatro eran asintomáticos. Se

Received on April 22nd, 2025. Accepted after evaluation on September 26th, 2025 • Dr. PATRICIO P. MANZONE • manzonepatricio@hotmail.com https://orcid.org/0000-0002-3987-267X
How to cite this article: Manzone PP, Fernández CA, Salom M, Moreiro ME, Amarilla N, Silveri C, et al. Large Osteochondromas During Growth: A Case Series and Literature Review. *Rev Asoc Argent Ortop Traumatol* 2026;91(2):XXX. https://doi.org/10.15417/issn.1852-7434.2026.91.2.2156

usaron las imágenes preoperatorias de resonancia magnética para definir el volumen; el volumen general promedio fue 65 cm^3 (43,75-904,78 cm^3). La cirugía incluyó resección marginal (10 casos), amplia (8 casos) e intralesional (2 casos). Tiempo medio de seguimiento: 4 años y 8 meses. Hubo 2 complicaciones posoperatorias inmediatas, y 2 complicaciones posoperatorias alejadas y una recidiva. **Conclusiones:** Considerar la ablación quirúrgica de osteocondromas voluminosos de extremidades y extracanalares raquídeos, aun sin síntomas, ante la posibilidad de malignización. Evitar la ablación intralesional por los riesgos de recidiva. El procedimiento adecuado es la resección marginal; algunos casos seleccionados requieren resección amplia con reconstrucción.
Palabras clave: Osteocondroma voluminoso; niños; estadificación; tratamiento quirúrgico.
Nivel de Evidencia: IV

INTRODUCTION

Osteochondromas are the most common benign osteocartilaginous tumors[1] and are typically located in the lower extremities, with an estimated prevalence ranging from 0.44% to 4.5%.[2] Surgical resection is indicated when lesions are symptomatic, when associated complications are present, for cosmetic reasons, or when malignant transformation is suspected.[3] Size alone is rarely an indication for surgery in skeletally immature patients.

Reports of large osteochondromas are generally limited to isolated cases, and surgical management is relatively uncommon.[4–6]

The aim of this study was to evaluate our own case series of large osteochondromas in a skeletally immature population undergoing surgery, to analyze their main characteristics and the treatments performed, as well as short- and mid-term outcomes, and to conduct a literature review.

MATERIALS AND METHODS

A multicenter, retrospective cohort study was conducted across Orthopedic and Traumatology Departments in three countries (8 sites), through review of cases recorded over the past 20 years (2004–2023).

Patients <18 years of age or skeletally immature (based on bone age), with large osteochondromas who underwent surgical treatment and had a minimum follow-up of one year, were included. To be eligible, patients were required to have osteochondromas with a volume >40 cm^3; this threshold was selected because a pedunculated osteochondroma of the knee typically has a smaller volume.

Patients with intraspinal osteochondromas were excluded. However, patients with extraspinal vertebral osteochondromas without neurological risk were included if they met the specified volume criterion. Table 1 summarizes the variables analyzed in each case.

As this was a multicenter observational study, each participating institution's Ethics Committee determined that formal approval was not required. Nevertheless, all parents, legal guardians, or patients (depending on age, clinical context, and local regulations) provided informed consent for participation in the study and for publication of their data and images, ensuring preservation of patient confidentiality.

Statistical Analysis

Parametric variables were analyzed using Student's *t* test, and nonparametric variables using the chi-square test.

Preoperative tumor volume was estimated as an approximation of the actual volume based on the best available imaging study: tumor shape was matched to the closest geometric form, and volume was subsequently calculated mathematically (Figure 1). Although these measurements were approximate rather than exact, they were close to the true values.

Table 1. Variables analyzed in the study.

Sex
Associated syndromes or conditions
Age at the time of surgery
Anatomical location
Affected bone and location within the bone
Preoperative imaging studies
Estimated tumor volume
Preoperative symptoms
Preoperative biopsy*
Type of resection**
Use of grafts, bone substitutes, or other reconstruction methods
Postoperative immobilization*
Early complications
Fixation/osteosynthesis used*
Histopathological findings
Need for additional treatment
Follow-up duration
Age at last follow-up
Late complications
Recurrence
Sequelae and functional outcomes at follow-up
Follow-up imaging studies

* If applicable.
**According to the Enneking staging system.

Figure 1. Magnetic resonance imaging of the distal thigh in coronal and sagittal planes. Example of volume estimation of a distal femoral osteochondroma approximated to a truncated cone (case 4) (see Table 2).

RESULTS

A total of 20 patients (16 males and 4 females) with a mean age of 14 years at the time of surgery (range 10 years 8 months-18 years) from eight sites in three countries were included (Table 2).

Table 2. Characteristics of patients included in the study.

Case	1	2	3	4	5	6	7	8	9	10	11	12	13	14	15	16	17	18	19	20
Sex	M	M	M	M	M	F	M	M	M	M	M	M	M	F	M	M	M	M	F	F
Associated conditions and syndromes	-	-	Down syndrome	-	MO	-	-	-	-	-	-	-	-	-	-	MO	-	-	MO	MO
Age at surgery (years)	14	11.7	15.3	13.5	14	12	17	12	12.3	15	10	18	16	18	17	15.3	10.64	14.08	11.72	11.8
Affected bone	Distal femur	Proximal humerus	Proximal humerus	Distal femur	Proximal tibia	Proximal fibula	Distal femur	Scapula, body	T6 Vertebra, posterior arch	Distal femur	Proximal humerus	Proximal femur	Proximal fibula	Proximal femur	Distal tibia	Proximal fibula	Humerus	Proximal femur	Proximal humerus	Humerus
Tumor volume (approx. in cm^3)	209.84	57.5	179.6	273.68	70.5	135.12	904.78	56.5	103 (extra-canal)	53.27	60	65	65	65	65	217.6	43.75	46.8	79.5	51.84
Preoperative symptoms	No (mass detected)	No (mass detected)	Pain	No (mass detected)	Pain + deformity	CFN Paresthesia + Deformity	Pain	Pain	Painless mass that grows	Pain	Pain + paresthesia	Pain + limited mobility	Pain	Pain + limited mobility	Post-activity pain	Painless mass that is growing	No (mass found)	Pain	Painless mass that is growing	Painful mass
Previous biopsy	Yes/C-shaped	No	No	No	No	No	Yes/CT	No	Yes/CT	No	No	No	No	No	No	No	No	No	No	No
Resection (margins)	Marginal	Marginal	Marginal	Wide	Marginal	Marginal	Wide	Marginal	Intralesional	Marginal	Wide	Wide	Wide	Wide	Wide	Wide	Marginal	Intralesional	Marginal	Marginal
Surgical technique	Partial femoral resection with tumor mass + reconstruction and IF	Partial humeral resection with tumor mass + phenolization + reconstruction and IF	Partial humeral resection with tumor mass + phenolization + reconstruction and IF	Partial femoral resection with tumor mass + phenolization + reconstruction and IF	Complete en bloc resection	Complete en bloc resection	Complete en bloc resection	Complete en bloc resection	Posterior approach + fragment resection + IF	Complete en bloc resection	Complete en bloc resection	Complete en bloc resection	Complete en bloc resection	Complete en bloc resection	Complete en bloc resection	Complete en bloc resection	Complete en bloc resection	Partial resection (residual tissue remains)	Complete en bloc resection	Complete en bloc resection
Type of reconstruction	Graft + BS	BS	BS	Graft + BS	No	No	No	No	No	No	No	No	No	No	No	No	No	No	No	No
IF	Solid titanium IN + SL plates	Elastic IN	Titanium L-plates + wires	Extra-long titanium plate	No	No	No	No	Pedicle fixation	No	No	No	No	No	No	No	No	No	No	No
Early complications	No	No	No	No	No	No	No	No	No	No	No	Joint stiffness	CFN deficit	No	No	No	No	No	No	No
Follow-up (years)																				
Age at final follow-up (years)	16.5	18.6	18.3	15.5	21	18	19	18	13.5	16	12	19	18	22	18	19.6	13	19.4	12.4	13.9
Late complications	No	No	Humeral pseudoarthrosis	No	No	No	No	No	No	No	No	No	No	No	No	No	No	Adductor pain	No	No
Recurrence	No	No	No	No	No	No	No	No	No	No	No	No	No	No	No	No	No	Yes	No	No
Sequelae at final follow-up	No	No	Limited shoulder abduction	No	No	No	No	No	Scoliosis (12°)	No	No	No	No	No	No	No	No	No	No	No

M = male; F = female; MO = multiple osteochondromatosis; CF = in the territory of the common fibular nerve; CT = computed tomography; IF = internal fixation; BS = bone substitutes; IN = intramedullary nail; SL = self-locking; CFN = external popliteal sciatic nerve.

Five patients had associated conditions (4 with multiple osteochondromatosis and 1 with Down syndrome). The anatomical locations are shown in Figure 2: 12 lesions were in the lower extremities, 7 in the upper extremities, and 1 in the spine. No statistically significant differences were found between sex and age (p = 0.6), nor between sex and anatomical location (p = 0.53).

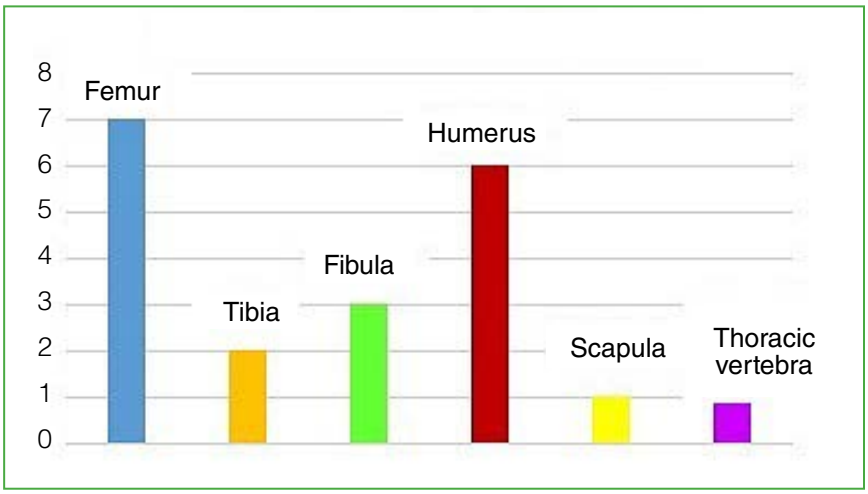

Figure 2. Anatomical distribution of skeletal osteochondromas.

Four patients were asymptomatic preoperatively; in these cases, the indication for surgery was based on tumor volume or patient and family concern. In the remaining 16 cases, symptoms included pain (12 cases) (Figure 3), progressive deformity or mass (4 cases), limitation of joint motion (3 cases), and neurological symptoms (regional paresthesia in 2 cases).

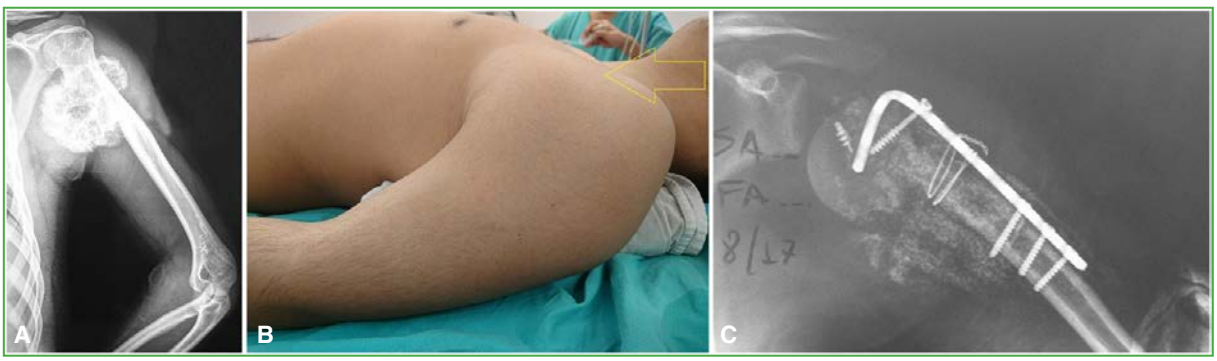

Figure 3. Case 3. Proximal humeral osteochondroma.**A.** Preoperative anteroposterior radiograph of a left proximal humeral osteochondroma (179.6 cm³). **B.** Preoperative clinical appearance. **C.** Radiograph at 18 months postoperatively showing pseudarthrosis.

All patients underwent plain radiographs; all but one also underwent magnetic resonance imaging (MRI), and 12 additionally underwent computed tomography (CT). MRI was primarily used to assess tumor volume. The mean tumor volume was 65 cm³ (range 43.75-904.78). No statistically significant differences were found in tumor volume between sexes (p = 0.51), nor between osteochondromas of the upper and lower extremities (p = 0.27).

Only three patients underwent image-guided percutaneous biopsy prior to resection; histopathological findings were consistent with the final surgical specimen.

Ten patients were treated with marginal resection, eight with wide resection, and two with intralesional ablation. All tumors were sessile osteochondromas on histopathological examination, with no evidence of malignancy or soft tissue invasion, and a cartilage cap thickness ≥3 cm.

The most performed procedure was simple tumor resection (16 cases: 15 in the extremities and 1 in the spine), either en bloc or piecemeal; reconstruction was required in only four cases. In the spinal osteochondroma, the procedure was supplemented with arthrodesis and pedicle instrumentation, without reconstruction.

Two early minor postoperative complications occurred, both in patients with extremity osteochondromas, and both resolved completely: one case of joint stiffness and one case of transient common fibular nerve deficit. No patient required additional treatment.

The mean follow-up was 4 years and 8 months (range 1–24 years), and the mean age at follow-up was 17 years and 2 months (range 12–22 years). Two late complications were observed: one case of proximal humeral pseudarthrosis that was not treated because it did not affect activities of daily living (patient with Down syndrome and significant cognitive impairment) (Figure 4), and one case of persistent pain in the adductor region, which resolved with injections and tenotomies.

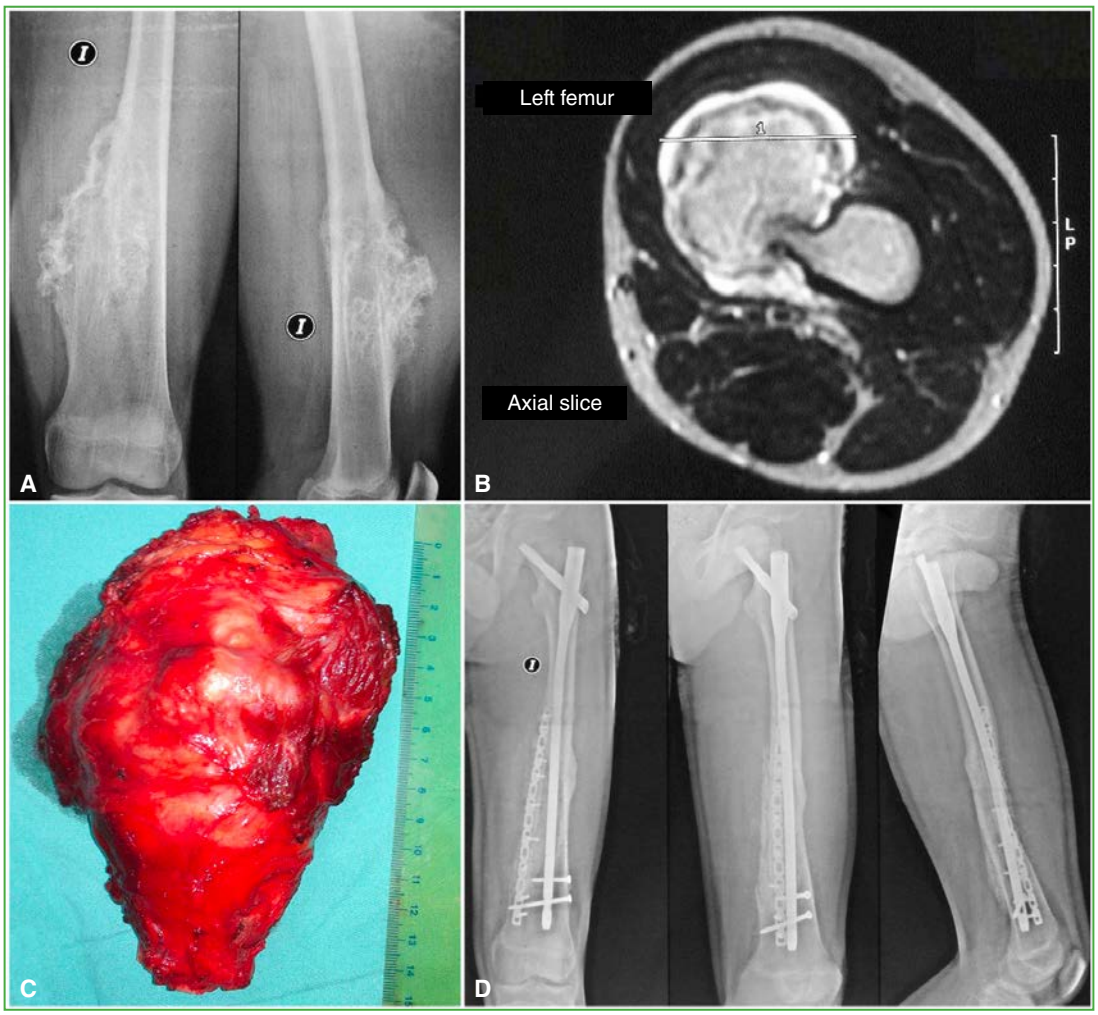

Figure 4. Case 1. Large osteochondroma of the left femur (209.8 cm^3). **A.** Preoperative radiographs of the distal femur in anteroposterior and lateral views. **B.** Preoperative MRI of the same anatomical region, axial plane. **C.** Surgical specimen. **D.** Radiographs of the entire femur, including the hip and knee, in anteroposterior, lateral, and oblique views at 6 months postoperatively, after partial femoral resection including the tumor mass, followed by reconstruction with autologous fibular and iliac crest grafts, addition of bone substitutes, and osteosynthesis with a locked solid titanium intramedullary nail (proximal and distal locking), along with locking plates for the fibular graft.

Considering both early and late complications together, for extremity osteochondromas (n = 19), no statistically significant differences were found between upper and lower extremities (p = 0.53).

One recurrence occurred after incomplete resection, and the patient received expectant management (case 18).

Two patients had residual sequelae: one with limited active shoulder abduction (case of proximal humeral pseudarthrosis), and another with mild right thoracic scoliosis (12°), secondary to ablation; neither required further treatment.

DISCUSSION

The surgical indications for excision of osteochondromas in the immature skeleton are well established in the literature.[7] Tumor volume alone does not justify surgical resection; however, an increase in size after completion of skeletal growth has been associated with a higher risk of malignant transformation, although this relationship has not been clearly defined.[7]

We did not identify published case series of large osteochondromas treated surgically similar to this cohort, nor reliable methods for volumetric measurement on imaging studies. Therefore, preoperative tumor volume (CT, MRI) was estimated by approximating tumor morphology to the closest geometric shape.

Large osteochondromas of the extremities usually produce symptoms depending on their location; however, four patients in our series were referred while asymptomatic after incidental detection of a mass. In contrast, spinal osteochondromas are typically exophytic lesions arising from the posterior elements (Case 9, Table 2; Figure 5) and extending outside the spinal canal. They usually present as a palpable mass and rarely cause symptoms or neurological compromise.[8] In some cases, they may lead to secondary deformity.[9] However, growth toward the spinal canal, regardless of size, may result in severe neurological deficits, particularly in the cervical and thoracic regions.[10]

Biopsy is generally not required in cases of typical osteochondromas. In three patients in our series, biopsy was performed due to suspicion of malignant transformation based on rapid growth, although cartilage cap thickness and morphology remained within benign parameters.

Although spontaneous regression of osteochondromas has been described in children,[11] complete excision with free margins remains the treatment of choice.

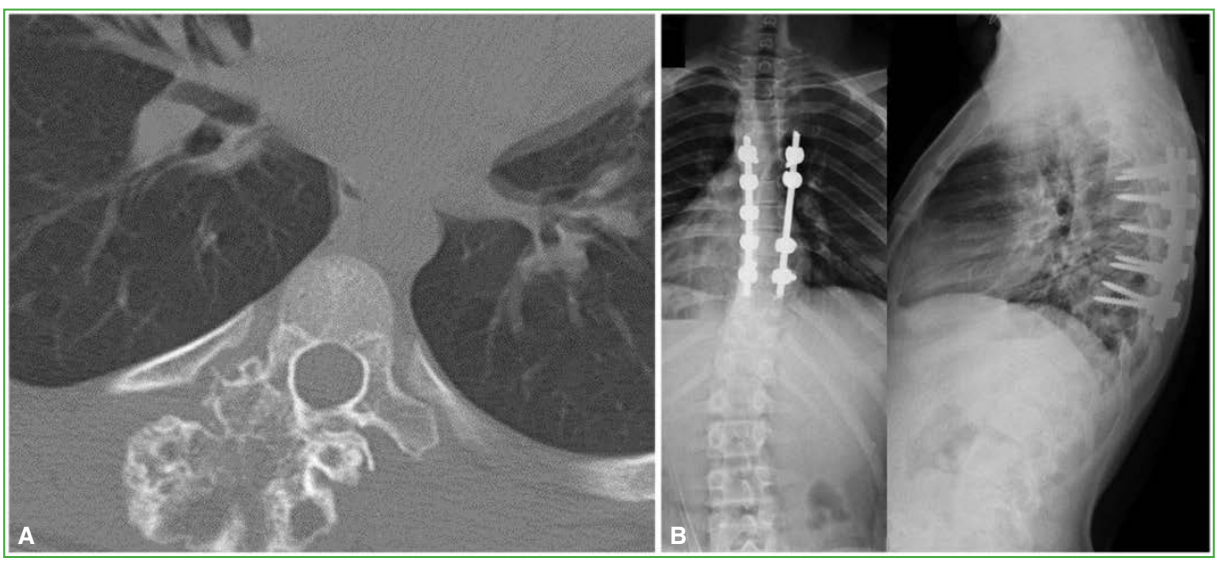

Figure 5. Case 9. **A.** Computed tomography of the thoracic spine, axial plane, showing a large extracanal osteochondroma (103 cm³) at T6. **B.** Anteroposterior and lateral radiographs of the thoracic spine at 1 year and 5 months postoperatively, following intralesional resection and arthrodesis with pedicle instrumentation. Note the absence of tumor recurrence.

In large or rapidly growing tumors, the main concern, although uncommon, is malignant transformation into chondrosarcoma; osteosarcoma and other neoplasms have also been reported.[12,13] The risk of malignant transformation to chondrosarcoma is estimated to be <1% in solitary osteochondromas and 2–5% in multiple osteochondromatosis.[14,15] Four patients in our series had multiple osteochondromatosis. Although malignant transformation is more common in adults, pediatric cases have been reported;[13] secondary chondrosarcomas account for more than half of cases in children and adolescents.[15]

In addition to tumor growth and multiplicity, the literature consistently highlights an increased risk of malignant transformation in lesions located in the spine and in the girdles (shoulder and pelvic), as well as in recurrent tumors.[15]

The differential diagnosis between osteochondroma and low-grade chondrosarcoma is based on clinical presentation (pain and progressive enlargement suggest malignancy) and imaging findings: size >5 cm, irregular margins, cortical disruption, soft tissue invasion, and cartilage cap thickness >2–3 cm should raise suspicion of malignant transformation.[3,16] We consider MRI an essential imaging modality for this evaluation.

Rapid tumor growth and a large mass in skeletally immature patients support surgical excision, even in the absence of symptoms. When malignant transformation is suspected, wide resection should be performed.[17,18] Image-guided percutaneous biopsy may not be representative in large tumors, as it may miss areas of histological atypia.[19] Furthermore, the differential diagnosis with low-grade chondrosarcoma is often challenging, which reinforces the indication for wide surgical resection.[16]

Most cases in this series were symptomatic or showed rapid growth, justifying surgical treatment. Four asymptomatic patients underwent surgery due to tumor volume and family concern.

There is no consensus on classifying osteochondromas of the extremities as active or aggressive according to the Enneking system; however, wide resection is generally accepted for aggressive lesions and marginal resection for active ones,[20] and marginal resection is adequate for most osteochondromas.[7] Wide resections may require reconstruction and tailored osteosynthesis (cases 1, 2, 3, and 4, Table 2).

In this cohort, the decision to perform wide resection was based on the following principles: (1) in very large osteochondromas, limited resection may fail to include occult atypical areas;[18] (2) as all tumors were sessile, margins were established through healthy tissue to reduce the risk of recurrence; and (3) when the tumor base involves a large portion of the bone circumference, excision may result in postoperative structural weakness or spinal instability (cases 1, 2, 3, 4, and 9; Figures 3, 4, and 5). Therefore, associated osteosynthesis with reconstruction or arthrodesis is essential in these cases.

In general, long-term functional outcomes are excellent for osteochondromas around the knee treated with marginal resection alone (cases 5, 6, and 13).[21] However, resection of osteochondromas located at the proximal fibula carries a risk of injury to the common fibular nerve (Figure 6).[22] One patient in our series developed a transient deficit following wide resection (case 14).

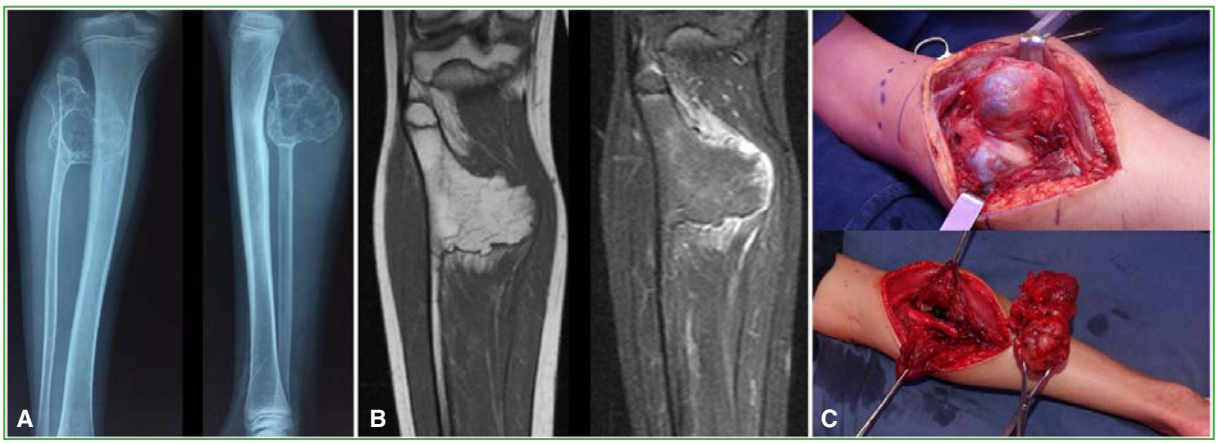

Figure 6. Case 6. **A.** Anteroposterior and lateral radiographs of the left leg showing a large proximal fibular osteochondroma (135.12 cm³). **B.** MRI of the same anatomical region, sagittal T1- and T2-weighted sequences. **C.** Intraoperative images.

We found no reports describing recurrence or prolonged postoperative pain in proximal humeral osteochondromas. However, one patient in our series developed proximal humeral pseudarthrosis following a postoperative fracture, despite osteosynthesis and reconstruction (Figure 3). In such cases, intramedullary nailing appears to be a more appropriate option (Figure 7).[5]

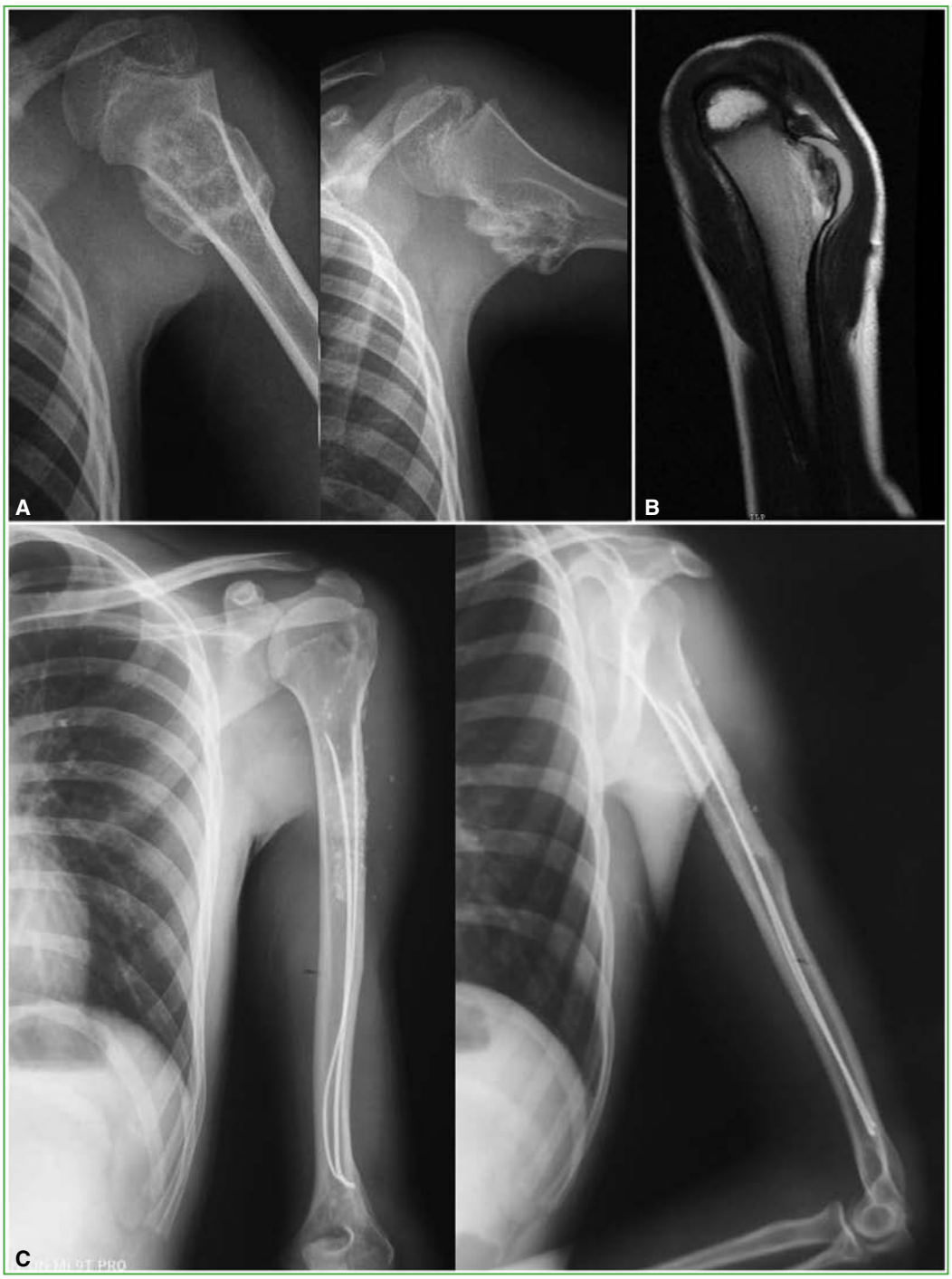

Figure 7. Case 2. **A.** Anteroposterior and lateral radiographs of the proximal humerus showing an osteochondroma (57.5 cm³). **B.** T1-weighted MRI of the shoulder in the coronal plane. Tumor dimensions and cartilage cap are visualized. **C.** Anteroposterior and lateral radiographs of the humerus more than 6 years after surgery, showing stable reconstruction.

In general, symptom resolution exceeds 90% when resection is complete in limb osteochondromas.[23]

Intracanal spinal osteochondromas frequently cause neurological deficits, even when small. In such cases, the indication for surgery depends on location rather than size.[24]

The postoperative recurrence rate is reported to be <2% after complete resection.[3] The only recurrence in our series occurred after intralesional resection (case 18; volume 46.8 cm³). The patient with a large exophytic thoracic vertebral osteochondroma (case 9; volume 103 cm³) showed no recurrence (Figure 5). Recurrence does not appear to be related to Enneking staging system stage, as it has been described even in latent lesions.[25] These findings suggest that recurrence is more closely related to intralesional resection than to tumor volume or stage.

The main limitations of this study are its retrospective design and the relatively small sample size, despite its multicenter nature. However, this cohort is highly specific, involving large osteochondromas in skeletally immature patients, and the number of cases appears sufficient for analysis. We found no comparable studies; most published data consist of case reports. The international multicenter nature of this series, including 20 patients, reflects both the rarity of large osteochondromas and current variability in diagnostic and therapeutic approaches.

CONCLUSIONS

Surgical resection of large osteochondromas of the extremities should be considered, particularly those located in the girdles (shoulder and pelvic) or in proximal regions, as well as large extracanal spinal osteochondromas, even in the absence of symptoms, given the potential for malignant transformation.

Intralesional resection of large osteochondromas should be avoided due to the risk of recurrence or residual tumor. Marginal resection is usually sufficient; however, in selected cases, wide excision may be indicated.

Conflict of interest: The authors declare no conflicts of interest.

C. A. Fernández ORCID ID: https://orcid.org/0000-0003-2350-3885
M. Salom ORCID ID: https://orcid.org/0000-0002-8626-2401
M. E. Moreiro ORCID ID: https://orcid.org/0009-0000-5590-9738
N. Amarilla ORCID ID: https://orcid.org/0009-0009-9432-7605
C. Silveri ORCID ID: https://orcid.org/0000-0002-2607-7749
P. Stoppiello ORCID ID: https://orcid.org/0000-0003-2085-6968
G. Bianchi ORCID ID: https://orcid.org/0000-0001-8222-4435
N. Casales ORCID ID: https://orcid.org/0000-0003-0318-8654
L. Gaiero ORCID ID: https://orcid.org/0000-0002-1182-1627
P. Amador ORCID ID: https://orcid.org/0009-0001-2888-7569
S. Fiscina ORCID ID: https://orcid.org/0000-0003-2655-4063
S. Innocenti ORCID ID: https://orcid.org/0000-0001-5650-1056

REFERENCES

1. Hakim DN, Pelly T, Kulendran M, Caris JA. Benign tumors of the bone: A review. *J Bone Oncol* 2015;4(2):37-41. https://doi.org/10.1016/j.jbo.2015.02.001
2. Collier CD, Nelson GB, Conry KT, Kosmas C, Getty PJ, Liu RW. The natural history of benign bone tumors of the extremities in asymptomatic children: a longitudinal radiographic study. *J Bone Joint Surg Am* 2021;103(7):575-80. https://doi.org/10.2106/JBJS.20.00999
3. Tepelenis K, Papathanakos G, Kitsouli A, Troupis T, Barbouti A, Vlachos K, et al. Osteochondromas: An updated review of epidemiology, pathogenesis, clinical presentation, radiological features and treatment options. *In vivo* 2021;35(2):681-91. https://doi.org/10.21873/invivo.12308
4. Taheriazam A, Saeidinia A. One-stage surgical excision of a huge bilateral multiple osteochondroma of the hip: a case report. *Electron Physician* 2017;9(9):5310-17. https://doi.org/10.19082/5310
5. Allagui M, Amara K, Aloui I, Hamdi MF, Koubaa M, Abid A. Historical giant near-circumferential osteochondroma of the proximal humerus. *J Shoulder Elbow Surg* 2019;19(6):e12-e15. https://doi.org/10.1016/j.jse.2010.04.004
6. Matthewson G, Singh M, Thompson S. Large osteochondroma of the scapula in a 2-year-old. *J Pediatr Surg Case Rep* 2019;42:12-6. https://doi.org/10.1016/j.epsc.2018.12.010

7. Unni KK, Inwards CY. Osteochondroma (osteocartilaginous exostosis). In: Unni K, Carrie Y (ed). *Dahlin's bone tumors: General aspects and data on 10,165 cases*. 6th ed. Philadelphia: Mayo Foundation for Medical Education and Research. Lippincott Williams & Wilkins; 2010, p. 9-21.
8. Sharma C, Acharya M, Kumawat BL, Parekh J. Giant spinal exostosis. *BMJ Case Rep* 2014:2014:bcr2014203819. https://doi.org/10.1136/bcr-2014-203819
9. Fiechtl JF, Masonis JL, Frick SL. Spinal osteochondroma presenting as atypical spinal curvature: a case report. *Spine (Phila Pa 1976)* 2003;28(13):E252-5. https://doi.org/10.1097/00007632-200307010-00026
10. Assan BR, Simon AL, Violas P, Sales de Gauzy J, Thepaut M, Ould-Slimane M, et al. Surgical outcomes of spinal osteochondroma in children: A multicentre observational study. *Orthop Traumatol Surg Res* 2022;108(6):103239. https://doi.org/10.1016/j.otsr.2022.103239
11. Valdivielso-Ortiz A, Barber I, Soldado F, Aguirre-Canyadell M, Enriquez G. Solitary osteochondroma: spontaneous regression. *Pediatr Radiol* 2010;40(10):1699-1701. https://doi.org/10.1007/s00247-010-1783-7
12. Park YK. Multiple osteochondromatosis. In: Santini-Araujo E, Kalil RK, Bertoni F, Park Y-K (eds.). *Tumors and tumor-like lesions of bone: For surgical pathologists, orthopedic surgeons and radiologists*. London: Springer-Verlag; 2015, p. 273-6.
13. Bukara E, Buteera AM, Karakire R, Manirakiza F, Muhumuza S, Rudakemwa E, et al. Osteoblastic osteosarcoma arising beneath an osteochondroma in an 11-year-old male with multiple hereditary exostoses. *Case Rep Orthop* 2018:2018:8280415. https://doi.org/10.1155/2018/8280415
14. Sonne-Holm E, Wong C, Sonne-Holm S. Multiple cartilaginous exostoses and development of chondrosarcomas--a systematic review. *Dan Med J* 2014;61(9):A4895. PMID: 25186537
15. Puri A, Gulia A, Kurisunkal VJ, Sukuma V, Rekhi B. Chondrosarcomas in adolescents: are they different? *J Pediatr Orthop B* 2020;29(5):505-9. https://doi.org/10.1097/BPB.0000000000000641
16. Choi JH, Ro JY. The 2020 WHO classification of tumors of bone: an updated review. *Adv Anat Pathol* 2021;28(3):119-38. https://doi.org/10.1097/PAP.0000000000000293
17. Tsuda Y, Gregory JJ, Fujiwara T, Abudu S. Secondary chondrosarcoma arising from osteochondroma. *Bone Joint J* 2019;101-B(10):1313-20. https://doi.org/10.1302/0301-620X.101B9.BJJ-2019-0190.R1
18. Laitinen MK, Parry MC, Morris G, Kurisunkal V, Stevenson JD, Jeys LM. Can the cartilaginous thickness determine the risk of malignancy in pelvic cartilaginous tumors, and how accurate is the preoperative biopsy of these tumors? *Clin Orthop Relat Res* 2022;482:1006-16. https://doi.org/10.1097/CORR.0000000000003065
19. Majd N, Theriault RV, Darrow MA, Thorpe SW, Chen DC. Osteochondroma-like parosteal osteosarcoma: A case highlighting diagnostic challenge and surgical advances. *Radiol Case Rep* 2024;19:4091-9. https://doi.org/10.1016/j.radcr.2024.06.045
20. Drumond JMN. Efficacy of the Enneking staging system in relation to treating benign bone tumors and tumor-like bone lesions. *Rev Bras Ortop* 2010;45(1):46-52. https://doi.org/10.1016/S2255-4971(15)30216-0
21. Wu M, Zheng ET, Anderson ME, Miller PE, Spencer SA, Heyworth BE. Surgical treatment of solitary periarticular osteochondromas about the knee in pediatric and adolescent patients: Complications and functional outcomes. *J Bone Joint Surg Am* 2021;103(14):1276-83. https://doi.org/10.2106/JBJS.20.00998
22. Birch CM, Smit KM, Sucato DJ. Peroneal nerve function before and following surgical excision of a proximal fibular osteochondroma. *J Pediatr Orthop* 2021;41(1):61-6. https://doi.org/10.1097/BPO.0000000000001688
23. Bottner F, Rodl R, Kordish I, Winkelmann W, Gosheger G, Lindner N. Surgical treatment of symptomatic osteochondroma: a three-to eight-year follow-up study. *J Bone Joint Surg Br* 2003;85(8):1161-5. https://doi.org/10.1302/0301-620x.85b8.14059
24. Gille O, Pointillart V, Vital JM. Course of spinal solitary osteochondromas. *Spine (Phila Pa 1976)* 2005;30(1):E13-9. PMID: 15626967
25. Sciubba DM, Macki M, Bydon M, Germscheid NM, Wolinsky J-P, Boriani S, et al. Long-term outcomes in primary spinal osteochondroma: a multicenter study of 27 patients. *J Neurosurg Spine* 2015;22(6):582-8. https://doi.org/10.3171/2014.10.SPINE14501

Custom Reverse Shoulder Arthroplasty for Severe Postoperative Glenoid Bone Defects: A Retrospective Case Series

Diego J. Gómez, Nadia Gabotto Loredo, Gonzalo M. Viollaz, Gustavo Teruya, Álvaro Muratore, Alejandro Tedeschi, Lucio Gutiérrez, Rafael Durán, Santiago Ávila Posada, Daniel Moya
Upper Limb Team, Hospital Británico de Buenos Aires, Autonomous City of Buenos Aires, Argentina

ABSTRACT

Introduction: Glenoid bone loss complicates revision reverse shoulder arthroplasty. Patient-specific 3D-printed glenoid implants allow accurate reconstruction of severe defects. **Objective:** To evaluate the clinical and radiographic outcomes of customized glenoid baseplates in revision reverse shoulder arthroplasty with severe glenoid defects, and to record intraoperative and postoperative complications. **Materials and Methods:** A retrospective series of eight consecutive patients (June 2022–May 2023) with Gohlke type ≥3 defects who underwent revision reverse shoulder arthroplasty with 3D-planned titanium glenoid baseplates based on computed tomography. Range of motion, function, pain, surgical time, and radiographic integration were analyzed, with a 12-month follow-up. **Results:** Range of motion improved significantly: forward elevation increased by 78.8° ($p < 0.001$), external rotation by 7.5° ($p = 0.019$), and internal rotation improved from the gluteal level (trochanter–L5) to a mean of T12 (range: T7–gluteal level). Pain decreased by 6.4 points ($p < 0.001$). The Constant-Murley score increased by 48.9 points ($p < 0.001$). Complete osseointegration was observed in 7 cases; the remaining case showed radiolucent lines without loosening. No major complications were recorded. **Conclusions:** In revision reverse shoulder arthroplasty with severe glenoid bone defects, 3D-printed glenoid baseplates restore anatomy, significantly improve function, and reduce pain at one year, with a high rate of integration and low morbidity.
Keywords: Reverse shoulder arthroplasty; glenoid bone defects; patient-specific implants; 3D printing; revision surgery.
Level of Evidence: IV

Artroplastia inversa de hombro personalizada para defectos óseos glenoideos severos posoperatorios. Estudio retrospectivo de casos clínicos

RESUMEN

Introducción: La pérdida ósea glenoidea complica las revisiones de una artroplastia inversa de hombro. Los implantes glenoideos personalizados impresos en 3D permiten reconstruir, con precisión, defectos severos. **Objetivos:** Evaluar los resultados clínicos y radiográficos de las metaglenas personalizadas en revisiones de artroplastias inversas de hombro con defectos glenoideos severos, así como registrar las complicaciones intra y posoperatorias. **Materiales y Métodos:** Serie retrospectiva de 8 pacientes consecutivos (junio 2022-mayo 2023) con defectos tipo Gohlke ≥3 sometidos a una artroplastia inversa de hombro de revisión con metaglenas de titanio planificadas en 3D sobre una tomografía. Se analizaron la movilidad y la función, el dolor, el tiempo quirúrgico y la integración radiográfica; seguimiento de 12 meses. **Resultados:** Los rangos de movilidad se incrementaron: la elevación anterior aumentó 78,8° ($p < 0,001$); la rotación externa, 7,5° ($p = 0,019$); la rotación interna, desde el nivel glúteo (trocánter-L5) a un promedio de T12 (rango T7-nivel glúteo). El dolor disminuyó 6,4 puntos ($p < 0,001$). La escala de Constant-Murley aumentó 48,9 puntos ($p < 0,001$). Se constató la integración ósea completa en 7 casos; el restante tenía líneas radiolúcidas sin aflojamiento. No se registraron complicaciones mayores. **Conclusiones:** En las revisiones de artroplastias inversas de hombro con defectos glenoideos severos, las metaglenas impresas en 3D restauran la anatomía, mejoran significativamente la función y reducen el dolor al primer año, con una alta tasa de integración y baja morbilidad.
Palabras clave: Artroplastia inversa de hombro; defectos óseos glenoideos; implantes personalizados; impresión 3D; revisión quirúrgica.
Nivel de Evidencia: IV

Received on July 22nd, 2025. Accepted after evaluation on October 20th, 2025 • Dr. NADIA GABOTTO LOREDO • Loredogabottonadia@gmail.com https://orcid.org/0009-0001-8122-0237
How to cite this article: Gómez DJ, Gabotto Loredo N, Viollaz GM, Teruya G, Muratore Á, Tedeschi A, et al. Custom Reverse Shoulder Arthroplasty for Severe Postoperative Glenoid Bone Defects: A Retrospective Case Series. *Rev Asoc Argent Ortop Traumatol* 2026;91(2):103-117. https://doi.org/10.15417/issn.1852-7434.2026.91.2.2199

INTRODUCTION

In recent decades, reverse shoulder arthroplasty has emerged as an effective treatment option for rotator cuff tear arthropathy. Due to its favorable outcomes, its indications have expanded to include four-part proximal humeral fractures in elderly patients, massive irreparable rotator cuff tears without arthropathy, and revision of failed osteosynthesis and hemiarthroplasties.[1-3]

Loss of glenoid bone stock is a common and challenging problem when performing reverse shoulder arthroplasty.[4,5] Glenoid bone defects are more frequently found in revision procedures, due to prosthetic loosening (septic or aseptic), periprosthetic glenoid fractures, and traumatic defects secondary to migration or protrusion of implants used for proximal humeral fractures.[6-8]

Various complex techniques have been described to address glenoid bone loss, including one- or two-stage revision procedures using iliac crest or humeral head bone grafts, the use of metal-augmented baseplates, Mark Frankle's alternative centerline technique, and even salvage hemiarthroplasty.[4,5] More recently, patient-specific implants manufactured using 3D printing based on precise preoperative digital planning have been introduced, which adapt to each patient's specific anatomical defects. This technology provides a better management of complex glenoid bone defects by optimizing surgical accuracy and primary implant stability.[5–11]

Given the novelty of this technology and the limited available evidence, we have not yet determined which technique provides the best outcomes.

The aim of this study was to evaluate the clinical and radiological outcomes at one year of follow-up in patients undergoing revision reverse shoulder arthroplasty for severe postoperative glenoid bone defects using patient-specific glenoid components, as well as to record intraoperative and postoperative complications.

MATERIALS AND METHODS

A retrospective analysis was conducted of a consecutive series of patients with severe glenoid bone defects associated with prior surgery, treated with reverse shoulder arthroplasty using patient-specific glenoid implants, between June 2022 and May 2023. Adults with severe postoperative glenoid bone defects (≥3 according to the Gohlke classification) and a minimum clinical and radiographic follow-up of one year were included. Patients undergoing primary arthroplasty, those with a history of shoulder infection, and those with neurological deficits in the affected limb were excluded.

Glenoid defects were classified according to the Gohlke classification.[12]

- Type 1: mild bone loss, central or eccentric, with retroversion <15°.
- Type 2: moderate contained bone loss, with an intact glenoid vault.
- Type 3: severe eccentric defect with retroversion >20° or significant loss of glenoid width.
- Type 4: moderate medialization of the glenoid surface.
- Type 5: defect with residual depth <10 mm for implant fixation.

All patients underwent a preoperative protocol that included true anteroposterior and axial radiographs of the affected shoulder, thin-slice computed tomography (CT) with 3D reconstruction, and laboratory tests including erythrocyte sedimentation rate and C-reactive protein.

In the postoperative period, clinical and radiographic evaluations were performed immediately after surgery, at 1 month, 6 months, 1 year, and at the final follow-up. Operative time (in minutes) was recorded based on surgical reports, and intraoperative and postoperative complications were documented during scheduled follow-up visits.

The treating surgeon assessed shoulder range of motion preoperatively and at follow-up visits. Evaluation parameters included active motion, measured as forward elevation in the scapular plane, external rotation with the elbow at the side, and internal rotation estimated according to the highest vertebral level reached by the thumb. In addition, pain was assessed using the visual analog scale, and function was evaluated using the Constant–Murley score.

Statistical Analysis

Categorical variables are expressed as frequencies and percentages, and continuous variables as mean and standard deviation or median and interquartile range, depending on their distribution. Normality of differences between pre- and postoperative values was assessed using the Shapiro–Wilk test. When normality was confirmed, the paired Student's t-test was used; otherwise, the nonparametric Wilcoxon signed-rank test was applied. A p value <0.05 was considered statistically significant. All analyses were performed using GraphPad Prism 9.0 (La Jolla, CA, USA).

Custom Implant Design

Preoperative computed tomography (CT) scans were used for implant design and manufacturing. Preoperative planning was performed using 3D Slicer (version 5.6.2) and Meshmixer (version 3.5.474, Autodesk Inc., San Rafael, CA, USA). This allowed detailed evaluation of the bone defect and creation of a 3D biomodel of the patient's scapula (Figure 1).

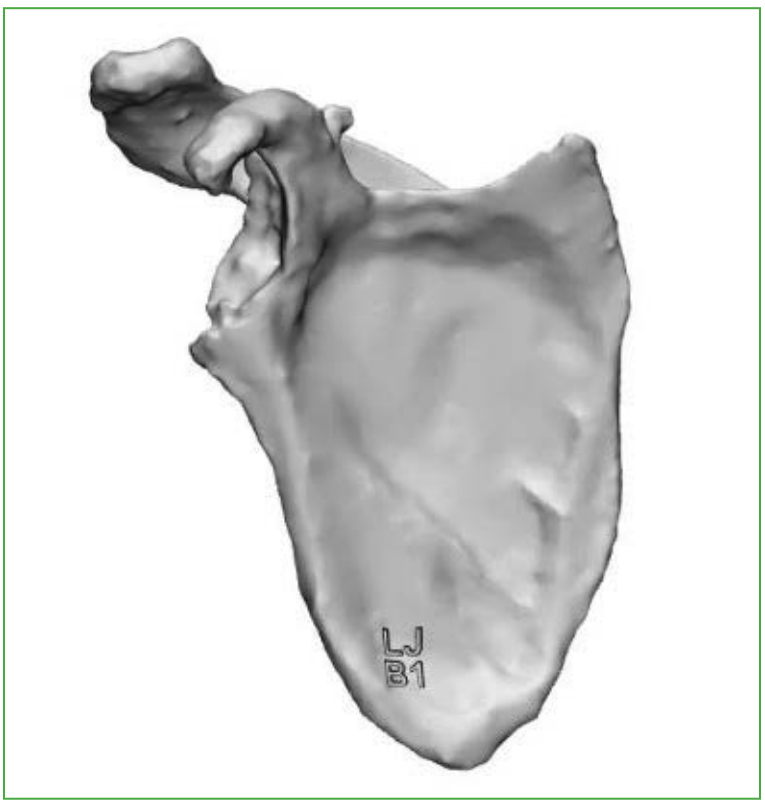

Figure 1. Use of 3D computed tomography for preoperative planning.

The patient-specific glenoid baseplate was designed in collaboration with a biomedical engineer, developing a component precisely adapted to the patient's bone defect, with the aim of reproducing the glenoid lateralization, inclination, and version specified by the surgeon (Figure 2).

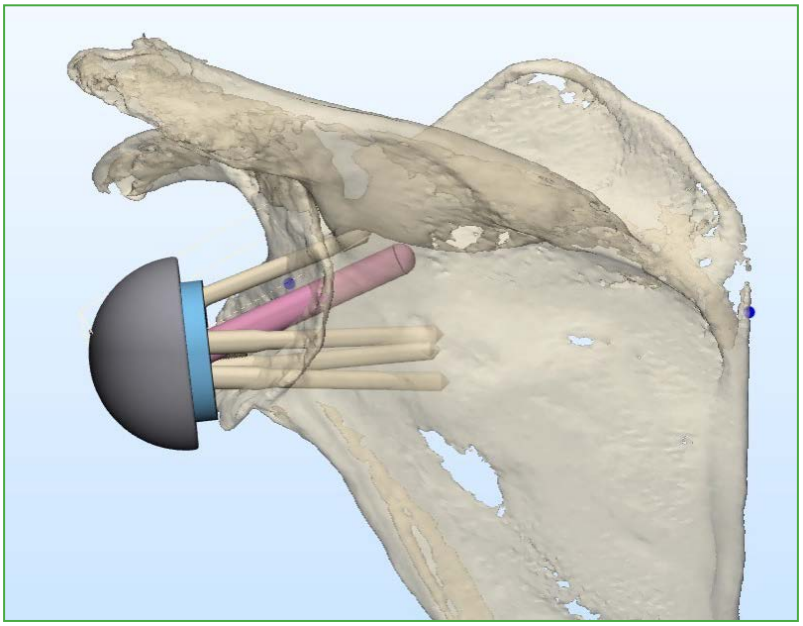

Figure 2. Design of the glenoid baseplate adapted to the patient's bone defect.

When the bone defect was so severe that premorbid lateralization could not be reliably estimated, superimposition was performed using a CT scan obtained prior to the initial surgery (if available) or, alternatively, from the contralateral shoulder (Figure 3).

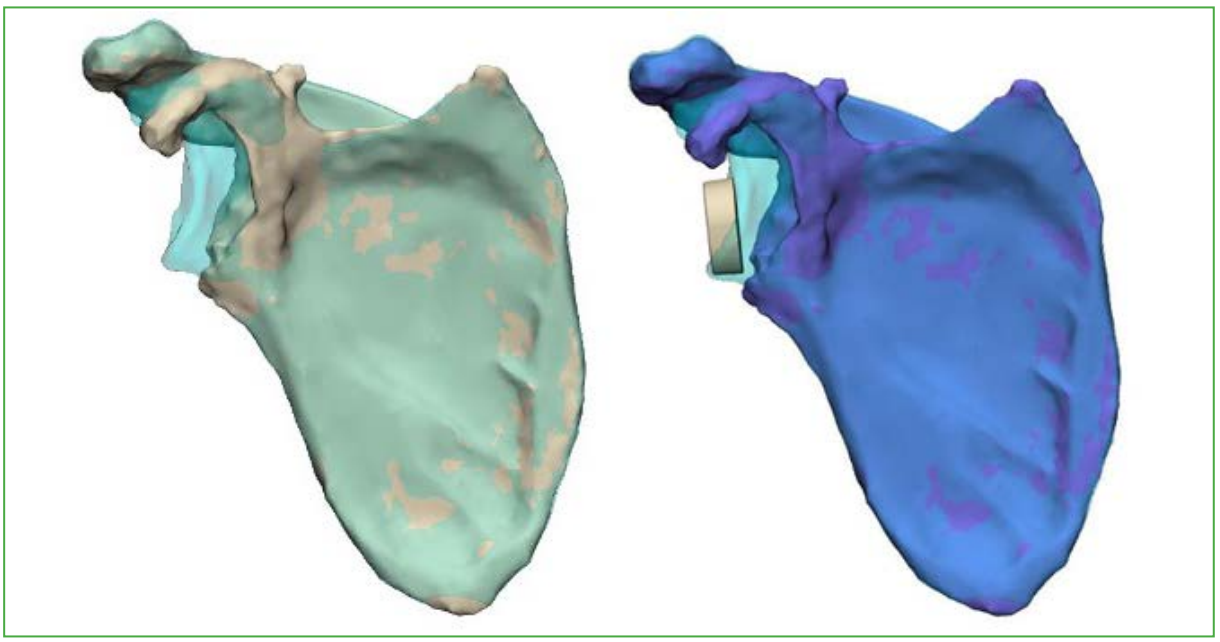

Figure 3. Use of preoperative CT scans and superimposition to calculate lateralization values.

The direction and length of the screws were subsequently planned according to each patient's bone quality and bone stock. The goal, whenever possible, was to achieve at least 1 cm of contact between the central peg and native bone, along with the placement of at least two screws measuring 4.5 mm in diameter and 30 mm in length (Figure 4).

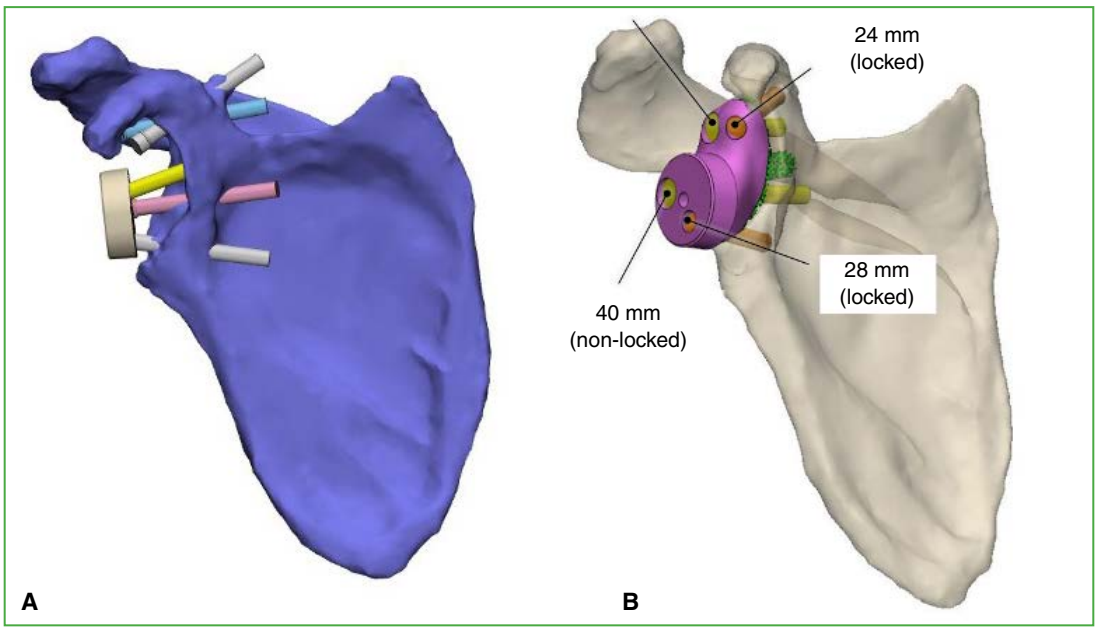

Figure 4. Planning of screw orientation (A) and measurement (B) for the glenoid baseplate.

The custom baseplate was designed to be Morse taper-compatible with a 36-mm Unique® glenosphere (Bioprotece, Villa Ballester, Buenos Aires, Argentina).

Once the implant was designed, patient-specific surgical guides were developed, and the implant was manufactured using 3D printing in titanium (Figures 5 and 6).

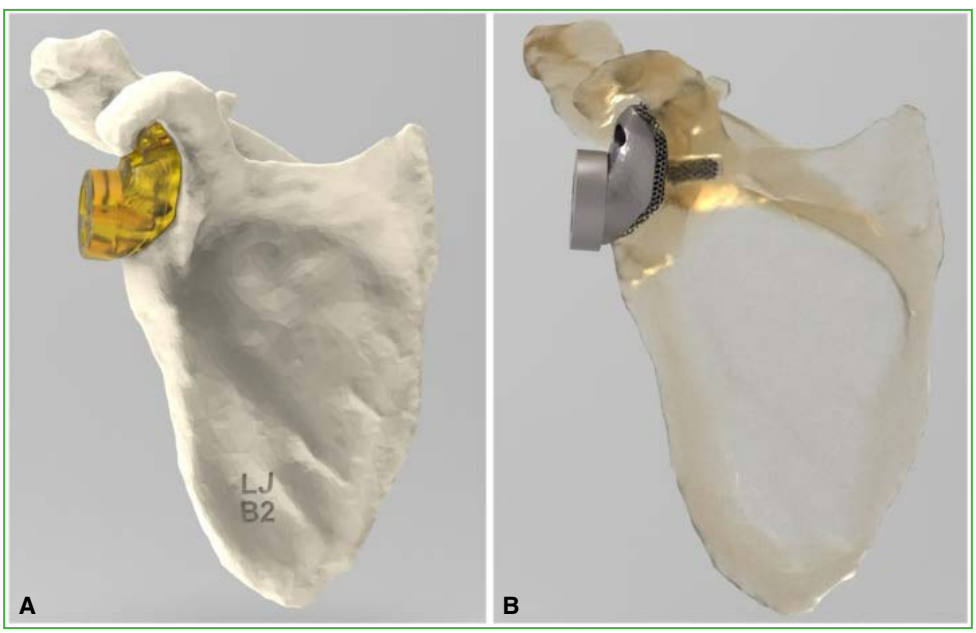

Figure 5. A. Patient-specific glenoid baseplate model in plastic. **B**. Titanium glenoid baseplate model adapted to the glenoid defect.

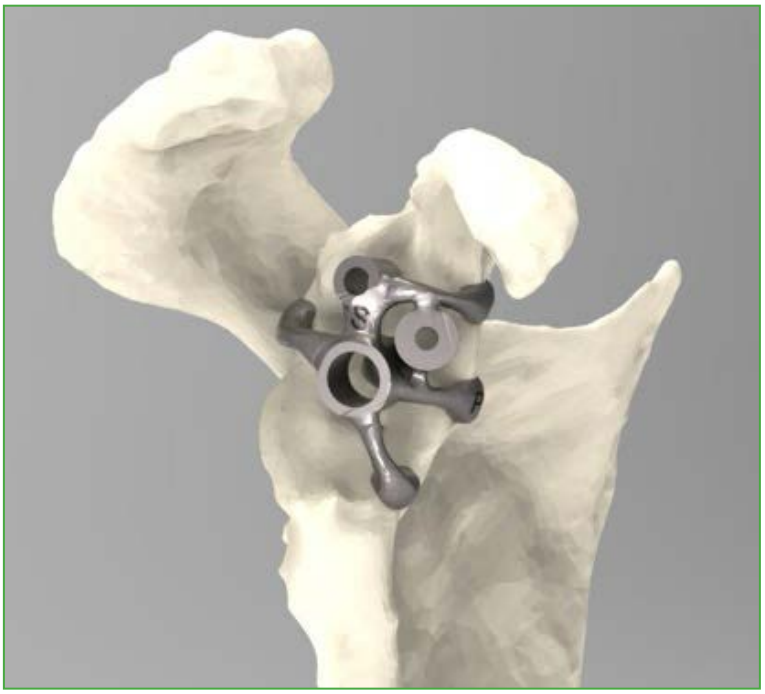

Figure 6. Patient-specific surgical guides tailored to the defect.

The guides were designed with four points of support on peripheral glenoid landmarks, considering retractor placement, to allow precise positioning of the central guide pin or drill.

Prior to final manufacturing, full scapular biomodels and full-scale plastic prototypes of the baseplates were produced (Figure 7). This enabled the surgeon to become familiar with the intraoperative scenario and, if satisfactory, approve the final design.

The definitive patient-specific baseplate was manufactured using 3D printing technology in ELI grade 5 trabecular titanium, with a trabecular metal interface of 0.4 mm thickness, 70% porosity, and an additional sandblasted surface treatment to enhance osseointegration (Figures 8 and 9).

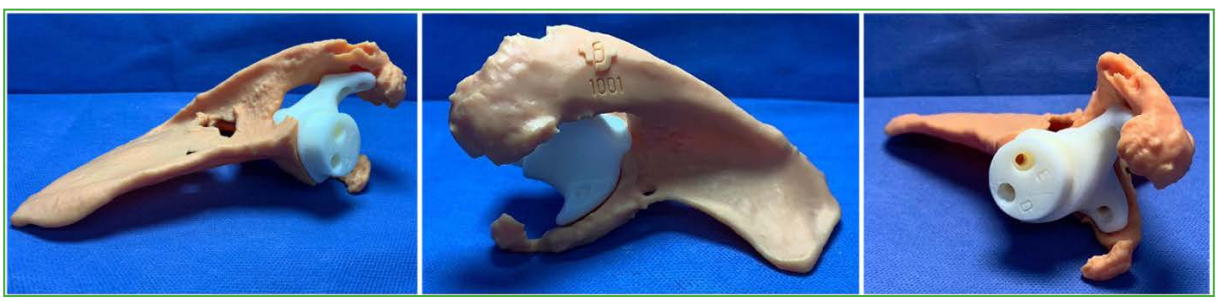

Figure 7. Biomodels of the entire scapula and full-scale plastic prototypes of the glenoid baseplates.

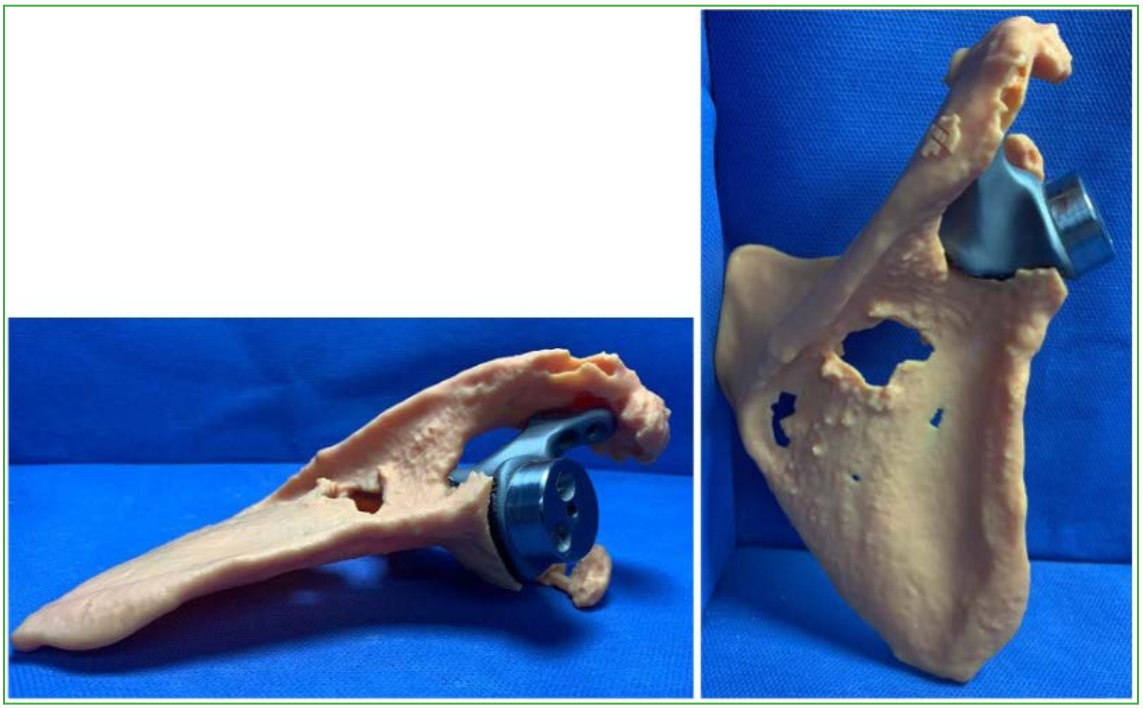

Figure 8. Patient-specific glenoid baseplate made of trabecular titanium.

Figure 9. Glenosphere coupled to the patient-specific glenoid baseplate.

Surgical Technique

Patients underwent surgery in the beach-chair position under sedation and regional anesthesia of the affected limb. A deltopectoral approach was used in all cases. After release of adhesions and resection of fibrotic tissue, osteosynthesis hardware or prosthetic components were removed as appropriate.

Following circumferential release of the glenoid, bony landmarks were identified for placement of the 3D-printed titanium guide, which was used as a template to guide drilling for the central peg (Figure 10).

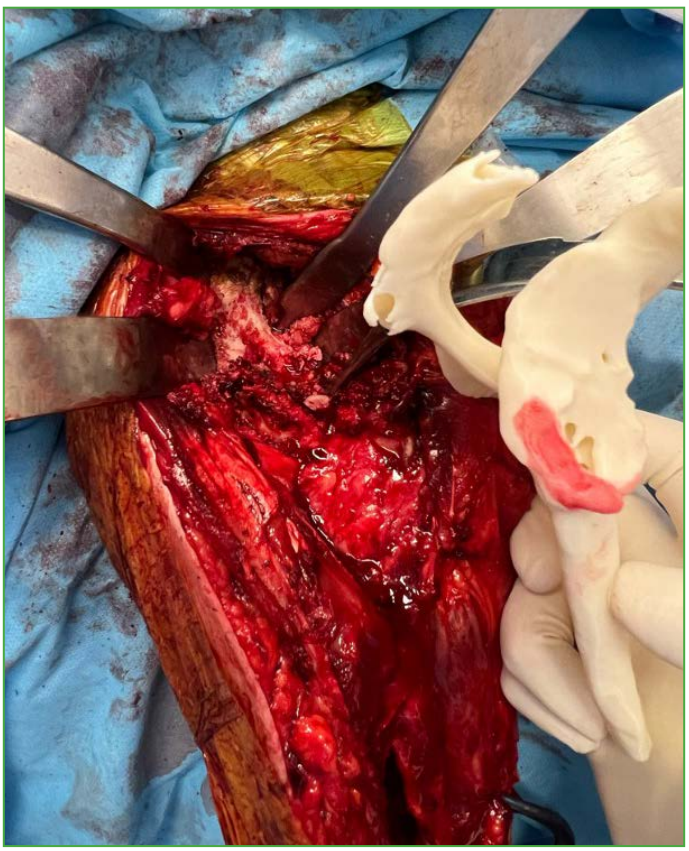

Figure 10. Glenoid defect and bony landmarks for positioning the 3D guide.

A full-scale plastic prototype of the baseplate was used to verify fit, followed by implantation of the definitive patient-specific component (Figures 11 and 12).

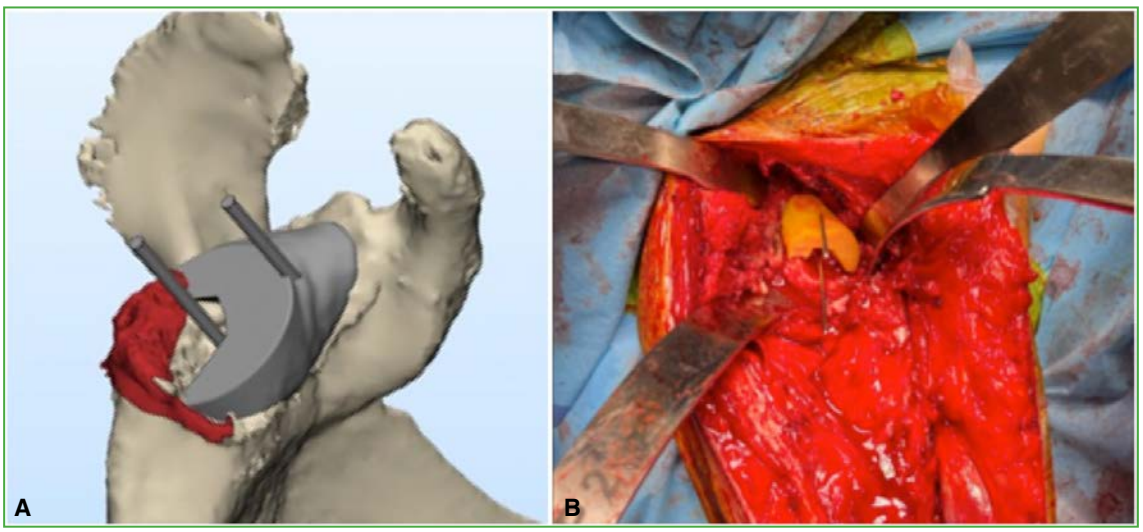

Figure 11. A. Planning of central pin placement. **B.** Placement of the central post pin and reaming stop guide using the plastic glenoid baseplate prototype.

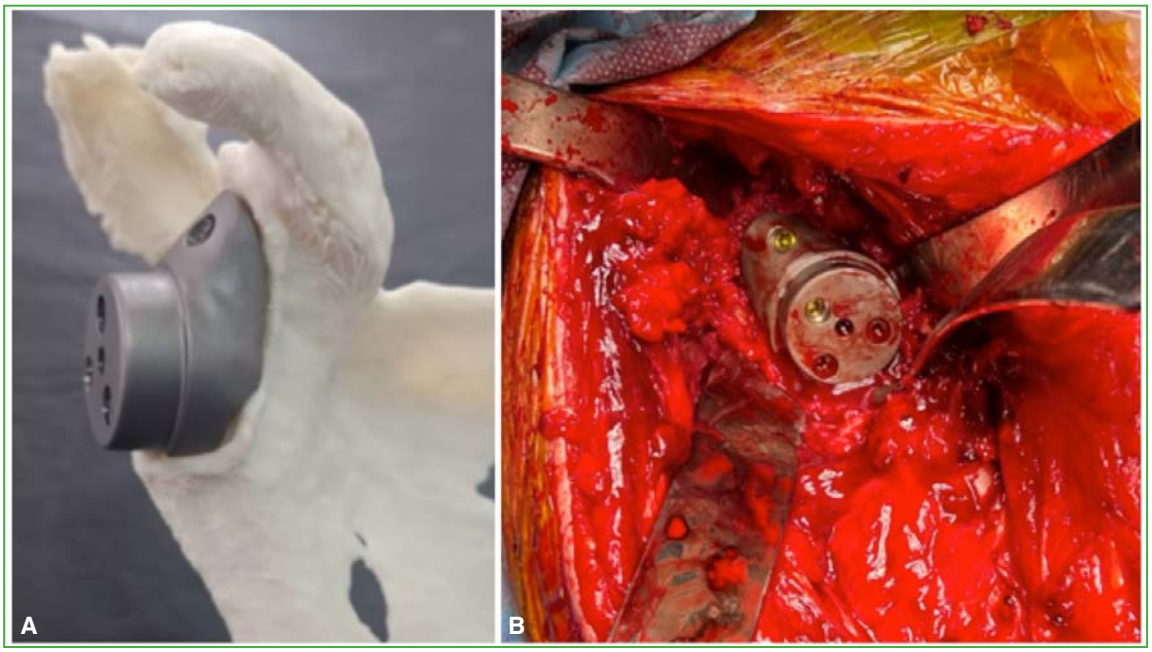

Figure 12. **A.** Final patient-specific implant in a plastic model. **B.** Final patient-specific implant in vivo.

The humeral component was addressed as required (either as a primary implantation, revision procedure, or retention of the existing implant) depending on the case.

All patients followed the same postoperative protocol: immobilization in a sling for the first 6 weeks, combined with gentle passive range-of-motion exercises. From week 6 onward, assisted active exercises were introduced to improve mobility, followed by progressive strengthening beginning at week 12. Full recovery was expected within 6 to 12 months.

RESULTS

The series comprised eight consecutive patients with a minimum follow-up of 12 months. The mean age was 67.3 years (range 38-84). Seventy-five percent were women and 25% were men. The affected shoulder was the right in six patients and the left in the remaining two (Table 1).

Table 1. Demographic data.

Variables		
Age	67.3 years (38–84 years)	
Sex	Male	Female
	6 (75%)	2 (25%)
Dominant side	Right	Left
	6 (75%)	2 (25%)

The mean operative time was 142.5 minutes (range 105-180) (Table 2).

Table 2. Operative time per patient.

Patient	Operative time (min)	Preoperative diagnosis	Number of previous surgeries	Treatment
1	145	Glenoid loosening	3	Glenoid revision
2	105	Spacer	4	Humeral + glenoid revision
3	155	Failed hemiarthroplasty	2	Humeral + glenoid revision
4	180	Failed osteosynthesis	1	Humeral + glenoid revision
5	180	Failed osteosynthesis	1	Humeral + glenoid revision
6	120	Failed hemiarthroplasty	1	Humeral + glenoid revision
7	130	Glenoid loosening	1	Glenoid revision
8	125	Failed osteosynthesis	2	Humeral + glenoid revision

The distribution of bone defects according to the Gohlke classification was as follows: type 3 (25%), type 4 (50%), and type 5 (25%).

In this series, significant improvements were observed in all analyzed variables. Forward elevation increased by a mean of 78.8° (95% confidence interval [CI] 65.0-92.5; $p < 0.001$), external rotation improved by 7.5° (95% CI 1.6-13.4; $p = 0.019$), and internal rotation improved from the gluteal level (trochanter-L5) to a mean of T12 (range T7-gluteal level). Pain, measured using the visual analog scale, decreased by 6.4 points (95% CI -7.6 to -5.2; $p < 0.001$). The Constant–Murley score increased by 48.9 points (95% CI 42.6-55.1; $p < 0.001$) (Table 3).

Table 3. Relationship between preoperative and postoperative clinical and functional parameters.

	Preoperative values (SD)	Postoperative values (SD)	p
Anterior elevation	45 ± 14.1°	123.8 ± 16.9°	<0.001
External rotation	8.8 ± 9.9°	16.2 ± 5.2°	0.019
Internal rotation	Gluteus-L5	T12 (T7-gluteus)	0.022
VAS	8.0 ± 1.3	1.6 ± 0.7	<0.001
Constant-Murley Scale	16.9 ± 4.7	65.8 ± 9.6	<0.001

VAS = visual analog scale.

Radiographic analysis showed appropriate implant integration in seven of the eight cases (Figures 13 and 14).

Figure 13. A and B. Anteroposterior and axial shoulder radiographs, one-year postoperative follow-up, showing correct implant osseointegration. **C**. Functional outcome one year after surgery.

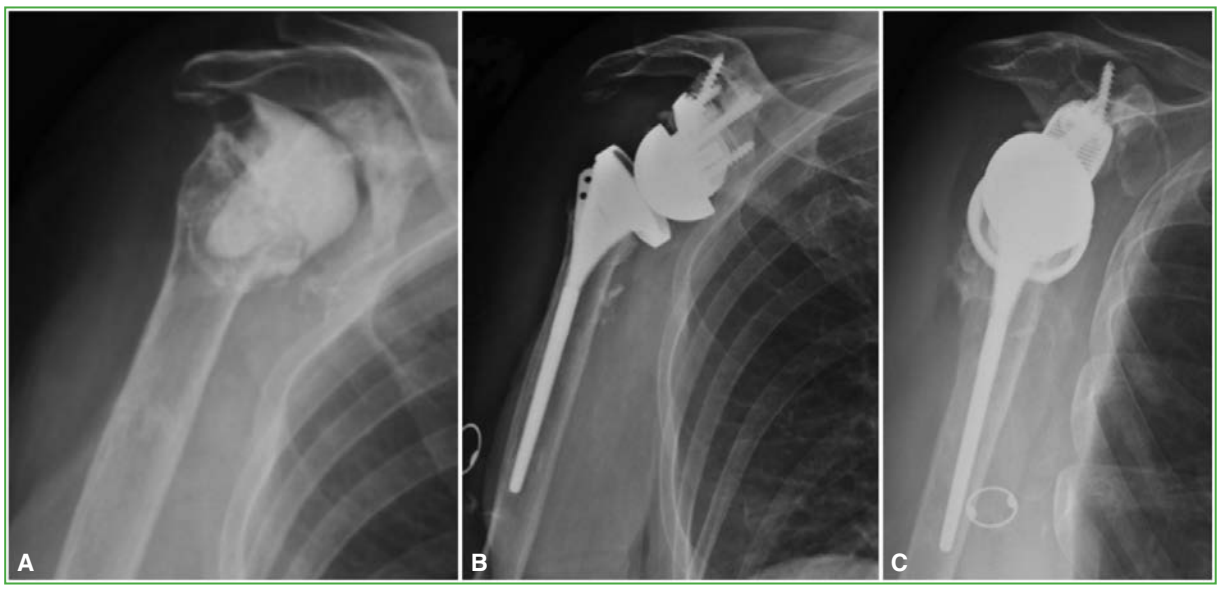

Figure 14. A. Preoperative radiograph of a patient with a severe glenoid defect. **B and C**. Anteroposterior and lateral shoulder radiographs, one-year postoperative follow-up, showing correct implant osseointegration.

In one patient with sequelae of a previously treated proximal humeral fracture with a PHILOS plate and severe glenoid erosion caused by the implant screws, loosening of the glenoid baseplate with mild migration was observed. This resulted in moderate functional limitation, although pain control remained adequate. The patient was satisfied with pain relief and declined further surgical intervention; therefore, conservative management was adopted (Figure 15).

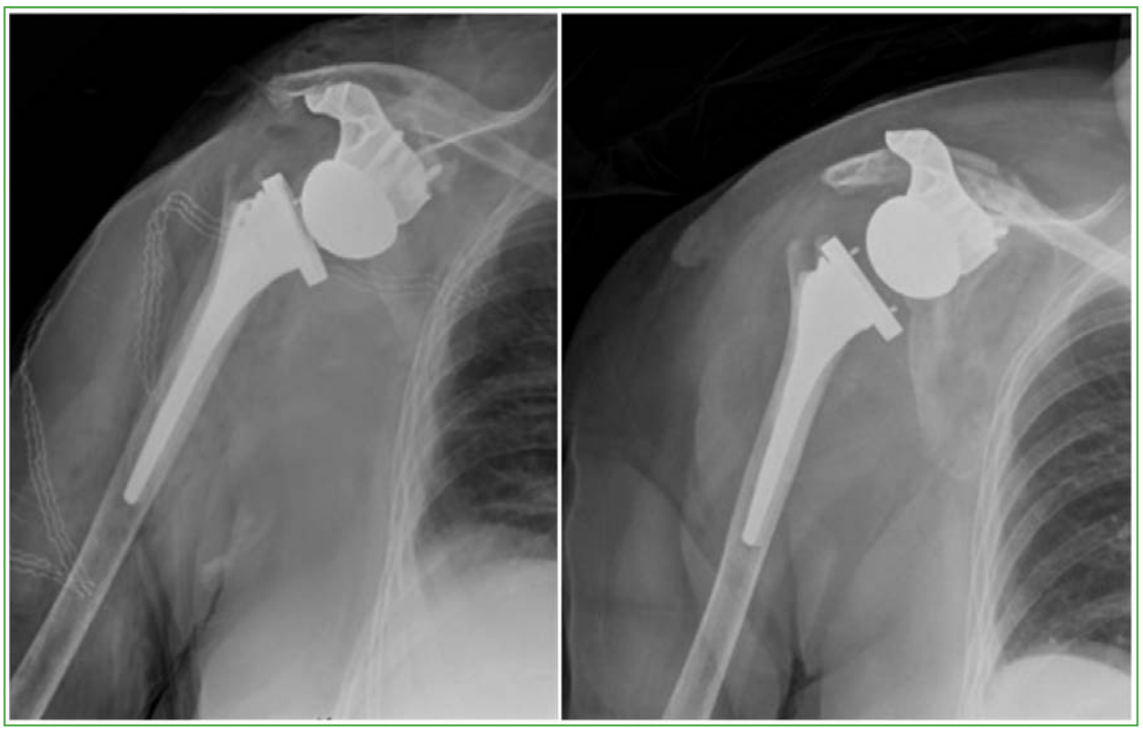

Figure 15. Radiographs of a patient with glenoid component loosening and migration, without clinical consequences.

DISCUSSION

Our results demonstrate that the use of patient-specific glenoid implants is a technically feasible option for the treatment of severe glenoid defects in revision surgery. Despite the complexity of the included cases, only one complication related to loosening of the glenoid component was observed, highlighting the stability achieved in most patients over a minimum follow-up of 12 months.

These findings are consistent with previous studies, although differences exist in patient populations and surgical indications. Chammaa et al.,[6] in a series of 37 patients, the largest reported to date, described favorable outcomes at a mean follow-up of 60 ± 25 months, with significant improvements in the Oxford Shoulder Score (from 11 to 27 points) and the Subjective Shoulder Value (from 23% to 60%). Active elevation increased from 39° ± 23° to 64° ± 38°, and external rotation from 6° ± 16° to 15° ± 17°.

However, their study focused on primary arthroplasties, whereas our series includes only revision procedures, which reinforces the relevance of our findings by demonstrating that patient-specific implants are also effective in more complex scenarios. In addition, it is important to note that the implant used in the study by Chammaa et al. was not patient-specific but rather based on a design concept similar to that of hip arthroplasty, which may limit its effectiveness compared with implants specifically designed for shoulder anatomy.

Likewise, Rangarajan et al. reported notable improvements in the Constant-Murley score (from 24.6 to 60.4) and the ASES score (from 32 to 79), as well as in range of motion, with increases in forward elevation (from 53° to 124°), abduction (from 42° to 77°), and external rotation (from 17° to 32°) in a series of 19 patients. However, that study included both primary and revision arthroplasties, resulting in a more heterogeneous cohort, which

may limit direct comparability with our findings. In the present series, patients had a mean of 1.3 prior surgeries (range 1-4), reflecting a more complex clinical scenario; nevertheless, the functional improvements observed were comparable.[11]

Bodendorfer et al. and Ortmaier et al. reported similar outcomes in terms of range of motion and function, with a minimum follow-up of 24 months, in series of 11 and 9 patients, respectively.[2,4] In the study by Bodendorfer et al., improvements were observed in forward elevation (from 95° to 150°), external rotation (from 13° to 40°), and internal rotation (from the sacrum to L3).[4] Ortmaier et al. reported improvements in the Constant-Murley score (from 10.9 to 51.7), the Subjective Shoulder Value (from 11% to 52%), and abduction (from 19° to 121°).[2] It is important to note that, in the series by Bodendorfer et al., surgeries were performed by four surgeons across three different institutions, which may have introduced variability in both technique and surgical experience.[4]

In our series, no intraoperative complications were observed. A single postoperative complication related to the glenoid component was recorded: one patient with a type 5 defect according to the Gohlke classification developed signs of baseplate loosening during follow-up. Although this rate (12.5%) is comparable to that reported in other series, studies such as that by Chammaa et al. reported a complication rate of 24% (9 of 37 patients), and Rangarajan et al. reported a rate of 21% (4 of 19 patients), including infections, hematomas, and intraoperative fractures.[6,11] Other authors, such as Porcellini et al., described minor radiographic findings and one dislocation in a series of six patients,[5] whereas Bodendorfer et al.,[4] and Ortmaier et al.[2] reported no complications. This variability may be attributable to differences in the defects treated, surgical experience, technique, and duration of follow-up.

Patient-specific glenoid implants offer several important advantages. They allow precise adaptation to complex bone defects, improving surgical accuracy and optimizing implant fixation and primary stability. This is particularly relevant in patients with severe defects in whom conventional implants may not provide an adequate solution.[2] Preoperative planning using the described methodology enables accurate assessment of bone stock and density, maximizing contact with the native glenoid and optimizing screw positioning, trajectory, and length. This results in improved primary stability and subsequent osseointegration, as observed in our series. Furthermore, the ability to design patient-specific implants allows effective management of anatomical variability and the specific characteristics of each glenoid defect.

However, this technique has certain drawbacks, such as a steep learning curve due to the low incidence of cases, which may impact operative time. In our series, variability in operative time was directly related to the type of procedure performed; although all cases involved revision arthroplasty, in two patients only the glenoid component was revised, whereas in the remaining cases both components were addressed. In cases of failed osteosynthesis, additional time required for hardware removal must be considered; similarly, failed hemiarthroplasties required removal of the humeral component, generally involving a humeral osteotomy. Another limitation is the delay between acquisition of the 3D CT scan and surgery. In our experience, once preoperative planning is approved, the implant can be manufactured and made available to the surgeon within a minimum of 5 weeks. The cost of patient-specific implants is higher than that of standard off-the-shelf implants, which may represent a limiting factor in certain settings.

This study has several limitations that should be considered. First, it is a retrospective study without a control group, which may limit interpretation of the results. Although the number of patients included is comparable to that of published international studies, the small sample size (eight patients) limits generalizability and may not capture the full variability of the population with severe glenoid defects. This small sample also precludes statistical power calculation, thereby limiting the validity of comparisons and introducing a potential risk of Type II error. Therefore, the results should be interpreted as preliminary and descriptive, and studies with larger sample sizes are required to confirm the effectiveness of patient-specific implants. In addition, the follow-up period was relatively short (12 months), precluding adequate assessment of long-term implant survival.

Furthermore, no independent evaluator was used to assess range of motion, as measurements were performed by the treating surgeon during clinical follow-up visits. Another limitation is that imaging follow-up was performed exclusively with plain radiographs in two projections (true anteroposterior and scapular axial views). Given the complex three-dimensional structure of these implants, CT evaluation could have provided more pre-

cise information regarding osseointegration; however, it was not performed due to additional costs and radiation exposure.

The novelty of this technique and its limited indications also restrict the number of patients treated with patient-specific glenoid implants to date, which further limits generalizability. Longer follow-up and larger cohorts are required to draw more robust conclusions regarding implant survival and complication rates.

Despite these limitations, this study has several notable strengths. To our knowledge, it is the first study published in a national and Latin American setting evaluating patient-specific glenoid implants with a minimum follow-up of one year, thereby providing a valuable contribution. The homogeneity of the study population is another important strength, as all patients underwent revision arthroplasty, allowing comparison with similar series. In addition, all procedures were performed by a single surgeon at a single institution, ensuring consistency in surgical technique and experience, and minimizing variability in outcomes.

CONCLUSIONS

Our study reports promising preliminary findings on the use of patient-specific glenoid implants in revision reverse shoulder arthroplasty, demonstrating positive outcomes in terms of range of motion, function, and pain reduction, with a low complication rate. Although further studies with larger cohorts and longer follow-up are required, these preliminary results support the use of this technology in patients with severe glenoid defects.

Conflicts of interest: The authors declare no conflicts of interest.

D. J. Gómez ORCID ID: https://orcid.org/0000-0003-0258-6802
G. M. Viollaz ORCID ID: https://orcid.org/0000-0002-4573-883X
G. Teruya ORCID ID: https://orcid.org/0000-0001-7342-1859
Á. Muratore ORCID ID: https://orcid.org/0000-0001-7540-7137
A. Tedeschi ORCID ID: https://orcid.org/0000-0001-5704-3122
L. Gutiérrez ORCID ID: https://orcid.org/0009-0000-4603-313X
R. Durán ORCID ID: https://orcid.org/0000-0002-8789-3221
S. Ávila Posada ORCID ID: https://orcid.org/0009-0008-8035-3522
Daniel Moya ORCID ID: https://orcid.org/0000-0003-1889-7699

REFERENCES

1. Burton R, Adam J, Holland P, Rangan A. A review of custom implants for glenoid bone deficiency in reverse shoulder arthroplasty. *J Orthop* 2023;36:65-71. https://doi.org/10.1016/j.jor.2022.11.016
2. Ortmaier R, Wierer G, Gruber MS. Functional and radiological outcomes after treatment with custom-made glenoid components in revision reverse shoulder arthroplasty. *J Clin Med* 2022;11(3):551. https://doi.org/10.3390/jcm11030551
3. Thati B, Bodanki C, Badam VK, Reddy MV, Reddy AVG. Custom 3D printed jigs in salvage reverse shoulder arthroplasty for failed four-part proximal humerus fracture fixation: a case report. *J Orthop Case Rep* 2020;10(2):25-8. https://doi.org/10.13107/jocr.2020.v10.i02.1682
4. Bodendorfer BM, Loughran GJ, Looney AM, Velott AT, Stein JA, Lutton DM, et al. Short-term outcomes of reverse shoulder arthroplasty using a custom baseplate for severe glenoid deficiency. *J Shoulder Elbow Surg* 2021;30(5):1060-7. https://doi.org/10.1016/j.jse.2020.08.002
5. Porcellini G, Micheloni GM, Tarallo L, Paladini P, Merolla G, Catani F. Custom-made reverse shoulder arthroplasty for severe glenoid bone loss: review of the literature and our preliminary results. *J Orthop Traumatol* 2021;22(1):2. https://doi.org/10.1186/s10195-020-00564-6
6. Chammaa R, Uri O, Lambert S. Primary shoulder arthroplasty using a custom-made hip-inspired implant for the treatment of advanced glenohumeral arthritis in the presence of severe glenoid bone loss. *J Shoulder Elbow Surg* 2017;26(1):101-7. https://doi.org/10.1016/j.jse.2016.05.027

7. Murphy J, Todd E, Wright MA, Murthi AM. Evaluation of clinical and radiographic outcomes after total shoulder arthroplasty with inset Trabecular Metal-backed glenoid. *J Shoulder Elbow Surg* 2022;31(5):971-7. https://doi.org/10.1016/j.jse.2021.10.014
8. Debeer P, Berghs B, Pouliart N, Van den Bogaert G, Verhaegen F, Nijs S. Treatment of severe glenoid deficiencies in reverse shoulder arthroplasty: the Glenius Glenoid Reconstruction System experience. *J Shoulder Elbow Surg* 2019;28(8):1601-8. https://doi.org/10.1016/j.jse.2018.11.061
9. Peri G, Troiano E, Colasanti GB, Mondanelli N, Giannotti S. Custom-made glenoid baseplate and intra-operative navigation in complex revision reverse shoulder arthroplasty: a case report. *J Shoulder Elb Arthroplast* 2024;8:1-6. https://doi.org/10.1177/17585732231225968
10. Rashid MS, Cunningham L, Shields DW, Walton MJ, Monga P, Bale RS, et al. Clinical and radiologic outcomes of Lima ProMade custom 3D-printed glenoid components in primary and revision reverse total shoulder arthroplasty with severe glenoid bone loss: a minimum 2-year follow-up. *J Shoulder Elbow Surg* 2023;32(10):2017-26. https://doi.org/10.1016/j.jse.2023.04.020
11. Rangarajan R, Blout CK, Patel VV, Bastian SA, Lee BK, Itamura JM. Early results of reverse total shoulder arthroplasty using a patient-matched glenoid implant for severe glenoid bone deficiency. *J Shoulder Elbow Surg* 2020;29(7S):S139-48. https://doi.org/10.1016/j.jse.2020.04.024
12. Gohlke F, Werner B. Humerale und glenoidale Knochendefekte in der Schulterendoprothetik: Klassifikation und Behandlungsprinzipien. *Orthopade* 2017;46(12):1008-14. https://doi.org/10.1007/s00132-017-3484-5

Preoperative Evaluation of Osteoporosis in Spinal Fusion Surgery: A Survey of Argentine and Latin American Surgeons

Pedro L. Bazán,[*] Guillermo A. Ricciardi,[**] Esteban Calcagni,[#] Enrique A. Casco,[##] Nicolás Galli,[§] Alexandre Fogaça Cristante,[§§] José Antonio Rosado Pardo,[**] Enrique Gobbi;[I] Grupo de Estudio de la Sociedad Argentina de Patología de la Columna Vertebral (SAPCV)

[*]*Spinal Pathology Unit, Department of Orthopedics and Traumatology, Hospital Interzonal General de Agudos San Martín, La Plata, Buenos Aires, Argentina*

[**]*Department of Orthopedics and Traumatology, Hospital General de Agudos "Dr. Teodoro Álvarez", Autonomous City of Buenos Aires, Argentina*

[#]*Centro Artro, Autonomous City of Buenos Aires, Argentina*

[##]*Department of Orthopedics and Traumatology, Hospital de Trauma, Asunción, Paraguay*

[§]*CEDEFCO, Montevideo, Uruguay*

[§§]*Institute of Orthopedics and Traumatology, School of Medicine, University of São Paulo, Brazil*

[I]*CEMIC, Buenos Aires, Argentina*

ABSTRACT

Objective: To analyze the preoperative evaluation of osteoporosis during surgical planning for adult patients undergoing spinal fusion surgery, from the perspective of spine surgeons in Argentina and Latin America. **Materials and Methods:** A descriptive, cross-sectional study was conducted among orthopedic spine surgeons practicing in Argentina and other Latin American countries. A structured questionnaire based on a simulated clinical case was developed to explore preoperative management of a 70-year-old patient scheduled for elective spinal fusion surgery. **Results:** A total of 154 spine surgeons from Argentina, Brazil, Paraguay, and Uruguay were surveyed. Significant differences were found in the use of full-length spine radiographs ($p < 0.001$), dynamic radiographs ($p = 0.001$), computed tomography ($p = 0.002$), magnetic resonance imaging ($p < 0.001$), and Hounsfield unit assessment ($p = 0.014$). The use of bone density scans showed a marginal statistical trend ($p = 0.058$), with higher rates in Uruguay (52.4%) and Argentina (42.9%). Vitamin D testing was requested in 40.3% of cases, with no significant differences between countries ($p = 0.803$), highlighting the limited assessment of this marker related to bone metabolism. **Conclusions:** There is a clear trend toward underestimation of osteoporosis screening in the preoperative evaluation for spinal fusion surgery. Fewer than 50% of surgeons considered requesting a DEXA scan, Hounsfield unit assessment, or vitamin D measurement.

Keywords: Osteoporosis; preoperative evaluation; spine surgery; arthrodesis; spinal fusion.

Level of Evidence: IV

Evaluación preoperatoria de la osteoporosis en la cirugía de fusión vertebral: encuesta a cirujanos de la Argentina y America Latina

RESUMEN

Objetivo: Analizar la evaluación preoperatoria de la osteoporosis durante la planificación quirúrgica de pacientes adultos candidatos a una cirugía de fusión vertebral, según la perspectiva de cirujanos de columna de la Argentina y América Latina. **Materiales y Métodos:** Estudio descriptivo y transversal de médicos traumatólogos, cirujanos de columna, que se desempeñan en centros de la Argentina y otros países de América Latina. Se confeccionó un cuestionario estructurado basado en un caso clínico simulado, diseñado para explorar el manejo preoperatorio frente a un paciente de 70 años candidato a una cirugía de fusión vertebral programada. **Resultados:** Se encuestaron 154 cirujanos de columna de la Argentina, Brasil, Paraguay y Uruguay. Se detectaron diferencias significativas en la solicitud de espinogramas ($p < 0{,}001$), radiografías dinámicas ($p = 0{,}001$), tomografía computarizada ($p = 0{,}002$), resonancia magnética ($p < 0{,}001$) y valoración de las unidades Hounsfield ($p = 0{,}014$). La solicitud de densitometría mostró una tendencia estadística marginal ($p=0{,}058$), con mayor solicitud por sujetos de Uruguay (52,4%) y Argentina (42,9%). La determinación de vitamina D fue solicitada en el 40,3% de los casos, sin diferencias significativas entre países ($p = 0{,}803$), lo

Received on August 11th, 2025. Accepted after review on February 12th, 2026 • Dr. PEDRO L. BAZÁN • pedroluisbazan@gmail.com https://orcid.org/0000-0003-0060-6558

How to cite this article: Bazán PL, Ricciardi GA, Calcagni E, Casco EA, Galli N, Fogaça Cristante A, et al, Grupo de Estudio de la Sociedad Argentina de Patología de la Columna Vertebral (SAPCV). Preoperative Evaluation of Osteoporosis in Spinal Fusion Surgery: A Survey of Argentine and Latin American Surgeons. *Rev Asoc Argent Ortop Traumatol* 2026;91(2):118-125. https://doi.org/10.15417/issn.1852-7434.2026.91.2.2214

que destaca una baja evaluación de este marcador relacionado con el metabolismo óseo. **Conclusiones:** Se observó una clara tendencia a la subestimación del cribado de osteoporosis en la evaluación preoperatoria para una cirugía de fusión vertebral. Menos del 50% de los cirujanos consideró solicitar una densitometría, unidades Hounsfield o medición de vitamina D.
Palabras clave: Osteoporosis; evaluación preoperatoria; cirugía de columna; artrodesis; fusión.
Nivel de Evidencia: IV

INTRODUCTION

Osteoporosis is the most common metabolic bone disease and represents a major global public health problem. It is characterized by reduced bone mass and deterioration of bone quality, leading to increased susceptibility to fractures.[1] Fragility fractures are its most relevant clinical outcome and have become a true global epidemic, with substantial health and economic impact.[2] It has been reported that the costs associated with hospitalizations for fragility fractures exceed those related to acute myocardial infarction, stroke, and breast cancer.[3]

Fragility fractures are not the only clinically relevant outcome in patients with osteoporosis. This is particularly evident in the context of spine surgery, where the prevalence of osteoporosis exceeds 30% in patients older than 50 years. In this setting, osteoporosis has been identified as a risk factor for multiple complications, extensively documented in both cervical and thoracolumbar procedures and across a broad spectrum of conditions (adult spinal deformity, unstable fractures, and degenerative disease).[4] Among the most common complications are implant loosening or failure, pseudarthrosis, proximal junctional kyphosis, interbody cage subsidence, and the development of new fractures.[5-9]

There is broad consensus on the importance of optimizing the patient's general condition prior to elective spine surgery in older adults. This includes correcting anemia, improving nutritional status, optimizing body mass index, managing pain, and promoting smoking cessation.[10] Within this comprehensive approach, optimization of bone metabolism has emerged as a key strategy to prevent complications associated with poor bone quality.[11] In line with current evidence, clinical guidelines recommend that preoperative osteoporosis assessment in adult patients undergoing surgery for spinal deformity be performed routinely.[12,13]

However, the rate of preoperative bone health assessment among spine surgeons remains low.[4] Several cross-sectional studies have highlighted variability in the diagnostic and therapeutic approaches adopted.[14,15] In light of the available evidence, we hypothesized that adherence among spine surgeons in Latin America to current recommendations for the preoperative evaluation of osteoporosis is low.

In this context, our objective was to evaluate preoperative osteoporosis assessment during surgical planning in adult patients undergoing spinal fusion, from the perspective of spine surgeons in Argentina and other Latin American countries.

MATERIALS AND METHODS

A descriptive, cross-sectional, exploratory study was conducted using a survey administered to orthopedic surgeons specializing in spine surgery, working at centers in Argentina and other Latin American countries, between April 1 and June 1, 2025.

A non-probability purposive sample was obtained from the database of spine surgeons of the Argentine Society of Spine Pathology, supplemented by snowball sampling through messaging applications and email.

Participants were selected according to predefined eligibility criteria. The study included orthopedic surgeons practicing as spine surgeons in Latin American centers who routinely perform spinal fusion procedures in adult patients and who agreed to complete the survey. Trainees (orthopedic residents and spine surgery fellows) and questionnaires with more than 50% missing responses were excluded.

Data Collection Instrument

A structured questionnaire based on a simulated clinical case was developed to assess preoperative management of a 70-year-old patient candidate for elective spinal fusion surgery. The questionnaire was designed by the research team and included items aimed at evaluating the use of imaging studies, laboratory tests, and other specific preoperative assessments for the diagnosis of osteoporosis and surgical planning. Responses were closed-ended (multiple choice).

The instrument was peer-reviewed to ensure clarity, relevance, and internal consistency. Prior to final administration, a pilot test was conducted on the first 20 responses to refine its format and content. The survey was distributed using Google Forms and remained open for a three-month period.

Statistical Analysis

Categorical variables are presented as absolute frequencies and percentages. Comparisons between groups were performed using the χ^2 test or Fisher's exact test, as appropriate based on sample size and expected frequencies. A p-value <0.05 was considered statistically significant. Statistical analyses were performed using SPSS Statistics version 25.

The study adhered to the principles of the Declaration of Helsinki for research involving human subjects, ensuring data confidentiality and participant anonymity. Informed consent was obtained from all participants upon agreeing to complete the survey, after receiving appropriate information regarding the study objectives and procedures. Collected data were coded, stored with restricted access, and used exclusively for the purposes of this study.

RESULTS

A total of 154 spine surgeons from Argentina, Brazil, Paraguay, and Uruguay were included (Figure).

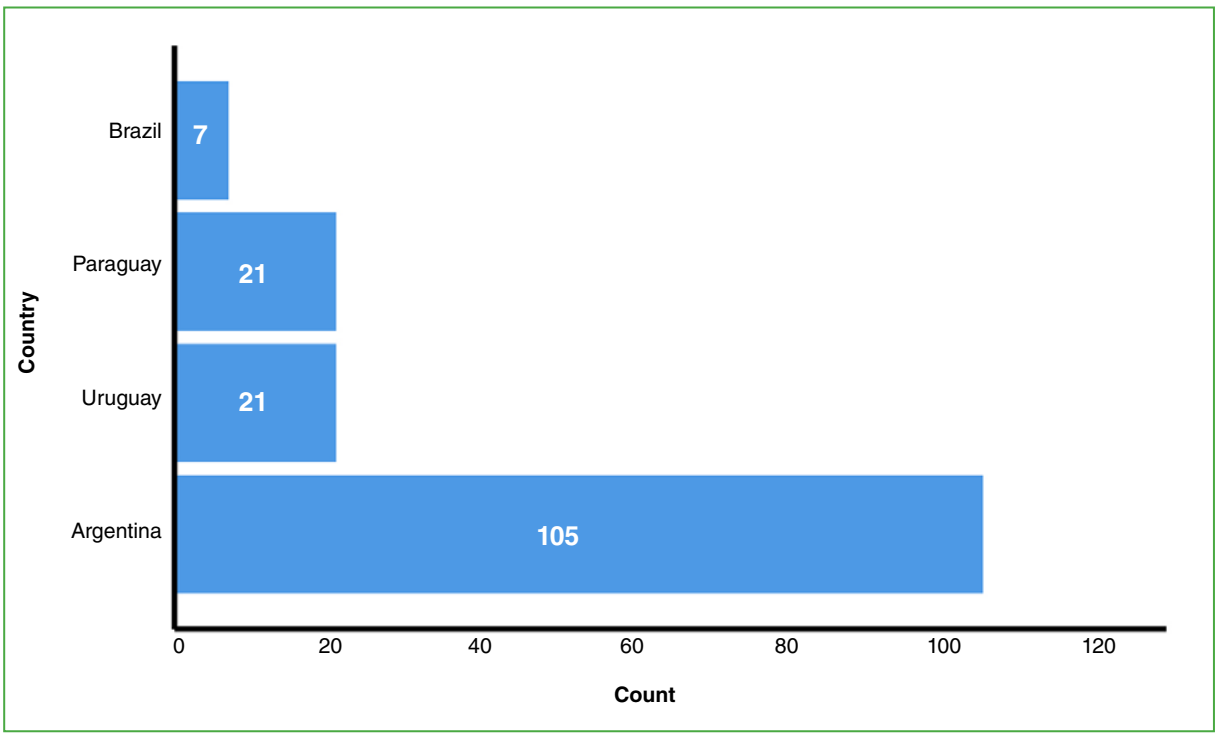

Figure. Bar chart showing the distribution of patients by country.

Imaging Studies

The most frequently requested studies were magnetic resonance imaging (MRI) (92.9%), dynamic radiographs (78.6%), full-spine radiographs (75.3%), and computed tomography (CT) (67.5%). Specific screening for osteoporosis using bone density scan and Hounsfield units was less frequent (40.3% and 37.7%, respectively).

When comparing by country, significant differences were observed in the use of full-spine radiographs ($p < 0.001$), dynamic radiographs ($p = 0.001$), CT ($p = 0.002$), MRI ($p < 0.001$), and Hounsfield unit assessment ($p = 0.014$). Bone density scan showed a marginal statistical trend ($p = 0.058$), being more frequently requested in Uruguay (52.4%) and Argentina (42.9%) (Table 1).

Table 1. Distribution of requested tests and comparison by country of origin.

Stydy		Total		Argentina		Brazil		Paraguay		Uruguay		p
		n	%	n	%	n	%	n	%	n	%	
Full-spine radiograph		116	75.3	92	87.6	5	71,4	4	19.0	15	71.4	<0.001
Dynamic radiograph		121	78.6	89	84.8	7	100.0	10	47.6	15	71.4	0.001
CT		104	67.5	79	75.2	4	57.1	7	33.3	14	66.7	0.002
MRI		143	92.9	103	98.1	0	0.0	19	90.5	21	100.0	<0.001
PET		3	1.9	1	1.0	0	0.0	2	9.5	0	0.0	0.06
Bone scintigraphy		1	0.6	1	1.0	0	0.0	0	0.0	0	0.0	0.925
Osteoporosis screening	Bone density scan	62	40.3	45	42.9	0	0.0	6	28.6	11	52.4	0.058
	HU	58	37.7	33	31.4	4	57.1	7	33.3	14	66.7	0.014

CT = computed tomography; MRI = magnetic resonance imaging; PET = positron emission tomography; HU = Hounsfield units.

Laboratory Parameters

Overall, no significant differences were observed between countries in most laboratory tests requested as part of the preoperative evaluation of the clinical case. The most frequently requested tests were complete blood count (98.1%), blood glucose (93.5%), and renal function assessment (92.9%), followed by glycated hemoglobin (74.7%), serum protein electrophoresis (66.2%), and acute-phase reactants (48.7%). Vitamin D was requested in 40.3% of cases, with no significant differences between countries ($p = 0.803$), highlighting the low rate of assessment of this marker related to bone metabolism. Statistically significant differences between countries were observed only for blood glucose testing ($p < 0.001$) and serum protein electrophoresis ($p = 0.017$), the latter being more frequently requested in Paraguay and Argentina (Table 2).

Table 2. Distribution of laboratory parameters by country.

Laboratory parameters	Total		Argentina		Brazil		Paraguay		Uruguay		p
	n	%	n	%	n	%	n	%	n	%	
Complete blood count	151	98.1	103	98.1	7	100.0	20	95.2	21	100.0	0.699
Blood glucose	144	93.5	102	97.1	6	85.7	16	76.2	20	95.2	0.004
Renal function	143	92.9	100	95.2	7	100.0	19	90.5	17	81.0	0.107
Serum protein electrophoresis	102	66.2	73	69.5	4	57.1	17	81.0	8	38.1	0.017
HbA1c	115	74.7	79	75.2	7	100.0	17	81.0	12	57.1	0.100
Acute-phase reactant	75	48.7	56	53.3	2	28.6	11	52.4	6	28.6	0.135
Vitamin D	62	40.3	41	39.0	2	28.6	10	47.6	9	42.9	0.803

Preoperative Risk Assessment

Regarding preoperative cardiovascular and respiratory tests, no statistically significant differences were observed between countries. Electrocardiography was the most frequently requested test (97.4% of the total sample), followed by spirometry (42.2%), lower-limb Doppler ultrasound (29.9%), and exercise stress testing (16.2%) (Table 3).

Table 3. Distribution of cardiorespiratory studies by country.

Studies	Total		Argentina		Brazil		Paraguay		Uruguay		p
	n	%	n	%	n	%	n	%	n	%	
ECG	150	97.4	103	98.1	6	85.7	20	95.2	21	100.0	0.177
Spirometry	65	42.2	48	45.7	1	14.3	10	47.6	6	28.6	0.202
Lower extremity Doppler ultrasound	46	29.9	35	33.3	3	42.9	5	23.8	3	14.3	0.265
Exercise testing	25	16.2	17	16.2	1	14.3	4	19.0	3	14.3	0.977

DISCUSSION

Osteoporosis is a critical factor in the preoperative evaluation of patients undergoing instrumented spine surgery, as it is a major predictor of mechanical complications, particularly those related to implant failure and sagittal imbalance. Its impact is especially relevant in complex procedures, such as adult spinal deformity surgery, which typically require long constructs and involve greater biomechanical demands.[5-9]

In a cross-sectional study of 349 spine surgeons in Latin America, Pantoja and Molina reported the regional clinical scenario, in which 79.6% indicated having managed osteoporosis-related complications and 71.6% reported having revised instrumentation due to failures associated with this condition.[16]

Recent AOSpine clinical recommendations on osteoporosis in adults with spinal deformity highlight the importance of systematic evaluation of osteoporosis in these patients. Although high-quality evidence is still needed, these recommendations emphasize that all clinicians treating adults with scoliosis should consider bone health as a key component for improving surgical outcomes and minimizing complications.[15] Nevertheless, and in line with previous cross-sectional studies, we identified a low level of awareness regarding the preoperative evaluation of osteoporosis.[14-16] Compared with the frequent use of initial imaging studies, such as full-spine radiographs (75.3%) and magnetic resonance imaging (92.9%), fewer than half of respondents used specific methods to detect osteoporosis, such as bone density scan (40.3%) and Hounsfield unit measurement (37.7%). No significant differences were found in the use of density scan according to country of origin, whereas a higher proportion of surgeons in Uruguay reported using Hounsfield unit measurement (66.7%; p = 0.014).

It should be noted that, although bone density scan has traditionally been the gold standard for diagnosing osteoporosis, it has limitations in patients with spondylarthrosis, in whom bone quality may be overestimated.[17] This has led to the investigation of additional methods for assessing bone health, such as Hounsfield unit measurement, the trabecular bone score, and fracture risk calculators, such as the FRAX® tool.[18-20] St. Jeor et al. evaluated 140 patients undergoing spinal fusion to compare preoperative assessment methods and reported a 32% rate of osteoporosis-related complications. Multivariable binary logistic regression analysis showed that lower mean Hounsfield unit values were an independent predictor of osteosynthesis-related complications. The odds of developing a complication increased 1.7-fold for every 25-unit decrease in mean Hounsfield values.[19]

Considering the best available evidence together with accessible resources for evaluating osteoporosis in vulnerable patients, routine clinical practice should include a bone density scan of the spine and wrist as an additional anatomical site, as well as analysis of Hounsfield units obtained from preoperative CT, to achieve a more accurate assessment of osteoporosis.[15,20]

In a systematic review of nine studies, Bazán et al. concluded that Hounsfield unit measurement may optimize surgical planning and reduce osteoporosis-related complications, with a low level of evidence but promising perspectives.[20]

On the other hand, although Hounsfield unit-based assessment is increasingly used, it has important limitations. Hounsfield unit values may be influenced by multiple technical factors, including CT acquisition parameters, scanner calibration, reconstruction algorithms, and region-of-interest selection, which affect reproducibility and interinstitutional comparability.

According to the evidence-based guidelines of the *Congress of Neurological Surgeons* on the preoperative evaluation of osteoporosis in patients undergoing spinal surgery, at least one of the following assessments is recommended, each with its corresponding cutoff value associated with a high risk of complications: bone density scan with a T-score < −2.5; CT with Hounsfield units <97.9; or serum vitamin D3 levels <20 ng/mL.[12]

Vitamin D deficiency is extremely common, with prevalence rates ranging from 40% to 90% in adults.[21] Patients >50 years of age, smokers, and individuals with obesity are at higher risk of hypovitaminosis D.[21-23] It is estimated that more than 25% of adults scheduled for spinal surgery have this deficiency.[22] Preoperative measurement of vitamin D and calcium provides valuable information on bone metabolism.[20] Furthermore, patients undergoing spinal fusion may benefit from correction of this deficiency.[23] In our study, fewer than half of the surgeons requested vitamin D testing as part of the preoperative workup. Although higher-quality evidence is needed, the available data suggest that spine surgeons should consider the increased risk of adverse outcomes in patients with preoperative vitamin D deficiency.[24]

Our study has several limitations, including a small sample size, a limited number of preoperative and demographic variables assessed, and the recall bias inherent to cross-sectional survey-based designs. In addition, the overrepresentation of Argentina compared with other countries limits the generalizability of the results.

Nevertheless, a clear trend was identified that may help guide future strategies to optimize the implementation of recommendations from international publications and guidelines regarding the preoperative evaluation of patients undergoing spinal surgery who are at risk of osteoporosis. Further multinational studies with greater regional representation are needed.

CONCLUSIONS

A clear tendency to underestimate osteoporosis assessment during preoperative evaluation in the surgical planning of adult patients undergoing spinal fusion was observed.

Fewer than half of the surgeons considered ordering bone density scan (40.3%), Hounsfield unit measurement (37.7%), or vitamin D testing (40.3%).

The low proportion of surgeons from other Latin American countries represents a limitation of the study and restricts the direct generalization of the results to the entire region.

Conflicts of interest: The authors declare no conflicts of interest.

G. A. Ricciardi ORCID ID: https://orcid.org/0000-0002-6959-9301
E. Calcagni ORCID ID: https://orcid.org/0009-0009-5989-9288
E. A. Casco ORCID ID: https://orcid.org/0000-0002-6113-5123
N. Galli ORCID ID: https://orcid.org/0000-0003-3830-5902
A. Fogaça Cristante ORCID ID: https://orcid.org/0000-0002-7797-5274
J. A. Rosado Pardo ORCID ID: https://orcid.org/0000-0001-8467-3453
E. Gobb ORCID ID i: https://orcid.org/0000-0001-7310-6170

REFERENCES

1. Albergaria BH, Chalem M, Clark P, Messina OD, Pereira RMR, Vidal LF. Consensus statement: osteoporosis prevention and treatment in Latin America-current structure and future directions. *Arch Osteoporos* 2018;13(1):90. https://doi.org/10.1007/s11657-018-0505-x

2. Etxebarria-Foronda I, Caeiro-Rey JR, Larrainzar-Garijo R, Vaquero-Cervino E, Roca-Ruiz L, Mesa-Ramos M, et al. Guía SECOT-GEIOS en osteoporosis y fractura por fragilidad. Actualización. *Rev Esp Cir Ortop Traumatol* 2015;59(6):373-93. https://doi.org/10.1016/j.recot.2015.05.007
3. Singer A, Exuzides A, Spangler L, O'Malley C, Colby C, Johnston K, et al. Burden of illness for osteoporotic fractures compared with other serious diseases among postmenopausal women in the United States. *Mayo Clin Proc* 2015;90(1):53-62. https://doi.org/10.1016/j.mayocp.2014.09.011
4. Fan ZQ, Yan XA, Li BF, Shen E, Xu X, Wang H, et al. Prevalence of osteoporosis in spinal surgery patients older than 50 years: A systematic review and meta-analysis. *PLoS One* 2023;18(5). https://doi.org/10.1371/journal.pone.0286110
5. Diebo BG, Sheikh B, Freilich M, Shah NV, Redfern JAI, Tarabichi S, et al. Osteoporosis and spine surgery: A critical analysis review. *JBJS Rev* 2020;8(6):e0160. https://doi.org/10.2106/JBJS.RVW.19.00160
6. Gupta A, Cha T, Schwab J, Fogel H, Tobert D, Razi AE, et al. Osteoporosis increases the likelihood of revision surgery following a long spinal fusion for adult spinal deformity. *Spine J* 2021;21(1):134-40. https://doi.org/10.1016/j.spinee.2020.08.002
7. Shen T, Shahzad H, Sierra F, Wick JB, Pina D, Van BW, et al. Osteoporosis treatment and outcomes in patients undergoing adult spinal deformity surgery. *World Neurosurg* 2024;190:e1018-e1024. https://doi.org/10.1016/j.wneu.2024.08.053
8. Diebo BG, Scheer R, Rompala A, Veenema RJ, Shah NV, Beyer GA, et al. The impact of osteoporosis on 2-year outcomes in patients undergoing long cervical fusion. *J Am Acad Orthop Surg* 2023;31(1):e44-e50. https://doi.org/10.5435/JAAOS-D-22-00361
9. Karikari IO, Metz LN. Preventing pseudoarthrosis and proximal junctional kyphosis: How to deal with the osteoporotic spine. *Neurosurg Clin N Am* 2018;29(3):365-74. https://doi.org/10.1016/j.nec.2018.03.005
10. Daniels AH, Singh M, Knebel A, Thomson C, Kuharski MJ, De Varona A, et al. Preoperative optimization strategies in elective spine surgery. *JBJS Rev* 2025;13(2). https://doi.org/10.2106/JBJS.RVW.24.00210
11. Bernatz JT, Winzenried AE, Hare KJ, Mikula AL, Williams SK, Binkley NC, et al. Effect of bone health optimization on osteoporosis screening and treatment before thoracolumbar fusion. *J Am Acad Orthop Surg Glob Res Rev* 2022;6(3):e21.00253. https://doi.org/10.5435/JAAOSGlobal-D-21-00253
12. Dimar J, Bisson EF, Dhall S, Harrop JS, Hoh DJ, Mohamed B, et al. Congress of Neurological Surgeons Systematic Review and Evidence-Based Guidelines for Perioperative Spine: Preoperative Osteoporosis Assessment. *Neurosurgery* 2021;89(Suppl 1):S19-S25. https://doi.org/10.1093/neuros/nyab317
13. Kato S, Rocos B, Yoshida G, Sardar Z, Jones KE, Oe S, et al. AO Spine Clinical Practice Recommendations: Evaluation, implications and management of osteoporosis in adult spinal deformity. *Global Spine J* 2025;14:21925682251357200. https://doi.org/10.1177/21925682251357200
14. Dipaola CP, Bible JE, Biswas D, Dipaola M, Grauer JN, Rechtine GR. Survey of spine surgeons on attitudes regarding osteoporosis and osteomalacia screening and treatment for fractures, fusion surgery, and pseudoarthrosis. *Spine J* 2009;9(7):537-44. https://doi.org/10.1016/j.spinee.2009.02.005
15. Díaz-Romero R, Henríquez MS, Melián KA, Balhen-Martin C. Practice patterns of spine surgeons regarding osteoporosis: An international survey. *Int J Spine Surg* 2021;15(2):376-85. https://doi.org/10.14444/8049
16. Pantoja S, Molina M. Surgeon management of osteoporosis in instrumented spine surgery: AOSpine Latin America survey. *Global Spine J* 2019;9(2):169-72. https://doi.org/10.1177/2192568218785369
17. Sociedad Internacional de Densitometría Clínica. Posiciones Oficiales para Adultos 2019. Available at: https://iscd.org/learn/official-positions/adult-positions/
18. St Jeor JD, Jackson TJ, Xiong AE, Kadri A, Freedman BA, Sebastian AS, et al. Osteoporosis in spine surgery patients: what is the best way to diagnose osteoporosis in this population? *Neurosurg Focus* 2020;49(2):E4. https://doi.org/10.3171/2020.5.FOCUS20277
19. St Jeor JD, Jackson TJ, Xiong AE, Freedman BA, Sebastian AS, Currier BL, et al. Average lumbar Hounsfield units predict osteoporosis-related complications following lumbar spine fusion. *Global Spine J* 2022;12(5):851-7. https://doi.org/10.1177/2192568220975365
20. Bazán PL, Jordan RC, Cevallos JRM, Adaro AOG, Adaro JCS. Uso de unidades Hounsfield en la planificación de cirugía de columna: revisión sistemática y metanálisis. *Coluna/Columna* 2022;21:e264579. https://doi.org/10.1590/S1808-185120222103264579
21. Lehman RA Jr, Kang DG, Wagner SC. Management of osteoporosis in spine surgery. *J Am Acad Orthop Surg* 2015;23(4):253-63. https://doi.org/10.5435/JAAOS-D-14-00042

22. Stoker GE, Buchowski JM, Bridwell KH, Lenke LG, Riew KD, Zebala LP. Preoperative vitamin D status of adults undergoing surgical spinal fusion. *Spine (Phila Pa 1976)* 2013;38(6):507-15. https://doi.org/10.1097/BRS.0b013e3182739ad1
23. Kerezoudis P, Rinaldo L, Drazin D, Kallmes D, Krauss W, Hassoon A, et al. Association between vitamin D deficiency and outcomes following spinal fusion surgery: A systematic review. *World Neurosurg* 2016;95:71-6. https://doi.org/10.1016/j.wneu.2016.07.074
24. Bajaj A, Shah RM, Goodwin AM, Kurapaty S, Patel AA, Divi SN. The role of preoperative vitamin D in spine surgery. *Curr Rev Musculoskelet Med* 2023;16(2):48-54. https://doi.org/10.1007/s12178-022-09813-z

Results of Anatomical Repair of the Distal Biceps via an Implant-Free Anterior Approach

Ignacio Seré, Santiago Llumipanta, Juan Carrizo, Natalia Villa, Marcos Deimundo, Enrique Gobbi
Orthopedics and Traumatology Service, Hospital Universitario CEMIC, Autonomous City of Buenos Aires, Argentina

ABSTRACT

Introduction: There are numerous approaches for treating distal biceps injuries, each with varying success rates and associated complications. We describe an implant-free technique for anatomical reinsertion of the distal biceps through an anterior incision and report the clinical and functional outcomes. **Materials and Methods:** A retrospective review was conducted of 11 patients who underwent this surgical technique for the repair of their distal biceps injuries. The mean age was 43.8 years, and all patients were male. Demographic data were collected, as well as clinical and functional outcomes more than one year after surgery. **Results:** At the final assessment, no mobility deficits were found. All patients returned to their pre-injury work and sports activities. The mean residual pain score on the Visual Analog Scale was 0.22. The average QuickDASH score one year after surgery was 6.38. There were 3 cases with complications: 2 transient neuropraxias of the lateral antebrachial cutaneous nerve and one surgical wound infection. **Conclusions:** Our results with this technique for repairing distal biceps injuries are comparable to those obtained using implant-based techniques. Recovery was satisfactory in all cases, with a low complication rate. This technique may represent a viable alternative to other, more complex surgical approaches.

Keywords: Distal biceps injury; anterior approach; transosseous suture.
Level of Evidence: IV

Reparación anatómica del bíceps distal por un abordaje anterior sin el uso de implantes: resultados clínicos y funcionales

RESUMEN

Introducción: Existen múltiples enfoques quirúrgicos para abordar las lesiones del bíceps distal, con diferentes tasas de éxito y complicaciones asociadas. En este artículo, se describe una técnica quirúrgica sin implantes para la reinserción anatómica del bíceps distal a través de una incisión anterior, y se comunican los resultados clínicos y funcionales. **Materiales y Métodos:** Se evaluó retrospectivamente a 11 pacientes sometidos a esta técnica quirúrgica para la reparación de lesiones de bíceps distal. Todos eran hombres y la edad promedio era de 43.8 años. Se recopilaron parámetros demográficos, los resultados clínicos y funcionales a más de un año de la cirugía. **Resultados:** En la evaluación final, no se observaron déficits de movilidad. Todos los pacientes reanudaron sus tareas laborales y deportivas como antes de la lesión. El puntaje promedio de dolor residual en actividad, según la escala analógica visual, fue de 0,22. El puntaje de QuickDASH promedio después de un año de la operación fue de 6,38. Se produjeron 3 complicaciones: 2 neuropraxias transitorias del antebraquial cutáneo externo y una infección de la herida quirúrgica. **Conclusiones:** Nuestros resultados con esta técnica quirúrgica para la reparación de lesiones de bíceps distal son comparables con los obtenidos usando técnicas con implantes. La recuperación fue satisfactoria en todos los casos, con una tasa de complicaciones aceptable. Esta técnica podría representar una alternativa viable a otros enfoques quirúrgicos más complejos.

Palabras clave: Lesión; bíceps distal; abordaje anterior; sutura transósea.
Nivel de Evidencia: IV

INTRODUCTION

Avulsion of the distal biceps tendon from its insertion on the radial tuberosity of the proximal radius is uncommon (1.2–2.5 cases per 100,000 persons per year); it typically occurs when resisting a sudden load with the forearm in flexion and supination, as during weightlifting or when attempting to arrest the fall of a heavy object. Nonoperative treatment results in a 22-50% loss of supination strength and a 12-40% loss of flexion strength.[1,2]

Received on December 12th, 2025. Accepted after evaluation on February 13th, 2026 • Dr. IGNACIO SERÉ • ignaciosere@gmail.com https://orcid.org/0000-0002-3267-8073
How to cite this article: Seré I, Llumipanta S, Carrizo J, Villa N, Deimundo M, Gobbi E. Results of Anatomical Repair of the Distal Biceps via an Implant-Free Anterior Approach. *Rev Asoc Argent Ortop Traumatol* 2026;91(2):XXX. https://doi.org/10.15417/issn.1852-7434.2026.91.2.2270

Although there remains some controversy regarding the need for repair of acute distal biceps avulsion, surgical repair has been associated with better outcomes in terms of strength, endurance, and cosmesis compared with nonoperative management.[1,2]

Currently, numerous surgical techniques are available for reattachment of the distal biceps brachii tendon, including fixation to the radial tuberosity using Endobutton® systems (cortical fixation with a titanium button), specifically designed interference screws, suture anchors, or transosseous sutures. The most commonly used method is the Endobutton® system combined with an interference screw. An important aspect of the native distal biceps tendon insertion is its ulnar and posterior position on the radial tuberosity, which enables effective forearm supination through contraction by exploiting the cam effect of the radial tuberosity. As the radial tuberosity projects eccentrically from the central axis of the radius, it increases the distance between the biceps tendon and the axis of rotation, thereby enhancing its moment arm.[3,4] Classically, the anterior approach allows fixation of the tendon on the anterior surface of the radial tuberosity, as with Endobutton® systems or suture anchors, which may reduce supination strength. In contrast, the Boyd two-incision approach allows for posterior reinsertion, but may interfere with pronation and also fails to fully exploit the cam effect, as it has been shown that, with a posterior insertion, the tendon migrates proximally on the tuberosity during contraction, thereby diminishing the cam effect.[3-5]

The transosseous suture technique through a single anterior approach used in this series allows replication of the native biceps insertion, maximizing the contact surface between the tendon and the radius and restoring the cam function of the radial tuberosity (Figure 1). This is achieved using transosseous sutures without implants or anchors, with minimal impact on the structural integrity of the radial tuberosity.[6,7]

The objectives of this study were to describe the surgical technique and to evaluate clinical and functional outcomes at more than one year postoperatively.

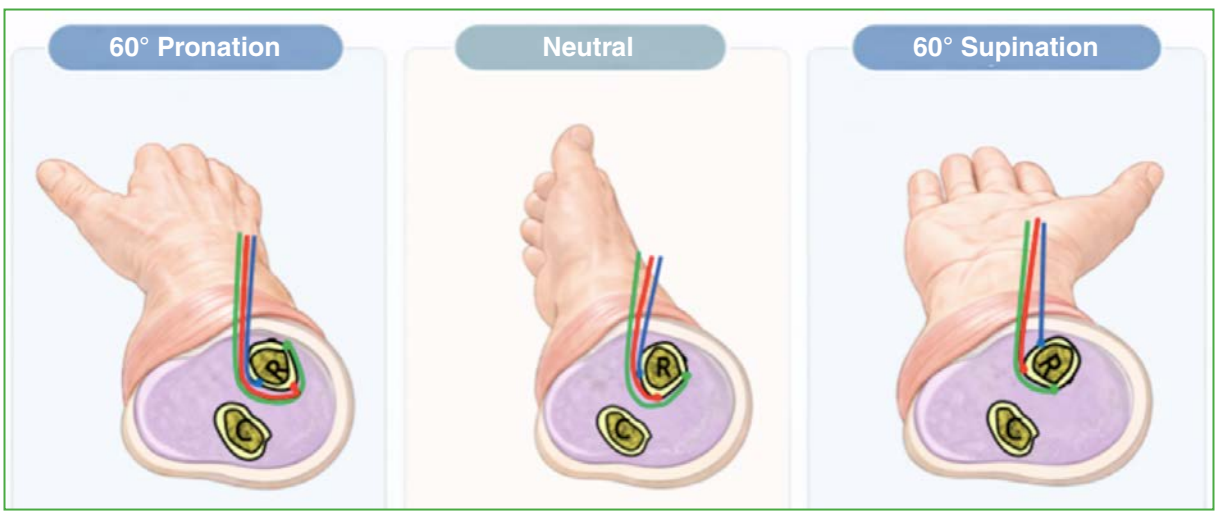

Figure 1. Schematic axial section of the proximal forearm at the level of the center of the bicipital tuberosity, in 60° pronation, neutral position, and 60° supination. With the native tendon insertion (red line), the bicipital tuberosity acts as a cam, increasing the moment arm of the biceps tendon by displacing its line of pull away from the axis of rotation of the radius. The anterior (more radial) insertion (blue line) shortens the moment arm, as does the posterior insertion (green line), since during effective contraction the biceps tendon migrates proximally and pulls over the superior edge of the tuberosity. R = radius; C = ulna. (Prepared by the authors.)

MATERIALS AND METHODS

We retrospectively reviewed the medical records of 14 patients who underwent distal biceps tendon repair between February 2021 and August 2024 and had a minimum postoperative follow-up of 12 months. Three patients were lost to follow-up and were excluded. The final study cohort consisted of 11 patients. All were men, with a mean age of 43.8 years (range 21-60; standard deviation [SD] 10.4). Four patients smoked more than 10 cigarettes per day, and two reported the use of creatine supplements to increase muscle mass. In eight cases, the injury in-

volved the dominant limb. The mechanism of injury was consistently a sudden eccentric load against resistance, with the elbow in flexion and supination: weightlifting (6 patients), lifting heavy objects (3 patients), and use of tools (2 patients). The mean time from injury to surgery was 15 days (range 6-55; SD 14.4). Mean follow-up was 35.5 months (range 12-53; SD 13.4).

All procedures were performed by the same surgeon with Level III experience according to the Tang classification (defined as a surgeon with substantial experience in the relevant techniques and more than 5 years of specialist practice).[8]

Surgical Technique

A standard Henry approach to the radial tuberosity of the proximal radius was used. The skin incision was made longitudinally under fluoroscopic guidance. Three surgical planes were identified:

- Subcutaneous plane, containing the major superficial veins, the lacertus fibrosus, and the lateral antebrachial cutaneous nerve;
- Muscular plane, defined superficially by the flexor carpi radialis and brachioradialis, and deeply by the pronator teres and supinator muscles. This plane contains the radial artery and its branches, the deep venae comitantes, and the terminal branches of the radial nerve (superficial sensory branch and posterior interosseous nerve); and
- Osseous plane, at the level of the radial tuberosity.

Immediately beneath the dermis lies the superficial venous system, composed, from medial to lateral, of the basilic vein, the median antebrachial vein, the cephalic vein, and the accessory cephalic vein. The median antebrachial vein divides into a lateral branch, the median cephalic vein, and a medial branch, the median basilic vein, which join their respective veins at the elbow (Figure 2).[9]

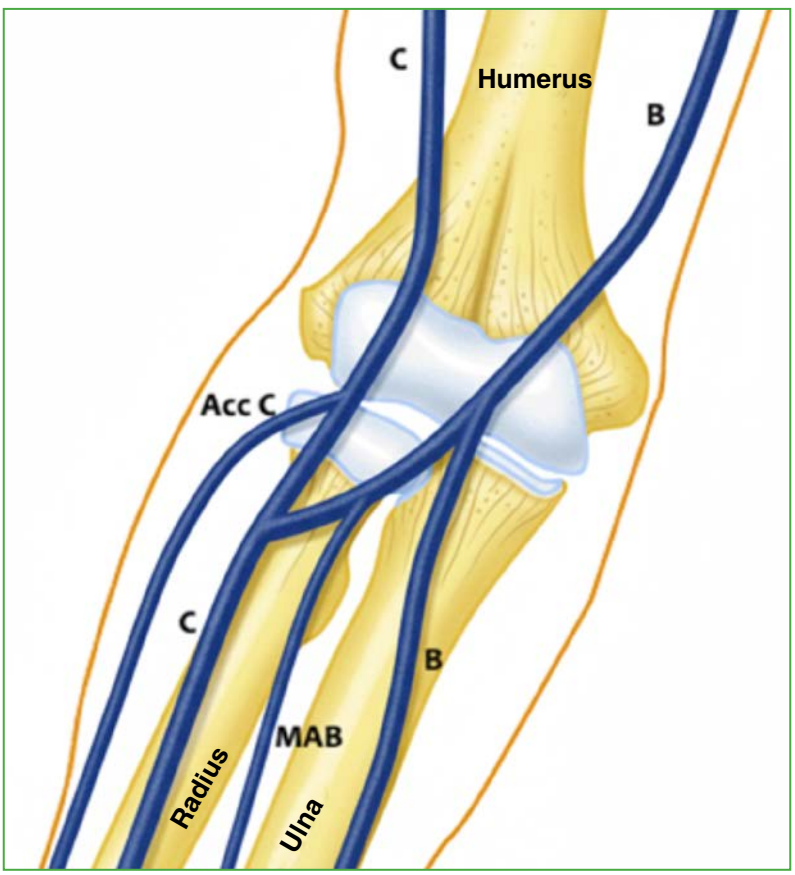

Figure 2. Superficial venous system at the anterior aspect of the elbow. Acc C = accessory cephalic vein; B = basilic vein; C = cephalic vein; MAB = median antebrachial vein. (Prepared by the authors.)

Deep to the cephalic vein lies the lateral antebrachial cutaneous nerve, a terminal branch of the musculocutaneous nerve, which enters the lateral bicipital groove of the elbow from the interval between the biceps brachii and brachialis muscles. It continues along the anterolateral aspect of the forearm, providing cutaneous innervation as far as the wrist (Figure 3).[1] The lacertus fibrosus originates from the musculotendinous junction of the distal biceps, extends over the flexor muscles of the forearm, blends with their superficial fascia, and inserts into the subcutaneous border of the ulna. It acts as a stabilizer of the distal biceps tendon (Figure 3).[1]

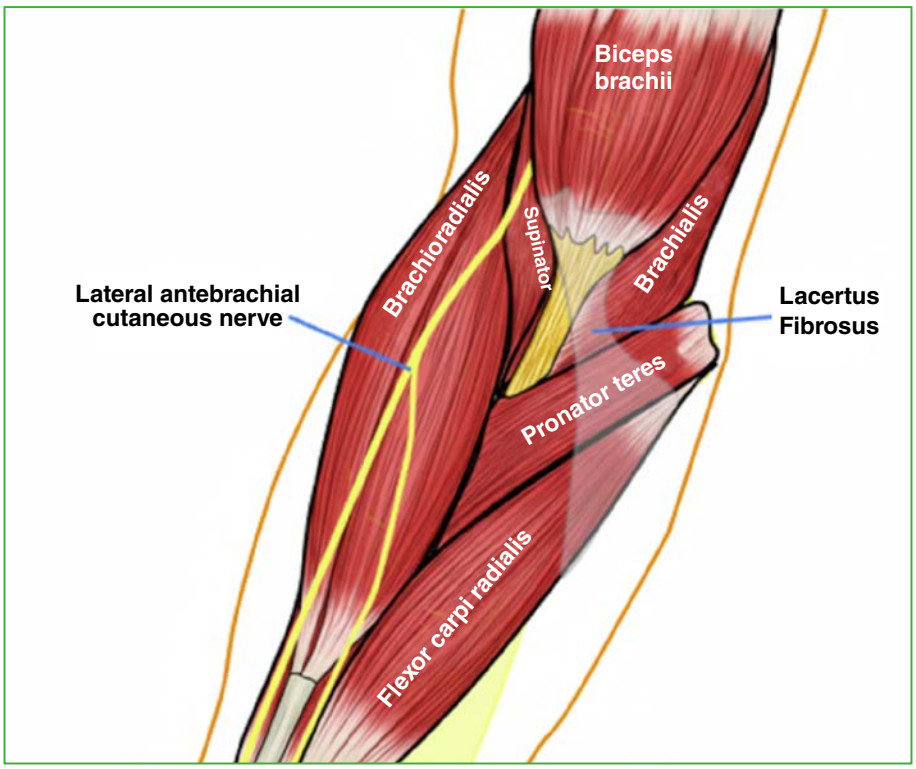

Figure 3. Anterior view of the muscular planes of the elbow, showing the lacertus fibrosus and the lateral antebrachial cutaneous nerve. (Prepared by the authors.)

The muscular planes (Figure 3) can be easily and safely separated by blunt dissection with the index finger. Although arterial variations are not uncommon, in approximately 47% of patients, the brachial artery (before bifurcating into the ulnar and radial arteries) gives rise to an accessory dorsal radial recurrent branch posterior to the biceps tendon (Figure 4). The radial artery courses just medial to the biceps tendon and gives rise to the radial recurrent artery, which runs anterior to the tendon, transversely across the forearm axis, approximately 4 mm proximal to the most proximal aspect of the radial tuberosity (Figure 5). This artery anastomoses with the anterior radial collateral artery (a branch of the profunda brachii artery), forming the so-called Henry vascular leash (Figure 4).[9] The deep venous system accompanies the arterial system in a more anterior plane as venae comitantes, with multiple anastomoses forming a venous plexus that communicates with the superficial venous system through perforating veins.[9] If the radial recurrent artery or its venae comitantes interfere with visualization or limit adequate exposure of the radial tuberosity, they may be ligated.[1,2,6,7,9]

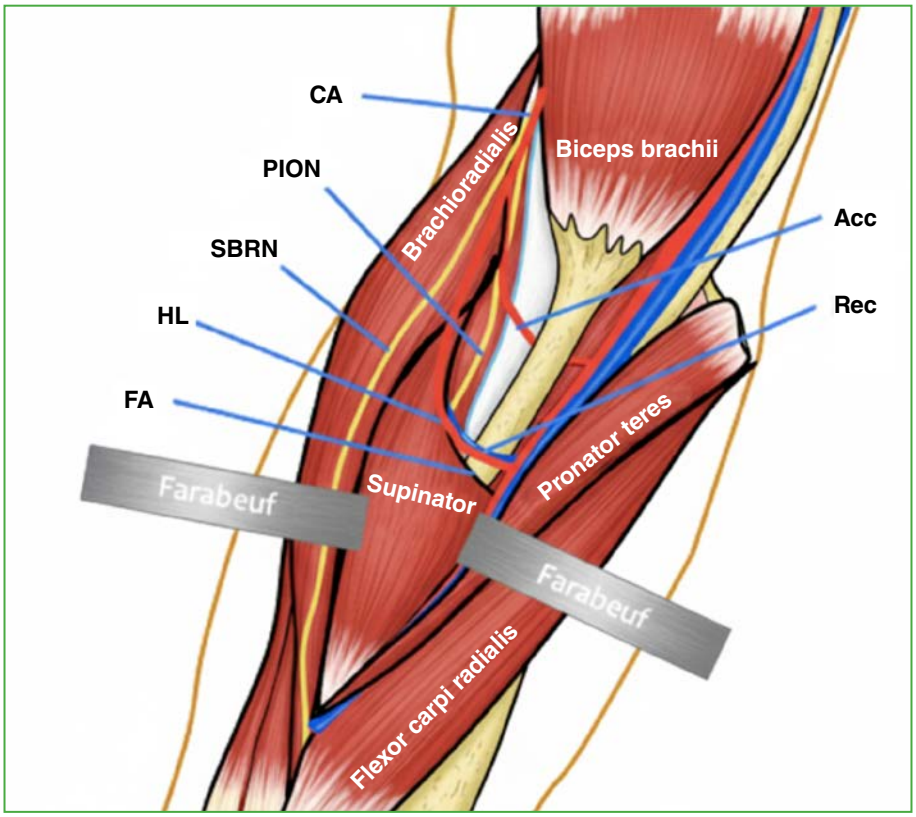

Figure 4. Schematic representation of the deep arterial and venous pattern (right elbow, anterior view): the dorsal accessory radial recurrent artery (Acc) arises from the brachial artery in 47% of cases and passes posterior to the biceps tendon. The radial recurrent artery (Rec) crosses anterior to the biceps tendon and anastomoses with the anterior radial collateral artery (CA), forming Henry's leash (HL). FA = Frohse's arcade; Farabeuf = Farabeuf retractor; PION = posterior interosseous nerve; SBRN = superficial sensory branch of the radial nerve. (Prepared by the authors.)

The radial nerve divides into its superficial (sensory) branch and its deep motor branch (posterior interosseous nerve) proximal to the arcade of the supinator muscle (arcade of Frohse).[10] The superficial sensory branch travels along the medial aspect of the brachioradialis muscle, accompanies the radial artery, and continues toward the wrist and hand. The deep motor branch, corresponding to the posterior interosseous nerve, continues distally in close contact with the lateral aspect of the radial neck, making it particularly vulnerable to injury when using Hohmann retractors at the lateral border of the radial neck. Forearm supination is recommended, as it moves the nerve into a more posterior and lateral position (whereas pronation shifts it anteriorly and medially),[10] along with a triangular retractor configuration to access the radial tuberosity, using two long-blade Farabeuf retractors laterally and a medial Hohmann retractor (Figure 5).[11]

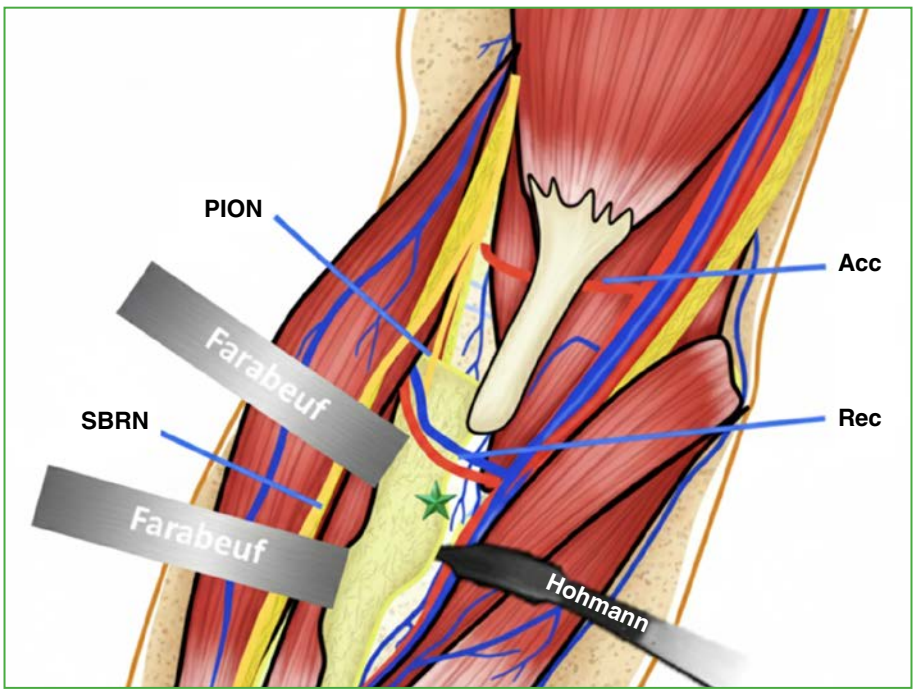

Figure 5. The biceps tendon is depicted as detached, and the supinator muscle is shown retracted laterally to access the bicipital tuberosity using a triangular configuration of two lateral Farabeuf retractors and one medial Hohmann retractor. The radial recurrent artery (Rec) crosses anterior to the biceps tendon approximately 4 mm proximal to the proximal edge of the bicipital tuberosity (green star). Acc = dorsal accessory radial recurrent branch; Farabeuf = Farabeuf retractor; PION = posterior interosseous nerve; SBRN = superficial sensory branch of the radial nerve. (Prepared by the authors.)

Dissection of the aforementioned anatomical structures allows access to the anterior surface of the radial tuberosity, whose apex, as a reference point, is oriented opposite to the radial styloid process.[4] The residual distal biceps tendon is detached from the tuberosity using a rongeur or curette. The tuberosity bed is then prepared on its posteromedial surface using a curette or rasp, which corresponds to the native insertion footprint.

With the forearm in 45° of supination, two holes are drilled using a 2-mm drill bit, approximately 1 cm apart. The drill is directed from the anterior aspect of the radial tuberosity at a 30° medial angle toward the dorsoulnar cortex of the radius (Figure 6A). The use of a soft-tissue protector facilitates the procedure. The 45° supination position and the ulnar direction of the drill holes facilitate suture passage and maximize the distance between the drill bit and the posterior interosseous nerve.[6,7,10]

A strong monofilament suture (Prolene, PDS, or 0 nylon) is then passed through the radius to serve as a shuttle suture, as follows: a standard right-angle clamp is introduced from the medial side to the posterior aspect of the radius, aligned with one of the drill holes (Figure 6B). An 18G spinal needle is inserted through the drill hole from anterior to posterior until the surgeon feels contact with the tip of the clamp. The clamp is slightly opened, the needle is advanced a few millimeters, and the clamp is then gently closed to grasp the needle. The stylet is removed, and the monofilament suture is passed through the needle lumen. The assistant advances the suture as far as possible; the clamp is then gently opened, and the needle is withdrawn a few millimeters while maintaining tension on the suture to prevent it from backing out. The clamp is then closed to grasp the suture, which is retrieved through the interval between the radius and ulna. The same procedure is repeated for the second drill hole, resulting in a monofilament shuttle suture in each hole, passing from the anterior cortex of the radius and exiting posteriorly into the radioulnar space (Figure 6C).

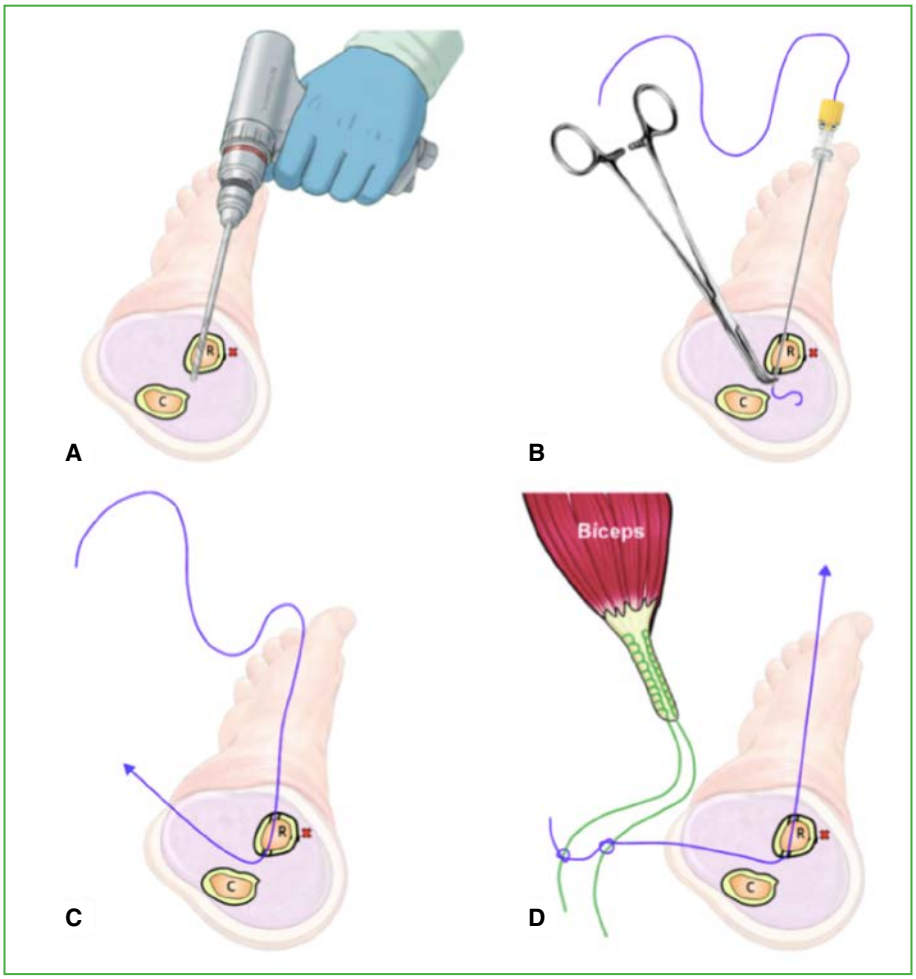

Figure 6. A. Drilling of the radial tuberosity with a 2-mm drill bit from anterior to posterior, angled 30° toward the ulna. The forearm is positioned in 45° supination. **B.** A strong monofilament suture (blue) is passed through a spinal needle and retrieved with a right-angle clamp from posterior into the radioulnar space. **C and D.** Monofilament shuttle suture in place, ready to pass the braided sutures (green) from the avulsed distal biceps tendon from posterior to anterior.
Red X = position of the posterior interosseous nerve; C = Ulna; R = radius. (Prepared by the authors.)

The avulsed distal biceps tendon is identified by digital proximal dissection, with the elbow flexed to bring the incision closer to the retracted tendon stump. Typically, a smooth anterior surface and a posterior surface can be distinguished, the latter often showing a lateral bundle (long head) and a medial bundle (short head). The tendon is secured using two Krackow locking sutures placed in a running fashion along each border, using high-strength flat braided nonabsorbable suture (No. 1.5 or 2), with the sutures overlapping so that the four free ends exit posteriorly 2–3 mm from the distal end of the tendon. This configuration provides a compressive effect, seating the tendon against its bony insertion site (Figure 7B). For a more anatomic repair, the external rotation of the tendon at its insertion must be considered: the long head inserts more proximally (superiorly) on the radial tuberosity, whereas the short head inserts more distally (inferiorly). Accordingly, the medial Krackow suture should be passed through the distal drill hole, and the lateral suture through the proximal drill hole, ensuring restoration of the tendon's native external rotation.[3,4] Intermediate sutures are passed one through each hole.

To pass the high-strength sutures through the radial drill holes, one end of each braided suture is tied to the posteromedial end of the monofilament shuttle suture previously passed through the radius (Figure 6D). Then, traction is applied to the monofilament from the anterior aspect, allowing the high-strength sutures to be shuttled from posterior to anterior. This process is repeated for the second hole. With the forearm in full supination and approximately 70° of flexion, an assistant applies traction to one pair of sutures, reducing the tendon onto the posteroulnar aspect of the radial tuberosity (Figure 7A). This reduction suture is maintained under tension while the surgeon ties the second high-strength suture over the anterior cortical bone bridge between the drill holes. The remaining suture is then tied over the same cortical bridge, completing the repair. After thorough irrigation and meticulous hemostasis, the wound is closed in layers, with skin closure only.

The mean operative time from skin incision to sling placement was 105.5 minutes (range 75-175; SD 32.12).

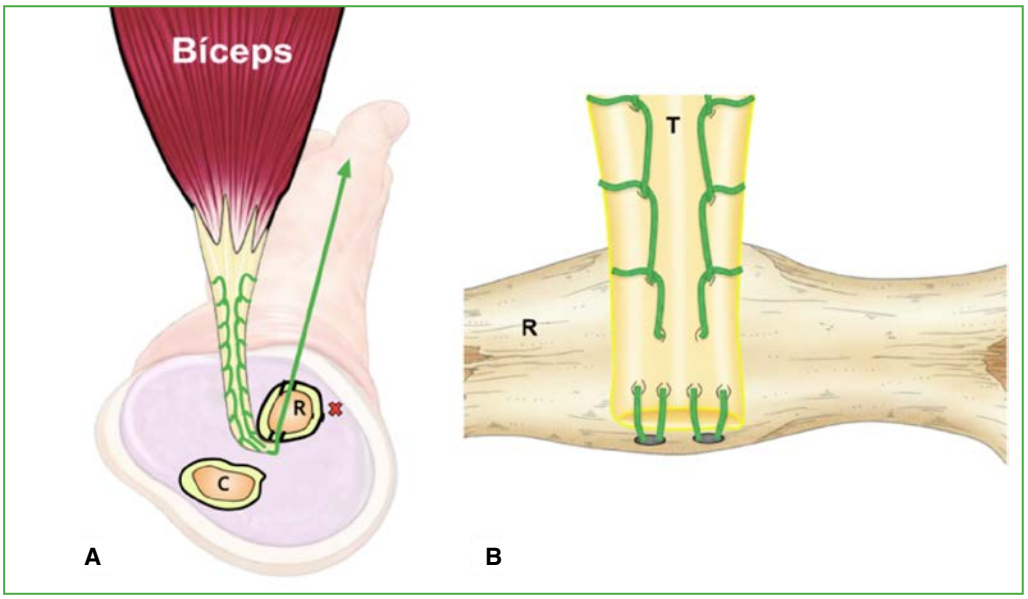

Figure 7. A. Traction on the anterior ends of the braided sutures reduces the distal biceps tendon, allowing the sutures to be tied over the anterior cortical bone bridge between the drill holes.
B. Posteromedial view of the bicipital tuberosity with the repaired tendon, demonstrating the compressive effect generated by posterior suture exit toward the bone. For proper anatomical orientation, the suture from the medial portion should be passed through the distal hole and the suture from the lateral portion through the proximal hole, restoring the native external rotation of the tendon.
C = Ulna; R = radius. (Prepared by the authors.)

Postoperative Protocol

A sling is applied with a short arm cast, with the elbow at 90° of flexion and the forearm in neutral rotation, for 10 days to reduce pain and edema. Passive range of motion is then initiated as tolerated, with limits of 30° of elbow extension and 30° of forearm rotation, while maintaining continuous sling use (removed only for exercises) until 4 weeks postoperatively. After this period, the sling is used only when going out and during sleep for an additional 2 weeks. At 6 weeks, the sling is discontinued and active range of motion is allowed, without resistance. Gradual and progressive strengthening is initiated at 12 weeks, and unrestricted use of the arm, according to tolerance, is permitted after 6 months.[12]

We reviewed the medical records of patients with at least 12 months of follow-up. Patients were evaluated using the QuickDASH score,[13] the visual analog scale (VAS) for pain,[14] and were asked whether they had returned to their pre-injury level of activity. The contralateral limb served as a control for assessing range of motion and subjective weakness. Patients were also asked whether their decision to undergo surgery was driven by functional or aesthetic concerns.

RESULTS

Eleven patients with postoperative follow-up >12 months were included. Eight reported undergoing surgery for both functional and aesthetic reasons, and three for functional reasons only. Eight of the repairs were performed on the dominant side. The mean follow-up was 35.5 months (range 12-53).

No differences were observed in pronation-supination or flexion-extension arcs compared with the contralateral side. Mean values were 138° of flexion, 3° of extension, 76° of pronation, and 75° of supination.

The mean QuickDASH score was 6.38 (range 2.7-13.6). The mean VAS score during exertion was 0.22/10 (range 0-2). Eight patients reported no postoperative symptoms. All patients returned to their usual work and sports activities, and were allowed to resume exertional activities 6 months after surgery.

The complications observed were as follows: two patients developed lateral antebrachial cutaneous nerve neuropraxia with transient symptoms that resolved after 4 months; and one patient developed a wound infection requiring surgical debridement and antibiotic therapy. This patient, who was also involved in a labor dispute, had the worst outcomes on the QuickDASH (13.6) and VAS (2/10 with exertion), and reported persistent subjective weakness.

In one patient with symptoms unrelated to the biceps tendon, postoperative magnetic resonance imaging of the elbow was performed. The images confirmed reinsertion of the tendon onto the posterior ulnar aspect of the radial tuberosity (Figure 8).

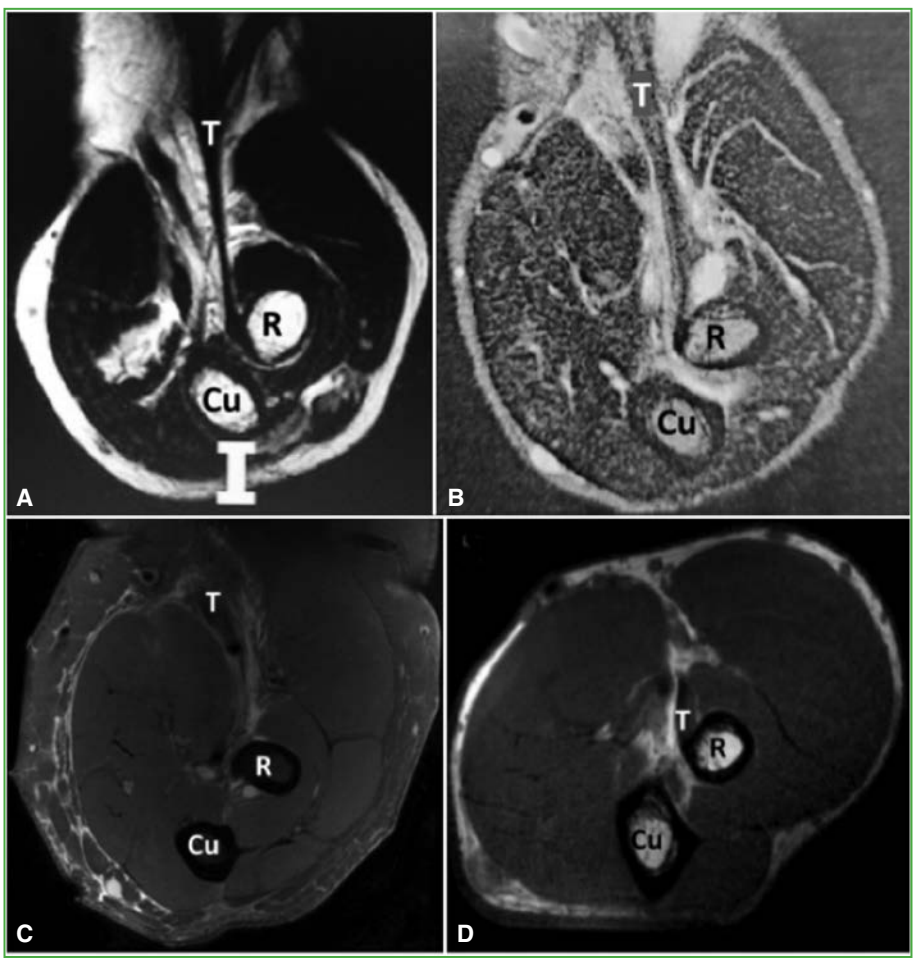

Figure 8. Magnetic resonance imaging of the proximal forearm, axial section at the level of the bicipital tuberosity, at different degrees of supination. **A**. 0° supination: normal insertion of the distal biceps tendon. **B**. 30° supination: partial tear of the distal biceps tendon. **C**. Maximum supination: complete avulsion of the distal biceps tendon. **D**. Reinsertion of the distal biceps tendon into the radial tuberosity using transosseous sutures in neutral pronosupination. Cu = Ulna; R = radius; T = distal biceps tendon.

DISCUSSION

The key to successful distal biceps tendon repair lies in a thorough understanding of regional anatomy. On the one hand, surgical exposure in the deep aspect of the elbow requires careful anticipation of the neurovascular structures encountered, allowing the surgeon to perform a safe and effective repair of the distal biceps tendon. On the other hand, accurate restoration of the native insertion footprint of the distal biceps tendon enables patients to achieve functional outcomes as close to normal as possible.

A crucial concept for understanding the supination function of the biceps is the generation of supination torque as a function of tendon position throughout forearm rotation. The native insertion of the distal biceps tendon wraps around the apex of the radial tuberosity, which plays a key biomechanical role by acting as a cam, displacing the line of pull away from the center of rotation of the radius and thereby enhancing supination strength.[3,7] Reinsertion of the distal biceps tendon is classically performed using either a single anterior approach or a two-incision technique.[5] Traditional anterior repairs (using suture anchors, interference screws, or cortical buttons), which fix the tendon to the anterior surface of the tuberosity, restore less than 10% of the native biceps footprint.[4] Schmidt et al. demonstrated that, in some cases, tendons repaired on the anterior surface of the radius may function as pronators near terminal supination.[3] Posterior repairs using the Boyd and Anderson two-incision technique may limit pronation and do not reproduce the additional cam effect of the radial tuberosity, as, during effective contraction, the tendon translates proximally and exerts its pull above the tuberosity.[4]

Maximal supination strength following both single-incision anterior and two-incision repairs may reach more than 90% of the contralateral side when assessed in mid-pronation; however, evaluation of supination strength throughout the full arc of forearm rotation is not commonly reported. In a study of anterior distal biceps repairs, a 33% deficit in supination strength was observed compared with the contralateral side when measured at 60° of supination.[3,6,7] In the technique used in our study, the biceps tendon is reattached to the posterior ulnar aspect of the radial tuberosity (Figure 6), thereby maximizing supination strength throughout all positions of forearm rotation.

From a clinical standpoint, both short- and long-term follow-up show no differences in mean outcome scores between the anterior approach and the two-incision technique. However, significantly more (minor) complications were observed in the single-incision group, primarily due to transient neuropraxias of the lateral antebrachial cutaneous nerve. Conversely, a higher incidence of significant loss of forearm rotation due to heterotopic ossification was observed with the two-incision approach.[5]

Aesthetics may play an important role, as many of our patients (8 of 11) acknowledged that it influenced their decision to undergo surgery. However, aesthetic outcomes are notably not included in commonly used instruments for evaluating elbow function.

Biomechanical studies evaluating various repair techniques have demonstrated the ability to withstand loads of 200-400 N, including those using transosseous tunnels similar to those employed in our technique.[3,6,7] This has encouraged us to initiate early active mobilization.

A simple cost analysis comparing the use of sutures alone with commercially available devices for distal biceps reinsertion reveals substantial cost savings with this technique. Furthermore, the implants used in distal biceps repair are not free from complications, such as osteolysis, migration, or failure of fixation systems (Figure 9).

Complications have been reported with all repair techniques, the most common being sensory nerve disturbances. In our series of 11 patients, two cases of transient neuropraxia of the lateral antebrachial cutaneous nerve were observed. Although the rate of re-tear remains unclear, such events have been reported; however, no cases were observed in our series at the time of study closure.

This study has several limitations, including the small sample size, retrospective design, absence of a control group, and reliance on subjective outcome measures. Another limitation is the lack of objective assessment of supination strength. In this regard, there is currently no consensus regarding the optimal method for evaluating forearm supination strength following distal biceps repair. Isotonic, isometric, and isokinetic methods have been described, and even within these categories, different testing parameters have been used.[3] Current outcome scoring systems also appear to have limitations and have not provided data that clearly differentiate between repair techniques.

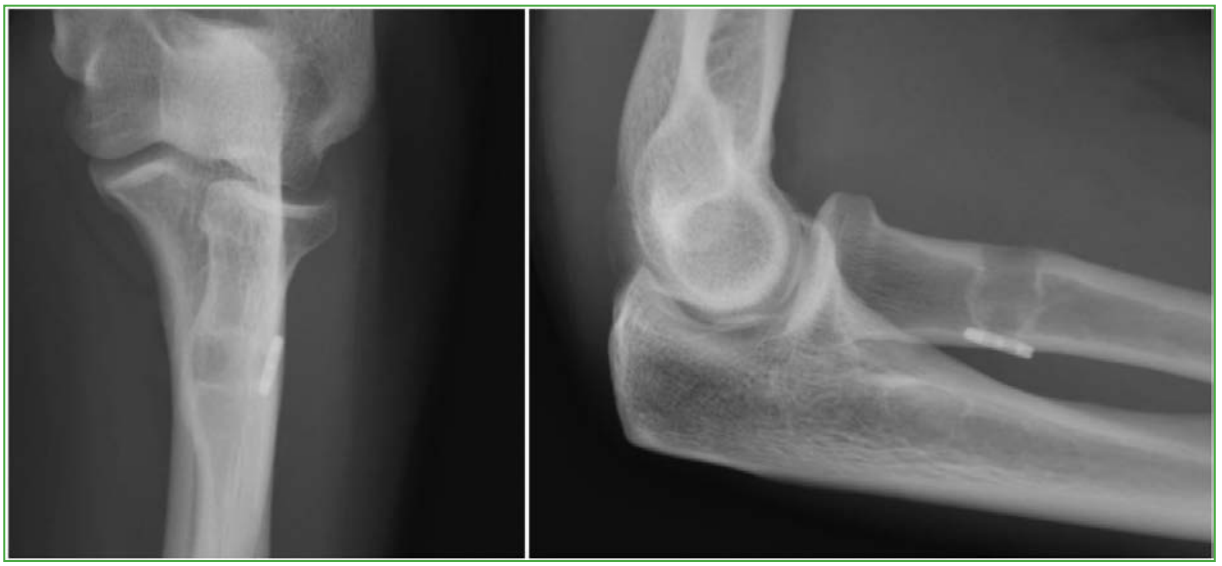

Figure 9. Anteroposterior and lateral elbow radiographs of a patient treated with a cortical button and interference screw for distal biceps repair. Note the marked osteolysis of the proximal radius, which may result in an area of bone weakness.

CONCLUSIONS

We describe a distal biceps repair technique that restores native insertion through an anterior approach. By reproducing the anatomical footprint, this technique may maximize supination strength without compromising range of motion. Additionally, by eliminating the need for anchors or specialized implants, the procedure is cost-effective and may preserve the structural integrity of the radius. However, further studies are required to evaluate the long-term outcomes of this technique and to compare it with other established surgical approaches.

Conflicts of interest: The authors declare no conflicts of interest.

S. Llumipanta ORCID ID: https://orcid.org/0009-0009-4869-1158
J. Carrizo ORCID ID: https://orcid.org/0009-0004-5706-7131
N. Villa ORCID ID: https://orcid.org/0009-0007-2984-2235
M. Deimundo ORCID ID: https://orcid.org/0000-0002-2822-4394
E. Gobbi ORCID ID: https://orcid.org/0000-0001-7310-6170

REFERENCES

1. Tjoumakaris FP, Bradley JP. Distal biceps injuries. *Clin Sports Med* 2020;39(3):661-72. https://doi.org/10.1016/j.csm.2020.02.004
2. Almigdad A, Saleem S, Malhas A. Distal biceps brachii rupture. *Clin Orthop Surg* 2025;17(2):267-73. https://doi.org/10.4055/cios24185
3. Schmidt CC, Weir DM, Wong AS, Howard M, Miller MC. The effect of biceps reattachment site. *J Shoulder Elbow Surg* 2010;19(8):1157-65. https://doi.org/10.1016/j.jse.2010.05.027
4. van den Bekerom MP, Kodde IF, Aster A, Bleys RL, Eygendaal D. Clinical relevance of distal biceps insertional and footprint anatomy. *Knee Surg Sports Traumatol Arthrosc* 2016;24(7):2300-7. https://doi.org/10.1007/s00167-014-3322-9

5. Castioni D, Mercurio M, Fanelli D, Cosentino O, Gasparini G, Galasso O. Single- versus double-incision technique for the treatment of distal biceps tendon rupture. *Bone Joint J* 2020;102-B(12):1608-17. https://doi.org/10.1302/0301-620X.102B12.BJJ-2020-0822.R2
6. Tanner C, Johnson T, Muradov P, Husak L. Single incision power optimizing cost-effective (SPOC) distal biceps repair. *J Shoulder Elbow Surg* 2013;22(3):305-11. https://doi.org/10.1016/j.jse.2012.10.044
7. Li J, Seiler LM, Hoekzema NA, Johnson TR, Lee J, Ridenauer JL, Tanner CM. Distal biceps reconstruction: a long-term follow-up of the complications and durability of the single-incision power optimizing cost-effective (SPOC) repair. *JSES Int* 2023;7(6):2547-52. https://doi.org/10.1016/j.jseint.2023.07.016
8. Tang JB. Re: Levels of experience of surgeons in clinical studies. *J Hand Surg Eur Vol* 2009;34(01):137-8. https://doi.org/10.1177/17531934097321
9. Zeltser DW, Strauch RJ. Vascular anatomy relevant to distal biceps tendon repair. *J Shoulder Elbow Surg* 2016;25(2):283-8. https://doi.org/10.1016/j.jse.2015.08.042
10. Arrigoni P, Cucchi D, Menon A, Guerra E, Nicoletti S, Colozza A, et al. The posterior interosseous nerve crosses the radial head midline and increases its distance from bony structures with supination of the forearm. *J Shoulder Elbow Surg* 2019;28(2):365-70. https://doi.org/10.1016/j.jse.2018.08.019
11. Ding DY, Ryan WE, Strauss EJ, Jazrawi LM. Chronic distal biceps repair with an Achilles allograft. *Arthrosc Tech* 2016;5(3):e525-9. https://doi.org/10.1016/j.eats.2016.02.016
12. Horschig A, Sayers SP, Lafontaine T, Scheussler S. Rehabilitation of a surgically repaired rupture of the distal biceps tendon in an active middle aged male: a case report. *Int J Sports Phys Ther* 2012;7(6):663-71. PMID: 23316429
13. Bersusky E, Arzac Ulla I, Loterzo L, Ricciardi GA, Zanotti G, Patiño J. Puntajes II. *Rev Asoc Argent Ortop Traumatol* 2022;87(3):447-53. https://doi.org/10.15417/issn.1852-7434.2022.87.3.1583
14. Vicente Herrero MT, Delgado Bueno S, Bandrés Moyá M, Ramírez Iñiguez de la Torre V, Capdevila García L. Valoración del dolor. Revisión comparativa de escalas y cuestionarios. *Rev Soc Esp Dolor* 2018;25(4):228-36. https://doi.org/10.20986/resed.2018.3632/2017

Modified Frailty Index as a Predictor of Postoperative Complications in Surgery for Pyogenic Spinal Infections

Guillermo A. Ricciardi,[*] Santiago Formaggin,[**] Ignacio Garfinkel,[**] Gabriel Carrioli,[**] Daniel Ricciardi[**]
[*]*Orthopedics and Traumatology Service, Hospital General de Agudos "Dr. Teodoro Álvarez", Autonomous City of Buenos Aires, Argentina*
[**]*Spine Team, Sanatorio Güemes, Autonomous City of Buenos Aires, Argentina*

ABSTRACT

Introduction: Pyogenic spinal infection is a potentially deadly and disabling condition with specific surgical indications. Its surgical management requires a precise risk-benefit assessment. Our objective was to evaluate the modified frailty index as a predictor of early postoperative complications in patients undergoing surgery for pyogenic spondylodiscitis. **Materials and Methods:** We conducted an observational, analytical, and retrospective study of patients who underwent surgery for pyogenic spondylodiscitis between 2022 and 2025. The association between the modified frailty index and the incidence of postoperative complications (classified according to Clavien-Dindo), as well as clinical, microbiological, and surgical variables, was analyzed. **Results:** Serious complications were recorded in 54.5% of patients, with a mortality rate of 13.6%. Bivariate analysis showed significant associations between serious complications and male sex, diabetes, cervical location, neurological deficit, and hypoalbuminemia. Although a modified frailty index ≥0.27 did not reach statistical significance as a categorical variable (p=0.082), its analysis as a continuous variable revealed a significantly higher value in the group with serious complications (p=0.006). **Conclusion:** Preoperative frailty, assessed by the modified frailty index as a continuous variable, was significantly associated with severe postoperative complications.
Keywords: Pyogenic spondylodiscitis; spinal infections; frailty; modified frailty index.
Level of Evidence: III

Índice de fragilidad modificado como predictor de complicaciones posoperatorias en cirugías de infecciones vertebrales piógenas

RESUMEN

Introducción: La infección vertebral piógena es una enfermedad potencialmente mortal e invalidante, y tiene indicaciones quirúrgicas precisas. El abordaje quirúrgico exige una adecuada relación riesgo-beneficio. Nuestro objetivo fue evaluar el índice de fragilidad modificado como predictor de complicaciones posoperatorias tempranas en pacientes sometidos a una cirugía por espondilodiscitis piógena. **Materiales y Métodos:** Estudio observacional, analítico y retrospectivo de pacientes operados por espondilodiscitis piógena entre 2022 y 2025. Se analizó la asociación entre el índice de fragilidad modificado y la ocurrencia de complicaciones posoperatorias clasificadas según Clavien-Dindo, junto con variables clínicas, microbiológicas y quirúrgicas. **Resultados:** El 54,5% de los pacientes sufrió complicaciones graves y la tasa de mortalidad fue del 13,6%. El análisis bivariado mostró una asociación significativa entre complicaciones graves y sexo masculino, diabetes, localización cervical, déficit neurológico e hipoalbuminemia. Aunque el índice de fragilidad modificado ≥0,27 no alcanzó significación como variable categórica (p = 0,082), su análisis como variable continua reveló un valor significativamente mayor en el grupo con complicaciones graves (p = 0,006). **Conclusión:** La fragilidad preoperatoria, evaluada mediante el índice de fragilidad modificado como variable continua, se asoció significativamente con complicaciones graves posoperatorias.
Palabras clave: Espondilodiscitis piógenas; infecciones vertebrales; fragilidad; índice de fragilidad modificado.
Nivel de Evidencia: III

Received on October 9th, 2025. Accepted after review on March 10th, 2026 • Dr. GUILLERMO A. RICCIARDI • guillermoricciardi@gmail.com https://orcid.org/0000-0002-6959-9301
How to cite this article: Ricciardi GA, Formaggin S, Garfinkel I, Carrioli G, Ricciardi D. Modified Frailty Index as a Predictor of Postoperative Complications in Surgery for Pyogenic Spinal Infections. *Rev Asoc Argent Ortop Traumatol* 2026;91(2):138-150. https://doi.org/10.15417/issn.1852-7434.2026.91.2.2232

INTRODUCTION

Pyogenic vertebral infections comprise a group of clinical conditions that may involve the spine, including the intervertebral disc, vertebral body, epidural space, paravertebral muscles, psoas muscle, and facet joints.[1] The term *spondylodiscitis* is used to describe infections affecting both the intervertebral disc and the vertebral body. It accounts for 3–5% of all cases of osteomyelitis, and its incidence ranges from 1:100,000 to 1:250,000 inhabitants in developed countries.[2]

This is a potentially life-threatening disease associated with the risk of neurological compromise and severe sequelae. In this context, early diagnosis and targeted antibiotic therapy are essential to achieve therapeutic success. Surgical treatment, in turn, is an alternative with well-defined indications, including neurological compromise, hemodynamic instability secondary to sepsis, local deformity, mechanical instability, failure of conservative treatment, and the presence of a compressive epidural abscess.[3–5]

When spinal surgery is required, the clinical context may influence both timing and surgical strategy, as spondylodiscitis is more common in patients with chronic diseases and risk factors such as diabetes, cardiovascular disease, intravenous drug use, renal failure, chronic dialysis, and cancer.[1,2,6–8] Additionally, older adults represent a particularly vulnerable group.[1-3] Therefore, the indication for surgery requires careful risk–benefit assessment, aiming to provide treatment that is both effective and safe.

Frailty is a syndrome characterized by an age-related decline in physiological reserve and reduced resilience to stressors, leading to adverse health outcomes.[9] Frailty has recently gained importance as a predictor of complications in spine surgery, particularly in adult spinal deformity procedures and in cases of vertebral metastases requiring surgical treatment.[9-12]

Despite its relevance, controversies persist regarding its clinical definition and how it should be assessed. The modified Frailty Index (mFI), described by Velanovich et al., is one of the most widely used tools,[10] and has proven to be a reliable predictor of complications in surgery for vertebral tumors.[11,12] However, there are few specific reports in the context of pyogenic vertebral infections.[13] Vettivel et al. reported a series of 76 cases of pyogenic spondylodiscitis, including 30 surgically treated patients, in which the mFI was associated with 30-day mortality in the bivariate analysis but was not a significant predictor in the multivariable analysis.[13]

The aim of this study was to evaluate the mFI as a predictor of early postoperative complications in patients undergoing surgery for pyogenic vertebral infections.

MATERIALS AND METHODS

An observational, analytical, retrospective cohort study was conducted in patients diagnosed with pyogenic spondylodiscitis who underwent surgery between April 1, 2022, and April 1, 2025, by a single surgical team at a high-complexity tertiary care center in the Autonomous City of Buenos Aires.

A non-probability purposive sample was obtained, including all patients who underwent surgery for pyogenic spondylodiscitis. Patients >18 years of age with a diagnosis of pyogenic spondylodiscitis were included according to the criteria proposed by the Infectious Diseases Society of America (IDSA, 2015) clinical practice guidelines, which recommend integration of clinical, radiological, and microbiological findings.[14] The diagnosis was confirmed when the patient presented with axial pain accompanied by compatible magnetic resonance imaging findings and at least one positive culture (blood culture, percutaneous aspirate, or intraoperative sample), or when there was a favorable clinical course under empiric antibiotic therapy in the absence of another identifiable infectious focus. As imaging criteria, T2 hyperintensity of the disc and post-gadolinium enhancement of the adjacent vertebral bodies and intervertebral disc were considered characteristic.[1–3,14]

Additional inclusion criteria were surgical treatment of the vertebral infection with therapeutic intent (decompression, stabilization, or both) and a minimum postoperative clinical follow-up of 30 days.

The indication for surgery was established by the surgical team of our institution based on clinical care criteria, in accordance with indications formally documented in the literature. Surgery was indicated in the presence of neurological compromise, clinical or radiological progression of the disease, or recurrence despite adequate antimicrobial therapy. The presence of actual or potential mechanical instability was also considered, defined by radiological findings such as vertebral collapse >50%, evident translation, or segmental kyphosis >25°.[15]

Additional inclusion criteria were surgical treatment of the vertebral infection with therapeutic intent (decompression, stabilization, or both) and a minimum postoperative clinical follow-up of 30 days.

The indication for surgery was established by the surgical team of our institution based on clinical care criteria, in accordance with indications formally documented in the literature. Surgery was indicated in the presence of neurological compromise, clinical or radiological progression of the disease, or recurrence despite adequate antimicrobial therapy. The presence of actual or potential mechanical instability was also considered, defined by radiological findings such as vertebral collapse >50%, evident translation, or segmental kyphosis >25°. Table 1 presents the Clavien–Dindo classification validated for complications in spine surgery.[16] The following outcome measures were also evaluated: length of hospital stay; white blood cell count and acute-phase reactants at discharge; consolidation or fusion of the involved segment at the last available follow-up (according to radiographs or computed tomography); and evolution of neurological status.

Table 1. Classification of complications according to Clavien-Dindo

Grade	Definition
I	Any deviation from the normal postoperative course without the need for pharmacological, surgical, endoscopic, or radiological treatment. Analgesics, antipyretics, antiemetics, diuretics, electrolytes, and physical therapy are permitted.
II	Requires pharmacological treatment with drugs other than those permitted in Grade I. Includes transfusions and parenteral nutrition.
IIIa	Requires surgical, endoscopic, or radiological intervention without general anesthesia.
IIIb	Requires intervention under general anesthesia.
IVa	Potentially life-threatening complication requiring management in the Intensive Care Unit; single-organ dysfunction.
IVb	Potentially life-threatening complication with multiorgan dysfunction.
V	Death

The primary independent variable was the mFI-11, which includes the 11 variables described in Table 2.[9] A cut-off value of ≥0.27 was used, based on previous studies evaluating risk of complications in spine surgery.[10]

Other variables with potential predictive value for postoperative complications were also recorded: 1) clinical-demographic variables: age (years), sex (male/female), nutritional status (serum albumin level), immunocompromised status (pharmacologic immunosuppression, active neoplastic disease, human immunodeficiency virus infection), Charlson Comorbidity Index, and ASA (American Society of Anesthesiologists) score;[17,18] 2) microbiological variables: type of isolated pathogen, presence of multidrug-resistant organisms (resistance to 3 or more antibiotic classes), empiric treatment initiated, and duration of antibiotic therapy; 3) vertebral infection characteristics: number of affected foci (single vs. multiple), presence of epidural or paravertebral abscess on imaging, anatomical level involved (cervical, thoracic, lumbar), presence and type of neurological deficit according to the American Spinal Injury Association classification (complete/incomplete), duration of the deficit in hours, presence of mechanical instability (vertebral collapse >50%, kyphosis >25°, evident translation), recurrence or clinical/radiological progression during antibiotic treatment, and Pola classification type;[15] 4) surgical variables: type of surgery performed (decompression alone or instrumented surgery), surgical approach (anterior, posterior, or combined), number of instrumented vertebrae, operative time (minutes), and use of coated implants (nanosilver); 5) preoperative laboratory values: hemoglobin, albumin, total white blood cell count ($\times 10^3/mm^3$), platelet count, coagulopathy (defined as International Normalized Ratio >1.5 or prolonged activated partial thromboplastin time), C-reactive protein, and erythrocyte sedimentation rate; 6) preoperative life support: requirement for mechanical ventilation or vasoactive drugs (inotropes) within 24 hours prior to surgery.

Table 2. Variables of the Modified Frailty Index-11 (mFI-11)

Variable
Functional dependence
History of diabetes mellitus
History of chronic obstructive pulmonary disease (COPD)
History of congestive heart failure
History of acute myocardial infarction
History of percutaneous coronary intervention, coronary artery bypass grafting, or angina
Hypertension requiring medication
History of cerebrovascular accident or transient ischemic attack
History of cognitive impairment or dementia
Peripheral vascular disease or intermittent claudication
History of cerebrovascular disease with residual deficit

The mFI-11 is calculated by assigning one point for each present comorbidity. The total score is divided by 11 to obtain a value between 0 and 1. For example, if a patient has 3 of the 11 listed conditions, their mFI-11 will be 0.27.

Statistical Analysis

Categorical variables are presented as absolute and relative frequencies (n and %) and were compared using the χ^2 test or Fisher's exact test, as appropriate. Continuous variables were analyzed according to their distribution, assessed with the Shapiro-Wilk normality test. Variables with a normal distribution are presented as mean and standard deviation (SD) and were compared using Student's *t* test for independent samples. Variables with a non-normal distribution are presented as median and interquartile range (IQR) and were compared using the Mann-Whitney *U* test. A p value <0.05 was considered statistically significant. Statistical analysis was performed using IBM SPSS Statistics (version 25).

RESULTS

A total of 22 patients who underwent surgery for pyogenic spondylodiscitis were included. Mean age was 62.36 years (SD ± 10.918; range 32-81), and 13 (59.1%) were men and 9 (40.9%) were women. All patients had at least one comorbidity; the median Charlson Comorbidity Index was 4 points (IQR 2.75-5.25). Most patients were classified as ASA III or IV (n = 20; 90.9%). Diabetes was the most frequent comorbidity (n = 15; 68.2%) (Table 3).

Table 3. Clinical variables and laboratory parameters

	Mean	Standard deviation	Median	25th percentile	75th percentile
Axillary temperature (°C)	36.5	0.7	36.3	36.0	37.1
Hemoglobin (g/dL)	10.9	1.8	10.8	10.4	11.3
Albumin (g/dL)	2.93	0.56	2.90	2.50	3.30
White blood cells (x10³/mm³)	19190	36883	11375	8470	13820
Urea	49.8	32.9	38.0	23.6	71.0
Creatinine	.94	0.47	0.88	0.60	1.12
CRP (mg/L)	321.3	537.7	115.8	36.3	160.0
ESR (mm/h)	73	31	81	55	97

CRP = C-reactive protein; ESR = erythrocyte sedimentation rate.

The most frequently isolated pathogen was *Staphylococcus aureus* (n = 11; 50%), followed by *Pseudomonas aeruginosa* (n = 4; 18.1%) and *Escherichia coli* (n = 2; 9%). One patient had a polymicrobial infection (*P. aeruginosa* + *K. pneumoniae*) (Figure 1).

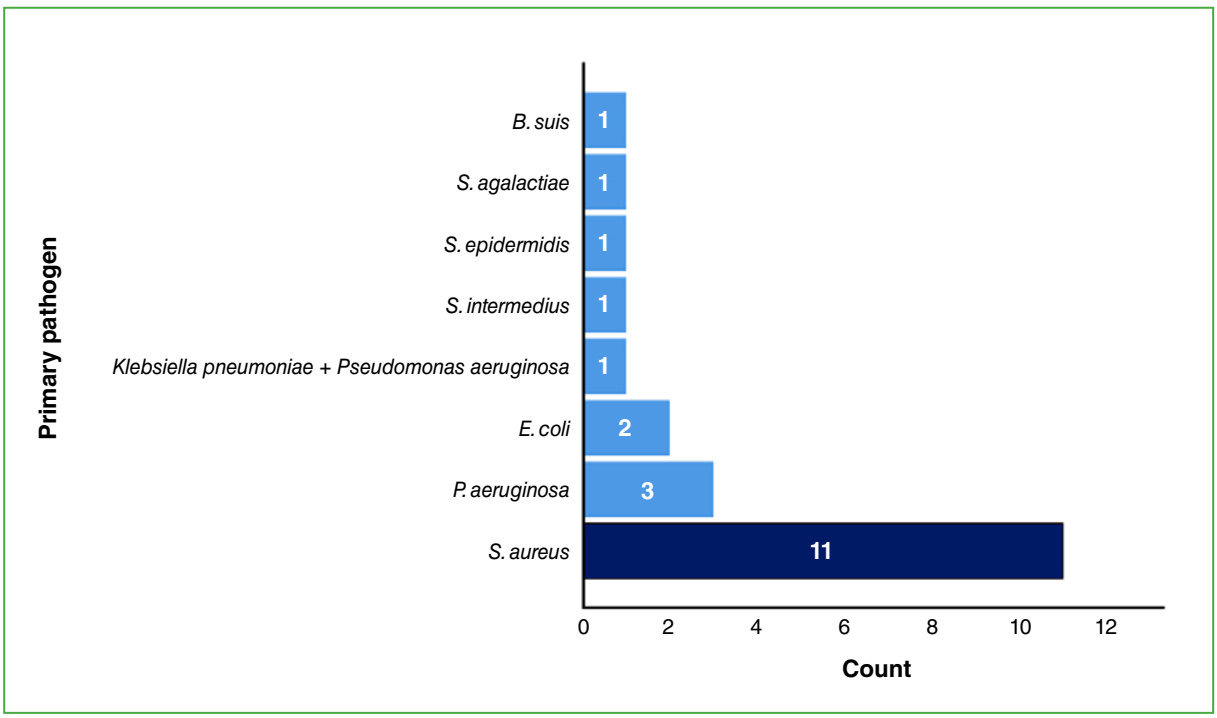

Figure 1. Bar chart showing the distribution of etiologies.

Four patients (18.2%) had multidrug-resistant strains. Empiric antibiotic therapy was used in most cases (n = 19; 86.4%), with subsequent adjustment of the regimen according to the identified etiology. Median duration of antibiotic treatment was 8 weeks (IQR 8–12). In one patient, no pathogen was isolated. In four patients (18.2%), the organism was isolated from a computed tomography-guided aspiration sample. Only nine patients (40.9%) had undergone prior computed tomography-guided aspiration, with a diagnostic yield of 44.4%. Surgical cultures were positive in 10 cases (45.5%), blood cultures in 12 (54.5%), and in two patients (9.1%), the pathogen was isolated from samples obtained during debridement of the index procedure.

Thoracic spondylodiscitis was the most frequent location (n = 11; 50%), followed by lumbar (n = 7; 31.8%) and cervical (n = 4; 18.2%). Infection most commonly involved a single vertebral segment (n = 17; 77.3%). Associated epidural abscess was observed in 19 patients (86.4%), paravertebral abscess in 14 (63.6%), and psoas abscess in four (18.2%). More than half of the patients had a neurological deficit (n = 15; 68.1%): six (27.3%) were complete and nine (40.9%) were incomplete. In most cases (85.7%), symptom duration at the time of surgery was >72 hours (median 13.5 days; IQR 7–33.25).

Criteria for mechanical instability were identified in 15 patients (68.2%), and in four cases (18.2%), surgery was indicated after failure of initial conservative antibiotic treatment. According to the Pola classification, the most frequent type was C (n = 18; 81.8%). Figure 2 shows the distribution of cases according to the Pola classification.

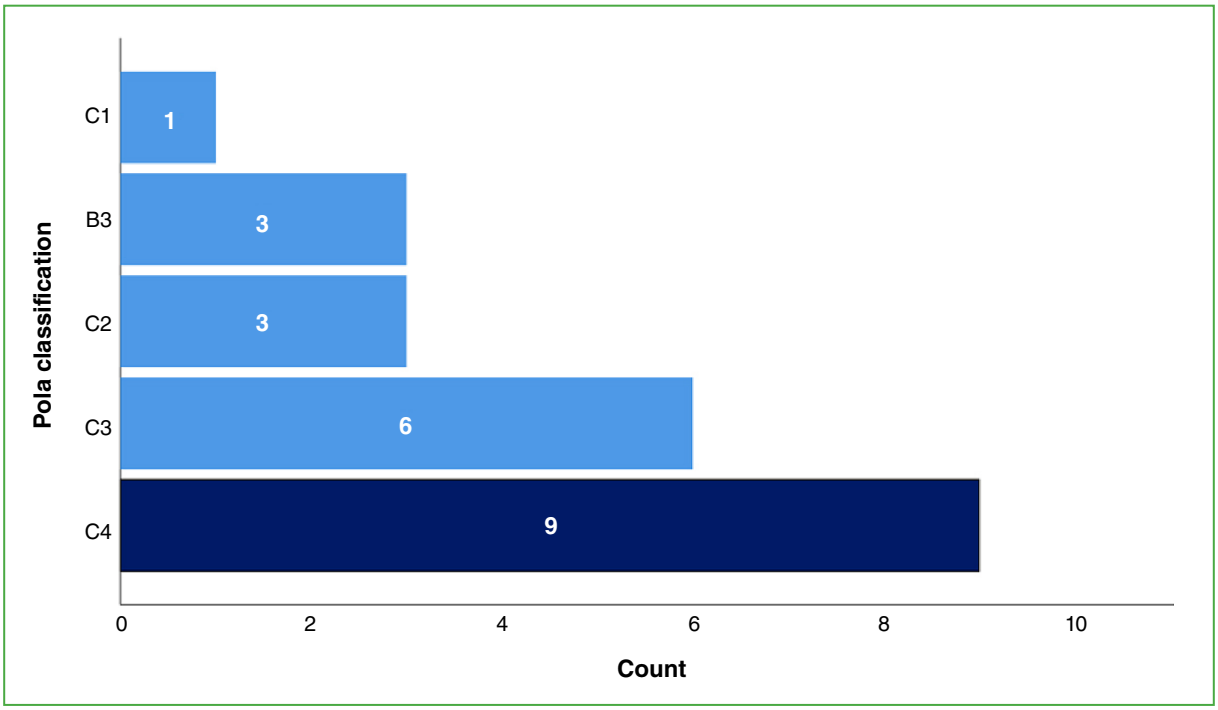

Figure 2. Bar chart showing the distribution of patients according to the Pola classification.

On admission, only one patient had an axillary temperature >38 °C (median 36.2 °C; IQR 36.0-37.1). Most patients were anemic (n = 17; 77.3%), and 10 (45.5%) had impaired renal function. Additionally, 13 (59.1%) had serum albumin levels consistent with malnutrition. Less than half presented with leukocytosis at admission (n = 10; 45.5%). In contrast, acute-phase reactants were elevated in all patients. None required vasoactive support or mechanical ventilation prior to surgery. Clinical and laboratory variables are detailed in Table 3.

Nineteen of the 22 patients (86.4%) underwent decompression combined with arthrodesis, while three (13.6%) underwent isolated decompression with drainage and surgical debridement. In most cases, a single conventional posterior approach was used (n = 17; 77.3%). In four cases (18.2%) with cervical involvement, an exclusive anterior approach with corpectomy was performed, and one patient (4.5%) with involvement of the lumbosacral junction was treated using a combined approach. In four of the 19 instrumented arthrodesis cases (21%), a nanosilver-coated implant was used. Surgical indications are detailed in Figure 3; notably, several patients met more than one indication for surgery. The median number of instrumented levels was 5 (IQR 3–7). Mean operative time was 152.14 minutes (SD ± 56.5).

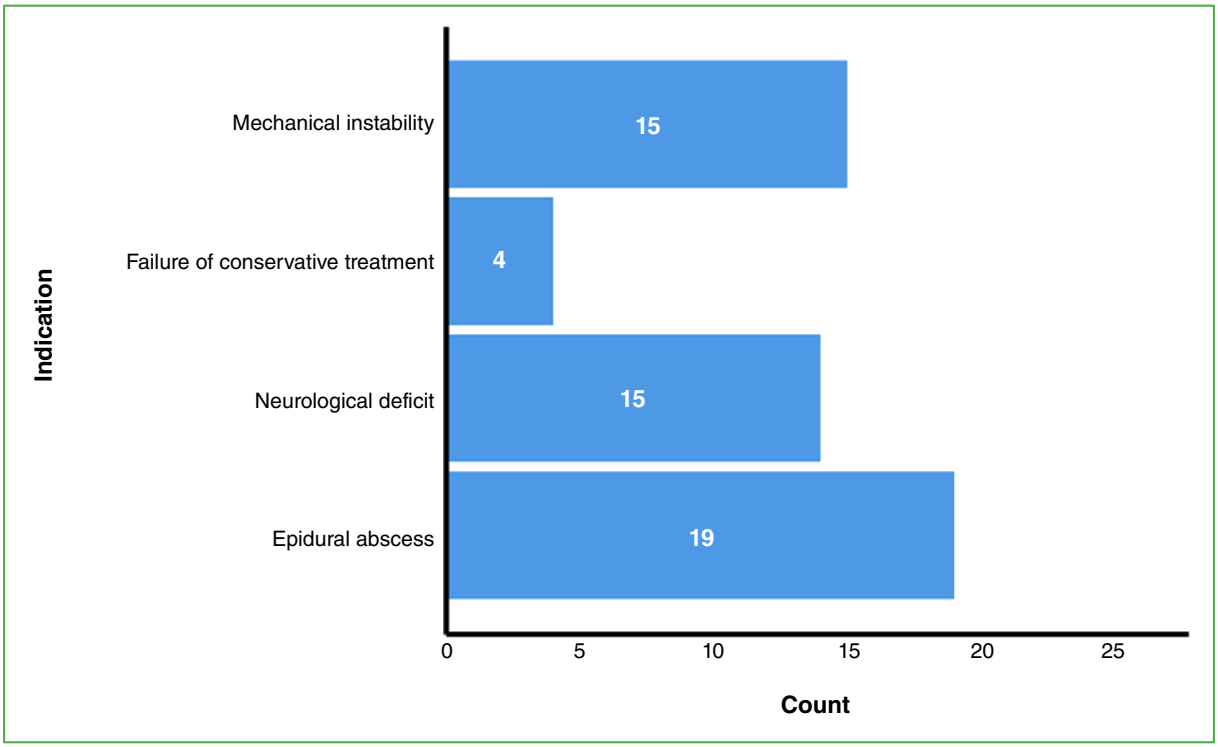

Figure 3. Horizontal bar chart showing the number of patients by surgical indication.

A total of 40 complications were recorded in 22 patients, classified according to severity using the Clavien-Dindo scale (Table 4).

During the postoperative period, 12 patients (57.1%) experienced at least one complication of grade III or higher. When mild complications (grade II or lower) were also considered, 18 patients (81.8%) experienced at least one adverse event. The most frequent severe complications were septic shock (n = 3; 13.6%), persistent infection requiring surgical debridement (n = 3; 13.6%), and heart failure (n = 3; 13.6%). These were followed by pneumonia (n = 2; 9.1%), implant-related complications (one case of loosening and one of mechanical failure; n = 2; 9.1%), and *C. difficile* infection (n = 2; 9.1%).

When comparing the occurrence of complications according to mFI-11, nine patients had a high frailty status (mFI-11 >0.27; i.e., ≥3 positive frailty variables). The median mFI-11 was 0.18 (moderate frailty; IQR 0.09–0.27). The presence of severe postoperative complications (Clavien-Dindo grade ≥III) was significantly associated with male sex (83.3% vs. 30%; p = 0.027), diabetes (58.3% vs. 40%; p = 0.020), cervical involvement (33.3% vs. 0%; p = 0.016), neurological deficit at admission (91.7% vs. 30%; p = 0.005), and serum albumin levels <3.2 mg/dL (83.3% vs. 33.3%; p = 0.029). A non-significant trend toward a higher comorbidity burden was also observed (median Charlson score: 4.5 vs. 3; p = 0.093).

Table 4. Complications*

Complication	Total	Clavien-Dindo <3	Clavien-Dindo 3 or higher
SIADH	4	4	0
Pressure injuries	4	2	2
Persistent infection	3	0	3
Urinary tract infection	3	0	2
Septic shock	3	0	3
Acute kidney injury	3	2	1
Heart failure	3	0	3
Instrument-related complications	2	0	2
Pneumonia	2	0	2
Deep vein thrombosis	2	2	0
Clostridium difficile infection	2	0	2
Hepatotoxicity	1	1	0
Bicytopenia	1	1	0
Gastrointestinal bleeding	1	0	1
COVID-19	1	1	0
Partial intestinal obstruction	1	1	0
Cognitive impairment	1	1	0
Septic arthritis	1	0	1
Epistaxis	1	0	1
Spondylodiscitis	1	0	1
Total	40	11	14

SIADH = Syndrome of Inappropriate Antidiuretic Hormone secretion.
*40 complications in 22 patients.

Preoperative frailty as a categorical variable (mFI-11 ≥0.27: 58.3% vs. 20%; p = 0.082) was associated with severe complications, although this did not reach statistical significance. However, when mFI-11 was analyzed as a non-parametric continuous variable using the Mann-Whitney U test, a significantly higher median value was observed in the group with severe complications [0.27 (IQR 0.18-0.33) vs. 0.09 (IQR 0.00-0.20); p = 0.006] (Figure 4).

No significant differences were found with respect to age, type of surgery, presence of abscesses, microbiological isolation, or preoperative white blood cell count. Median length of hospital stay was 55 days (IQR 37-75), median intensive care unit (ICU) stay was 3.5 days (IQR 2-14), and median clinical follow-up was 246.5 days (IQR 102-726). No significant differences in follow-up duration were observed according to the presence or absence of severe complications (291 vs. 226.5 days; p = 0.923). However, patients who developed severe complications required a significantly longer ICU stay (median 6 vs. 2 days; p = 0.009) and a longer total hospital stay, with borderline statistical significance (57.5 vs. 40 days; p = 0.050). No association was found between overall or ICU length of stay and the degree of preoperative frailty.

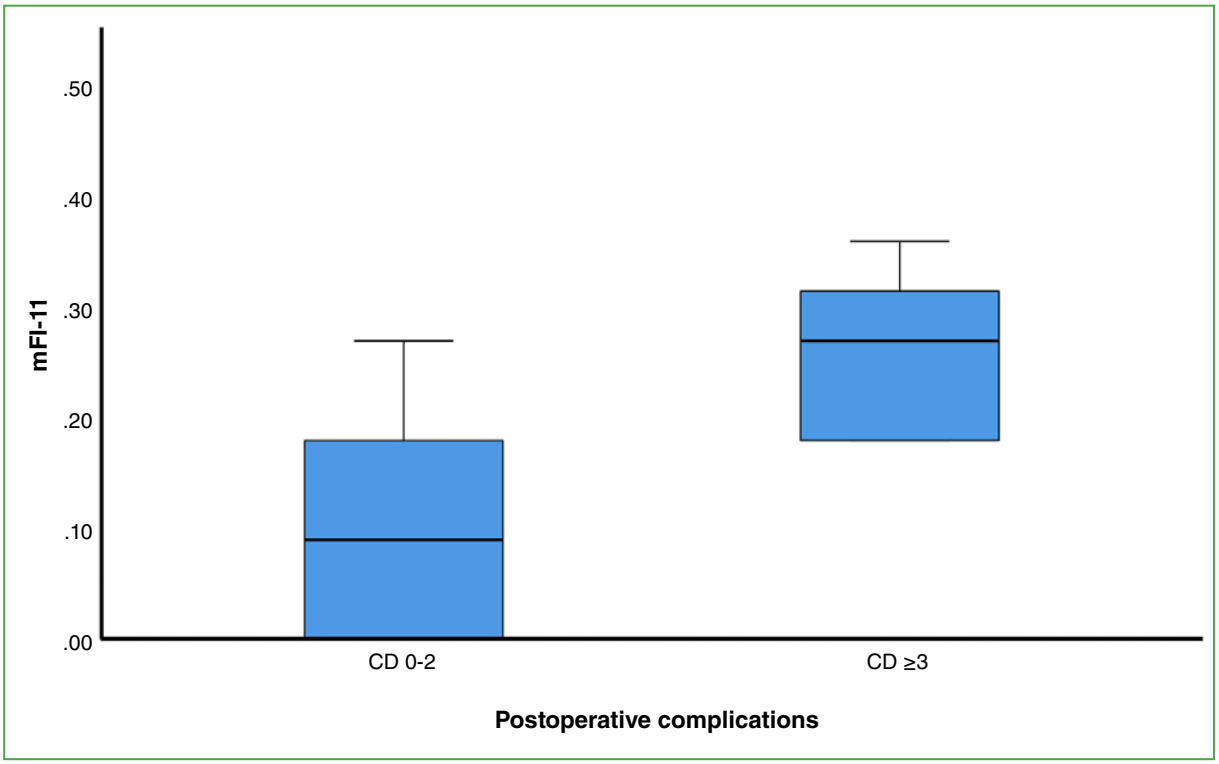

Figure 4. Box plot showing the distribution of mFI-11 values according to the presence of complications.

The mortality rate was 13.6% (n = 3). Among the remaining patients, fusion of the involved segment at 90 days was confirmed in 52.6% of cases (10 of 19 patients) (Figure 5). During hospitalization, inflammatory markers decreased significantly. Median white blood cell count decreased from 10,640/mm³ (IQR 8,037-13,332) at admission to 6,986/mm³ (IQR 5,130-11,741) at discharge (p = 0.04). Similarly, erythrocyte sedimentation rate decreased from 78.5 mm/h (IQR 43.7-96.7) to 32.5 mm/h (IQR 21.7-53.7) (p = 0.013), and C-reactive protein decreased from a median of 89.9 mg/L (IQR 23.2-160) to 10.2 mg/L (IQR 4.1-56.7) (p = 0.005). Neurological improvement of at least one grade on the ASIA scale was documented in 9 of 15 patients (60%) (Figure 6).

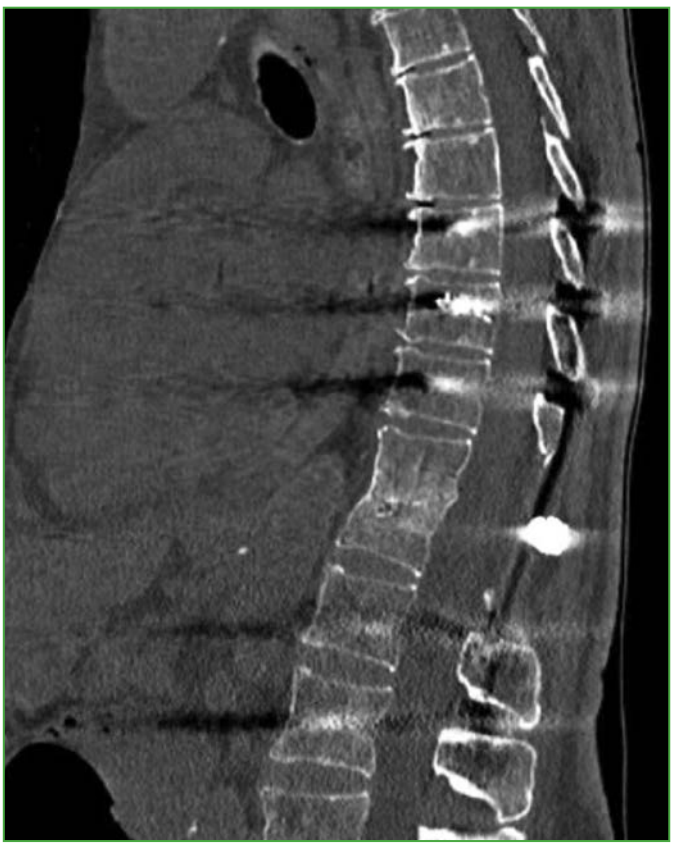

Figure 5. Sagittal computed tomography scan of the thoracic spine, 90 days after the onset of thoracic spondylodiscitis, showing segmental fusion and spinal stability.

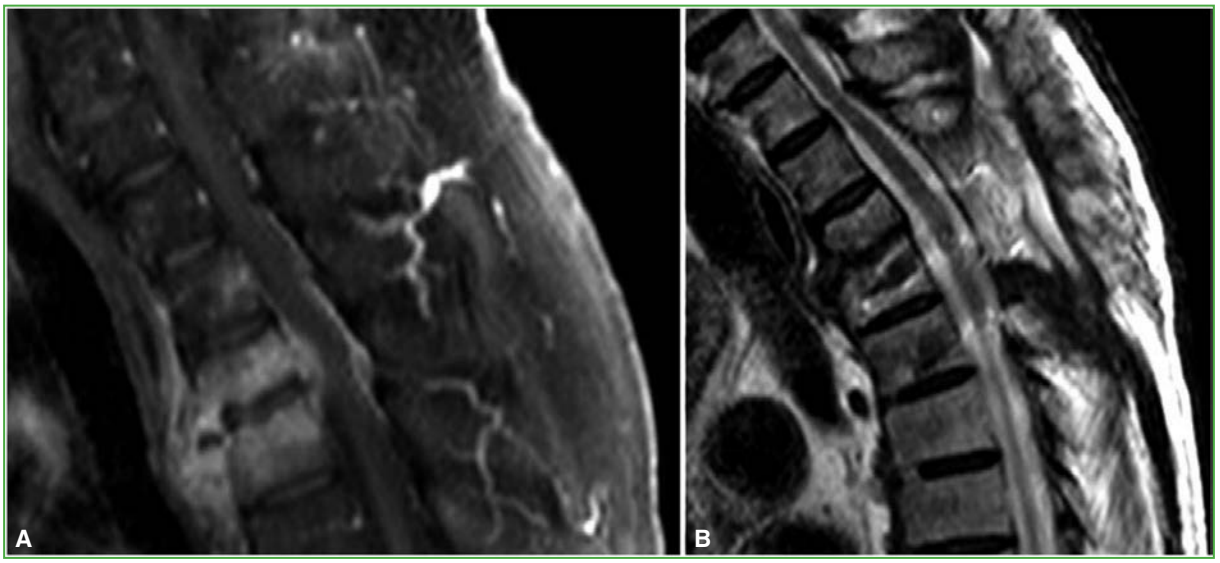

Figure 6. Magnetic resonance imaging of the thoracic spine in a patient with spondylodiscitis complicated by an epidural abscess and spinal cord involvement, at admission (**A**) and one year later (**B**). **A.** Contrast-enhanced T1-weighted sequence showing the characteristic enhancement of spondylodiscitis, with involvement of the intervertebral disc space, adjacent vertebral bodies, anterior paravertebral soft tissues, and epidural space. **B.** T2-weighted sequence at 1-year follow-up showing resolution of the abscess, decompression of the spinal cord, and no signal abnormalities. These findings correlate with complete neurological recovery from an incomplete spinal cord injury.

DISCUSSION

Pyogenic spondylodiscitis is a severe and potentially devastating disease that predominantly affects vulnerable populations, in whom multiple risk factors have been identified, including intravenous drug use, immunosuppression, and clinical frailty. Mortality rates of up to 20% have been reported in some series.[19] In our cohort of surgically treated patients, those with severe frailty accounted for a considerable proportion and were characterized by a high burden of comorbidities, a high rate of severe complications (54.5%), and early mortality (13.6%).

The morbidity and mortality associated with this condition are partly related to neurological involvement, epidural space invasion, and, in cases of severe structural damage, mechanical instability.[1,2,5] Our cohort consisted predominantly of patients with advanced disease: more than half presented with neurological deficits at admission (n = 15; 68.1%), and 85.7% underwent surgery after more than 72 hours of symptom evolution. In addition, 15 patients (68.2%) met criteria for mechanical instability. The occurrence of severe complications was significantly associated with preoperative neurological deficit (p = 0.005).

Although the surgical indication for spondylodiscitis remains a matter of debate in certain aspects, there is consensus in the literature regarding its fundamental role in cases of instability, neurological compression, or failure of antibiotic therapy. This underscores the need for a careful risk-benefit assessment when determining surgical timing and indication. In this context, several studies have sought to identify predictors of postoperative complications.[20–23] In addition, various scoring systems have been developed to predict complications in this patient population, although their predictive performance remains limited.[24] Bazán et al. proposed a morphological classification of epidural abscesses that helps guide therapeutic planning.[25]

In a series of 143 surgically treated patients, Ukon et al. identified the following factors associated with severe complications: a high Charlson Comorbidity Index, chronic lung disease, diabetes, Gram-negative infection, pyogenic osteoarthritis, leukocytosis, and preoperative thrombocytopenia.[20,21] Pola et al., in a cohort of 207 patients (47 of whom underwent surgery), reported negative blood cultures, neurological deficit at diagnosis, and underlying endocarditis as negative prognostic factors.[22] Camino-Willhuber et al. analyzed 627 patients who underwent surgery for pyogenic spondylodiscitis using the American College of Surgeons National Surgical Quality Improvement Program (ACS-NSQIP) database, a validated multicenter source for surgical outcomes research.[23] They reported a complication rate of 14.6%, a readmission rate of 9.4%, and a reoperation rate of 6.2%. The most frequent complications were wound infection, pneumonia, septic shock, and death (1.8%). Hypoalbuminemia and the need for dialysis were associated with increased perioperative morbidity and mortality.

Consistent with previous findings, in our cohort, severe complications were significantly associated with male sex (83.3% vs. 30%; p = 0.027), diabetes (58.3% vs. 40%; p = 0.020), cervical involvement (33.3% vs. 0%; p = 0.016), preoperative neurological deficit (91.7% vs. 30%; p = 0.005), and hypoalbuminemia (<3.2 mg/dL; 83.3% vs. 33.3%; p = 0.029). A non-significant trend toward a higher comorbidity burden was also observed in the group with severe complications (median Charlson score: 4.5 vs. 3; p = 0.093).

Numerous studies have identified preoperative frailty as a predictor of complications and mortality in patients with spinal disease, particularly in settings such as vertebral metastases, deformities, and degenerative conditions. However, its role has been less extensively studied in spinal infections.[13] In our series, preoperative frailty showed a relevant association with severe complications. Although the categorical analysis of the mFI-11 (≥0.27) demonstrated only a non-significant trend (58.3% vs. 20%; p = 0.082), when analyzed as a continuous variable, patients with severe complications had a markedly higher median mFI-11, with a statistically significant difference. This finding suggests that quantitatively assessed frailty may represent a useful prognostic marker for anticipating postoperative adverse events in this population.

Our findings, in line with the available literature, suggest that specific risk factors may help identify patients at increased risk of severe complications. Future studies should evaluate whether emerging technologies, such as minimally invasive or percutaneous approaches, may reduce surgical trauma and, consequently, complication rates in this complex setting.[26–28]

This study has limitations inherent to its retrospective design and small sample size. Nevertheless, it provides relevant findings regarding the role of frailty as a risk factor in the surgical treatment of pyogenic spondylodiscitis, an aspect that remains insufficiently explored in adult spinal infections.

CONCLUSIONS

In patients with pyogenic spondylodiscitis undergoing surgery, preoperative frailty was significantly associated with a higher rate of severe complications, particularly when analyzed as a continuous variable. These findings support the need for a comprehensive patient assessment that includes frailty indices to optimize surgical decision-making and timing in this vulnerable population.

Conflict of interest: The authors declare no conflicts of interest.

S. Formaggin ORCID ID: https://orcid.org/0000-0002-7103-2937
I. Garfinkel ORCID ID: https://orcid.org/0000-0001-9557-0740
G. Carrioli ORCID ID: https://orcid.org/0000-0003-4160-9712
D. Ricciardi ORCID ID: https://orcid.org/0009-0002-1586-4904

REFERENCES

1. Boody BS, Tarazona DA, Vaccaro AR. Evaluation and management of pyogenic and tubercular spine infections. *Curr Rev Musculoskelet Med* 2018;11(4):643-52. https://doi.org/10.1007/s12178-018-9523-y
2. Duarte RM, Vaccaro AR. Spinal infection: state of the art and management algorithm. *Eur Spine J* 2013;22(12):2787-99. https://doi.org/10.1007/s00586-013-2850-1
3. Rutges JP, Kempen DH, van Dijk M, Oner FC. Outcome of conservative and surgical treatment of pyogenic spondylodiscitis: a systematic literature review. *Eur Spine J* 2016;25(4):983-99. https://doi.org/10.1007/s00586-015-4318-y
4. Taylor DG, Buchholz AL, Sure DR, Buell TJ, Nguyen JH, Chen CJ, et al. Presentation and outcomes after medical and surgical treatment versus medical treatment alone of spontaneous infectious spondylodiscitis: a systematic literature review and meta-analysis. *Global Spine J* 2018;8(4 Suppl):49S-58S. https://doi.org/10.1177/2192568218799058
5. Blecher R, Frieler S, Qutteineh B, Pierre CA, Yilmaz E, Ishak B, et al. Who needs surgical stabilization for pyogenic spondylodiscitis? Retrospective analysis of non-surgically treated patients. *Global Spine J* 2023;13(6):1550-7. https://doi.org/10.1177/21925682211039498
6. Babic M, Simpfendorfer CS. Infections of the spine. *Infect Dis Clin North Am* 2017;31(2):279-97. https://doi.org/10.1016/j.idc.2017.01.003
7. Guerado E, Cerván AM. Surgical treatment of spondylodiscitis: an update. *Int Orthop* 2012;36(2):413-20. https://doi.org/10.1007/s00264-011-1441-1
8. Moskven E, Charest-Morin R, Flexman AM, Street JT. The measurements of frailty and their possible application to spinal conditions: a systematic review. *Spine J* 2022;22(9):1451-71. https://doi.org/10.1016/j.spinee.2022.03.010
9. Velanovich V, Antoine H, Swartz A, Peters D, Rubinfeld I. Accumulating deficits model of frailty and postoperative mortality and morbidity: its application to a national database. *J Surg Res* 2013;183(1):104-10. https://doi.org/10.1016/j.jss.2013.01.021
10. Kweh BTS, Lee HQ, Tan T, Tew KS, Leong R, Fitzgerald M, et al. Risk stratification of elderly patients undergoing spinal surgery using the modified frailty index. *Global Spine J* 2023;13(2):457-65. https://doi.org/10.1177/21925682221094053
11. Matsuo T, Kanda Y, Sakai Y, Yurube T, Takeoka Y, Miyazaki K, et al. Modified frailty index as a novel predictor for the incidence and severity of postoperative complications after spinal metastases surgery. *Bone Joint J* 2024;106-B(12):1469-76. https://doi.org/10.1302/0301-620X.106B12.BJJ-2024-0100.R1

12. Xu ZY, Hao XY, Wu D, Song QY, Wang XX. Prognostic value of 11-factor modified frailty index in postoperative adverse outcomes of elderly gastric cancer patients in China. *World J Gastrointest Surg* 2023;15(6):1093-103. https://doi.org/10.4240/wjgs.v15.i6.1093
13. Vettivel J, Bortz C, Passias PG, Baker JF. Pyogenic vertebral column osteomyelitis in adults: analysis of risk factors for 30-day and 1-year mortality in a single-center cohort study. *Asian Spine J* 2019;13(4):608-14. https://doi.org/10.31616/asj.2018.0295
14. Berbari EF, Kanj SS, Kowalski TJ, Darouiche RO, Widmer AF, Schmitt SK, et al. 2015 Infectious Diseases Society of America clinical practice guidelines for the diagnosis and treatment of native vertebral osteomyelitis in adults. *Clin Infect Dis* 2015;61(6):e26-46. https://doi.org/10.1093/cid/civ482.
15. Pola E, Autore G, Formica VM, Pambianco V, Colangelo D, Cauda R, et al. New classification for the treatment of pyogenic spondylodiscitis: validation study on a population of 250 patients with a 2-year follow-up. *Eur Spine J* 2017;26(Suppl 4):479-88. https://doi.org/10.1007/s00586-017-5043-5
16. Dindo D, Demartines N, Clavien PA. Classification of surgical complications: a new proposal with evaluation in a cohort of 6336 patients and results of a survey. *Ann Surg* 2004;240(2):205-13. https://doi.org/10.1097/01.sla.0000133083.54934.ae
17. Charlson ME, Pompei P, Ales KL, MacKenzie CR. A new method of classifying prognostic comorbidity in longitudinal studies: development and validation. *J Chronic Dis* 1987;40(5):373-83. https://doi.org/10.1016/0021-9681(87)90171-8
18. Mayhew D, Mendonca V, Murthy BVS. A review of ASA physical status: historical perspectives and modern developments. *Anaesthesia* 2019;74(3):373-9. https://doi.org/10.1111/anae.14569
19. Rawall S, Hiatt LA, Rajaram SM, Theiss S. Management of pyogenic spondylodiscitis in adults. *J Am Acad Orthop Surg* 2025;33(22):1257-64. https://doi.org/10.5435/JAAOS-D-24-01088
20. Ukon Y, Takenaka S, Makino T, Kashii M, Iwasaki M, Sakai Y, et al. Preoperative risk factors affecting outcome in surgically treated pyogenic spondylodiscitis. *Global Spine J* 2023;13(8):2201-9. https://doi.org/10.1177/21925682221077918
21. Ukon Y, Takenaka S, Hirai H, Sugiura T, Sakai Y, Fujimori T, et al. Establishment of scoring to predict severe complication after pyogenic spondylodiscitis surgery. *Clin Spine Surg* 2025;38(8):353-9. https://doi.org/10.1097/BSD.0000000000001756
22. Pola E, Taccari F, Autore G, Giovannenze F, Pambianco V, Cauda R, et al. Multidisciplinary management of pyogenic spondylodiscitis: epidemiological and clinical features, prognostic factors and long-term outcomes in 207 patients. *Eur Spine J* 2018;27(Suppl 2):229-36. https://doi.org/10.1007/s00586-018-5598-9
23. Camino-Willhuber G, Franklin A, Rosecrance K, Oyadomari S, Chan J, Holc F, et al. Preoperative hypoalbuminemia and dialysis increase morbidity/mortality after spine surgery for primary pyogenic spinal infections (ACS-NSQIP study). *Surg Neurol Int.* 2022;13:193. https://doi.org/10.25259/SNI_330_2022
24. Gamada H, Funayama T, Ogata Y, Setojima Y, Nakagawa T, Sunami T, et al. Challenges and limitations of the existing scoring systems for postoperative outcomes in thoracolumbar pyogenic spondylitis: a multicenter retrospective cohort study. *Eur Spine J* 2025;34(10):4717-27. https://doi.org/10.1007/s00586-025-08933-7
25. Bazán PL, Godoy Adaro AO, Padini E, Casco EA, Maruñak M. Aspectos morfológicos del absceso epidural espinal piógeno. *Rev Asoc Argent Ortop Traumatol* 2023;88(2):148-55. https://doi.org/10.15417/issn.1852-7434.2023.88.2.1513ID
26. Youn MS, Shin JK, Goh TS, Lee JS. Minimally invasive percutaneous endoscopic treatment for acute pyogenic spondylodiscitis following vertebroplasty. *Eur Spine J* 2018;27(Suppl 3):458-64. https://doi.org/10.1007/s00586-018-5478-3
27. Tong YJ, Liu JH, Fan SW, Zhao FD. One-stage debridement via oblique lateral interbody fusion corridor combined with posterior pedicle screw fixation in treating spontaneous lumbar infectious spondylodiscitis: a case series. *Orthop Surg* 2019;11(6):1109-19. https://doi.org/10.1111/os.12562
28. Madhavan K, Vanni S, Williams SK. Direct lateral retroperitoneal approach for the surgical treatment of lumbar discitis and osteomyelitis. *Neurosurg Focus* 2014;37(2):E5. https://doi.org/10.3171/2014.6.FOCUS14150

Osteopoikilosis ("Spotted Bone Disease"): A Benign Bone Finding. A Case Report

Víctor A. Avendaño Arango,[*] Ricardo Londoño García,[*] Gustavo A. Molina,[**] Laura Moreno,[#] Miguel A. Murcia Hernández[**]
[*]*Universidad Pontificia Bolivariana, Medellín, Colombia*
[**]*Oncologic Orthopedics Department, Hospital Pablo Tobón Uribe, Medellín, Colombia*
[#]*Universidad Pontificia Javeriana, Cali, Colombia*

ABSTRACT
We report the case of a woman with osteopoikilosis who was evaluated by the orthopedic oncology service due to blastic lesions in the left proximal femur identified on pelvic radiography and increased uptake on bone scintigraphy. The patient reported a one-year history of polyarthralgia of unknown origin, with pain in the spine, hips, and knees, which worsened during the menstrual cycle and when ascending or descending stairs. Magnetic resonance imaging of the pelvis and left femur was performed, confirming the findings. **Conclusion:** Osteopoikilosis is a rare benign sclerosing bone dysplasia; however, lack of awareness of this condition may lead to unnecessary invasive studies and emotional distress. This case is presented to raise awareness of its existence and its importance as a differential diagnosis of malignant diseases.
Keywords: Osteopoikilosis; Albers-Schoenberg disease; benign bone tumor.
Level of Evidence: IV

Osteopoiquilosis, "la enfermedad de los huesos manchados": un hallazgo óseo benigno. A propósito de un caso clínico

RESUMEN
Se comunica el caso de una mujer con osteopoiquilosis, evaluada en el Servicio de Ortopedia Oncológica, por presentar lesiones blásticas en el fémur proximal izquierdo detectadas en una radiografía de pelvis e hipercaptación en la gammagrafía ósea. La paciente refirió que, desde hacía un año, tenía poliartralgias de origen desconocido, dolor en la columna, las caderas y las rodillas, que se exacerbaba con el ciclo menstrual, y al bajar y subir escaleras. Se solicitó una resonancia magnética de pelvis y de fémur izquierdo, con la que se confirmaron los hallazgos. **Conclusiones:** La osteopoiquilosis es una displasia ósea esclerosante benigna con una baja incidencia; sin embargo, desconocer esta enfermedad lleva a indicar estudios invasivos y a generar un malestar emocional. Se presenta este caso clínico con la intención de concientizar sobre su existencia y la importancia como diagnóstico diferencial de enfermedades malignas.
Palabras clave: Osteopoiquilosis; enfermedad de Albers-Schoenberg; tumor óseo benigno.
Nivel de Evidencia: IV

INTRODUCTION

Osteopoikilosis, also known as disseminated condensing osteopathy, is an autosomal dominant disorder associated with heterogeneous mutations in the LEMD3 gene, which encodes a protein of the inner nuclear membrane. It was first described by Heinrich Albers-Schönberg in 1915 and is currently recognized as a rare condition, with an estimated prevalence of 1 in 50,000 individuals.[1] In some studies, mutations have been identified in familial cases of osteopoikilosis.[2] Its incidence is similar in both sexes, it can occur at any age, and it primarily affects the epiphyses of long bones. It has three patterns of presentation: spotted, striated, and mixed.

Most patients are asymptomatic; only 20% experience symmetric joint pain and edema.[2,3] Additionally, 25%

Received on October 18th, 2024. Accepted after evaluation on May 2nd, 2025 • Dr. VÍCTOR A. AVENDAÑO ARANGO • avendano7245@gmail.com https://orcid.org/0000-0002-2976-3269
How to cite this article: Avendaño Arango VA, Londoño García R, Molina GA, Moreno L, Murcia Hernández MA. Osteopoikilosis ("Spotted Bone Disease"): A Benign Bone Finding. A Case Report. *Rev Asoc Argent Ortop Traumatol* 2026;91(2):151-156. https://doi.org/10.15417/issn.1852-7434.2026.91.2.2050

may present with other conditions, such as cardiac disease, dacryocystitis, and renal and endocrine malformations. It may occur in isolation or in association with melorheostosis (hyperostosis of the cortical bone of tubular bones resembling dripping candle wax over the surface of long bones, usually unilateral and asymmetric), dermatofibrosis lenticularis disseminata, forming Buschke-Ollendorff syndrome,[4] or with Gardner syndrome, which includes osteopoikilosis and colonic polyposis.[5]

From a radiological standpoint, it is characterized by multiple small (2–3 mm), well-defined, round or ovoid radiodense sclerotic lesions. Histologically, focal areas of compact lamellar bone are observed within cancellous bone.[3,5]

For this reason, the diagnosis is usually incidental. It should be emphasized that the condition does not undergo malignant transformation or affect bone strength, and it does not require specific treatment.[1,6] To differentiate it from metastatic disease, its distribution must be considered, as it involves long bones as well as phalanges, carpal bones, metacarpals, tarsal bones, and the pelvis, with a symmetrical pattern but uneven distribution, and only rarely involves the skull, ribs, clavicles, and vertebrae. In addition, there is no evidence of bone destruction.[5,6] Its course is typically benign, and most patients remain asymptomatic, with diagnosis often being incidental. However, associations between osteopoikilosis and other malformations, such as duplicated ureter, coarctation of the aorta, precocious puberty, and exostoses, have been reported.[7]

The aim of this article is to highlight the characteristics of this condition and how it differs from metastatic disease, with emphasis on avoiding unnecessary invasive procedures, which may cause significant emotional distress for patients and impose an economic burden on the healthcare system.

CASE REPORT

A 30-year-old woman presented with bilateral knee pain radiating to the left thigh, with a one-year history. She also reported occasional thoracolumbar spine pain that worsened during the menstrual cycle and when climbing or descending stairs. Additionally, she described a nonspecific sensation of decreased strength.

Bilateral radiographs of the pelvis and femurs were obtained, revealing rounded, bead-like sclerotic lesions in both femurs, without signs of malignancy (Figure 1).

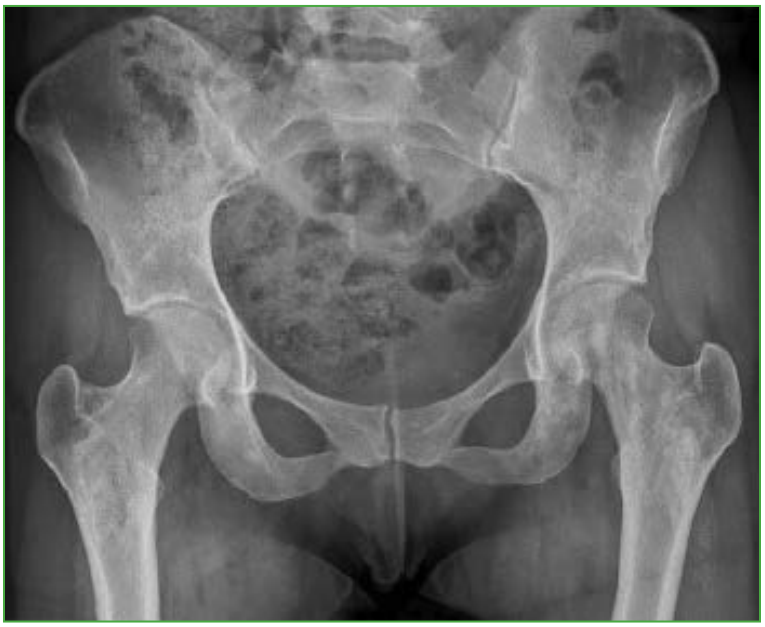

Figure 1. Anteroposterior radiograph of the pelvis showing multiple rounded sclerotic foci measuring <1 cm in the cancellous bone of the proximal femur and pelvis, sparing the cortex, with no periosteal reaction.

Magnetic resonance imaging showed multiple millimetric punctate lesions, hypointense on both T1- and T2-weighted sequences, predominantly visible on T1-weighted images. These lesions were bilateral and relatively symmetrical, involving the lower right limb, mainly at the periarticular level in the distal knee region. They had ill-defined margins, with no associated edema, expansile effect, or contrast enhancement (Figures 2 and 3).

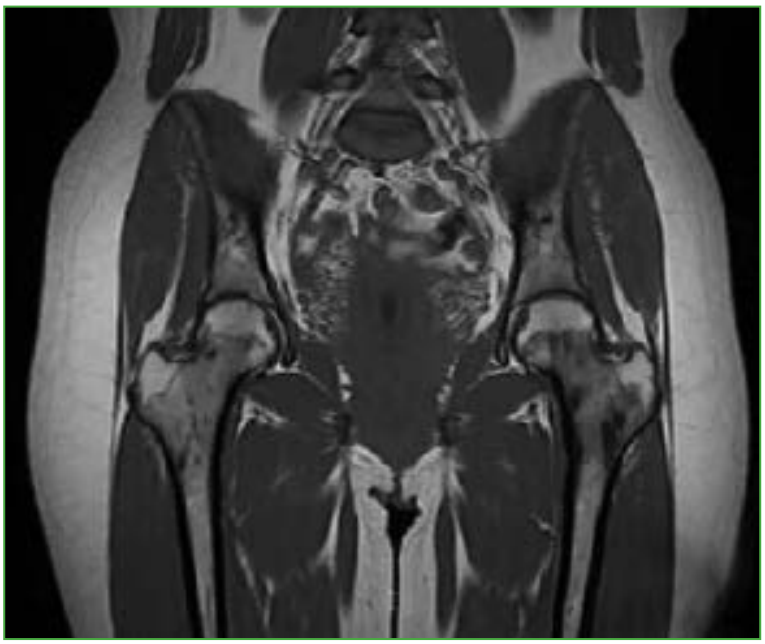

Figure 2. Magnetic resonance imaging of the pelvis, coronal section, T1-weighted sequence, showing multiple small hypointense lesions in the proximal femur.

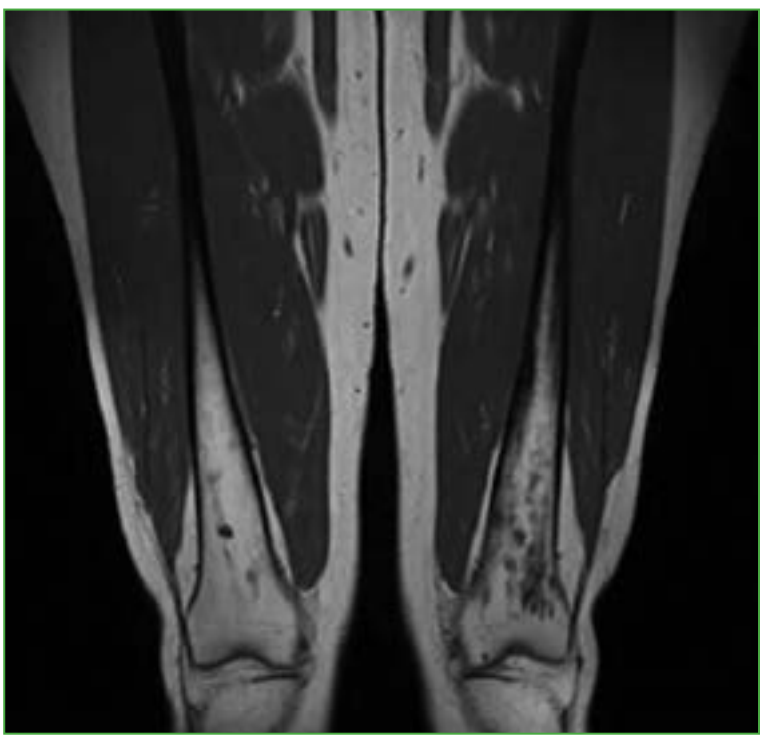

Figure 3. Magnetic resonance imaging of the distal femur, coronal section, T1-weighted sequence, showing multiple small hypointense lesions.

A bone scintigraphy was also performed, demonstrating areas of increased uptake consistent with osteopoikilosis (Figure 4).

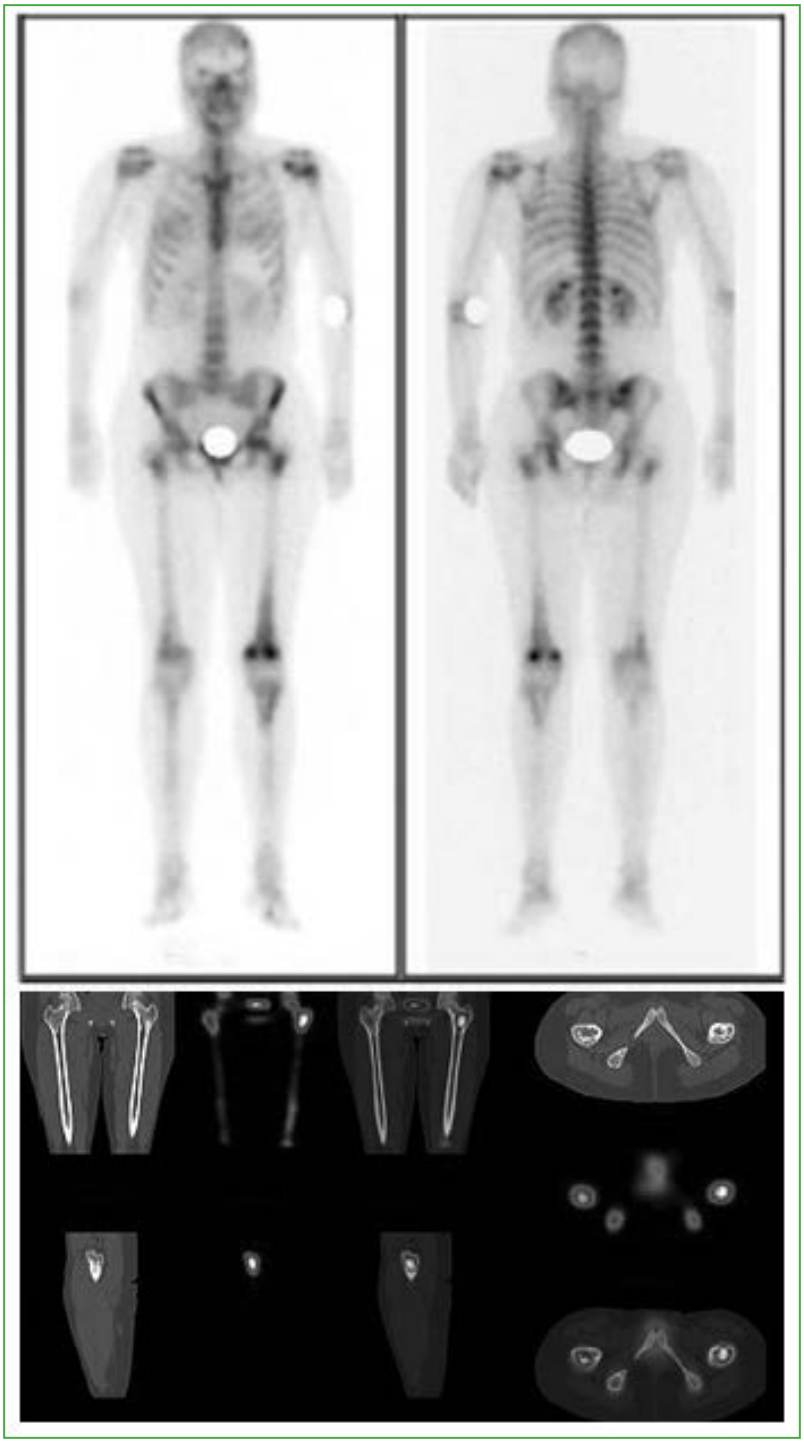

Figure 4. Bone scintigraphy showing areas of increased uptake in the bilateral proximal humeri, pelvis, and proximal and distal femora.

Based on these findings, the patient was evaluated by the Orthopedic Oncology Service, where left patellofemoral pain and hip pain on rotation were identified, along with right-sided hyporeflexia.

A discrepancy between the clinical presentation and imaging findings was noted. A consultation with the Rheumatology Department was requested, and comparative follow-up radiographs of the spine, pelvis, and femurs were obtained. These showed normal bone density, preserved joint relationships, and well-defined radiodense lesions in the distal femur and bilateral proximal tibia, more pronounced on the left side. There was no bone expansion, cortical disruption, or soft tissue component, and no changes compared with the previous study.

DISCUSSION

On magnetic resonance imaging, osteopoikilosis may appear as multiple benign bone islands distributed throughout the axial and appendicular skeleton, appearing as small hypointense lesions on both T1- and T2-weighted images.[6] These findings are attributed to a failure of resorption of secondary cancellous bone and are typically clustered around large joints.[7,8] In our patient, the main characteristic features (symmetrical involvement of long bones) were present, and clinical suspicion was confirmed by the imaging studies. However, one of the most important differential diagnoses is osteoblastic metastases, as well as Erdheim-Chester disease.[7,8] Therefore, bone scintigraphy was required to rule out findings such as osteolysis or periosteal reaction suggestive of malignancy and to exclude these diagnostic possibilities.[9] It should also be emphasized that the radiological findings of osteopoikilosis are sufficiently characteristic to avoid misdiagnosis and prevent unnecessary invasive procedures, such as biopsy.[10]

Patients with osteopoikilosis may also be associated with autoimmune disorders, as the LEMD3 gene influences the expression of transforming growth factor β1, a modulator of immune responses. Therefore, a thorough clinical examination and detailed medical history are warranted, along with referral to the Rheumatology Department to rule out such conditions. In our patient, the clinical findings did not correlate with the imaging findings, which prompted interdisciplinary evaluation.

It should be noted that this condition may predispose to excessive fibrous tissue formation, which may increase the risk of joint stiffness and disability following surgical procedures. Therefore, early diagnosis and appropriate follow-up are essential.[6]

Currently, there is no consensus regarding treatment. Some studies suggest the use of nonsteroidal anti-inflammatory drugs for pain management. Analgesics, such as acetaminophen, and opioids may also be used.[11]

CONCLUSIONS

It is essential to recognize osteopoikilosis to avoid misdiagnosis as a malignant condition, and to ensure timely referral for multidisciplinary evaluation to rule out associated autoimmune disorders.

Conflicts of interest: The authors declare no conflicts of interest.

R. Londoño García ORCID ID: https://orcid.org/0000-0002-6568-9166
G. A. Molina ORCID ID: https://orcid.org/0009-0007-3351-2298
L. Moreno ORCID ID: https://orcid.org/0009-0006-6429-7722
M. A. Murcia Hernández ORCID ID: https://orcid.org/0009-0006-8611-8625

REFERENCES

1. Lewis M. Skeletal displasias and related conditions. In: Buikstra JE. *Ortner's Identification of Pathological Conditions in Human Skeletal Remains*. London, UK: Academic Press; 2019, chapter 18. https://doi.org/10.1016/B978-0-12-809738-0.00018-1
2. Mukai T, Morita Y. Osteopoikilosis. *Rheumatology* 2022;61(2):879-80. https://doi.org/10.1093/rheumatology/keab436
3. Mohsenpour B, Ahmadi A. Osteopoikilosis: a case report. *J Med Case Rep* 2023;17(1):292. https://doi.org/10.1186/s13256-023-04025-6
4. Pendino JC, Navas MDL, Sasia G. Osteopoikilosis: an incidental finding. *Medicina (B Aires)* 2023;83(6):1030. PMID: 38117729
5. Nascimento AF, Araújo FC. Osteopoikilosis – the importance of recognizing a rare but benign bone disorder. *ARP Rheumatol* 2022;1(2):177-8. PMID: 35810377
6. Fu L, Tian C, Zeng X. Cinematic rendering of osteopoikilosis. *Rheumatology (Oxford)* 2024;63(7):e206-e207. https://doi.org/10.1093/rheumatology/keae234
7. Syrycka J, Kubicka E, Polowczyk B, Bolanowska-Tyszko A, Podgajny Z, Bolanowski M. Low back pain and osteosclerotic bone lesions suggestive of metastases: a mask of osteopoikilosis. *Pol Arch Intern Med* 2020;130(3):249-51. https://doi.org/10.20452/pamw.15158
8. Goyal G, Young JR, Abeykoon JP, Shah MV, Bennani NN, Sartori-Valinotti JC, et al. Impact of a multidisciplinary tumor board on the care of patients with histiocytic disorders: The Histiocytosis Working Group experience. *Oncologist* 2022;27(2):144-8. https://doi.org/10.1093/oncolo/oyab031
9. Woyciechowsky TG, Monticielo MR, Keiserman B, Monticielo OA. Osteopoikilosis: what does the rheumatologist must know about it? *Clin Rheumatol* 2012;31(4):745-8. https://doi.org/10.1007/s10067-011-1916-x
10. Ozdemirel AE, Burcu DC, Erdem HR, Koc B. A rare benign disorder mimicking metastasis on radiographic examination: a case report of osteopoikilosis. *Rheumatol Int* 2011;31(8):1113-6. https://doi.org/10.1007/s00296-010-1664-2
11. Appenzeller S, Castro GR, Coimbra IB. Osteopoikilosis con gammagrafía ósea anormal: seguimiento a largo plazo. *J Clin Rheumatol* 2007;13:291-2. https://doi.org/10.1097/RHU.0b013e318156d987

Management of Radial Shaft Nonunion with Fixation Failure Using the Masquelet Technique: A Case Report

Italo J. Mejía Sabando, Rafael Maia, Raphael W. Campos Cunha, Francisco G. Mero Cañarte, Kevin M. Armijos Montaño, Jean C. Muñoz Macías

Orthopedics and Traumatology Service, Santa Casa de Misericórdia Hospital of Rio de Janeiro, Pontifícia Universidade Católica do Rio de Janeiro, Rio de Janeiro, Brazil

ABSTRACT

Nonunion represents a challenge for orthopedic surgeons, and although several treatment options exist, there is no clear consensus. We report the successful use of the Masquelet technique as an alternative approach. This technique, commonly used for the treatment of large bone defects in the extremities, has reported success rates ranging from 82% to 100%. Although it is widely used in the lower limbs, there is limited evidence regarding its application in the upper limbs. We present a case of radial shaft nonunion with fixation failure, successfully treated using this technique. **Conclusion:** Bone union was achieved at approximately 8 months, with symptom resolution and functional recovery, demonstrating the effectiveness of this therapeutic option.

Keywords: Bone graft; Masquelet technique; Nonunion.

Level of Evidence: IV

Manejo de la seudoartrosis diafisaria de radio con falla de síntesis mediante la técnica de Masquelet. Presentación de un caso

RESUMEN

La seudoartrosis representa un desafío para el cirujano y, aunque existen diferentes alternativas de tratamiento, no hay un consenso claro. Presentamos el uso exitoso de la técnica de Masquelet como alternativa. Esta técnica, conocida por tratar defectos óseos largos en las extremidades, tiene tasas de éxito del 82% al 100%. Aunque su uso es común en los miembros inferiores, hay poca evidencia sobre su aplicación en los miembros superiores. En este reporte, se presenta un caso de seudoartrosis en la diáfisis radial con falla del material de osteosíntesis, tratado exitosamente con esta técnica. **Conclusión:** La consolidación ósea ocurrió en aproximadamente 8 meses, los síntomas se aliviaron y se logró la recuperación funcional, lo que demuestra la eficacia de esta opción terapéutica.

Palabras clave: Injerto óseo; técnica de Masquelet; seudoartrosis.

Nivel de Evidencia: IV

INTRODUCTION

Forearm fractures affect upper limb function and require appropriate treatment to prevent complications such as nonunion, which represents a challenge for the surgeon. Nonunion is defined as the absence of bone healing within the expected timeframe, without the potential for spontaneous consolidation. In clinical practice, its diagnosis is complex and depends on factors such as fracture type, initial treatment, time elapsed, and bone condition; therefore, clinical and radiographic criteria are essential.[1]

The treatment of nonunion depends on its origin and characteristics, and proper classification is key. When biological potential is adequate, proper alignment and stable osteosynthesis are sufficient; in nonviable lesions, additional measures are required to promote bone healing.[2]

Received on June 5th, 2024. Accepted after evaluation on June 25th, 2025 • Dr. ITALO J. MEJÍA SABANDO • italomej94@gmail.com https://orcid.org/0009-0008-4337-9061

How to cite this article: Mejía Sabando IJ, Maia R, Campos Cunha RW, Mero Cañarte FG, Armijos Montaño KM, Muñoz Macías JC. Management of Radial Shaft Nonunion with Fixation Failure Using the Masquelet Technique: A Case Report. *Rev Asoc Argent Ortop Traumatol* 2026;91(2):157-164. https://doi.org/10.15417/issn.1852-7434.2026.91.2.1981

Options for the treatment of large bone defects in the upper extremity include autografts, allografts, distraction osteogenesis, and bioactive materials. Each technique has specific indications and limitations: autografts require a well-vascularized bed and offer better integration in poorly vascularized areas, but they involve greater surgical complexity; allografts avoid donor-site morbidity, but may lead to complications such as infection and fracture.[3]

The Masquelet technique is based on the use of an autologous bone graft within an induced biological membrane and is an effective and relatively simple method for treating segmental bone defects in both the upper and lower extremities. It can be applied in aseptic or septic settings and does not require advanced microsurgical techniques.[4]

This technique is performed in two stages: first, debridement and bone stabilization are carried out with placement of a cement spacer and fixation material; approximately 4 weeks later, after formation of the induced membrane, the spacer is removed and the defect is filled with an autologous bone graft.[2]

This grafting approach is effective for treating bone defects of several centimeters in length in the extremities, with union rates ranging from 82% to 100%. Most currently published studies focus on bone defects in the lower extremities.[3] There are few reports on its use in the upper extremity, which underscores the relevance of the clinical case presented here: a radial diaphyseal nonunion successfully treated with this technique.

CLINICAL CASE

A 29-year-old man with no relevant past medical history sustained a fall from a motorcycle, resulting in trauma to the left upper limb. He presented with a diaphyseal fracture of the left radius classified as AO 2R2B2 (Figure 1). Initial management consisted of analgesia, immobilization, and hospital admission for surgical treatment. Two days after the injury, the fracture was treated with a dynamic compression plate through a volar approach.

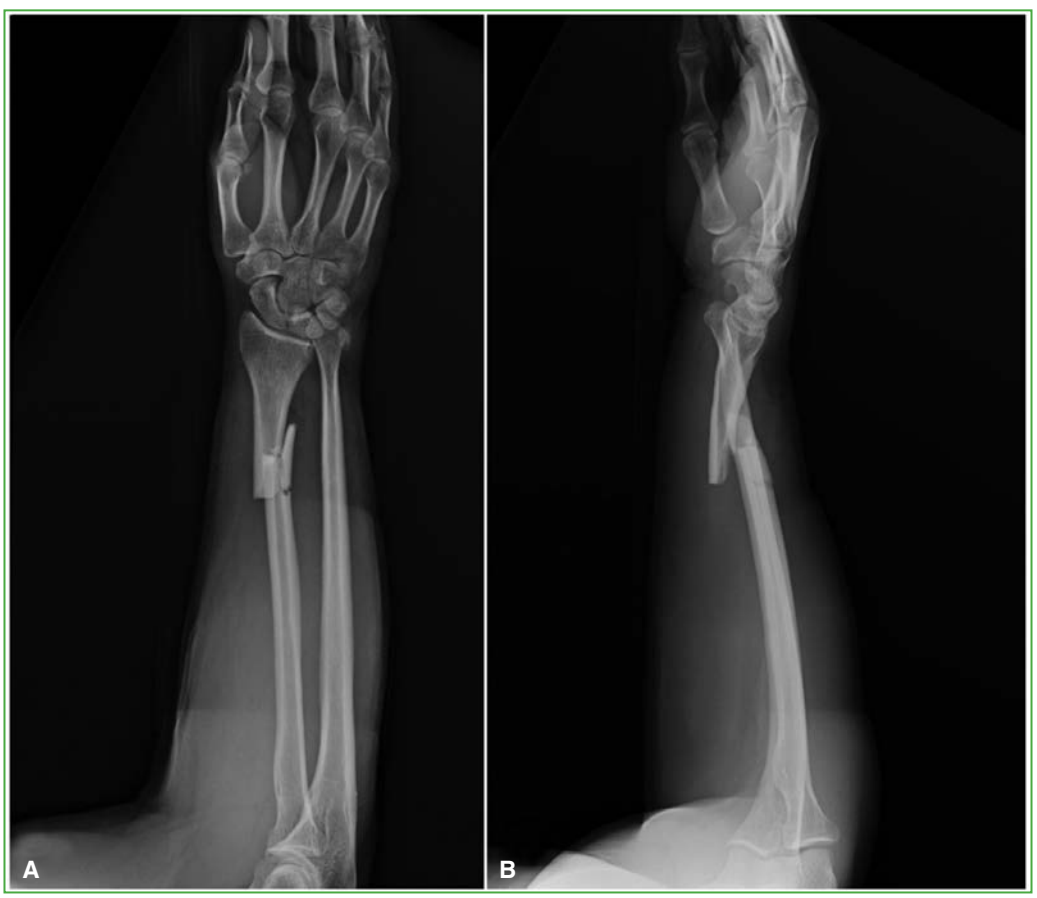

Figure 1. Anteroposterior (**A**) and lateral (**B**) radiographs of the forearm showing an AO 2R2B2 radial diaphyseal fracture.

Two months after surgery, the patient returned for follow-up, and control radiographs showed delayed union (Figure 2).

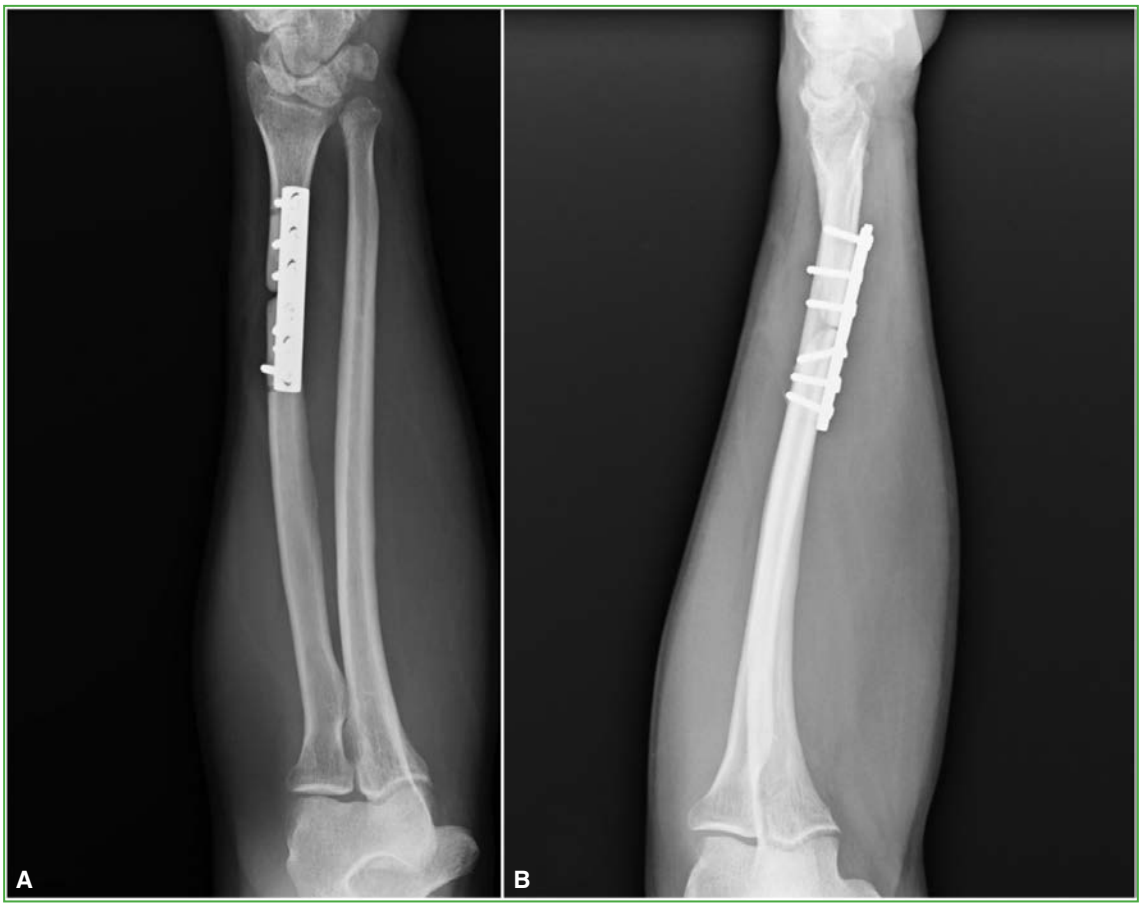

Figure 2. Anteroposterior (**A**) and lateral (**B**) radiographs of the forearm showing delayed union.

Eight months later, he presented to the emergency department with deformity of the left forearm. He denied recent trauma or fever, and the surgical wound was in good condition, without inflammatory changes or signs of infection. Radiographic evaluation revealed a radial diaphyseal nonunion associated with failure of the fixation hardware (Figure 3). Complete laboratory tests were requested, including erythrocyte sedimentation rate and C-reactive protein.

The patient underwent surgery consisting of resection of all nonviable bone and removal of the fixation hardware, through the previous volar approach, which was extended. During the procedure, no signs of infection were observed at the nonunion site. The residual bone defect after debridement measured approximately 10 cm. An antibiotic-free orthopedic bone cement spacer was placed in the defect. For stabilization, a Kirschner wire was inserted within the cement to function as an intramedullary support, and a second wire was used to perform temporary arthroereisis of the distal radioulnar joint (Figure 4).

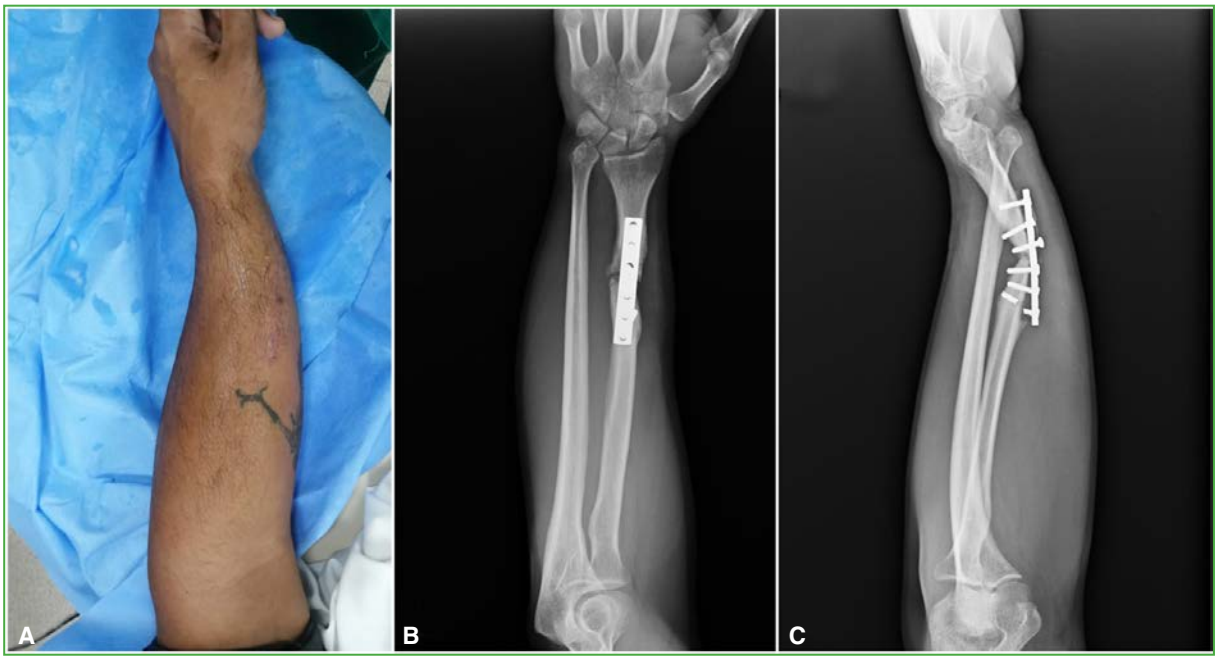

Figure 3. **A.** Obvious deformity of the forearm. Anteroposterior (**B**) and lateral (**C**) radiographs of the forearm showing a radial diaphyseal nonunion associated with failure of the fixation hardware.

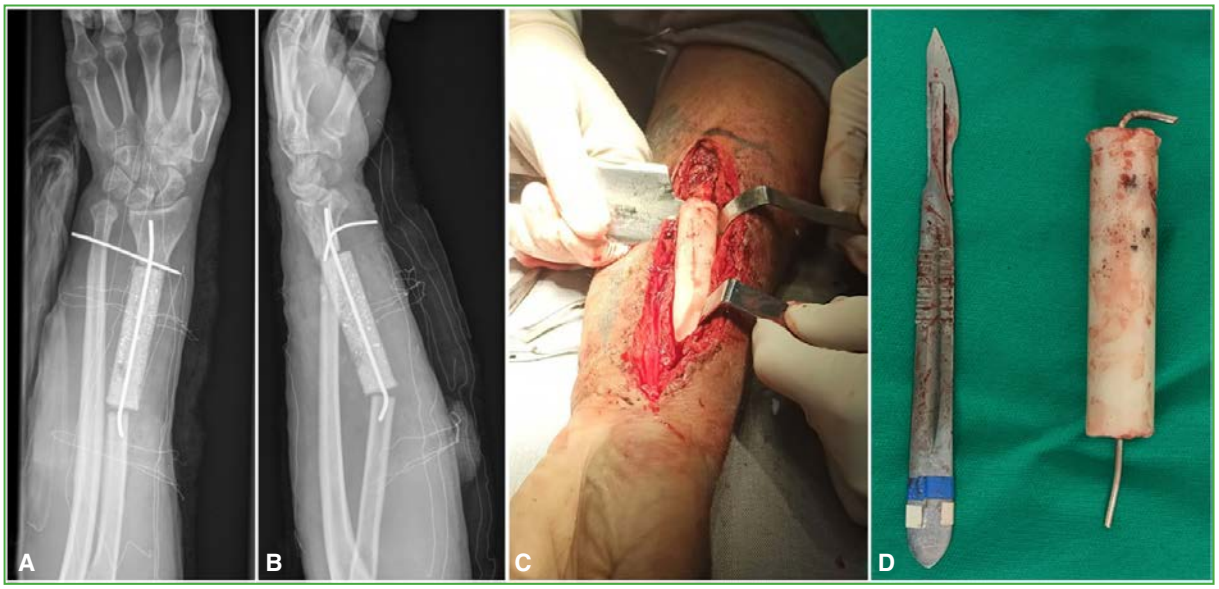

Figure 4. Anteroposterior (**A**) and lateral (**B**) radiographs of the forearm in the immediate postoperative period, showing orthopedic cement associated with Kirschner wires. **C and D.** Visualization and placement of orthopedic cement.

No postoperative complications were observed. Four weeks after cement placement, the patient underwent the second stage of the procedure. During this stage, the cement spacer was removed, and the formation of the induced membrane was confirmed intraoperatively. The bone defect was then filled with autologous cancellous bone graft harvested from the iliac crest. A locking dynamic compression plate was applied in neutralization mode, and an additional Kirschner wire was placed to maintain distal radioulnar joint arthroereisis (Figure 5).

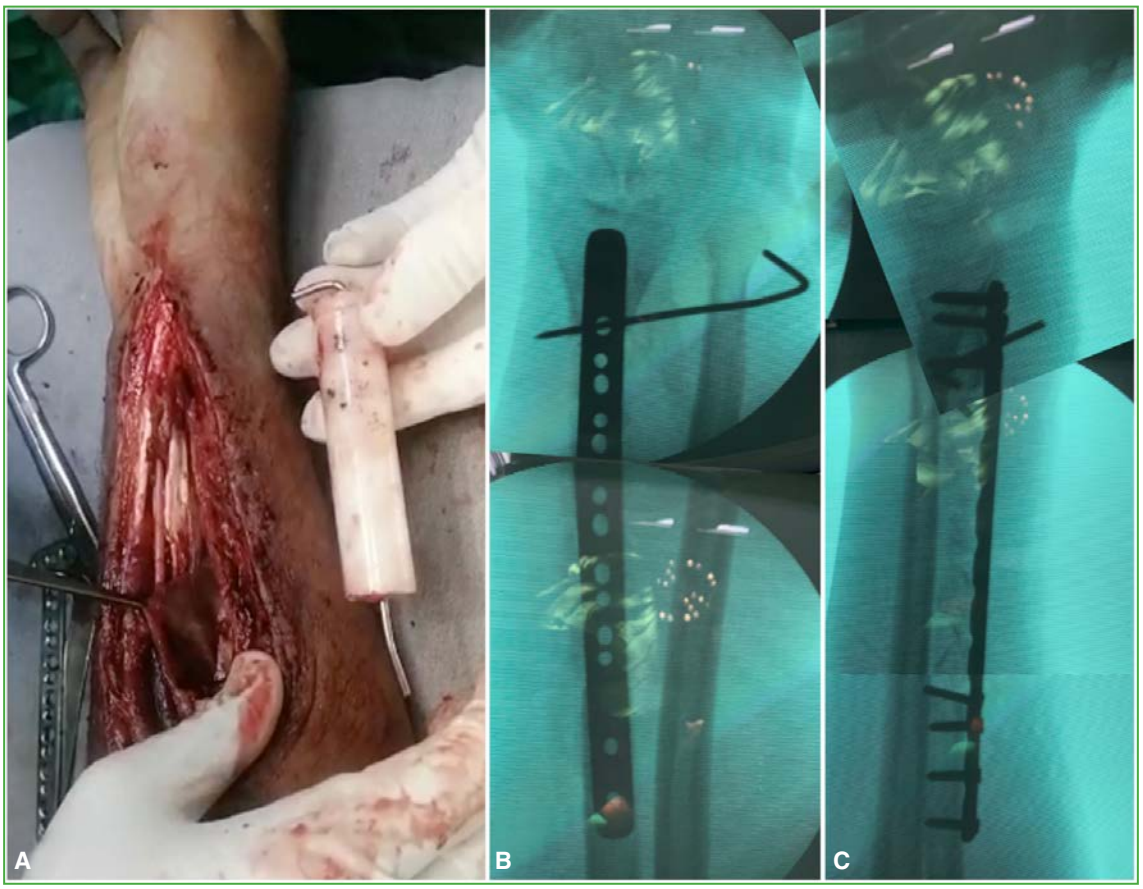

Figure 5. A. Removal of the orthopedic cement with visualization of the induced membrane (tip of the forceps). Anteroposterior (**B**) and lateral (**C**) radiographs of the forearm in the immediate postoperative period, showing the bone graft and fixation hardware.

The patient showed favorable progression, with the surgical wound in good condition and no signs of infection or pain. Follow-up radiographs at 1 month (Figures 6A and B) and 3 months (Figures 6C and D) demonstrated good progression of bone healing. The Kirschner wire was removed, and rehabilitation was initiated.

One year after surgery, complete bone union was observed on radiographs (Figures 7A and B). The patient reported no pain, had no neurovascular deficits or signs of infection, and maintained range of motion, with pronation of 60° and supination of approximately 70° (Figures 7C and D).

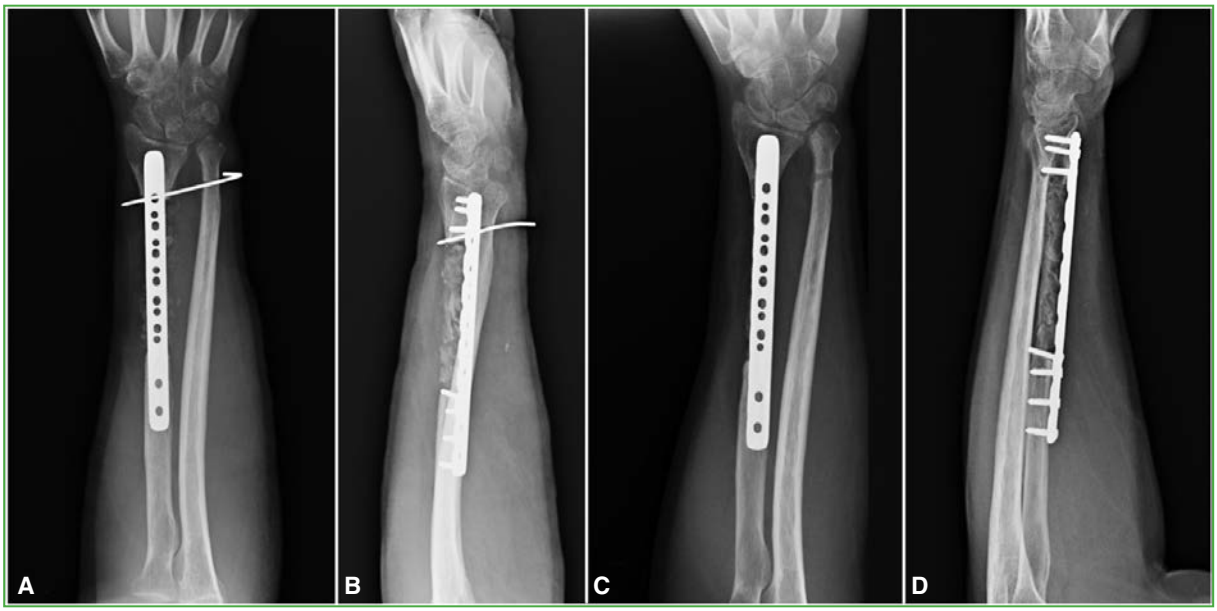

Figure 6. Anteroposterior (**A**) and lateral (**B**) radiographs of the forearm at 1 month and 3 months after surgery (**C and D**).

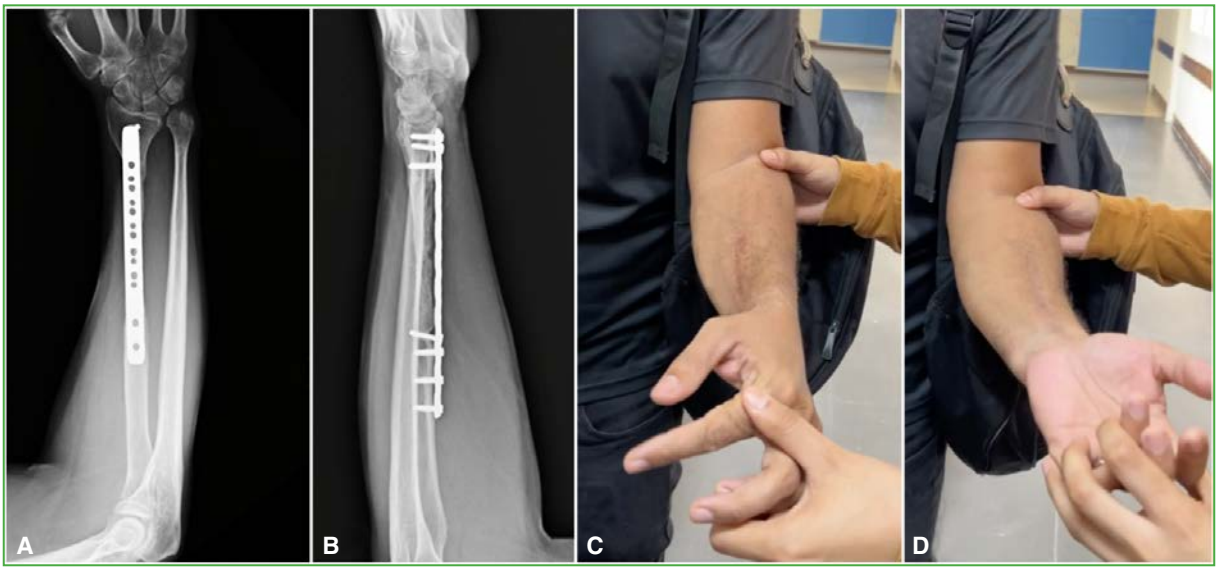

Figure 7. Anteroposterior (**A**) and lateral (**B**) radiographs of the forearm 1 year after surgery, showing bone union. **C and D.** Range of motion: pronation and supination, respectively.

DISCUSSION

The induced membrane technique described by Masquelet has consistently established itself as an effective and reliable method for the treatment of segmental bone defects. Although its initial applications were limited, its use has progressively expanded to include the long bones of the upper extremity.

In a review of this technique for fractures with segmental bone loss in the upper extremity, Braswell et al.[5] reported favorable outcomes, with an overall union rate of 91.3% and a mean time to union of 20 weeks. Similarly, Pederiva et al.[6] reported a union rate of 96%, with a mean time to union of 5.5 months and an average defect length of 4.5 cm. In a case report of an infected radial diaphyseal nonunion treated with this technique, Nitai et al.[7] reported favorable outcomes, with complete graft ossification at 10 months.

Micev et al.[3] proposed an optimal interval of 4 weeks for bone grafting within the induced membrane. In a randomized group of 14 patients treated with the Masquelet technique, membrane vascularization peaked at 1 month and decreased to less than 60% in samples obtained at 3 months. One-month samples showed the highest levels of vascular endothelial growth factor, interleukin-6, and type I collagen, whereas 2-month membranes exhibited less than 40% of the levels observed at 1 month.

Compared with data from oncologic reconstruction of the upper extremity, O'Connor et al.[8] concluded that the induced membrane technique compares favorably. They also reported no significant clinical differences compared with free bone grafting, despite the latter demonstrating shorter time to union. Furthermore, the Masquelet technique allows limb salvage in cases where microvascular bone flaps are not feasible.

In a comparative study of this technique and vascularized fibular grafting in open forearm fractures with segmental bone defects, Zhou et al.[9] concluded that clinical and radiographic outcomes are similar; however, with the Masquelet technique, operative time, hospital stay, and intraoperative blood loss were reduced. A military study reported a high success rate with this technique for the management of open fractures, bone loss, or infections (common complications in combat settings) since, in the military environment, there are limitations to other procedures, such as bone transport or vascularized bone grafting.[10]

Rohilla et al.[11] compared the Masquelet technique with bone transport in a prospective study of 25 patients with infected tibial nonunion and bone loss of up to approximately 6 cm. The authors reported that both techniques achieved functional outcomes, but bone transport was superior in terms of bone healing.

Among the main complications of this technique, some studies report nonunion requiring unplanned reoperations,[5] while others identify infection as one of the most frequent complications.[8] Pederiva et al.[6] reported a complication rate of 21% and failure in only 6 of 156 patients.

This technique yields good functional outcomes but requires strong commitment from both the patient and the surgeon, as well as effective communication, with patients being informed of the possibility that multiple procedures may be required until bone union is achieved.[12]

CONCLUSIONS

The Masquelet technique proved to be an effective option for the treatment of a radial diaphyseal nonunion with significant bone loss, achieving complete bone union and satisfactory functional recovery. This outcome supports the use of the Masquelet technique as a safe and viable alternative for bone reconstruction in the upper extremity, provided that appropriate surgical timing is respected and good adherence to treatment is ensured.

Conflicts of interest: The authors declare no conflicts of interest.

R. Maia ORCID ID: https://orcid.org/0009-0002-2613-9265
R. W. Campos Cunha ORCID ID: https://orcid.org/0009-0003-3386-8180
F. G. Mero Cañarte ORCID ID: https://orcid.org/0009-0005-5403-2264
K. M. Armijos Montaño ORCID ID: https://orcid.org/0000-0002-7246-9305
J. C. Muñoz Macías ORCID ID: https://orcid.org/0009-0000-9311-3669

REFERENCES

1. Wildemann B, Ignatius A, Leung F, Taitsman LA, Smith RM, Pesántez R, et al. Non-union bone fractures. *Nat Rev Dis Primers* 2021;7(1):57. https://doi.org/10.1038/s41572-021-00289-8
2. Masquelet AC, Fitoussi F, Begue T, Muller GP. [Reconstruction of the long bones by the induced membrane and spongy autograft]. *Ann Chir Plast Esthet* 2000;45(3):346-53. [French] PMID: 10929461
3. Micev AJ, Kalainov DM, Soneru AP. Masquelet technique for treatment of segmental bone loss in the upper extremity. *J Hand Surg Am* 2015;40(3):593-98. https://doi.org/10.1016/j.jhsa.2014.12.007
4. Kołodziejczyk K, Ropielewski A, Garlewicz R, Złotorowicz M, Czubak J. Clinical observations of the effectiveness of the Masquelet induced membrane technique in the treatment of critical long-bone defects of the lower and upper extremities. *Medicina (Kaunas)* 2024;60(12):1933. https://doi.org/10.3390/medicina60121933
5. Braswell MJ, Bulloch LR, Gaston RG, Garcia RM. Outcomes after use of the induced membrane technique for fractures of the upper extremity. *J Hand Surg Am* 2023;48(7):735.e1-735.e7. https://doi.org/10.1016/j.jhsa.2022.01.018
6. Pederiva D, de Luca L, Faldini C, Vergano LB. Masquelet's induced membrane technique in the upper limb: a systematic review of the current outcomes. *J Orthop Traumatol* 2025;26(1):4. https://doi.org/10.1186/s10195-024-00815-w
7. Nitai K, Eran K, Yaniv, K. Radial diaphysis infected non-union treated with combination of Masquelet technique and autologous bone grafting harvested by RIA: A case report. *Trauma Case Rep* 2022;39:100621. https://doi.org/10.1016/j.tcr.2022.100621
8. O'Connor CM, Perloff E, Drinane J, Cole K, Marinello PG. An analysis of complications and bone defect length with the use of induced membrane technique in the upper limb: A systematic review. *Hand* 2022;17(3):572-77. https://doi.org/10.1177/1558944720918368
9. Zhou M, Ma Y, Jia X, Wu Y, Liu J, Wang Y, et al. Comparison of free vascularized fibular grafts and the Masquelet technique for the treatment of segmental bone defects with open forearm fractures: a retrospective cohort study. *J Orthop Traumatol* 2024;25(1):44. https://doi.org/10.1186/s10195-024-00787-x
10. Mathieu L, Bilichtin E, Durand M, de l'Escalopier N, Murison JC, Collombet JM, et al. Masquelet technique for open tibia fractures in a military setting. *Eur J Trauma Emerg Surg* 2020;46(5):1099-105. https://doi.org/10.1007/s00068-019-01217-y
11. Rohilla R, Sharma PK, Wadhwani J, Das J, Singh R, Beniwal D. Prospective randomized comparison of bone transport versus Masquelet technique in infected gap nonunion of tibia. *Arch Orthop Trauma Surg* 2022;142(8):1923-32. https://doi.org/10.1007/s00402-021-03935-8
12. Herrera Caballero ZV, Sierra Pérez M, Hernández Frías E, Ceballos Sánchez JA, de los Santos Montoya FA. Técnica de Masquelet en no unión atrófica de tibia con osteomielitis crónica, su descripción. *Acta Médica Grupo Ángeles* 2021;19(2):280-4. https://doi.org/10.35366/100456

Pretibial Ganglion Cyst Secondary to Anterior Cruciate Ligament Reconstruction and Its Conservative Management: A Two-Case Report

Tania Alvarado Chávez,[*] Cecilia Rentería Lascano,[**] Roy Luna Alvarado,[#] Raisa Vélez Albán[*]
[*]*Orthopedics and Traumatology Service, Hospital General "Dr. Enrique Ortega Moreira", Durán, Ecuador*
[**]*Orthopedics and Traumatology Service, Hospital del Día "Mariana de Jesús", Guayaquil, Ecuador*
[#]*Orthopedics and Traumatology Service, Hospital General del Norte de Guayaquil, Guayaquil, Ecuador*

ABSTRACT

Introduction: We present two cases of pretibial ganglion cyst, an uncommon postoperative complication after arthroscopic anterior cruciate ligament (ACL) reconstruction. In both cases, hamstring autografts and biodegradable interference screws were used for fixation. We discuss the rarity and multifactorial etiology of this complication, including fixation material and graft micromotion. Both conservative (aspiration) and surgical (curettage and bone grafting) treatment options are reviewed; however, surgery appears to be more effective in preventing recurrence. The choice of fixation material is highlighted as a key preventive factor. **Conclusion:** Management should be individualized, and close follow-up is essential.

Keywords: Cyst; pretibial ganglion; anterior cruciate ligament.
Level of Evidence: IV

Ganglión pretibial secundario a la reconstrucción del ligamento cruzado anterior y su tratamiento conservador. Reporte de dos casos

RESUMEN

Se presentan dos casos clínicos de ganglión pretibial, una complicación posoperatoria infrecuente tras la reconstrucción artroscópica del ligamento cruzado anterior; en ambos casos, se recurrió a un injerto de isquiotibiales y la fijación con tornillos interferenciales biodegradables. Se analizan la rareza y la etiología multifactorial de esta complicación, inclusive el material de fijación y la micromovilidad del injerto. Se exploran las opciones de tratamiento conservador (punción) y quirúrgico (curetaje y relleno). La cirugía parece más efectiva para prevenir las recurrencias. La elección del material de fijación se subraya como un factor preventivo crucial. **Conclusión:** El manejo debe ser individualizado y el seguimiento continuo es fundamental.

Palabras clave: Quiste; ganglión pretibial; ligamento cruzado anterior.
Nivel de Evidencia: IV

INTRODUCTION

Anterior cruciate ligament (ACL) reconstruction is one of the most commonly performed procedures in knee surgery. With the evolution and variety of available surgical techniques and fixation materials, it has become a safer option with a high rate of favorable outcomes, leading to its increasing use. However, no surgical technique is free from complications. The most common postoperative complications associated with this procedure include pain, hemarthrosis, infection, deep vein thrombosis, arthrofibrosis, and saphenous neuropathy,[1-4] whereas less frequent complications include pretibial ganglion cyst and pigmented villonodular synovitis, among others.[5–13]

Received on April 6th, 2025. Accepted after evaluation on September 18th, 2025 • Dr. TANIA ALVARADO CHÁVEZ • dratanialvarado@hotmail.com https://orcid.org/0000-0002-2936-6802
How to cite this article: Alvarado Chávez T, Rentería Lascano C, Luna Alvarado R, Vélez Albán R. Pretibial Ganglion Cyst Secondary to Anterior Cruciate Ligament Reconstruction and Its Conservative Management: A Two-Case Report. *Rev Asoc Argent Ortop Traumatol* 2026;91(2):165-176. https://doi.org/10.15417/issn.1852-7434.2026.91.2.2151

We present two patients who underwent arthroscopic ACL reconstruction at different institutions and at different times and subsequently developed pretibial ganglion cysts as a complication. As previously mentioned, this is a rare complication that may occur even several years after surgery,[14] and multiple etiologies have been proposed.[15]

CLINICAL CASE 1

A 17-year-old female tennis player had undergone right ACL reconstruction using an autologous hamstring graft (semitendinosus-gracilis), fixed with a biodegradable interference screw in the tibial tunnel, in June 2022, and right meniscal allograft transplantation in August 2023. She also tended to develop keloids.

In July 2024, she presented with swelling near the surgical scar over the tibial tunnel that did not interfere with her athletic performance. She denied previous trauma.

On physical examination, a well-defined soft mass measuring approximately 2–3 cm was observed. It was painless, with no inflammatory signs. Keloid scars corresponding to previous arthroscopic portals were also noted, for which she was receiving dermatologic treatment (Figure 1). Magnetic resonance imaging showed an intact graft and preserved tibial tunnel, with no signs of local infection (Figure 2).

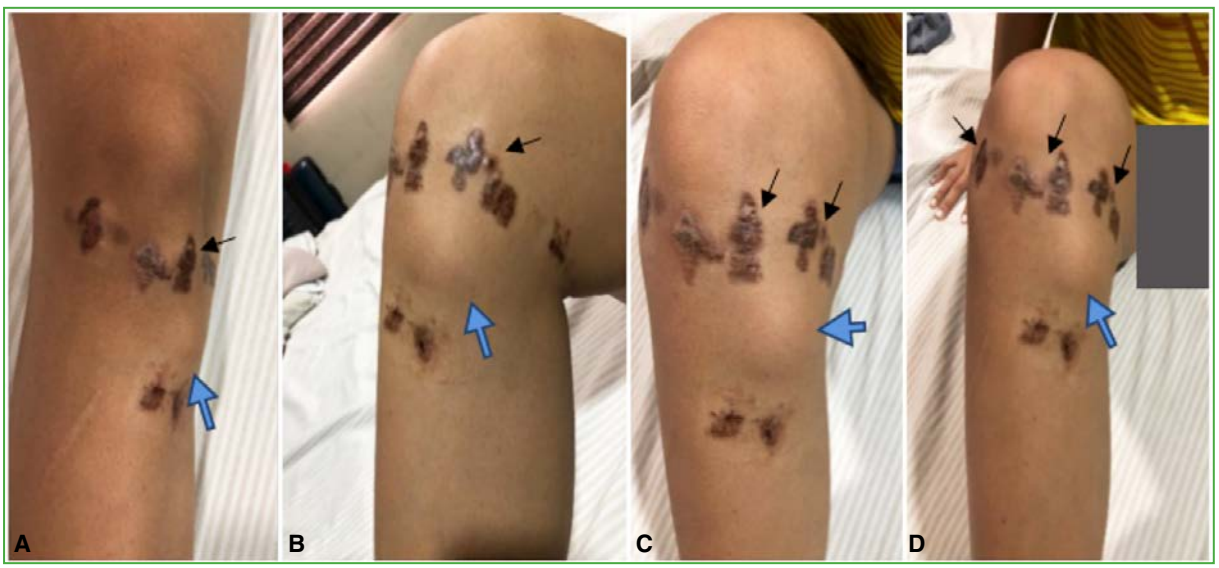

Figure 1. Anteroposterior (**A**), lateral (**B**), and oblique (**C and D**) views of the right knee. Swelling is observed in the anteromedial region of the knee at the tibial metaphysis (large arrows). The patient also presents keloid scars (small arrows) corresponding to previous arthroscopic portals, which were undergoing dermatologic treatment at the time the images were obtained.

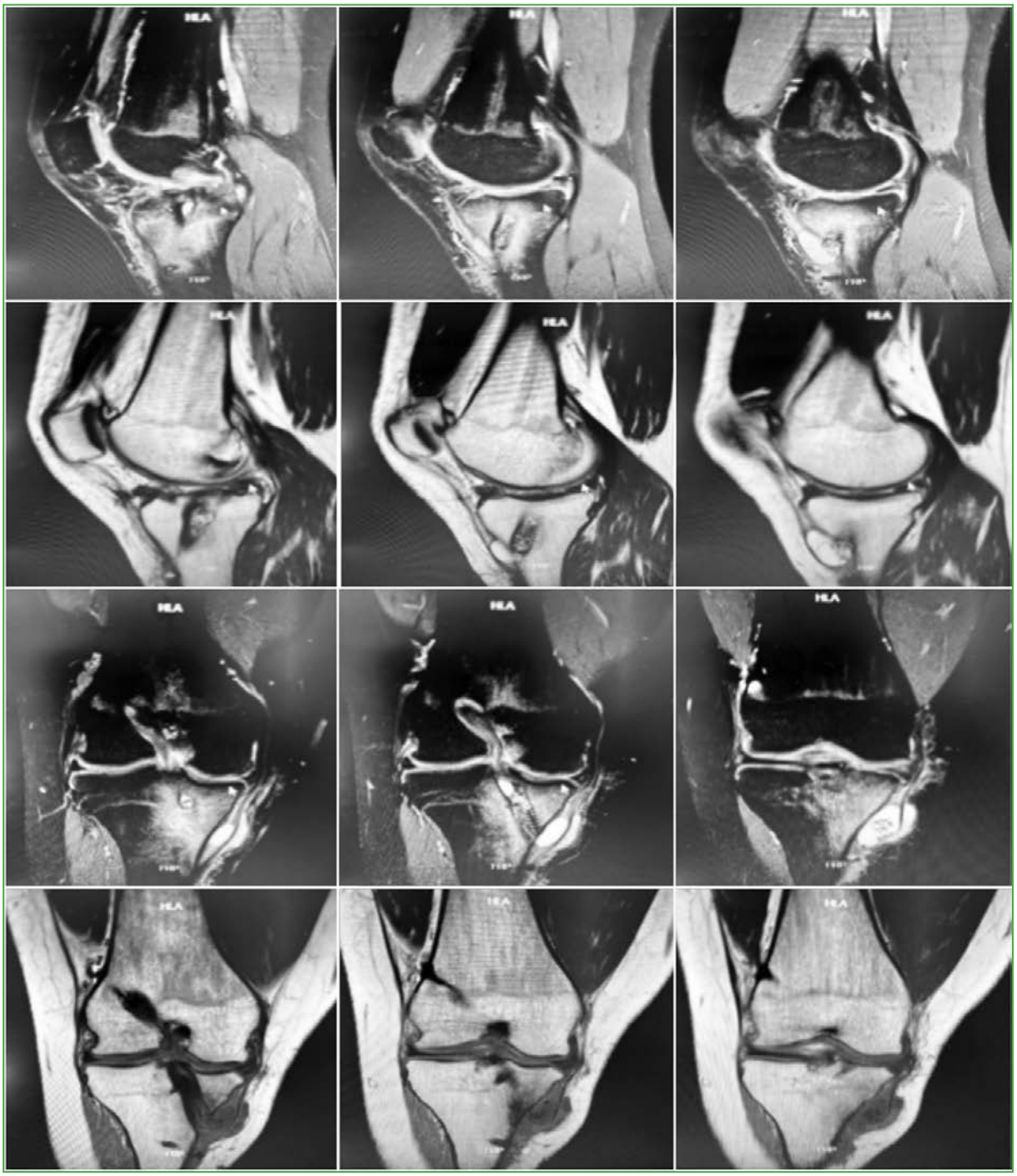

Figure 2. Magnetic resonance imaging of the right knee, sagittal and coronal T1-weighted and T2-weighted sequences, showing continuity of the graft along its course and preservation of its proximal and distal insertions, together with an anteromedial pretibial cystic mass and bone marrow edema around the tibial tunnel.

Surgical excision and biopsy of the ganglion cyst were proposed; however, the patient stated that she did not wish to undergo another procedure, having already had two surgeries in the previous two years. With her consent, ultrasound-guided aspiration of the pretibial ganglion cyst was performed in the outpatient clinic under sterile conditions (Figure 3). Clear, viscous fluid was aspirated (Figure 4). An elastic compressive dressing was then applied and indicated for 23 hours per day, and the patient was instructed regarding warning signs.

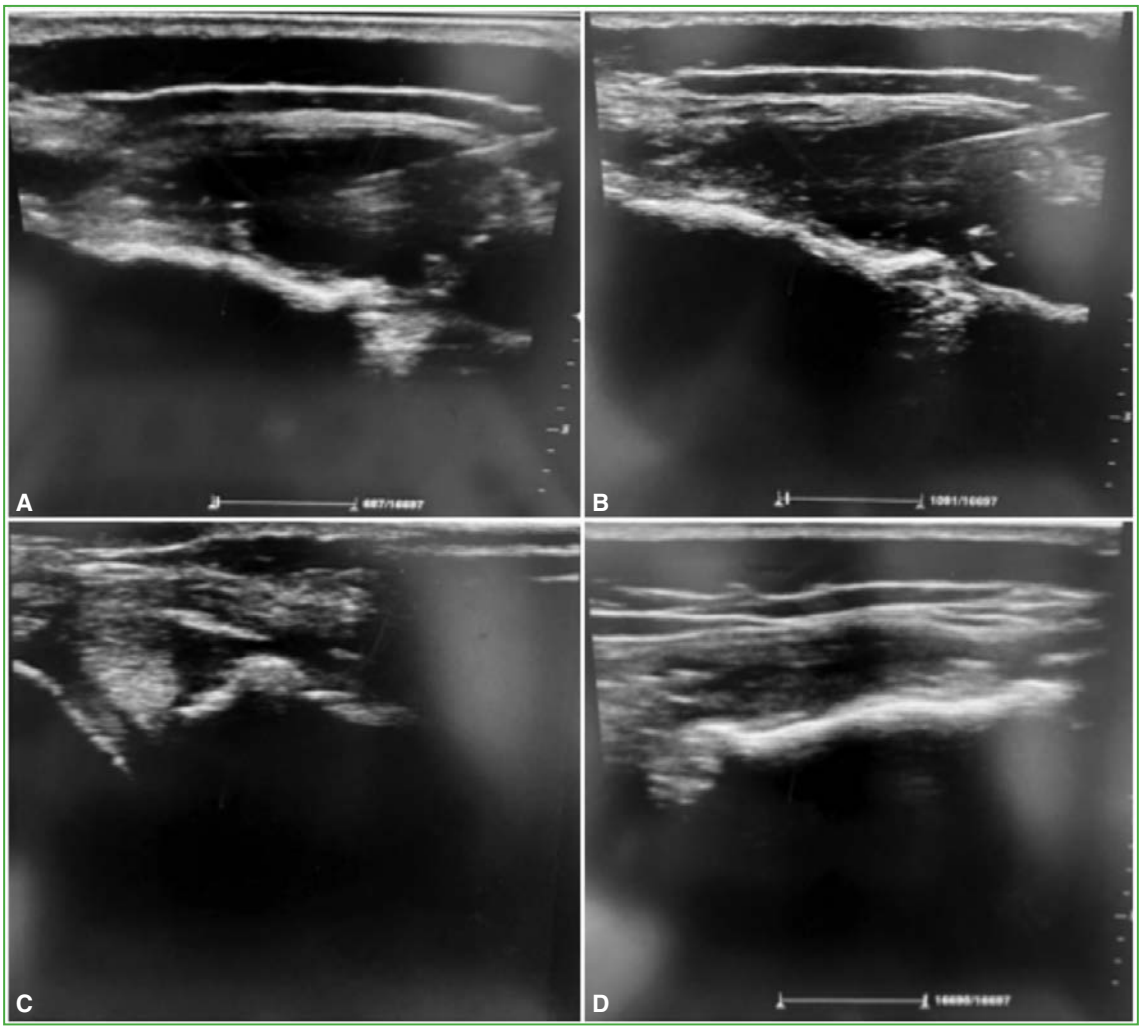

Figure 3. A and B. Ultrasound-guided aspiration and drainage of the pretibial ganglion cyst in the anteromedial region. **C and D.** Appearance after aspiration and drainage.

Figure 4. Clear, viscous fluid obtained during ultrasound-guided aspiration and drainage of the pretibial ganglion cyst.

At the two-month follow-up, the swelling had markedly decreased (Figure 5).

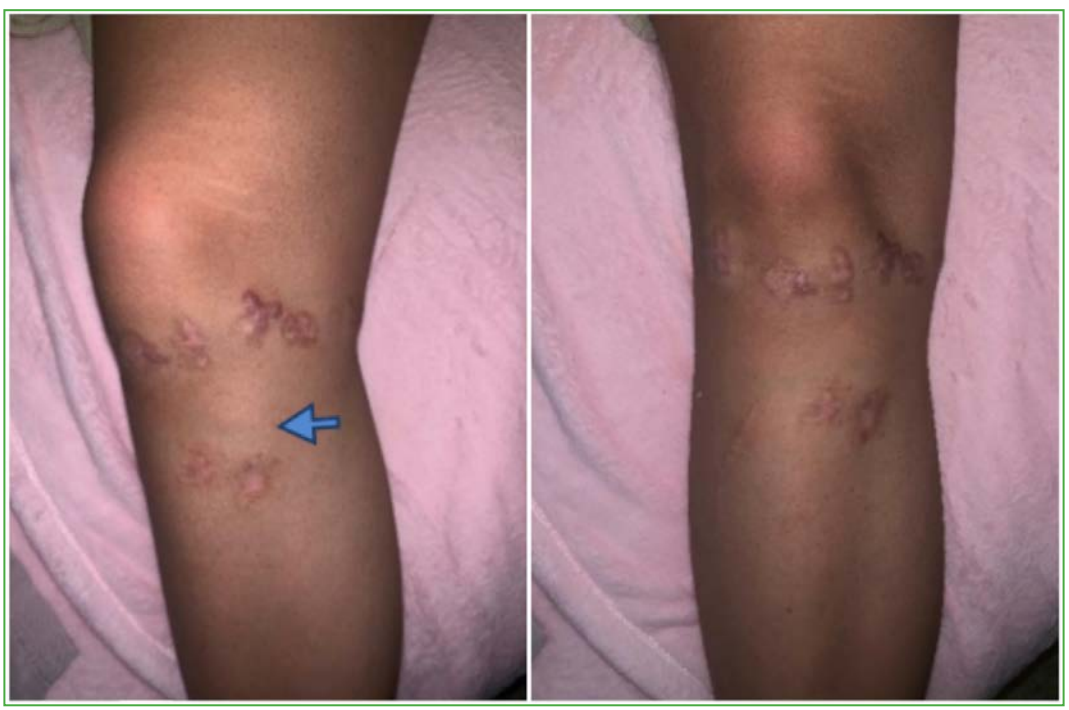

Figure 5. Case 1. Follow-up at 2 months after ultrasound-guided aspiration and drainage, showing marked reduction of swelling (blue arrow).

The patient returned one year after treatment and reported that she had not attended further follow-up visits because of symptomatic improvement and complete return to sports activity. Physical examination showed no relevant findings (Figure 6). During the visit, ultrasound examination of the anteromedial aspect of the proximal tibia revealed a small, collapsible hypoechoic image corresponding to the pretibial ganglion cyst capsule. The transplanted medial meniscus was also evaluated, with no pathological findings detected (Figure 7).

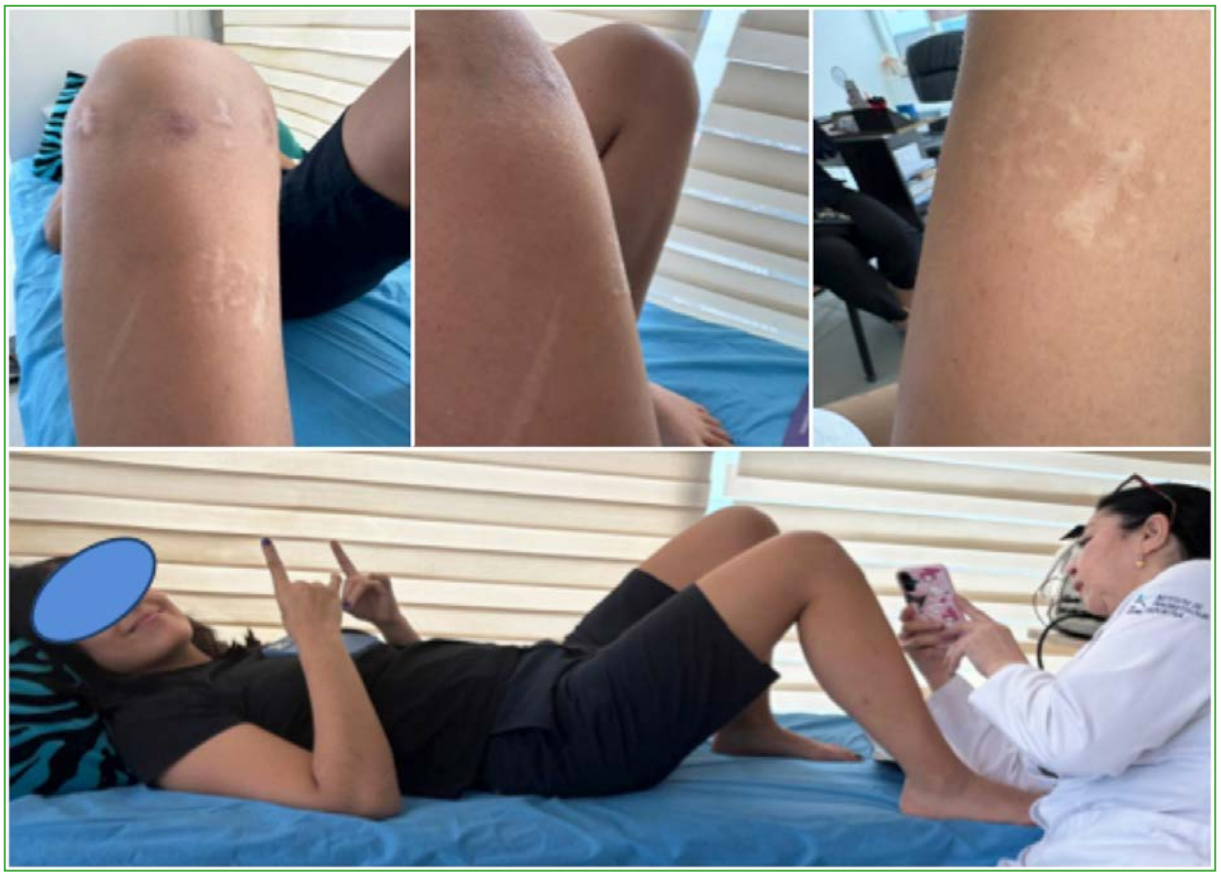

Figure 6. Case 1. Follow-up at 1 year after ultrasound-guided aspiration and drainage. Surgical scars from previous procedures are visible. The patient is asymptomatic.

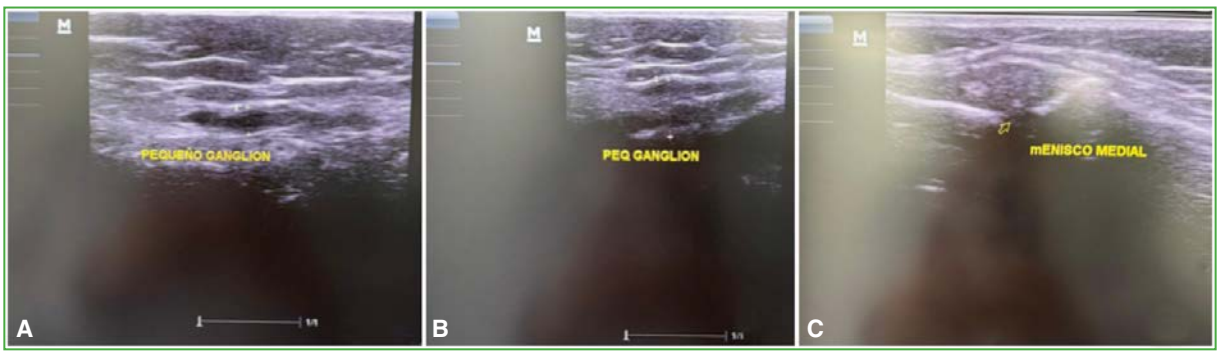

Figure 7. Ultrasound of the right knee, over the anteromedial region of the proximal tibia showing a hypoechoic, collapsible image, identified as the pretibial ganglion cyst (**A and B**). The transplanted medial meniscus was also evaluated, with no pathological findings (**C**).

CLINICAL CASE 2

A 41-year-old man employed by an electrical utility company had undergone arthroscopic right ACL reconstruction in 2017 using a double-bundle hamstring autograft (semitendinosus-gracilis), fixed with a biodegradable interference screw in the tibial tunnel.

One week after surgery, a soft mass developed over the anteromedial proximal region of the right tibia. Magnetic resonance imaging and ultrasound confirmed the presence of a cystic lesion related to the tibial tunnel exit site (Figures 8 and 9). Ultrasound-guided aspiration and drainage were performed under sterile conditions in the preoperative area, obtaining clear fluid (Figure 10). An elastic compressive dressing was immediately applied. Its use was indicated for 23 hours per day for 2 months, followed by physical therapy beginning 2 months after the procedure. Follow-up continued for one year, with no recurrence.

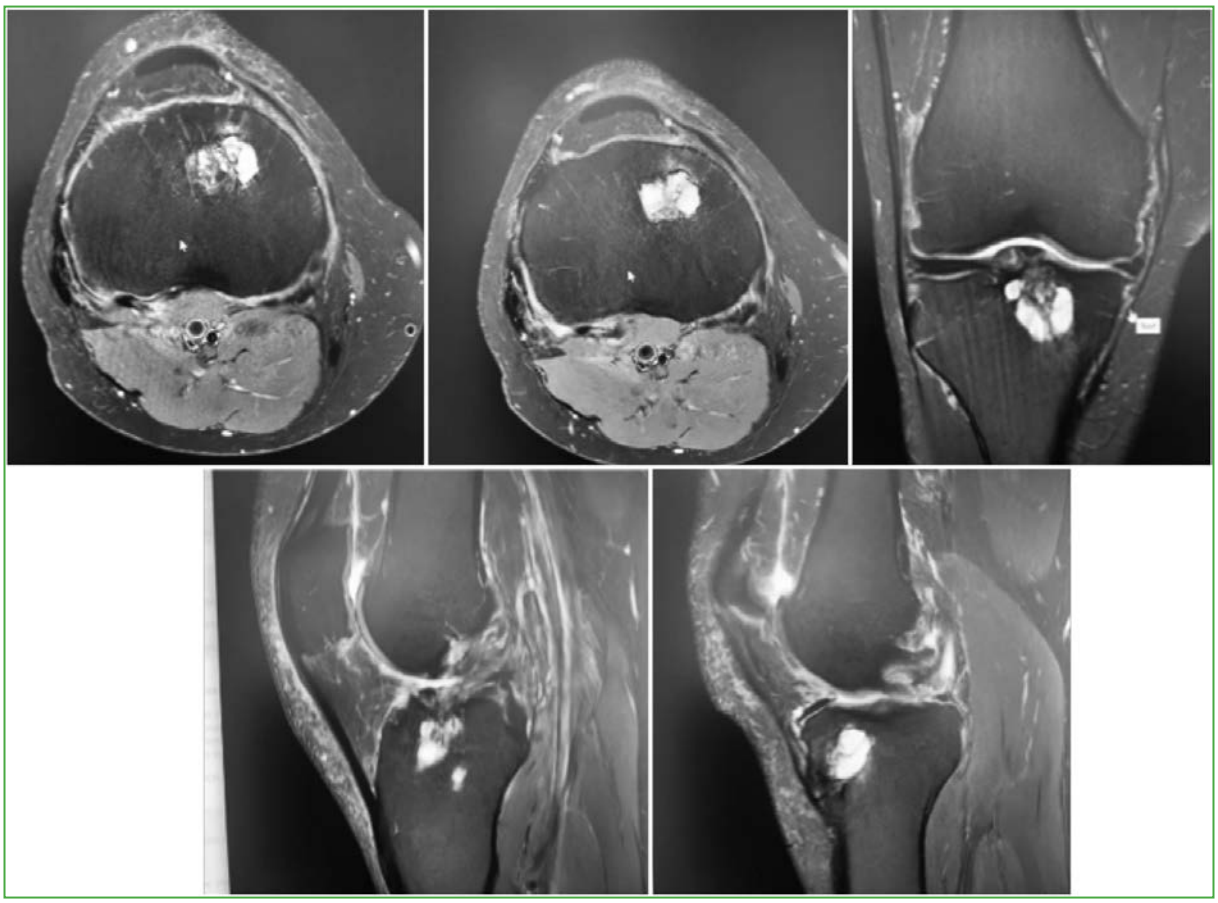

Figure 8. Magnetic resonance imaging of the right knee, axial and sagittal T2-weighted sequences, showing continuity of the graft along its course and preservation of its proximal and distal insertions, together with an anteromedial pretibial and intraosseous tibial cystic mass, as well as bone marrow edema around the tibial tunnel.

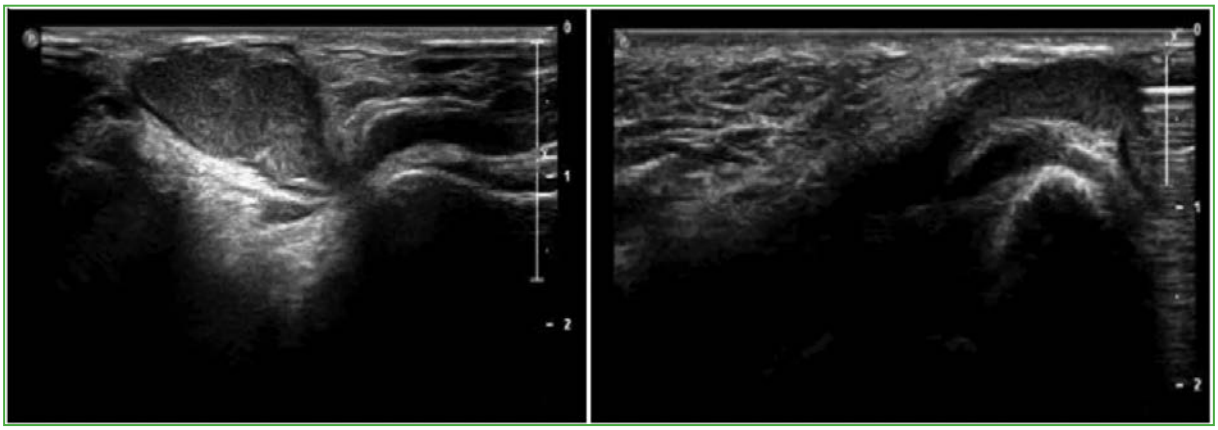

Figure 9. Ultrasound-guided aspiration and drainage of the pretibial ganglion cyst in the anteromedial region.

Figure 10. Clear, viscous fluid obtained during ultrasound-guided aspiration and drainage of the pretibial ganglion cyst.

Both patients developed a palpable soft mass located in the anteromedial proximal pretibial region, measuring approximately 2-3 cm in diameter, without signs of local infection or instability of the operated knee.

In the first case (17-year-old woman), the mass developed approximately two years after ACL reconstruction. Surgical treatment was proposed but declined because she had undergone two surgeries in the previous two years. Therefore, ultrasound-guided aspiration of the pretibial ganglion cyst was performed, followed by compressive bandaging, nonsteroidal anti-inflammatory drugs, temporary cessation of sports activity, and physical therapy. At two months, the reduction in lesion size was maintained, without recurrence (Figure 5). At the one-year follow-up, she reported being asymptomatic and having resumed her usual sports activity, which was the reason she had not returned for interim visits. She denied recurrence. Ultrasound examination demonstrated a small painless hypoechoic collapsible image corresponding to a residual pretibial ganglion cyst capsule (Figures 6 and 7).

In the second case (41-year-old man), pretibial swelling developed within days of arthroscopic surgery. Magnetic resonance imaging and ultrasound demonstrated a fluid-filled cystic pretibial lesion consistent with a ganglion cyst. Immediate aspiration of the pretibial ganglion cyst was performed (Figures 8-10), followed by strict compressive bandaging. Physical therapy began at two months, and serial follow-up was continued for one year. No recurrence occurred. The patient regained full painless range of motion and returned to his usual daily activities.

DISCUSSION

The development of pretibial ganglion cysts after ACL reconstruction is a relatively uncommon but clinically relevant complication. According to the review by Barbosa et al.,[8] these cysts may present with a wide range of symptoms, from painless swelling without functional impairment to limitation of range of motion. The estimated incidence ranges from 0.28% to 3.9%.[8,16,17]

Current evidence suggests a multifactorial etiology influenced by patient-related factors, fixation materials, surgical technique, and biological response.[8,15,18] Barbosa et al. reported that in approximately 44% of the publications included in their review (representing 84.56% of reported cases), pretibial cysts developed in the presence of bioabsorbable materials within the tibial tunnel, ranging from biodegradable screws to sutures, with predominance of poly-L-lactic acid (PLLA) interference screws. Only 11 studies (11.44% of reported cases) described cyst formation associated with nonabsorbable fixation devices.

In addition, 21% of the included studies reported associated factors such as tendon necrosis, inflammatory reaction to sutures, allograft use, infection, and graft micromotion. In the same review, magnetic resonance imaging demonstrated communication between the joint and the tibial tunnel in 14% of 93 patients.[8] However, these publications do not specify the time elapsed between identification of tunnel communication and cyst development.

Two meta-analyses[17,19] comparing bioabsorbable and metallic interference screws for ACL reconstruction found no significant differences in postoperative stability or recovery of joint function. However, both studies reported a higher frequency of joint effusion and tibial tunnel widening with bioabsorbable materials compared with metallic interference screws.

Although the mechanism underlying formation of these lesions remains unclear, a major contributing factor appears to be the use of biodegradable interference screws, particularly PLLA screws. Long-term follow-up studies evaluating these implants have shown a longer-than-expected resorption period, ranging from 7 to 10 years.[18,20] These authors suggest that such implants may induce a chronic inflammatory foreign-body reaction, thereby increasing the risk of pretibial cyst formation.[8,14,21]

Less commonly, this complication has also been reported in the presence of nonabsorbable fixation devices, where it has been associated with possible graft micromotion within the tunnel leading to a similar reaction.[8,22]

In one of the patients described here, the pretibial cyst developed approximately 2 years after surgery, whereas in the other, it appeared within days of the procedure. Most pretibial ganglion cysts reported after ACL reconstruction develop around 2 years postoperatively and, less frequently, after 5-7 years. In the second case, this short interval makes a chronic foreign-body inflammatory reaction less likely; communication with synovial fluid may reasonably be suspected as a facilitating factor, despite the absence of this finding on imaging studies.

In most published reports, pretibial ganglion cysts after ACL reconstruction have been managed surgically, either through an open or arthroscopic approach. Management generally consists of cyst excision and tunnel curettage, with removal of residual material from the primary procedure. Tunnel filling with autologous bone graft, allograft, or osteoconductive substitutes such as calcium hydroxyapatite has frequently been reported,[8,9,14,15,20,23,24] and the use of bone cement has also been described,[25] all with the aim of reducing recurrence. Among the reviews including the largest number of cases, the estimated recurrence rate ranges from 3% to 7.7%.[8,15,25] Two patients (of a total of six) were treated with excision and curettage alone.

Yacuzzi et al. and Munguina et al. reported patients initially treated with needle aspiration of the lesion without success, who subsequently underwent screw removal, curettage, and tunnel filling, achieving resolution.[15,25]

Recurrence of these cysts is not clearly characterized in the literature because this complication is uncommon (1.88%–14.28%).[8,15,20] Some studies suggest that when only drainage or cyst excision is performed, without tunnel resection or curettage with bone grafting, recurrence rates may be high.[25]

Complications associated with tibial cysts include recurrence, infection, and, in rare cases, the need for revision ACL reconstruction. Malhan et al.[26] and Ramsingh et al.[27] emphasized the importance of careful selection of fixation materials to minimize these risks. Yonga et al.[14] highlighted the need for long-term follow-up.

In the two cases presented here, pretibial ganglion cysts developed after ACL reconstruction using biodegradable interference screws. Neither patient reported pain nor showed local inflammatory signs other than swelling. Both patients, although treated at different institutions and at different times, underwent conservative management consisting of aspiration and drainage followed by elastic compressive bandaging and anti-inflammatory measures. In the first case, the patient's refusal of surgery justified the choice of a less invasive approach. In the second case, pretibial ganglion cyst developed one week after ACL reconstruction, and conservative treatment proved effective, with no recurrence during follow-up.

We have not identified other published reports describing a similar management strategy for this condition, which makes it difficult to determine with certainty the true recurrence rate associated with this approach. Current evidence suggests that it may provide short-term symptom relief, although with a higher risk of recurrence.

However, we believe that, in selected cases, conservative management with image-guided percutaneous aspiration may represent a valid alternative that does not require hospitalization and is less invasive, particularly in patients without significant functional impairment and with localized symptoms or no clear indication for surgery. Another advantage is that ultrasound is more cost-accessible, making it a particularly useful tool in the outpatient setting.

CONCLUSIONS

There is currently stronger evidence supporting surgical intervention as the safest option for definitive treatment of this complication and prevention of recurrence. However, we believe that in patients without concerning symptoms, aspiration of the lesion may be a reasonable initial management option when combined with appropriate follow-up, particularly given the advantages of avoiding hospitalization and being economically accessible.

The final decision should be based on an individualized assessment of each patient. Ongoing follow-up is essential to ensure favorable long-term outcomes and to address any complications that may arise. Further research is needed to establish best practices for management.

Conflicts of interest: The authors declare no conflicts of interest.

C. Rentería Lascano ORCID ID: https://orcid.org/0000-0002-7233-7169
R. Luna Alvarado ORCID ID: https://orcid.org/0009-0006-3712-6258
R. Vélez Albán ORCID ID: https://orcid.org/0000-0002-2401-7339

REFERENCES

1. Figueroa D, Gonzalez W, Figueroa L, Figueroa F, Vaisman A. Complications in anterior cruciate ligament reconstruction. *J Clin Orthop Trauma* 2025;61:102876. https://doi.org/10.1016/j.jcot.2024.102876
2. Eckenrode BJ, Carey JL, Sennett BJ, Zgonis MH. Prevention and management of post-operative complications following ACL reconstruction. *Curr Rev Musculoskelet Med* 2017;10(3):315-21. https://doi.org/10.1007/s12178-017-9427-2
3. Ochiai S, Hagino T, Senga S, Yamashita T, Oda K, Haro H. Injury to infrapatellar branch of saphenous nerve in anterior cruciate ligament reconstruction using vertical skin incision for hamstring harvesting: Risk factors and the influence of treatment outcome. *J Orthop Surg Res* 2017;12(1):1-7. https://doi.org/10.1186/s13018-017-0596-x

4. Egerci OF, Dogruoz F, Asoglu MM, Ertan MB, Yapar A, Kose O. The prognosis of iatrogenic saphenous nerve injuries during hamstring tendon harvesting in anterior cruciate ligament reconstruction. *J Orthop Surg Res* 2024;19(1):4-11. https://doi.org/10.1186/s13018-024-04929-z
5. Azar F, Robert Miller III. Knee injuries. In: Azar FM, Beaty JH (eds.). *Campbell's operative orthopaedics*. Philadelphia: Elsevier; 2020, vol. 4, p. 2308-9.
6. Rajani R, Ogden L, Matthews CJ, Parker Gibbs C. Diffuse pigmented villonodular synovitis as a rare cause of graft failure following anterior cruciate ligament reconstruction. *Orthopedics* 2018;41(1):e142-e144. https://doi.org/10.3928/01477447-20170719-06
7. Chen X, Li P, Zhang W, Yin X, Ma Q, Wang K. Higher incidence of diffuse pigmented villonodular synovitis in patients with ruptured cruciate ligament: A case report. *Int J Surg Case Rep* 2022;100:107720. https://doi.org/10.1016/j.ijscr.2022.107720
8. Barbosa NC, Campos JP, Capelão V, Kandhari V, Vieira TD, Sonnery-Cottet B. A comprehensive scoping review of tibial cysts after anterior cruciate ligament reconstruction. *J Exp Orthop* 2021;8(1):40. https://doi.org/10.1186/s40634-021-00356-9
9. Rossi W, Ranalletta M, Ranalletta A. Ganglión pretibial post reconstrucción de ligamento cruzado anterior. *Artroscopía* 2013;20:95-7. Available at: http://www.revistaartroscopia.com/ediciones-anteriores/2013/volumen-20-numero-3/91-volumen-05-numero-1/volumen-20-numero-3/635-ganglion-pretibial-post-reconstruccion-de-ligamento-cruzado-anterior
10. Borjali A, Mohseni M, Chizari M. Biomechanical modeling of a bone tunnel enlargement post ACL reconstruction. *bioRxiv* 2020.09.03.281915. https://doi.org/10.1101/2020.09.03.281915
11. Flury A, Wild L, Waltenspül M, Zindel C, Vlachopoulos L, Imhoff FB, et al. Tibial tunnel enlargement is affected by the tunnel diameter-screw ratio in tibial hybrid fixation for hamstring ACL reconstruction. *Arch Orthop Trauma Surg* 2023;143(4):1923-30. https://doi.org/10.1007/s00402-022-04408-2
12. Palazzolo A, Rosso F, Bonasia DE, Saccia F RRKCS. Uncommon complications after anterior cruciate ligament reconstruction. *Joints* 2018;6(3):188-203. https://doi.org/10.1055/s-0038-1675799
13. Andrés-Cano P, Godino M, Vides M, Guerado E. Postoperative complications of anterior cruciate ligament reconstruction after ambulatory surgery. *Rev Esp Cir Ortop Traumatol* 2015;59(3):157-64. https://doi.org/10.1016/j.recot.2014.09.001
14. Yonga Ö, Güven M, Akman B, Taşatan E. Unusual tibial ganglion cyst formation due to bioabsorbable screw 13 years after anterior cruciate ligament reconstruction: A case report. *Ann Orthop Trauma Rehabil* 2022;4(2):141. Available at: https://scientificliterature.org/Orthopaedics/Orthopaedics-22-141.pdf
15. Yacuzzi CH, Zicaro JP, Ranalletta M, Costa Paz M. Quiste sinovial en la tibia luego de la reconstrucción del ligamento cruzado anterior: evaluación de 14 pacientes. *Artroscopía* 2018;25(1):14-20. Available at: https://www.revistaartroscopia.com.ar/index.php/revista
16. Deie M, Sumen Y, Ochi M, Murakami Y, Fujimoto E, Ikuta Y. Pretibial cyst formation after anterior cruciate ligament reconstruction using auto hamstring grafts: Two case reports in a prospective study of 89 cases. *Magn Reson Imaging* 2000;18(8):973-7. https://doi.org/10.1016/s0730-725x(00)00207-1
17. Laupattarakasem P, Laopaiboon M, Kosuwon W, Laupattarakasem W. Meta-analysis comparing bioabsorbable versus metal interference screw for adverse and clinical outcomes in anterior cruciate ligament reconstruction. *Knee Surg Sports Traumatol Arthrosc* 2012;22(1):142-53. https://doi.org/10.1007/s00167-012-2340-8
18. Sprowson AP, Aldridge SE, Noakes J, Read JW, Wood DG. Bio-interference screw cyst formation in anterior cruciate ligament reconstruction-10-year follow up. *Knee* 2012;19(5):644-7. https://doi.org/10.1016/j.knee.2012.01.004
19. Shen C, Jiang SD, Jiang LS, Dai LY. Bioabsorbable versus metallic interference screw fixation in anterior cruciate ligament reconstruction: a meta-analysis of randomized controlled trials. *Arthroscopy* 2010;26(5):705-13. https://doi.org/10.1016/j.arthro.2009.12.011
20. Chevallier R, Klouche S, Gerometta A, Bohu Y, Herman S, Lefevre N. Bioabsorbable screws, whatever the composition, can result in symptomatic intra-osseous tibial tunnel cysts after ACL reconstruction. *Knee Surg Sports Traumatol Arthrosc* 2017;27(1):76-85. https://doi.org/10.1007/s00167-018-5037-9
21. Alonso B, Sobrón F, Vidal C, Vaquero J. Seudoquiste pretibial tras la reconstrucción del ligamento cruzado anterior con tornillo biocomposite. *Acta Ortop Mex* 2016;30(3):150- 3. Available at: https://www.scielo.org.mx/scielo.php?script=sci_arttext&pid=S2306-41022016000300150
22. Thapa S, Lamichhane A, Mahara D. Pretibial cyst after anterior cruciate ligament reconstruction with non-bioabsorbable interference screw. *J Inst Med Nepal* 2024;40(1):137-9. https://doi.org/10.59779/jiomnepal.892

23. Tsuda E, Ishibashi Y, Tazawa K, Sato H, Kusumi T, Toh S. Pretibial cyst formation after anterior cruciate ligament reconstruction with a hamstring tendon autograft. *Arthroscopy* 2006;22(6):691.e1-691.e6. https://doi.org/10.1016/j.arthro.2005.04.115
24. Sekiya JK, Elkousy HA, Fu FH. Recurrent pretibial ganglion cyst formation over 5 years after anterior cruciate ligament reconstruction. *Arthroscopy* 2004;20(3):317-21. https://doi.org/10.1016/j.arthro.2003.11.041
25. Sedou MSL, Mbombo CT, Kiama YT, Ndangi K, Nkodia E, Mwangala D, et al. Treatment of synovial cysts related to the tibial tunnel of anterior cruciate ligament grafts by filling the tunnel with acrylic cement. *Surg Sci* 2024;15:289-98. https://doi.org/10.4236/ss.2024.154027
26. Malhan K, Kumar A, Rees D. Tibial cyst formation after anterior cruciate ligament reconstruction using a new bioabsorbable screw. *Knee* 2002;9(1):73-5. https://doi.org/10.1016/s0968-0160(01)00109-0
27. Ramsingh V, Prasad N, Lewis M. Pre-tibial reaction to biointerference screw in anterior cruciate ligament reconstruction. *Knee* 2014;21(1):91-4. https://doi.org/10.1016/j.knee.2013.07.011

Retroperitoneal Incisional Hernia Secondary to Lumbar Revision Surgery. Description of the Surgical Repair Technique with Mesh and Intertransverse Fixation: A Case Report

Bryan A. Orellana Tapia,[*] Cecibel Y. Cevallos Agurto,[**] Juan Carlos Ortiz Calle,[#] Juan Diego Mora Tola[*]
[*]Universidad de Cuenca, Cuenca, Ecuador
***Hospital General Docente Vicente Corral Moscoso, Cuenca, Ecuador*
#Hospital de Especialidades José Carrasco Arteaga, Cuenca, Ecuador

ABSTRACT
Introduction: Lumbar spine revision surgery is a procedure performed when mechanical or biological complications arise after primary surgeries. The surgical approach can alter the anatomy of the posterior abdominal wall, weakening it and leading to hernias at this level. **Objective:** To describe the surgical technique for repairing an incisional hernia in the retroperitoneum after lumbar revision surgery, using mesh and intertransverse fixation. **Conclusions:** Lumbar incisional hernias secondary to lumbar spine revision surgery are rare. They can be repaired in the same surgical stage by placing a polypropylene mesh with intertransverse transosseous fixation, yielding good and reproducible results.
Keywords: Retroperitoneal incisional hernia; retroperitoneal herniorrhaphy; failed lumbar spine surgery.
Level of Evidence: IV

Hernia incisional retroperitoneal secundaria a una cirugía de revisión lumbar. Descripción de la técnica quirúrgica de reparación con malla y fijación intertransversa: a propósito de un caso

RESUMEN
Introducción: La cirugía de revisión de la columna lumbar es un procedimiento que se realiza cuando surgen complicaciones mecánicas o biológicas tras las cirugías primarias. El abordaje quirúrgico puede alterar la anatomía de la pared abdominal posterior, debilitándola, y generar hernias a este nivel. **Objetivo:** Describir la técnica quirúrgica de reparación con una malla y fijación intertransversa de una hernia incisional retroperitoneal secundaria a una cirugía de revisión lumbar,. **Conclusiones:** Las hernias incisionales lumbares secundarias a una cirugía de revisión de la columna vertebral lumbar son raras. Se las puede reparar en el mismo tiempo quirúrgico colocando una malla de polipropileno con fijación transósea intertransversa. Los resultados son buenos y reproducibles.
Palabras clave: Hernia incisional retroperitoneal; herniorrafia retroperitoneal; cirugía fallida de columna lumbar.
Nivel de Evidencia: IV

INTRODUCTION

Lumbar revision surgery is performed in patients with recurrent symptoms due to structural surgical failure or biological complications. This type of surgery is challenging because of preexisting anatomical alterations, the presence of scar tissue, and the increased risk of complications such as infection and dural injury.[1-5]

Received on October 20th, 2025. Accepted after evaluation on March 3rd, 2026 • Dr. BRYAN A. ORELLANA TAPIA • orellana_28@outlook.com https://orcid.org/0000-0001-5742-9471
How to cite this article: Orellana Tapia BA, Cevallos Agurto CY, Ortiz Calle JC, Mora Tola JD. Retroperitoneal Incisional Hernia Secondary to Lumbar Revision Surgery. Description of the Surgical Repair Technique with Mesh and Intertransverse Fixation: A Case Report. *Rev Asoc Argent Ortop Traumatol* 2026;91(2):177-183. https://doi.org/10.15417/issn.1852-7434.2026.91.2.2237

A lumbar incisional hernia is an anatomical defect of the posterior abdominal wall through which abdominal contents protrude, most commonly from the retroperitoneum.[6] The defect is bounded superiorly by the twelfth rib, inferiorly by the iliac crest, laterally by the external oblique muscle, and medially by the erector spinae muscle.[7] These hernias are rare, accounting for 1.5% of abdominal wall hernias; they may present as a well-defined reducible mass or as a large, poorly defined fascial defect.[6]

The aim of this report is to describe a surgical technique for the repair of a retroperitoneal incisional hernia using mesh and intertransverse fixation, secondary to lumbar revision surgery.

CLINICAL CASE

A 60-year-old woman with no relevant medical history was diagnosed with degenerative spondylolisthesis at L4-L5 and lumbar stenosis at L3-L5. She had undergone decompression, instrumentation, and posterior lumbar interbody fusion in 2017. Following the procedure, she developed an acute complication consisting of a cerebrospinal fluid fistula and multilevel vertebral osteomyelitis. She underwent multiple surgical debridements, hardware removal, fistula repair, and antibiotic therapy.

After resolution of the infection, the patient continued to experience severe mechanical low back pain that worsened with exertion. She was unable to tolerate prolonged standing or sitting, and her symptoms did not improve with analgesics or physical therapy. She reported no abdominal symptoms.

On physical examination, there was lumbar facet pain predominantly on the right side, as well as pain with active lumbar flexion and extension. She had residual right L4 paresis (Medical Research Council grade 4/5).

Lumbar MRI showed resolution of the infection and instability due to grade II L4-L5 spondylolisthesis secondary to pseudoarthrosis. At L3-L4, in the right posterolateral region, a retroperitoneal incisional hernia was identified, with a 1-cm hernial defect and a hernia sac measuring 10 x 5 x 5 cm, at risk of strangulation, classified as L4, W1, R1 according to the European Hernia Society (Figure 1).[8]

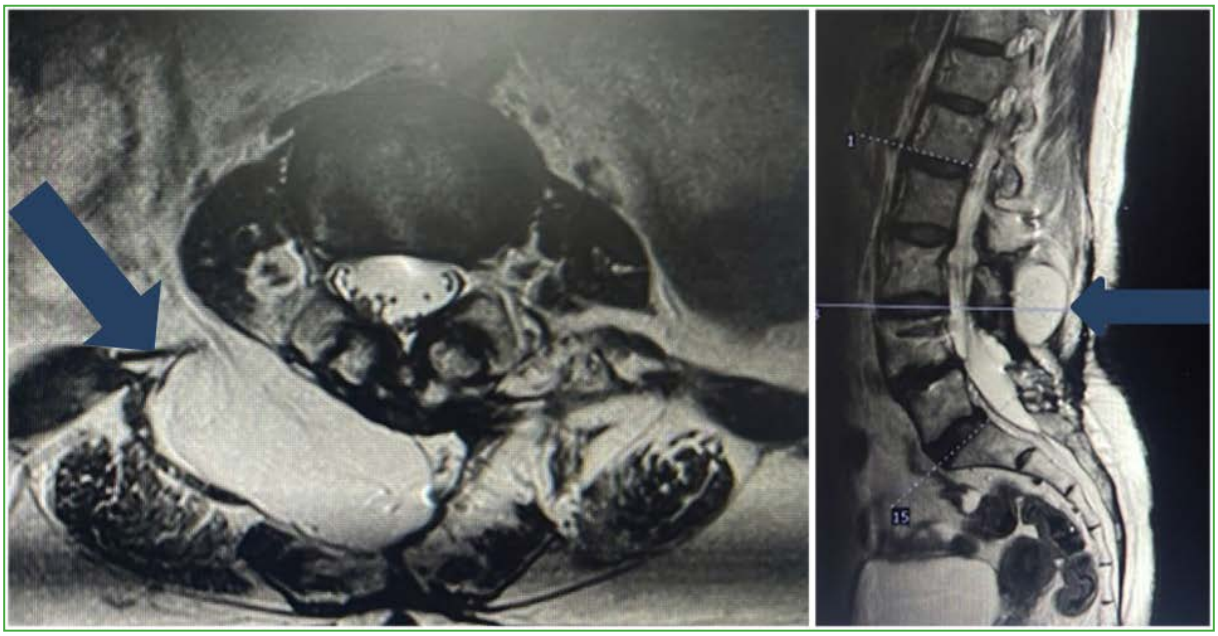

Figure 1. Magnetic resonance imaging of the lumbosacral region, axial and sagittal views. A hyperintense lesion measuring 10 x 5 x 5 cm is observed in the right posterolateral region, with a 1-cm hernial defect communicating with the retroperitoneal cavity.

Surgery was planned jointly by a spine surgeon and a general surgeon. A lumbar revision procedure was indicated to address pseudoarthrosis, along with repair of the retroperitoneal incisional hernia, given its interposition at the surgical approach site and the associated risk of iatrogenic bowel injury.

Layer-by-layer dissection was performed. The hernia sac (Figure 2A), its contents (omentum), and the hernial defect were identified, and a partial omentectomy was performed (Figure 2B).

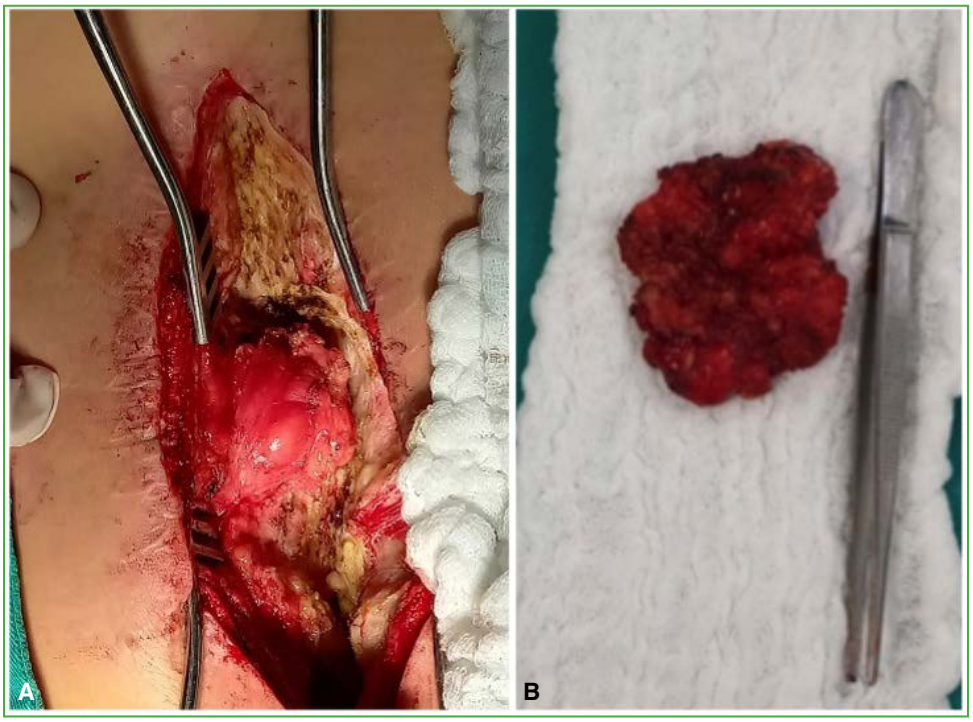

Figure 2. A. Right retroperitoneal incisional hernia. **B.** Partial omentectomy.

The hernia was reduced, and the fascial defect was repaired using a polypropylene mesh. Medially, the mesh was secured using a transosseous technique with Prolene™ 1 sutures to the right transverse processes of L3 and L4, which were drilled using a 1.5-mm drill bit; an additional suture was placed between the transverse processes (Figure 3).

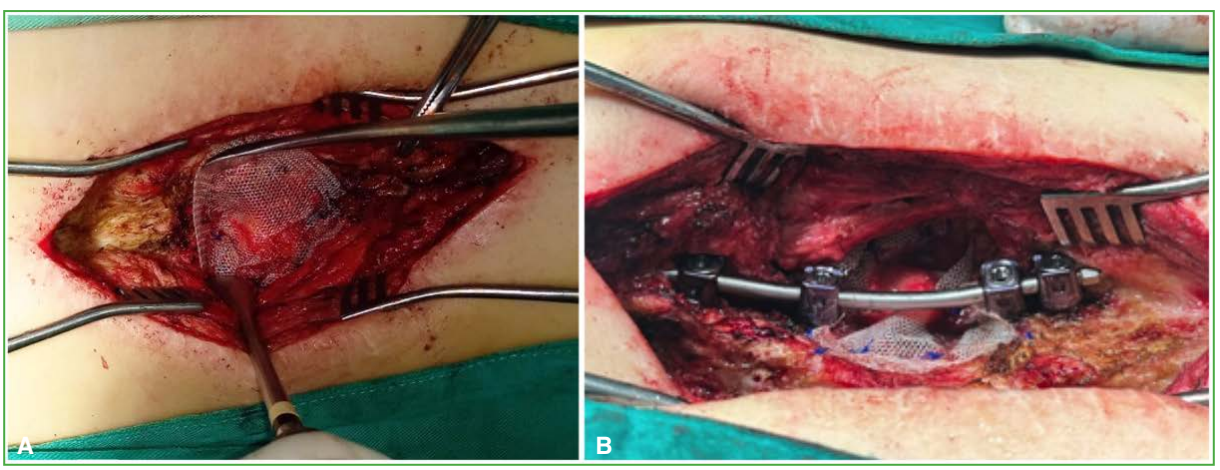

Figure 3. A. Hernia reduction and fixation of the polypropylene mesh. **B.** Lumbar instrumentation.

Laterally, the mesh was secured with three sutures to the remaining fascia and surrounding soft tissues (Figure 4). Subsequently, L2-S1 instrumentation was performed with intraoperative neuromonitoring, followed by posterolateral fusion using allograft. Postoperative radiographs confirmed appropriate lumbar instrumentation (Figure 5). The patient had a favorable outcome, with improved lumbar function and no pain or complications.

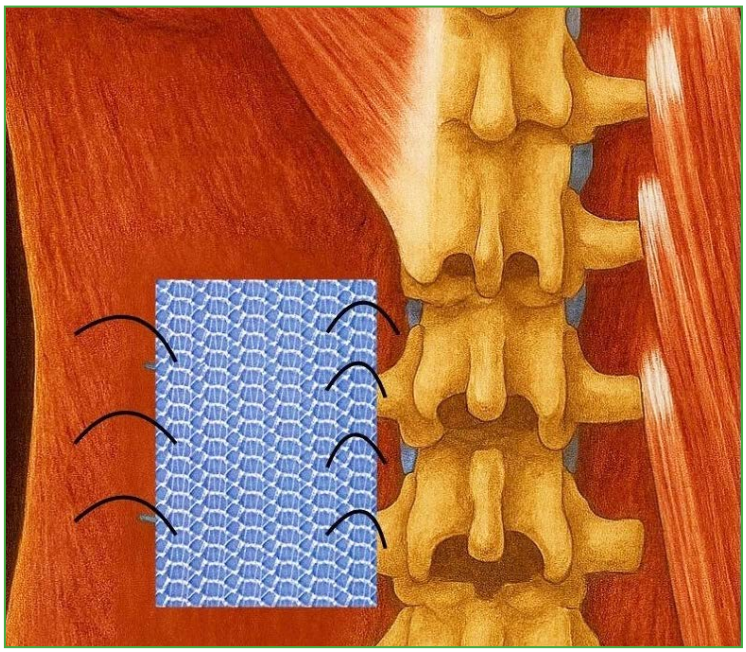

Figure 4. Representative image of the polypropylene mesh fixed to the fascia and surrounding soft tissues, as well as to the transverse processes of L3 and L4.

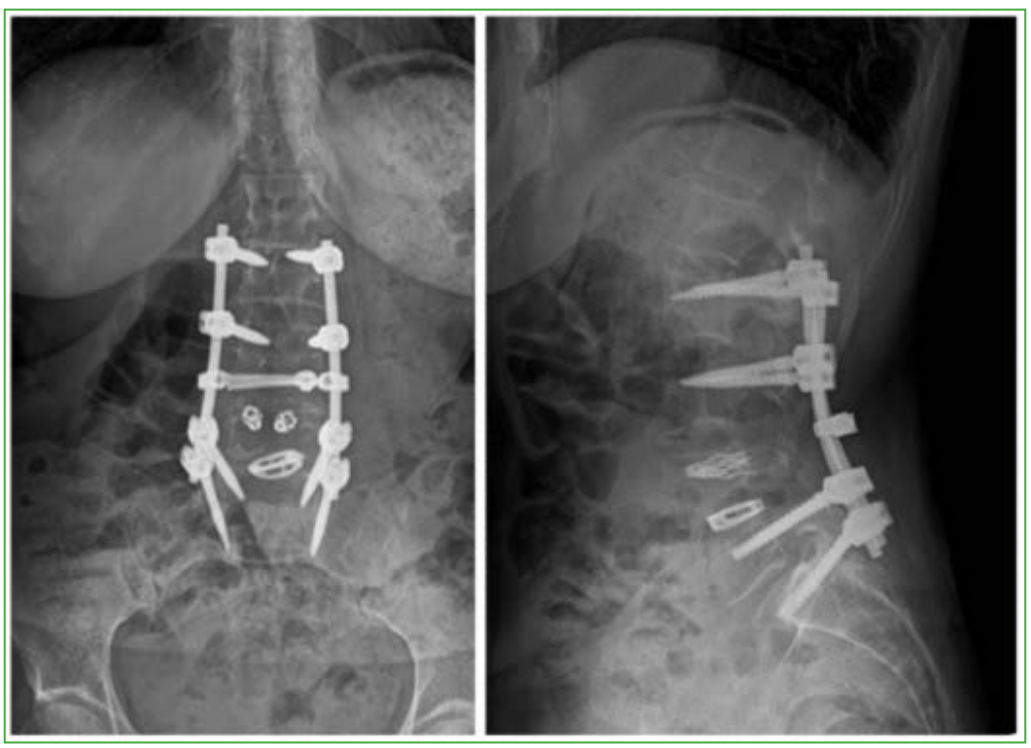

Figure 5. Anteroposterior and lateral radiographs of the lumbosacral region, postoperative follow-up. L2-S1 instrumentation.

At the 6-month postoperative follow-up, lumbar MRI demonstrated successful lumbar fusion and complete resolution of the retroperitoneal incisional hernia, with no evidence of recurrence (Figure 6).

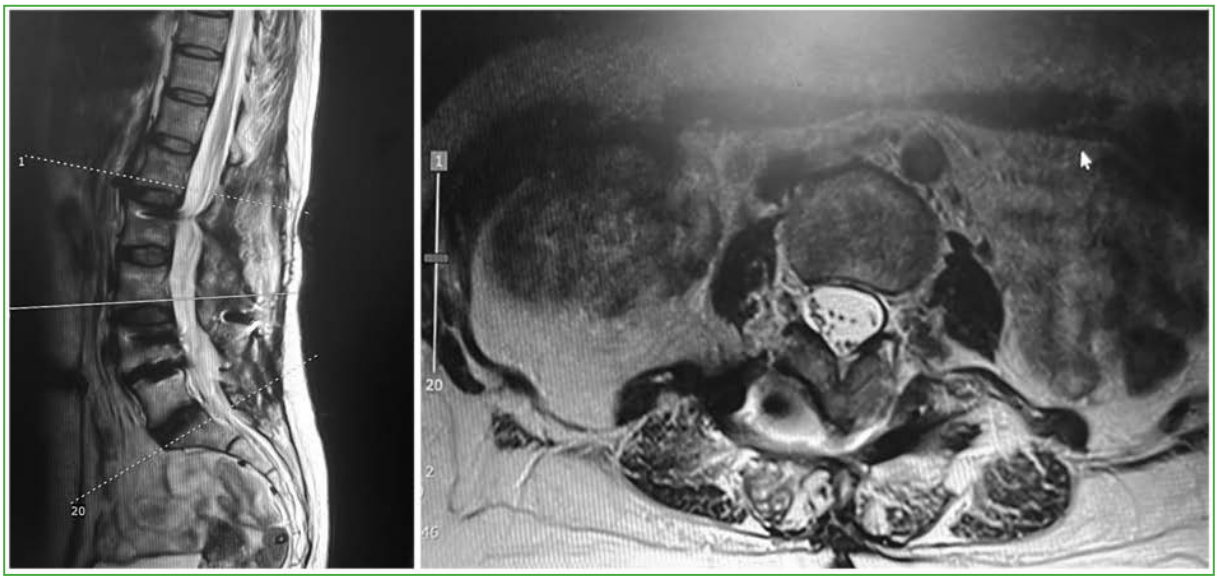

Figure 6. Magnetic resonance imaging of the lumbosacral region, sagittal and axial views, showing resolution of the retroperitoneal incisional hernia.

DISCUSSION

Retroperitoneal hernias secondary to lumbar revision surgery are rare and occur following loss of integrity of the posterior abdominal fascia. They may result from resection of postoperative fibrotic tissue or from muscle atrophy.[9] The patient underwent multiple lumbar procedures, which weakened the posterior abdominal fascia and led to the development of a retroperitoneal incisional hernia.

The natural history of hernias involves a gradual increase in size.[10] Luu et al.[11] conducted a retrospective study of 735 patients who underwent lumbar spine surgery via a paramedian approach; 20 developed a lumbar incisional hernia, and 14 required surgical repair.

There is no consensus regarding optimal treatment. However, the primary objective is to restore the functional and mechanical integrity of the abdominal wall.[12] Predisposing factors include short stature, pregnancy, ascites, obesity, and muscle atrophy. The typical clinical presentation consists of a slowly enlarging lumbar mass, posterior abdominal pain or low back pain, and a positive Valsalva maneuver.[13]

Flank incisions may lead to retroperitoneal hernia due to disruption of the posterior abdominal wall fascia, or to pseudohernia secondary to nerve injury, resulting in decreased muscle tone and atrophy. Diagnosis is established by computed tomography (CT) or magnetic resonance imaging (MRI), which can demonstrate the hernial defect, size, location, and contents, or isolated atrophic changes of the abdominal wall.[12] In the present case, the diagnosis was confirmed by MRI.

Approximately 70% of these hernias require surgical treatment. Repair is technically challenging due to the proximity of bony structures, which limits adequate dissection and mesh overlap.[14] Surgical management may be open or laparoscopic, depending on defect size.[12] Current evidence favors laparoscopic repair over open techniques, as it is associated with reduced analgesic requirements, less postoperative pain, faster recovery, and improved visualization of visceral contents, thereby decreasing the risk of intra-abdominal injury.[13]

Du et al.[15] evaluated 11 patients with lumbar retroperitoneal hernias (not secondary to lumbar spine surgery) treated using a laparoscopic technique with self-adhering mesh and reported favorable outcomes.

This case illustrates an innovative technique for the repair of lumbar retroperitoneal hernias, involving transosseous intertransverse fixation of a mesh to both the transverse processes and the residual fascia. This approach may provide greater stability and reduce the risk of mechanical failure, with favorable outcomes. Further studies are required to validate this surgical technique.

CONCLUSIONS

Retroperitoneal incisional hernias secondary to lumbar spine revision surgery are rare. They can be repaired during the same surgical procedure using a polypropylene mesh with transosseous intertransverse fixation, with favorable outcomes.

This intertransverse mesh fixation technique provides enhanced stability and has not yet been described in the literature. Therefore, we recommend further evaluation through case series to validate its efficacy and safety. It may represent a useful option in complex cases requiring multiple prior surgical procedures.

Conflicts of interest: The authors declare no conflicts of interest.

C. Y. Cevallos Agurto ORCID ID: https://orcid.org/0000-0002-0364-0121
J. C. Ortiz Calle ORCID ID: https://orcid.org/0000-0001-9384-3047
J. D. Mora Tola ORCID ID: https://orcid.org/0000-0002-5008-6573

REFERENCES

1. Lambrechts MJ, Toci GR, Siegel N, Karamian BA, Canseco JA, Hilibrand AS, et al. Revision lumbar fusions have higher rates of reoperation and result in worse clinical outcomes compared to primary lumbar fusions. *Spine J* 2023;23(1):105-15. https://doi.org/10.1016/j.spinee.2022.08.018
2. Mahamid A, Jayyusi F, Hodruj M, Mansour A, Fishman D, Behrbalk E. Comparative analysis of primary and revision single-level lumbar fusion surgeries: Predictors, outcomes, and clinical implications using big data. *J Clin Med* 2025;14(3):723. https://doi.org/10.3390/jcm14030723
3. Mehren C, Wanke-Jellinek L, Korge A. Revision after failed discectomy. *Eur Spine J* 2020;29(Suppl 1):14-21. https://doi.org/10.1007/s00586-019-06194-9
4. Wang W, Li J, Xu Y, Luo Y, Ding W, Zhang W. Predictors and tactics for revision surgery in lateral lumbar interbody fusion. *BMC Musculoskelet Disord* 2022;23(1):1101. https://doi.org/10.1186/s12891-022-06052-8
5. Kudo Y, Okano I, Toyone T, Matsuoka A, Maruyama H, Yamamura R, et al. Lateral lumbar interbody fusion in revision surgery for restenosis after posterior decompression. *Neurosurg Focus* 2020;49(3):E11. https://doi.org/10.3171/2020.6.FOCUS20361
6. Giacosa GA, Rodríguez M, Juárez Á, Begnis SS, Tabares Á. Incisional lumbar hernias: Current role of laparoscopic approach with intraperitoneal onlay mesh procedure. *Int J Abdom Wall Hernia Surg* 2024;7(1):1. https://doi.org/10.4103/ijawhs.ijawhs_59_23
7. Salameh JR, Salloum EJ. Lumbar incisional hernias: Diagnostic and management dilemma. *JSLS* 2004;8(4):391-4. PMID: 15554289
8. Marenco de la Cuadra B, Retamar Gentil M, Sánchez Ramírez M, Guadalajara Jurado J, Cano Matías A, López Ruiz JA. Tipos de hernias: Clasificaciones actuales. *Cir Andal* 2018;29(2):77-9. Available at: https://dialnet.unirioja.es/servlet/articulo?codigo=9041381
9. Gundanna M, Shah K. Delayed incisional hernia following minimally invasive trans-psoas lumbar spine surgery: Report of a rare complication and management. *Int J Spine Surg* 2018;12(2):126-30. https://doi.org/10.14444/5019
10. Park Y, Chung M, Lee MA. Traumatic lumbar hernia: clinical features and management. *Ann Surg Treat Res* 2018;95(6):340. https://doi.org/10.4174/astr.2018.95.6.340
11. Luu HY, Zobel MJ, Jonzzon S, Lin M, Lee D, Eichler C, et al. Predictors and outcomes of paramedian incisional hernia after anterior spine exposure. *J Surg Res* 2020;247:380-6. https://doi.org/10.1016/j.jss.2019.10.005

12. Moreno-Egea A, Olalla-Muñoz JR. Doble lesión de pared abdominal: hernia incisional lumbar izquierda y seudohernia por denervación y atrofia muscular derecha. Manejo laparoscópico conjunto. *Rev Hispanoam Hernia* 2014;2(4):161-8. https://doi.org/10.1016/j.rehah.2014.05.002
13. Heemskerk J, Leijtens JWA, van Steensel S. Primary lumbar hernia, review and proposals for a standardized treatment. *J Abdom Wall Surg* 2023;2:11754. https://doi.org/10.3389/jaws.2023.11754
14. Aparicio López D, Kälviäinen Mejía H, Gracia Roche C, Duque Mallén M. Post-traumatic lumbar hernia. Complex abdominal wall repair and associated cholecystectomy. *Cir Andal* 2023;34(4):486-9. https:/doi.org/10.37351/2023344.15
15. Du H, Shen Y, Yang H, Zhu Y. Retroperitoneal laparoscopic repair of primary lumbar hernia using self-gripping mesh. *Surg Innov* 2025;428-34. https://doi.org/10.1177/15533506251348535

Case Resolution

Juan Pablo Ghisi,[*] Joaquín Escotorín[**]
[*]Magnetic Resonance Imaging Department, Hospital General de Agudos "Dr. Juan A. Fernández", Autonomous City of Buenos Aires, Argentina
[**]Diagnostic Imaging Department, Sanatorio San Lucas, San Isidro, Buenos Aires, Argentina

Case Presentation on page 79.

Hydroxyapatite Crystal Deposition Disease

ABSTRACT
The disease is described, along with its imaging findings as observed with each diagnostic modality.
Keywords: Knee; calcifications; pain.
Level of Evidence: IV

Enfermedad por depósito de cristales de hidroxiapatita

RESUMEN
Se desarrolla la enfermedad y cómo se visualiza las imágenes, en cada caso, según el estudio.
Palabras clave: Rodilla; calcificaciones; dolor.
Nivel de Evidencia: IV

DIAGNOSIS

Hydroxyapatite crystal deposition disease.

DISCUSSION

Crystal deposition diseases comprise a group of conditions in which the accumulation of crystals within the joint space or periarticular tissues leads to acute or chronic inflammatory manifestations. From a practical standpoint, they can be classified into three main categories: those due to monosodium urate deposition (gout), those related to calcium pyrophosphate deposition, and those secondary to basic calcium phosphate deposition.[1-3]

Hydroxyapatite deposition disease belongs to the latter group. In the literature, it is referred to by various terms that partly reflect the anatomical structure involved and partly the clinical presentation: hydroxyapatite deposition disease, hydroxyapatite crystal deposition disease, basic calcium phosphate deposition, calcific tendinitis, calcific periarthritis, calcific bursitis, and, in intra-articular locations or more destructive forms, hydroxyapatite arthropathy. Within this spectrum, the so-called Milwaukee syndrome represents an advanced form of arthropathy associated with basic calcium phosphate crystals, most commonly described in the shoulder, although knee involvement has been reported in some series.[1-5]

Unlike calcium pyrophosphate deposition disease, which typically presents as chondrocalcinosis with linear or lamellar calcifications in cartilage and fibrocartilage, and urate deposition, which tends to produce bone erosions and tophi, hydroxyapatite deposition disease is characterized by amorphous, periarticular calcifications most commonly located in tendons, bursae, and the joint capsule, and less frequently in ligamentous structures. This distinction is important in imaging assessment, as it helps guide the differential diagnosis based on the pattern of distribution and the morphology of the calcifications.[1-4,6]

Received on March 13th, 2026. Accepted after evaluation on March 19th, 2026 • Dr. JUAN PABLO GHISI • jpghisi@gmail.com https://orcid.org/0000-0001-7991-9228
How to cite this article: Ghisi JP, Escotorín J. Postgraduate Orthopedic Instruction – Imaging. Case Resolution. *Rev Asoc Argent Ortop Traumatol* 2026;91(2):184-186. https://doi.org/10.15417/issn.1852-7434.2026.91.2.2324

From a pathophysiological perspective, three phases are described: precalcific, calcific, and postcalcific, a classification originally established for calcific tendinitis of the shoulder and applicable, by extension, to other periarticular locations. The calcific phase, in turn, includes formative, resting, and resorptive stages. The resorptive stage usually corresponds to the period of greatest clinical expression, as the deposit may fragment or liquefy and trigger a marked inflammatory response in the surrounding tissues. This evolutionary behavior explains the variability of imaging findings and the fact that the same lesion may appear as a well-defined calcification at one time and as a poorly defined lesion with perilesional edema at another.[1,3,6]

Although the shoulder is the most common site of involvement, the knee is also a recognized location. In this joint, the quadriceps tendon, patellar tendon, periarticular bursae, capsule, and ligamentous structures may be affected. Involvement of the medial collateral ligament is uncommon but of particular interest, as it may mimic enthesopathy, post-traumatic sequelae, or avulsion injuries.[1-4,6]

On radiographs, the condition typically appears as an amorphous, rounded, or oval calcification with variable density. During resting phases, it tends to be more homogeneous and well defined, whereas in symptomatic or resorptive phases, it may appear faint, cloud-like, or poorly defined. Radiography therefore remains the most useful initial modality for detecting calcifications and guiding diagnostic suspicion.[1,3,4,6]

Computed tomography allows more precise confirmation of the calcific nature of the deposit, accurate assessment of its size and location, and evaluation of possible cortical erosions or extension into adjacent tissues. It is also particularly useful in the differential diagnosis with mature ossification processes, such as Pellegrini-Stieda lesion, in which imaging typically shows trabecular or cortical organization, unlike the amorphous appearance characteristic of hydroxyapatite deposits.[1,3,6]

Ultrasound demonstrates the deposits as hyperechoic foci, with or without posterior acoustic shadowing, and allows real-time assessment of the inflammatory changes in adjacent soft tissues. In more active phases, Doppler imaging may show associated hyperemia. In addition, ultrasound has therapeutic value, as it enables image-guided procedures such as aspiration or lavage in selected cases.[1,3,6]

Magnetic resonance imaging is not the most sensitive modality for detecting calcifications but is highly useful for assessing the inflammatory context. Deposits typically appear as foci of signal void or hypointensity on all sequences, associated with perilesional edema, bursitis, or reactive synovitis. MRI may pose diagnostic challenges when interpreted in isolation, as the inflammatory changes may predominate over visualization of the deposit and mimic traumatic, infectious, or even neoplastic conditions. For this reason, correlation with radiography, CT, or ultrasound is essential.[1,3,6]

In the cases presented, the findings were located along the medial aspect of the knee, anterior to the femoral insertion of the medial collateral ligament, with calcific morphology and associated perilesional inflammatory changes. The anatomical distribution, the appearance of the deposits, and the adjacent soft-tissue reaction constitute a pattern consistent with hydroxyapatite deposition in the medial capsuloligamentous region. In one case, ultrasound confirmed the calcific nature of the finding, whereas in the other, radiography demonstrated faint calcifications in the same location, supporting this interpretation.[6]

In the differential diagnosis of medial knee calcifications around the insertion area, the following entities should be considered: enthesopathy, remote avulsion injury, post-traumatic ossification (Pellegrini-Stieda lesion), medial bursitis, and other crystal-induced arthropathies, particularly calcium pyrophosphate deposition disease. Recognition of the morphological pattern of the deposits and their multimodality correlation helps avoid misinterpretation and guides appropriate diagnostic and therapeutic management.[1-3,6]

From a therapeutic standpoint, this is generally a self-limiting condition initially managed conservatively with relative rest, physical therapy, and nonsteroidal anti-inflammatory drugs. In cases of persistent symptoms, interventional options may be considered, such as extracorporeal shock wave therapy and image-guided percutaneous aspiration or lavage. Arthroscopic or open surgery is reserved for severe or refractory cases. In this context, imaging plays a role not only in diagnosis but also in the planning and guidance of therapeutic procedures.[1,3]

CONCLUSIONS

These two cases illustrate a rare and likely underdiagnosed cause of medial knee pain: perinsertional calcific deposits of the medial capsuloligamentous complex, which, in their symptomatic phase, may be associated with marked inflammatory changes and mimic trauma, infection, or other arthropathies.

The diagnostic approach should be based on multimodality imaging correlation. Radiography is essential for identifying calcifications, even when subtle. Computed tomography confirms the deposit, precisely defines its location and extent, and helps differentiate calcification from ossification. Ultrasound confirms its calcific nature, may provide information about the stage of the process, and enables image-guided therapy. Finally, magnetic resonance imaging delineates the extent of edema and reactive changes, although it requires correlation with calcium-sensitive modalities to avoid misinterpretation.

In the medial knee, including this entity in the differential diagnosis when evaluating enthesopathy or Pellegrini-Stieda lesion helps prevent overdiagnosis of chronic ligament injury or post-traumatic sequelae and reduces unnecessary additional studies or interventions.

J. Escotorín ORCID ID: https://orcid.org/0009-0006-4115-1034

REFERENCES

1. Hayes CW, Conway WF. Calcium hydroxyapatite deposition disease. *Radiographics* 1990;10:1031-48. https://doi.org/10.1148/radiographics.10.6.2175444
2. Garcia GM, McCord GC, Kumar R. Hydroxyapatite crystal deposition disease. *Semin Musculoskelet Radiol* 2003;7(3):187-94. https://doi.org/10.1055/s-2003-43229
3. Hegazi T. Hydroxyapatite deposition disease: a comprehensive review of pathogenesis, radiological findings, and treatment strategies. *Diagnostics (Basel)* 2023;13:2678. https://doi.org/10.3390/diagnostics13162678
4. Bonavita JA, Dalinka MK, Schumacher HR Jr. Hydroxyapatite deposition disease. *Radiology* 1980;134:621-5. https://doi.org/10.1148/radiology.134.3.6243783
5. Halverson PB, McCarty DJ, Cheung HS, Ryan LM. Milwaukee shoulder syndrome: eleven additional cases with involvement of the knee in seven (basic calcium phosphate crystal deposition disease). *Semin Arthritis Rheum* 1984;14(1):36-44. https://doi.org/10.1016/0049-0172(84)90007-6
6. Hongsmatipa P, Cheng KY, Kim C, Lawrence DA, Rivera R, Smitaman E. Calcium hydroxyapatite deposition disease: imaging features and presentations mimicking other pathologies. *Eur J Radiol* 2019;120:108653. https://doi.org/10.1016/j.ejrad.2019.108653

Letter to the Editor

Dear Editor,

After reading the article *"Neonatal Vertebral Osteomyelitis: Case Report and Literature Review"* by Manzone P. and Ovejero MP, recently published in the AAOT Journal, which highlights the challenges in managing this severe condition based on the authors' experience,[1] I would like to comment on the relevance of the predominant pathogens in this entity and the empirical antibiotic approach, critical aspects for optimizing outcomes in these patients.

Neonatal vertebral osteomyelitis (NVO) is most associated with *Staphylococcus aureus*, including methicillin-resistant strains (MRSA), as in the case described in the original article, followed by *Streptococcus agalactiae*. Among Gram-negative organisms, *Klebsiella pneumoniae* and *Escherichia coli* are frequently identified, particularly in nosocomial sepsis or in preterm neonates. Early identification of the causative pathogen is essential, as antimicrobial resistance significantly impacts prognosis.[2]

Considering the most frequent pathogens, initial antibiotic therapy should provide coverage for both Gram-positive and Gram-negative organisms, prioritizing agents with adequate bone penetration and guided by local antimicrobial resistance patterns, which were not specified for the Centro Nicolás Andry, where the reported case was managed. In neonates without risk factors for multidrug-resistant organisms, the regimen used appears appropriate to cover the relevant pathogens. In nosocomial settings or in cases of severe sepsis, the use of carbapenems should be considered. Transition to oral therapy should be guided by culture results and clinical response, with a total treatment duration of 4-6 weeks.[3]

REFERENCES

1. Manzone P, Ovejero MP. Osteomielitis vertebral neonatal. Presentación de un caso y revisión bibliográfica. *Rev Asoc Argent Ortop Traumatol* 2025;90(1):80-9. https://doi.org/10.15417/issn.1852-7434.2025.90.1.2037
2. Zhan C, Zhou B, Du J, Chen L. Clinical analysis of 17 cases of neonatal osteomyelitis: A retrospective study. *Medicine (Baltimore)* 2019;98(2):e14129. https://doi.org/10.1097/MD.0000000000014129
3. Miller JM, Binnicker MJ, Campbell S, Carroll KC, Chapin KC, Gonzalez MD, et al. Guide to Utilization of the Microbiology Laboratory for Diagnosis of Infectious Diseases: 2024 Update by the Infectious Diseases Society of America (IDSA) and the American Society for Microbiology (ASM). *Clin Infect Dis* 2024;ciae104. https://doi.org/10.1093/cid/ciae104

José Manuel Morales Mena
General Practitioner, Independent Researcher, San José, Costa Rica
josemlmorales@hotmail.com

Jorge Merren Gallegos
General Practitioner, Independent Researcher, San José, Costa Rica

Meir Mendelewicz Montero
General Practitioner, Independent Researcher, San José, Costa Rica

Dr. JOSÉ MANUEL MORALES MENA • josemlmorales@hotmail.com

How to cite this article: Morales Mena JM, Merren Gallegos J, Mendelewicz Montero M. Letter to the Editor. *Rev Asoc Argent Ortop Traumatol* 2026;91(2):187. https://doi.org/10.15417/issn.1852-7434.2026.91.2.2181